

# **Geotechnical properties of the surficial soil of Sana'a The Yemen Arab Republic.**

**Khaled Abdallah Hasan Al-Gasous**

Civil Engineering

1988

Abstract

There is a paucity of geotechnical information about the surficial soil of Sana'a region. Therefore, this study is aimed at filling this gap by studying in detail the engineering properties of Sana'a soil.

The geotechnical properties of the surficial soils of an area of about 100 km in Sana'a region, the capital of Yemen Arab Republic were investigated. The study consisted of both field and laboratory investigation programs.

In the field investigation program, 32 locations were selected for the classification and inspection tests. Based on the obtained results, ten additional stations were selected for carrying the standard penetrations test and for studying the geotechnical properties in more detail by carrying out specific tests.

The laboratory testing program included classification tests, strength tests (consolidated undrained triaxial test), one dimensional consolidation test, X-Ray Diffraction analysis, X-Ray Fluorescence analysis, Energy Dispersive Spectrum, Scanning Electron Microscope analysis and chemical analysis. Based on these investigations seven different soil units, resulting mainly from both alluvial and wind depositional systems, were also identified. Depositional systems and soil distribution were identified. Soil profiles have been prepared. Soil composition, soil structure and engineering properties including index properties, strength properties and deformation characteristics were established.

Preliminary analysis indicated the existence of both collapsing soil, loessial soil and expansive soil, top layer. Appropriate design considerations for the expected moisture conditions, suitable foundation implementation and finally potential improvement techniques of the soil in the region were drawn.

# Geotechnical Properties of the Surficial Soil of Sana'a, The Yemen Arab Republic

by

Khaled Abdallah Hasan Al-Gasous

A Thesis Presented to the

FACULTY OF THE COLLEGE OF GRADUATE STUDIES

KING FAHD UNIVERSITY OF PETROLEUM & MINERALS

DHAHRAN, SAUDI ARABIA

In Partial Fulfillment of the  
Requirements for the Degree of

**MASTER OF SCIENCE**

In

**CIVIL ENGINEERING**

June, 1988

## **INFORMATION TO USERS**

**This manuscript has been reproduced from the microfilm master. UMI films the text directly from the original or copy submitted. Thus, some thesis and dissertation copies are in typewriter face, while others may be from any type of computer printer.**

**The quality of this reproduction is dependent upon the quality of the copy submitted. Broken or indistinct print, colored or poor quality illustrations and photographs, print bleedthrough, substandard margins, and improper alignment can adversely affect reproduction.**

**In the unlikely event that the author did not send UMI a complete manuscript and there are missing pages, these will be noted. Also, if unauthorized copyright material had to be removed, a note will indicate the deletion.**

**Oversize materials (e.g., maps, drawings, charts) are reproduced by sectioning the original, beginning at the upper left-hand corner and continuing from left to right in equal sections with small overlaps. Each original is also photographed in one exposure and is included in reduced form at the back of the book.**

**Photographs included in the original manuscript have been reproduced xerographically in this copy. Higher quality 6" x 9" black and white photographic prints are available for any photographs or illustrations appearing in this copy for an additional charge. Contact UMI directly to order.**

# **U·M·I**

University Microfilms International  
A Bell & Howell Information Company  
300 North Zeeb Road, Ann Arbor, MI 48106-1346 USA  
313/761-4700 800/521-0600

**Order Number 1355720**

**Geotechnical properties of the surficial soil of Sana'a, the  
Yemen Arab Republic**

**Al-Gasous, Khaled Abdallah Hasan, M.S.**

**King Fahd University of Petroleum and Minerals (Saudi Arabia), 1988**

**U·M·I**  
300 N. Zeeb Rd.  
Ann Arbor, MI 48106

**GEOTECHNICAL PROPERTIES OF THE SURFACIAL  
SOIL OF SANA'A, THE YEMEN ARAB REPUBLIC**

**BY**

**KHALED ABDALLAH HASAN AL-GASOUS**

**A Thesis Presented to the  
FACULTY OF THE COLLEGE OF GRADUATE STUDIES  
KING FAHD UNIVERSITY OF PETROLEUM & MINERALS  
DHAHRAN, SAUDI ARABIA**

**In Partial Fulfillment of the  
Requirements for the Degree of**

**MASTER OF SCIENCE  
In  
CIVIL ENGINEERING**

**LIBRARY  
KING FARD UNIVERSITY OF PETROLEUM & MINERALS  
Dhabran - 31261. SAUDI ARABIA**

**June, 1988.**

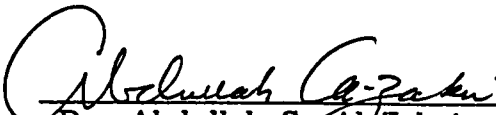
KING FAHD UNIVERSITY OF PETROLEUM & MINERALS  
DHAHRAN, SAUDI ARABIA

This thesis, written by

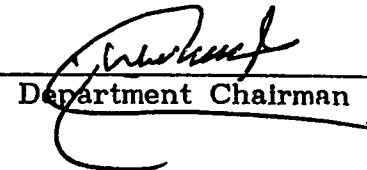
KHALED ABDALLAH HASAN AL-GASOUS

under the direction of his thesis committee, and approved by all the members, has been presented to and accepted by the Dean, College of Graduate Studies, in partial fulfillment of the requirements for the degree of

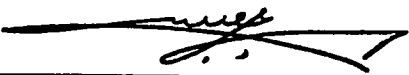
MASTER OF SCIENCE IN CIVIL ENGINEERING

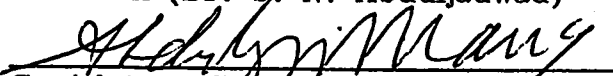
  
Dr. Abdullah S. Al-Zakri  
Dean, College of Graduate Studies

Date : July 12, 1988

  
Department Chairman

Thesis Committee

  
Chairman (Dr. S. N. Abduljawad)

  
Co-Advisor (Dr. A. I. Al-Mana)

  
Member (Dr. M.O. Faruque)



بِسْمِ اللَّهِ الرَّحْمَنِ الرَّحِيمِ

بِسْمِ اللَّهِ الرَّحْمَنِ الرَّحِيمِ

وَقُلْ أَغْبِئُوا فِسِيرَةَ اللَّهِ لِيُكْفِرَ بَرُّوهُمُ الْمُؤْمِنُونَ

سورة التوبة

In the name of God, Most Gracious, Most Merciful

Say unto them, work as ye will;  
but God will behold your work,  
and his apostle also, and  
the true believers.

SURAT. AL TAWBAH

DEDICATION

*Dedicated to my parents, wife and family without whose support and sacrifice this work would not have been accomplished.*

## ACKNOWLEDGEMENT

I am most grateful to Almighty ALLAH for providing me an opportunity and capability to complete this thesis. Acknowledgement is due to King Fahd University of Petroleum and Minerals for support of this research and also the support of Sana'a University and Ministry of Public Works, Government of Yemen Arab Republic for carrying out the field tests.

I am greatly indebted to my major advisor Dr. S. N. Abduljawad for his careful guidance throughout the completion of this research. His advice, enthusiastic interest, patience, constructive criticism at every stage of the work have been invaluable to me.

Appreciation and special thanks are also extended to my thesis Co-Adviser, Dr. Abdulaziz I. Al-Mana who endeavoured to thoroughly review this research and was helpful in providing assistance in conducting X-ray and Scanning Electron Microscope analysis at the Research Institute and for his valuable guidance throughout this research. I also appreciate the efforts of other committee member Dr. Muhammad Omar Faruque for his guidance and helpful comments while reviewing this thesis. I would also like to thank Dr. Waddah Akili for guiding me to select the thesis topic and for his valuable suggestions.

I am also thankful to my friends whose contribution is difficult

to be acknowledged explicitly. Among them are Messrs Kalalah, M., Al-Gassous, M., Al-Kohali, GH., Abduljabbar, S. and Musa, M. Thanks are due to Dr. Khatri, Mr. Naugn, of the Research Institute and Mr. Hasan Zakariya, Mr. Essam El-Deeb, Mr. Abdulappa and the staff of the Soil Lab at the Ministry of Public Works in Sana'a, for their help and cooperation in accomplishing the work.

Finally, I will express my profound gratitude to my parents, brothers and my wife for their love and affection. Their sacrifices and foresightedness made this work possible.

I also appreciate the kind help to me by Mr. Mumtaz Khan for typing this thesis.

## LIST OF SYMBOLS

- A = activity of the soil
- C = cohesion in term of total stresses
- Cc = curvature coefficient
- C.S.L. = critical state line
- Cu = uniformity coefficient
- DS = disturbed sample
- E = effective stress path
- FE = foundation excavation
- K = coefficient of permeability
- Kc = collapsing subsidence
- L.I. = liquidity index
- L.L. = liquid limit
- M = slope of the critical state line in  $q'$ - $p'$  space
- N = standard penetration value
- N.C.L. = normal consolidation line
- O.C.R. = over-consolidation ratio

P.I. = plastic index

PH = pithole excavation

P.L. = plastic limit

S = degree of saturation

SPT = Standard Penetration Test

T = total stress path

TE = trench excavation

US = Undisturbed sample

$v$  = specific volume ratio

$W_c$  = natural moisture content

$A_f$  = coefficient of pore water pressure

$C_c$  = compression index

$C_p$  = collapsing potential

$C_s$  = swelling index

$C_c'$  = field compression index

$C_v$  = coefficient of consolidation

$C'_{linuep}$  = cohesion in term of effective stresses

$D_{10}$  = effective diameter at 10 per cent fines passing

$e_L$  = voids ratio at liquid limit

$e_o$  = initial void ratio

$E_s$  = tangent modulus of elasticity

$G_s$  = specific gravity

$K_o$  = earth pressure coefficient at rest

$K_{av}$  = average value of earth pressure coefficient

$m_v$  = coefficient of volume compressibility

$m'_v$  = field coefficient of volume compressibility

$N$  = specific volume on critical state line at  $p' = 1.0$  kpa

$N_o$  = specific volume at  $p' = 1.0$  kpa

$p'$  = mean effective stresses

$p'_f$  = mean effective pressure at failure

$q_f$  = deviatoric stress at failure

- $S_p$  = swelling potential
- $S_1$  = settlement of soil with no change in moisture
- $S_2$  = settlement of soil caused by collapsing due to water addition
- $U_f$  = pore water pressure at failure
- $U_o$  = initial pore water pressure, back water pressure
- $v_f$  = specific volume at failure
- $v_o$  = initial specific volume
- $V_s$  = volume of solid part of the total volume of unity
- $\Delta H$  = settlement
- $\gamma_d$  = dry unit weight
- $\gamma_n$  = natural unit weight
- $\gamma_w$  = water unit weight
- $\Gamma$  = slope of the critical state line in  $V-\ln p'$  space
- $\lambda$  = slope of the normal consolidation in  $\ln p$  space
- $\kappa$  = slope of swelling line in  $v-\ln p'$  space

$\mu$  = Poisson's ratio

$\phi_{cu}$  = total friction angle resulted from CIU triaxial test

$\phi'_o$  = effective internal friction angle

$\phi'_{cu}$  = effective friction angle resulted from CIU triaxial test

$\sigma_c$  = total confining pressure

$\sigma_h$  = horizontal total stress

$\sigma'_o$  = effective confining pressure

$\sigma_p$  = maximum stress history

$\sigma_v$  = vertical total stress

$\sigma'_v$  = vertical effective pressure

$\sigma_{vo}$  = overburden pressure

$\sigma_1$  = Major principal vertical stress

$\sigma_3$  = Minor principal total stress

## TABLE OF CONTENTS

<i>Chapter</i>	<i>Page</i>
Acknowledgements .....	iii
Table of Symbols .....	v
Table of Contents.....	x
List of Tables .....	xiv
List of Figures .....	xvi
List of Plates .....	xxii
Abstract.....	xxiv
1. INTRODUCTION .....	1
1.1 General.....	2
1.2 Objectives and Scope of the Study .....	
2. PHYSIOGRAPHY AND GEOLOGY	
2.1 General.....	5
2.1.1 Location .....	5
2.1.2 Climate .....	5
2.2 Physiography .....	7
2.3 Geology.....	11
2.3.1 General Geology .....	11
2.3.2 Stratigraphy.....	12
2.3.3 Structure.....	21
3. METHODS OF INVESTIGATION	
3.1 General.....	22
3.2 Field Investigation .....	22
3.2.1 Exploration Study.....	24
3.2.2 Sampling.....	25
3.2.2.1 Disturbed Soil Samples.....	25
3.2.2.2 Undisturbed Soil Samples .....	26
3.2.2.3 Hand-carved Undisturbed Soil Samples .....	27

3.3	Insitu Testing .....	33
3.3.1	Types of Testing .....	33
3.3.2	Auger Testing .....	33
3.3.3	Standard Penetration Test (SPT).....	35
3.3.3.1	Definition.....	35
3.3.3.2	Suitability and Validity of SPT.....	37
3.3.3.3	General Remarks on SPT.....	37
3.4	Laboratory Test .....	38
3.4.1	Inspection Tests.....	38
3.4.2	Classification and General Tests .....	39
3.4.3	Laboratory Sampling and Specimens Preparation .....	41
3.4.3.1	Consolidation Specimens .....	41
3.4.3.2	Triaxial Specimens.....	41
3.4.4	Consolidated Undrained Triaxial Compression Tests with Pore Pressure Measurements (CIU-Strength Tests) .....	42
3.4.5	Oedometer Consolidation Tests .....	47
3.4.6	X-ray Diffraction Analysis.....	47
3.4.6.1	General .....	47
3.4.6.2	Specimen Preparation .....	48
3.4.7	X-ray Fluorescence Spectrometer (XRF) .....	49
3.4.8	Scanning Electron Microscope .....	50
3.4.9	Soil Chemical Analysis .....	51
3.4.9.1	pH Test.....	52
3.4.9.2	Organic Matter Test .....	52
3.4.9.3	Chemical Determination .....	53
3.4.9.4	Sulphate Determination .....	53
3.4.9.5	Cation Exchange Capacity Determination .....	54
4.	<b>SOIL FORMATION AND SOIL DISTRIBUTION</b>	
4.1	Soil Formation and Soil Deposition.....	56
4.1.1	Introduction .....	56
4.1.2	Depositional Systems .....	57
4.1.3	Soil Deposits.....	57
4.1.3.1	Alluvial Deposits.....	58
4.1.3.2	Wadi Deposits.....	60

4.1.3.3	Wind Deposits .....	71
4.1.3.4	Chemical Deposits.....	73
4.2	Soil Distribution .....	78
4.2.1	General Definition and Results .....	78
4.2.2	Soil Profile .....	85
4.2.3	Soil Units.....	95
<b>5.</b>	<b>SOIL COMPOSITION AND SOIL FABRIC</b>	
5.1	Mineral Composition of Soil Samples from XRD Analysis .....	139
5.1.1	Non-clay Minerals.....	141
5.1.1.1	Quartz ( $S_{12}O_3$ )	
5.1.1.2	Calcite ( $CaCO_3$ )	
5.1.1.3	Albite ( $NaAlS_{13}O_3$ )	
5.1.2	Clay Minerals .....	153
5.1.2.1	Clay Mineral Identification .....	154
5.1.2.2	Kaolinite ( $OH_8S_i4Al_4O_{10}$ )	
5.2	Soil Chemical Analysis .....	162
5.2.1	Soil Chemical by Energy Dispersive Spec- trum & X-Ray Fluorescence.....	162
5.2.2	Wet Chemical Analysis .....	167
5.2.3	Dispersive Soil Identification.....	172
5.3	Soil Fabric.....	174
5.3.1	General .....	178
5.3.2	Fabric of Soils .....	178
5.3.2.1	Metastable Fabric.....	187
5.3.2.2	Oriented Fabric of Lean Clay Soils .....	187
5.3.2.3	Clayey Sand Fabric.....	196
5.3.3	Cementation.....	196
<b>6.</b>	<b>SOIL DEFORMATION AND SHEAR STRENGTH CHARACTERISTICS</b>	
6.1	General.....	201

6.2	Consolidation and Collapsing Properties .....	201
6.2.1	Results of Consolidation Tests .....	201
6.2.2	Critical State Results .....	209
6.2.3	Analysis of Results .....	215
6.2.4	Collapsing Soils .....	229
6.2.4.1	General .....	229
6.2.4.2	Qualitative and Quantitative Methods of Predicting Soil Col- lapsing .....	230
6.2.4.3	Mechanism and Settlement of Collapsing Soils .....	237
6.3	Strength Properties .....	249
6.3.1	Introduction .....	249
6.3.2	Results .....	249
6.3.3	Analysis and Correlations .....	266
7.	CONSIDERATION AND SITE IMPROVEMENT .....	279
8.	CONCLUSION .....	293
	REFERENCES .....	296

**APPENDICES:**

- Appendix - A:
- Appendix - B:
- Appendix - C:
- Appendix - D:
- Appendix - E:

## LIST OF TABLES

<u>Tables</u>	<u>Page</u>
4.1 Recognition of water-laid deposits(adopted after Glemmie 1970) .....	72
4.2 Recognition of wind-laid deposits.....	74
4.3 Location of the obtained samples and their classifications .....	82
4.4 Index Properties of the Fine Soils.....	136
4.5 Index Properties and Engineering Classification of Windblown Deposits (after Peck, Hanson and Thurnborn, 1974) ...	137
5.1 Quantitative analysis of non-clay minerals by x-ray diffraction.....	147
5.2 Common non-clay minerals.....	151
5.3 Quantitative analysis of clay minerals by x-ray diffraction...	156
5.4 Cation exchange capacity of different clay minerals (after Joseph E. Powels, 1984) .....	159
5.5 Activities of Various Minerals .....	159
5.6 Chemical composition of granular soil by x-ray fluorescence spectrometer.....	165
5.7 Chemical composition of fine soil by x-ray fluorescence spectrometer .....	166
5.8 Wet chemical analysis of 1:1 extraction .....	168
5.9 Chemical engineering properties .....	169
5.10 Summary of soil fabric .....	200
6.1 Summary of results from one-dimensional consolidation test.....	206
6.2 Interrelated results of one-dimensional consolidation test.....	208
6.3 Critical state parameters results of sandy lean clay	

	calculated from Oedometer test results.....	213
6.4	Oedometer test results in form of critical state .....	216
6.5	Values of $C_c$ and $C_v$ of clay minerals (adopted after Mitchell, 1976).....	221
6.6	Order-of magnitude for permeability $k$ , based on description of soil by Unified Classification, m/s (After, Bowles, 1982) .....	221
6.7	Approximate relationship between total expansion, swelling potential, and plasticity index, (Mitchell, 1976) .....	224
6.8	Typical range of values for Poisson's ratio $\mu$ (Bowles, 1982) .....	227
6.9	Collapsing identification of the different soils of the study area.....	234
6.10	Relation of collapse potention to the Severity of Foundation Problems (after Clemence and Finbarr (1981) .....	239
6.11	Critical state model parameters of the different soils.....	253
6.12	Summary of the consolidated undrained triaxial results of partially saturated soils .....	254
6.13	Summary of the consolidated undrained triaxial results of the saturated soils .....	255
6.14	Typical range of values for the static stress-strain modulus, for selected soils (field values depend on stress history, water content, density, etc.(after Bowqles, 1982) .....	269
6.15	Empirical values for $\phi$ , $D_r$ and unit weight of granular soils based on the standard penetration number with corrections for depth and for fine saturated sands(Bowles 1982) .....	277
6.16	Characteristics of China Loess (after Wu Zhi-hui and Xie Ding-yi, ASCE, 1987).....	278
7.1	Methods of treating collapsible foundation soils (Soil Improvement, ASCE, 1978) .....	283

## LIST OF FIGURES

<u>Figure</u>	<u>Page</u>
2.1 The map of the study area .....	6
2.2 The physiography of main regions in Yemen Arab Republic .....	8
2.3 The geological map of Sana'a area and surrounding areas (adopted from Kruck, W. 1983) .....	13
2.4 Summary of geological formations of Sana'a Plain (Ital Consult, 1973) .....	19
3.1 Flow diagram of investigation program .....	23
3.2 Hand-curved undisturbed sampling .....	31
3.3 Used split spoon sampler in penetration testing .....	36
3.4 The layout of apparatus of consolidated-undrained tests on 1-1/2" diameter samples: with measurement of pore pressure .....	46
4.1 Block diagram of the depositional systems .....	65
4.2 Chemical deposits due to leaching as detected by (a) SEM, and (b) EDS .....	77
4.3 The regions and stations distribution .....	79
4.4 Longitudinal and transfer cross-section .....	86
4.5 Legend of the different soil profiles (Figs. 4.6-6.10) .....	87
4.6 Soil profiles resulted from the longitudinal cross-section A-A .....	88
4.7 Soil profiles resulted from the curved cross-section B-B .....	89
4.8 Soil profiles resulted from cross-section 1-1 .....	90
4.9 Soil profiles resulted from cross-section 2-2 .....	91
4.10 Soil profiles resulted from cross-section 3-3 .....	92

4.11	Bore Log of Station # 34 .....	99
4.12	Gradation curves of well to poorly graded gravel with sand .....	100
4.13	Gradation curves of well to poorly graded sand with gravel.....	103
4.14	Gradation curves of sand and gravel with silty clayey matrix.....	108
4.15	Bore log of Station # 41 .....	109
4.16	Bore log of Station # 37 .....	110
4.17	Bore log of Station # 36 .....	113
4.18	Gradation curves of sandy clay soils.....	114
4.19	Bore log of Station #35 .....	119
4.20	Gradation curves of sand silty soils .....	121
4.21	Gradation curves of sandy silty clay with gravel.....	124
4.22	Trends of gradation and plasticity for loess .....	125
4.23	Bore log of Station # 38 .....	127
4.24	Particle size distribution curves for wind-deposited sediments(adopted after Peck, Hanson and Thurnborn 1974).....	128
4.25	Gradation curve of lean clay soil selected from Station # 38 at 0.7m .....	132
4.26	Gradation curve of clayey sand soil selected from Station # 23 at 4.5m.....	134
5.1	Some standard X-ray powder diagrams.....	140
5.2	X-ray patterns of nonclay minerals of: (a) well to poorly graded sand with gravel, (b) well to poorly graded gravel with sand.....	142
5.3	X-ray patterns of nonclay minerals of: (a) sandy wilt soil taken from 2.5m depth (b) sandy soil taken from 4.5m depth.....	143
5.4	X-ray patterns of nonclay minerals of: (a) lean clay	

	taken from 0.7m, (b) sandy lean clay from 4.0m.....	144
5.5	X-ray patterns of nonclay minerals of: (a) clayey sand soil, (b) silty clayey sand with gravel .....	145
5.6	X-ray pattern and standard powdered diagrams of sandy silty clay with gravel Station # 38 at 20m .....	146
5.7	Cementation agents of calcium carbonate in form of (a) calcite with bulky form, Station 40 at 2.5m and (b) aragonite with needle form, Station # 41 at 2.0m.....	152
5.8	X-ray patterns of clay minerals.....	155
5.9	Heating effects on clay minerals identification.....	157
5.10	Kaolinite composition (a) SEM of kaolinite of air-dried specimen of sandy silty clay with gravel, vertical fracture, (b) schematic of kaolinite structure, (c) EDS-composition .....	161
5.11	Different forms of some chemical elements along with their EDS, (a) calcium, (b) manganese, and (c) iron oxide.....	163
5.12	Relationship between dispersibility (susceptibility to colloidal erosion) and dissolved pore waters salts based on pinhole tests and experience with erosion in nature (from Sherard, Dunningan, and Decker, 1976).....	175
5.13	Soil Fabric .....	177
5.14	(a) Loess microstructure of air-dried, vertical section, sandy silt, Station 33 at 1.8m, (b) EDS-spectrum of the loess specimen shown in (a).....	179
5.15	(a) Metastable fabric of sandy silt, loess soil, (Station # 33, at 1.8m), (b) schematic representation of particle assemblage (Collins and McGown, 1974) .....	180
5.16	(a) Microstructure of clothed silt and sand particles of undisturbed sample, air-dried and vertical section, (b) ED-spectrum, Station # 33 at 1.8m .....	182
5.17	(a) Loess microstructure of air-dried, vertical section, sandy silt, Station # 33 at 1.8m, (b) ED-spectrum of the loess specimen shown in (a).....	183
5.18	Open fabric of clothed granular interaction type .....	185

5.19	(a) Honeycombed open fabric structure of sand silts, loess deposit, Station # 33....., (b) Structure of open fabric after Casagrande (1932) and Mitchell (1976) .....	186
5.20	(a) microstructure of clay buttress selected from Station # 26 at 2.0m, (b) schematic of the fabric after Dudley, 1970 and others.....	188
5.21	(a) Scanning electronic microscope of flocculated face to face clay structure, (b) EDS of flocculated clay bonded by calcite and kaolinite .....	189
5.22	Oriented structure, close-packed of lean soils .....	190
5.23	High clay precipitation within silt particles .....	191
5.24	(a) Well oriented face to face aggregation with edge to edge of sandy lean clay soil, Station # 38 at 4.5m, (b) Layering in face of lean clay, Station # 33 at 0.7m .....	193
5.25	Structure fabric of lean clay, Station # 33 at 0.7m (a) Scanning Electronic Microscope of air-dried undisturbed sample, (b) EDS of lean clay soil .....	194
5.26	Microstructure of clayey sand, Station # 23 at 4.5m, (a) SEM of air-dried, vertical section of undisturbed sample, (b) EDS of clayey sand .....	197
6.1	e-Log $\sigma'_v$ curve of sandy silt soil selected from Station # 40 at 2.5m.....	202
6.2	e-Log $\sigma'_v$ curve of sandy silty clay with gravel selected from Station # 38 at 2.0m.....	203
6.3	e-Log $\sigma'_v$ curve of silty clay sand with gravel selected from Station # 41 at 2.0m.....	204
6.4	Coefficient of permeability k from time-compression curve (after Sandbakken and Lacasse, ASTM 892, 1986).....	210
6.5	v-lnp space of the sandy silty clay with gravel (Station # 38 at 2.0) .....	214
6.6	v-lnp space of the silty clay sand with gravel (Station # 41 at 2.0) .....	214

6.7	e-Log $\sigma'_v$ curve of lean clay soil selected from Station # 33 at 0.7m .....	
6.8	Classification chart for swelling potential (Mitchell, 1976).....	223
6.9	Collapsible and noncollapsible loess (Clemence, 1981).....	233
6.10	Collapsing potential as resulted from the oedometer test (sandy silt Station # 42 at 1.3m).....	238
6.11	Settlement calculation from double oedometer test: (a) normally consolidated soil; (b) overconsolidated soil (Clemence, 1981) .....	244
6.12	Double Oedometer Test of sandy silt soil (Station # 42 at 1.3m) .....	246
6.13	Calculation of collapsing settlement by using Double Oedometer Test.....	247
6.14	Stress strain relation of the sandy silty clay with gravel (Station # 38 at 4.0m).....	251
6.15	Stress strain relations of the sandy lean clay soil (Station # 26 at 4.0m).....	256
6.16	Stress path of the lean clay soil.....	257
6.17	Stress path of sandy silty clay soil with gravel in terms of (a) $q'$ vs. $p'$ , and (b) $v$ vs. $p'$ .....	260
6.18	Mohr's circles and failure envelopes in terms of (a) total stress, (b) effective stress .....	261
6.19	Partially saturated and fully saturated Mohr's envelope.....	262
6.20	Mohr envelope boundaries of the different soils for both natural and saturated conditions.....	264
6.21	Mohr envelope boundaries of the different soils in terms of the effective stress.....	265
6.22	Upper and lower boundaries of Mohr envelopes of loess under different moisture and densities .....	271
6.23	Ranges in effective stress failure envelopes for pure clay minerals and quartz (Olson, 1974) .....	274

7.1 Continuous strip footing in collapsing soil: (a) continuous in one direction with load bearing beam, and (b) continuous in two directions .....286

7.2 Effect of densification in reducing the collapsing potential tendency .....290

## LIST OF PLATES

<u>Plate</u>	<u>Page</u>
3.1	Block sampling from excavated trench having different levels in one of the sides while the other side was kept vertical. Sample was taken from 4.5m below the ground surface .....28
3.2	Block sampling from excavated trench at 1.8m depth, the level of the first berm .....30
3.3	Auger drilling and SPT testing by the tractor-mounted rig .....24
3.4	Resampling from the block sample by thin tubes through guide plates .....43
3.5	Jacking and trimming process .....44
4.1	The upper fan portion (Apex) at the base of Asser Mountain in the Western part of the study area .....61
4.2	Bed stream deposits .....62
4.3	The imbricated pebbles formation in granular soils .....63
4.4	Cross-stratification of water-laid deposits .....64
4.5	Granular soils of graded bedding form. The gravity soil in the bottom, while sandy soil is in the top. Indicated scale is 13 cm .....68
4.6	The reported layering system of water and wind-laid deposits as found in Wadi Area. Loess, wind-laid, interbedded by imbricated water laid deposit. Indicated scale is 13 cm .....69
4.7	Coarse-grained Minderbelt as shown in: (a) southern part and (b) central part of the study area.....70
4.8	Vertical root holes in the wind deposits, loess soil .....75
4.9	The pithole station.....80
4.10	Relative regular soil profile: (a) longitudinal section, (b) vertical section .....94

4.11	Conglomerates of sand, silt and fine particles interaction...	106
4.12	Light brown sandy silt layer interrupted by silty clayey sand with gravel. Indicated scale is 13 cm .....	118
4.13	Micro fissures and joints of lean clay soil .....	130
4.14	Occurance of the Tuff volcanic soil at surface in Hada Region.....	135
4.15	Different studied soils: (a) dark stiff lean clay, (b) redish to light brown loess, (c) cemented gravelly sand with silty matrix and pebbles, (d) stiff brown sandy clay, (e) sandy silty clay with sharp cemented gravel of sand stone, and (f) granular colour and form variations ...	138
5.1	Inspected erosion of top layers of an open excavation .....	171
6.1	Failure on masonry bearing wall of one floor building resting on the expanding lean clay, 'Merriah' .....	228
6.2	Collapsing in cementation agent of the sandy silt, loess as detected from oedometer test by SEM.....	241
6.3	Two failure types of triaxial compression specimens .....	268
6.4	Both grain to grain content and leaching of cementing agents at failure as detected by SEM, from the failure surface of triaxial specimen.....	275
7.1	Cracks on a reinforced concrete wall of one floor building resting on surficial collapsing soil in Hada Region.....	288

## ABSTRACT

FULL NAME OF STUDENT: AL-GASOUS KHALED ABDALLAH

TITLE OF STUDY: GEOTECHNICAL PROPERTIES OF THE  
SURFICIAL SOIL OF SANA'A, THE YEMEN  
ARAB REPUBLIC

MAJOR FIELD: CIVIL ENGINEERING (GEOTECHNICAL)

DATE OF DEGREE: June, 1988.

There is paucity of geotechnical information about the surfical soil of Sana'a region. Therefore, this study is aimed at filling this gap by studying in detail the engineering properties of Sana'a soil.

The geotechnical properties of the surficial soils of an area of about 100 km<sup>2</sup> in Sana'a region, the capital of Yemen Arab Republic were investigated. The study consisted of both field and laboratory investigation programs.

In the field investigation program, 32 locations were selected for the classification and inspection tests. Based on the obtained results, ten additional stations were selected for carrying the standard penetration test and for studying the geotechnical properties in more detail by carrying out specific tests.

The laboratory testing program included classification tests,

strength tests (consolidated undrained triaxial test), one dimensional consolidation tests, X-Ray Diffraction analysis, X-Ray Fluorescence analysis, Energy Dispersive Spectrum, Scanning Electron Microscope analysis and chemical analysis. Based on these investigations, seven different soil units, resulting mainly from both alluvial and wind depositional systems, were also identified. Depositional systems and soil distribution were identified. Soil profiles have been prepared. Soil composition, soil structure and engineering properties including index properties, strength properties and deformation characteristics were established.

Preliminary analysis indicated the existence of both collapsing soil, loessial soil and expansive soil, top layer. Appropriate design considerations for the expected moisture conditions, suitable foundation implementation and finally potential improvement techniques of the soil in the region were drawn.

**MASTER OF SCIENCE DEGREE**

**KING FAHD UNIVERSITY OF PETROLEUM AND MINERALS**

**Dhahran, Saudi Arabia**

**June, 1988.**

( الخلاصة )

الاسم : خالد عبدالله حسن القصوي  
عنوان الدراسة : الخواص الهندسية للتربة السطحية لمدينة صنعاء /  
الجمهورية العربية اليمنية .  
التخصص : هندسة مدنية .  
التاريخ : يونيه ١٩٨٨م

تعتبر المعلومات المتوفرة عن الخواص الهندسية ( هندسة التربة والاساسات ) لمنطقة صنعاء قليلة جدا لعدم وجود دراسات سابقة في هذا المجال، وعليه فان هذه الدراسة تهدف لسد هذه الفجوة وذلك بدراسة الخواص الهندسية لتربة صنعاء بالتفصيل.

لقد تم بحث ودراسة الخواص الهندسية للتربة السطحية لمساحة ١٠٠ كم مربع في منطقة صنعاء عاصمة الجمهورية العربية اليمنية. اشتملت هذه الدراسة على دراسة معملية ودراسة ميدانية. وقد اشتمل البحث الميداني على اجراء اختبارات بصرية واختبارات التصنيف وذلك على ٣٢ موقع . وبناءا على نتائج هذه الاختبارات ، تم اختيار عشرة مواقع اخرى اضافية وذلك لاجراء اختبار الاختراق القياسي والحصول على العينات التمثيلية النهائية والتي تم استخدامها في دراسة الخواص الهندسية بالتفصيل وذلك باجراء اختبارات خاصة.

وقد اشتملت الدراسة المعملية على الاختبارات التالية :

( التصنيف ، القوى ، الانضغاط الراسي المحيط ، الاشعة السينية الانتشارية ، تشتت الطاقة بتفلور الاشعة السينية ، المجهر المسحي الالكتروني وبعض اختبارات التحليل الكيميائي .

بناءا على نتائج التحاليل والاختبارات السابقة ، تم تحديد سبعة أنواع رئيسية مختلفة من التربة ناتجة من الترسيب المائي وترسيمات الرياح ( اللويس ) . كما تم تحديد نظم الترسيب وتوزيع التربة . لقد تم بيان التوزيع الراسي في صورة قطاعات طولية وعرضية . التركيب المعدني والتكوين الحبيبي والخواص الهندسية مشتملة على خواص القوى والتشكل تم تحديدها ووضعها في صورة جداول ومنحنيات واشكال.

لقد أوضح التحليل البدائي من هذه الدراسة على وجود كلا من التربة الانهيارية ( تربة اللويس ) والتربة التمددية السطحية . اعتبارات التصميم لحالات الرطوبة المختلفة والاساسات المناسبة تم اقتراحها مع ايضاح طرق التحسين الفني الضروري للتربة في المنطقة .

درجة الماجستير في العلوم  
جامعة الملك فهد للبترول والمعادن  
الظهران - المملكة العربية السعودية

يونيه ١٩٨٨م .

٢٥

## Chapter 1

### INTRODUCTION

#### 1.1 General

Yemen Arab Republic lies along the southern western part of the Arabian Peninsula. Sana'a the capital of the Yemen Arab Republic, whose population is about one million is the oldest, biggest and the most important city in the Republic. This population is about five times the population before 1962. Since 1962 great development and expansion in construction has taken place. The area that has been occupied by the new construction since 1962 is about three times the area of the old Sana'a city in 1962. Because Sana'a area is partially surrounded by mountains, this great urban development in construction has occurred over a limited area leading to the construction of multistory buildings in order to provide sufficient number of housing units.

In Yemen, combinations of different structural systems are the predominant types of structures for multistory buildings. Masonry and/or stonewall are often deployed with reinforced concrete in the same structure; either side by side or on top of one another. This practice requires extreme care in design and construction to safeguard against differential settlement which could jeopardize the safety of structure.

This recent upsurge in construction activities joined with limited local design, specifications and construction experience have placed great demands on the engineering and building construction community in the Yemen Arab Republic to establish the needed engineering design guidelines. An important design guidelines is a rational guidelines for foundation design with appropriate geotechnical parameters satisfying safe and economic design of a specific structure. To satisfy such need, pertinent geotechnical information and parameters should be compiled to serve as data base.

Available information on geotechnical data and characteristics for the Sana'a area are almost non-existent. Most of the available information are in terms of geologic profiles, maps and water well data, and can not be labeled as geotechnical per say. It is evident that there is paucity of geotechnical information about the soil of Sana'a region. This study is aimed at filling this gap by studying in detail the engineering properties of surficial soil of the Sana'a area down to 6.0 m below the ground surface.

## 1.2 Objective and Scope of the Study

The present research addresses the geotechnical properties of the surficial soils of Sana'a, the Yemen Arab Republic, and attempts to provide useful geotechnical data on Sana'a soils

Specifically, the objectives of this study are:

- 1) To identify and classify the surficial soils horizontally and vertically;
- 2) To study the stress - strain - strength behaviour of the surficial soils by triaxial tests;
- 3) To obtain compressibility parameters and stress history of selected samples using one dimensional consolidation theory;
- 4) To study the mineralogy of the surficial soils using - X-ray diffraction and X-ray fluorescence techniques;
- 5) To determine organic content and chemical composition by running selected chemical tests
- 6) To study the soil fabric by using Scanning Electronic microscope (SEM); and finally
- 7) To reduce and analyze the obtained data to draw appropriate conclusions for suitable foundation implementation and potential improvement techniques of the surficial soil in the region.

in;.of;.il 5 The present study include both field and laboratory testing programs. In the field program the site exploration and inspection were carried out on pit holes and excavations. Out of these locations 42 representative pit holes were selected from which all tested samples were obtained. Finally, Standard Penetration test was carried out on 8 out of the 42

locations. From these 8 locations both disturbed and undisturbed samples of block type were obtained for laboratory testing program. This last program included both specific and general tests. These tests are consolidated undrained triaxial tests of both saturated and partially saturated samples, consolidation tests, classification tests, engineering properties tests, Chemical and mineral composition determination using X-Ray diffraction, X-Ray flourances and chemical analysis techniques and finally; scanning electronic microscope tests of undisturbed samples.

The data obtained from the above investigation were analyzed. The appropriate conclusions for soil deposition and distribution, soil composition and soil fabric, shear strength and deformation parameters, suggested suitable foundation implementation and potential improvement techniques of the sub-soil in the region were drawn.

## Chapter 2

### PHYSIOGRAPHY AND GEOLOGY

#### 2.1 General

##### 2.1.1 Location

The study area, Sana'a, lies in a plain, which exists among the high mountain region in the Yemen Arab Republic. It is located between latitudes  $15.17^{\circ}$  N, longitude  $44.10^{\circ}$  E, and  $15.25^{\circ}$  N, longitude  $44.14^{\circ}$  E with an elevation of 2300 m above sea level. It is bounded by Iyban, Nogum and Al-Nahdien mountains on west, east and south respectively. Al-Rawdah town and Sana'a International Airport bounded the area on north(Fig.2.1). The study area is about 100 square kilometers, which is about the fifth of the total area of the plain. The southern part of the study area is little higher than the northern part which is the slope direction (0.4%)

##### 2.1.2 Climate

The climate of Sana'a area is characteristic of semi arid climate (Agha, S.; 1984). The temperature of the study area highly fluctuated not only from season to season but also during a day. A daily maximum temperature of  $32^{\circ}$  C in June and a minimum temperature of  $3^{\circ}$  C in December were recorded. The variation in temperature from midnight to midday reached  $18^{\circ}$  C (Italconsult, 1973).

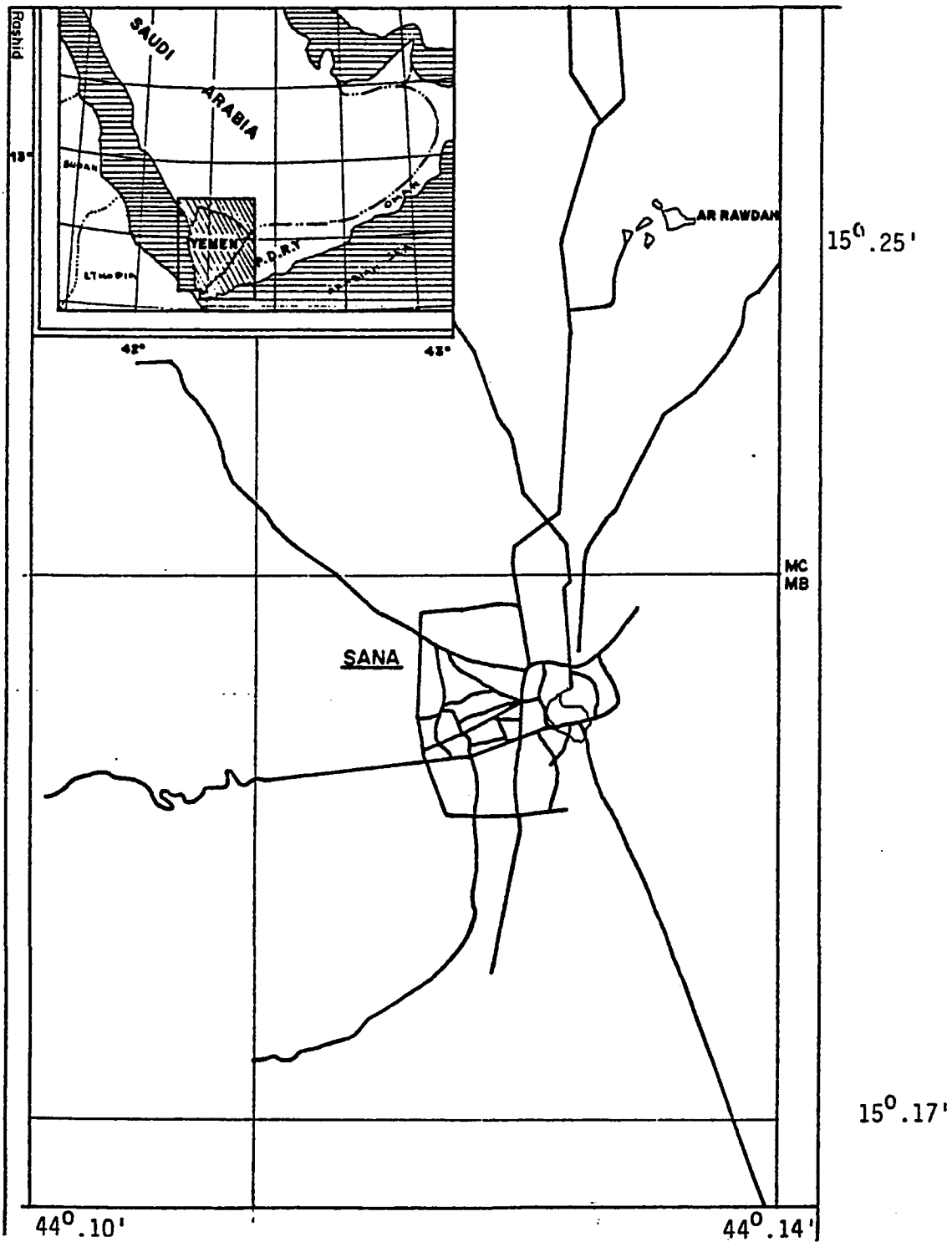


Fig. 2.1 : The Map of the Study Study Area, (adopted from Survey Department, Y.A.R., 1980).

The rainfall in Sana'a is seasonal with annual recorded of about 200-300 mm. It rains mainly in the summer season, but in some years it rains also during spring. About 2000 meter above the sea level the annual rainfall is less than the rate of evaporation which reaches 1500-2000 mm per year at the same level. The predominant and controlling wind in the study area is the northern wind due to the mountains which bounded the area from the west and the east (Agha, S., 1983).

## 2.2 PHYSIOGRAPHY

During the past millions of years the tectonic movements of Red Sea rift and high mountains creation have gradually affected the geological and tectonic feature of the Yemen Arab Republic (Y.A.R.) as a part of the Arabian Peninsula resulting in the present physiography of the country.

Physiographically, the Y.A.R. can be divided into five main regions (Fig.2.2). These regions from west to east as listed below are (Kings, J. and Abu Ghanem, 1983):

- 1) The Western Plain (Tihama Coastal Plain)
- 2) The Wester Slope (Red Sea Escarpment)
- 3) The Yemen Highlands (The central high mountains)
- 4) The Eastern Slope

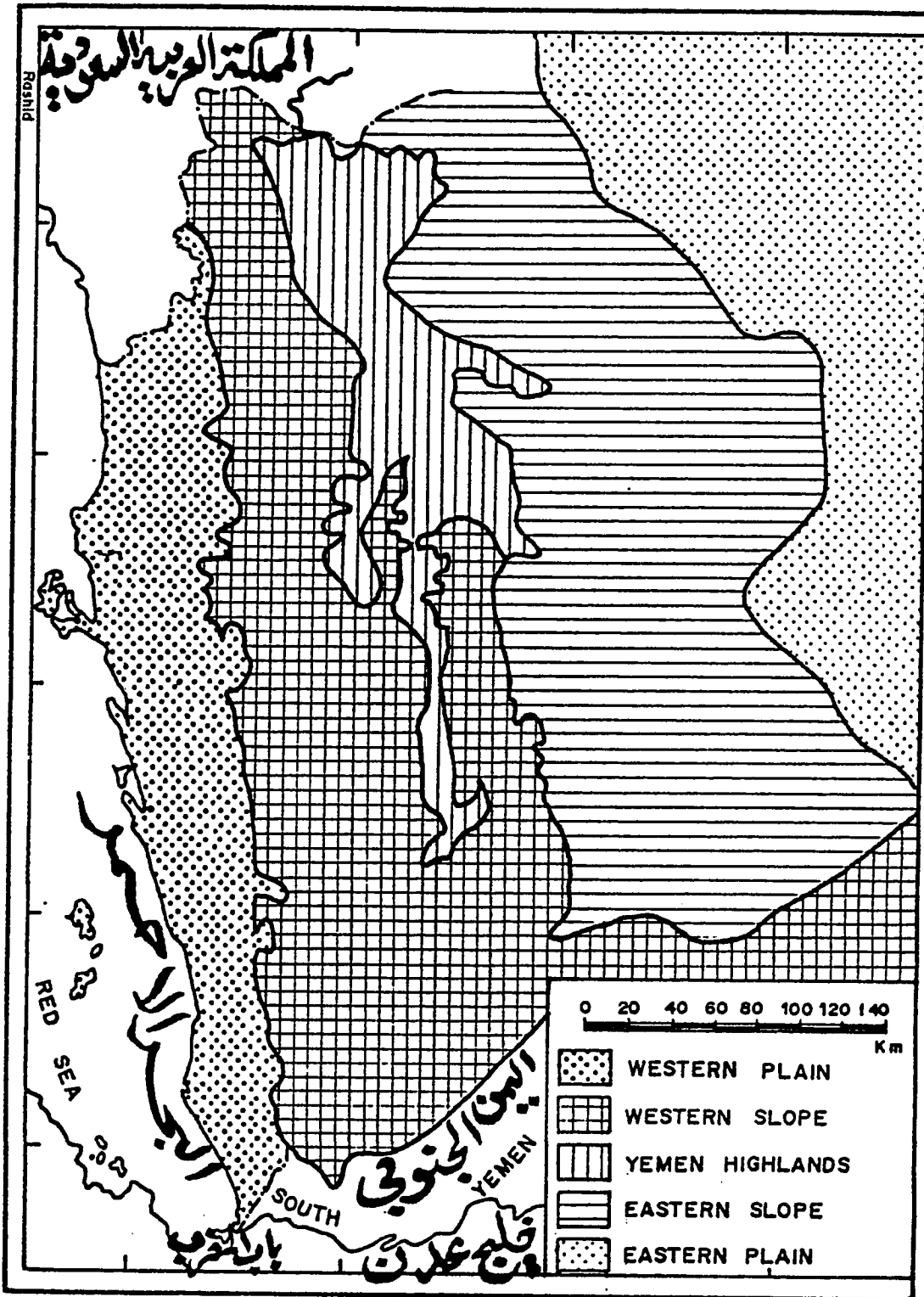


Fig. 2.2 : The Physiography main regions in Yemen Arab Republic. (After Mustafa, I., 1985).

##### 5) The Eastern Plain (including Wadi Al-Gawf)

The Highlands (high mountains) in Y.A.R. lie in the central part of the country with an elevation that varies from 1500 to 3800m and varies in width between 40 and 200 km. They extend from north to south and are parallel to the Red Sea coast (El-Anbaawy, 1985). These Highlands region are characterized by plains and complex topography. They occupy the west flank of a horst which lies between the Red Sea graben on the west and the Arabian Desert on the east (Geukens, 1966).

A great variation in the types of rock exists within this region such as Precambrian rocks, marine Jurassic rocks and Quaternary volcanic rocks. This region contains a series of high plains separates the discontinuous mountains in the region. These plains which extend from south to north, are Dhamar-Yerim, Sana'a, Amran and Sadah plain. They are filled with alluvium soils which are derived from volcanic debris (El-Anbaawy, 1985). Dhamar-Yerim plain is characterized by having calcareous silty soil, while Sadah and Sana'a plains are characterized by coarser alluvial deposits (Kings, J. and Abu Ghanem, 1983).

The present study area is located among the central high mountains on Sana'a basin with an elevation of 2300 meters above the sea level while the surrounding mountains rise 750 meters above the level of the plain (El-Anbaawy, 1985). Sana'a plain as other plains is covered with either fluvial, eolian or volcanic deposits

(Geukens, 1966).

The morphology of Sana'a Basin is characterized by flat tabular forms with deeply entrenched valley. It seems that the morphogenesis is quite recent occurring during the Quarternary. Quarternary rocks are of two types: Quarternary sediments and basalt volcanics with thickness varies from almost non existence to 300m (Italconsult, 1973).

The study area is filled by the alluvium deposits which carried through the scattered valleys (Wadis) around Sana'a region. "The southern part of Sana'a plain became a terrace by capture of the Wadi Walan tributaries. In other places, the plateaus are cut by faults which form depressed areas and appear as alluvium-filled valleys - notably the plains of Sana'a, Amran, Sadah and others" (Geunkens, 1966). Many of the valleys, were depressions due to the effects of faults and then reformed by the water floods action. Such as Wadi As Sair in the northern part of Sana'a and Wadi Ghayman in the southern part of the study area. The water flood plays a predominant factor in driving the quartz, lighter mica, calcium carbonate and silt-clay materials to fill Sana'a plain. Also the aeolian soils are carried out from nearby mountains and the far away deserts by wind action (Rub-al-Khali) (Agha, Sh. G., 1983).

The stratigraphy sequence of the study area, as a part of Sana'a Plain, includes both Tertiary Trap Volcanic series (Yemen Volcanics) and Quarternary sedimentaries and volcanic rocks. The

former one is surrounding the study area except from north, while the last one exists within the study area. The Quarternary volcanic rocks occur in terms of basaltic flow and cones such as Jabal Al-Nah-dyn and Dhahban while the Quarternary sediments occur as Wadi, washplain sand and basin alluvium (Italconsult, 1973 and W. Kruck, 1983).

## 2.3 Geology

### 2.3.1 General Geology

The Yemen Arab Republic (Y.A.R.) constitutes a part of the original Arabian Peninsula which is a part of Precambrian Arabian Nubian Massif. As a result of that the geology of Precambrian of Y.A.R. and its tectonic map are directly related to the tectonic history of the Arabian Shield (El-Anbaawy, 1985).

"Tectonic movements, resulting in faulted domes, affected especially the central part of the country, (in which the study area lies) where Jurassic and Cretaceous beds were removed by erosion at the beginning of the Tertiary" (Geukens, 1966). During most of the Tertiary the

vulcanic activity began and spread widely (mainly during the formation of the Red Sea Rift). In the Quarternary, vulcanic materials were distributed over whole country; large area of basalt flows and many craters characterize the central part of Yemen (Geukens, 1966).

### 2.3.2 Stratigraphy

Stratigraphically, the Sana'a Basin, together with the whole of Yemen, particularly since the Mesozoic sediments, shows a great affinity to the rest of the Arabian Peninsula, (Italconsult, 1973).

The subsurface stratigraphic sequence outcropping in the large Sana'a Plain including the study area ranges from Jurassic to Quaternary. The stratigraphic sequence can be divided into three major groups:

- Sedimentary rocks formations of Paleocene and Mesozoic
- Tertiary trap volcanic series (Yemen Volcanics)
- Quaternary sedimentary and volcanic rocks.

The geological map of the study area and surrounding areas (Fig.2.3) shows the distribution of the above formations (Italconsult, 1973). The descriptions of these formations based on Italconsult (1973), J. King and Abu Khanem (1983), Grolier and Overstreet (1978), Geunkins (1966), El-Anbaawy (1985) are as follow:

#### Group (1): Sedimentary Rocks Formations

There are three sets of sedimentary rocks in Sana'a Basin that are surrounding the study area:

- 1) *Jurassic, Amran Formation*: This formation bounded the study area mainly from the north and partially from north west. Grolier and Overstreet (1978) described this formation as consisting of limestone, marl and shale that are

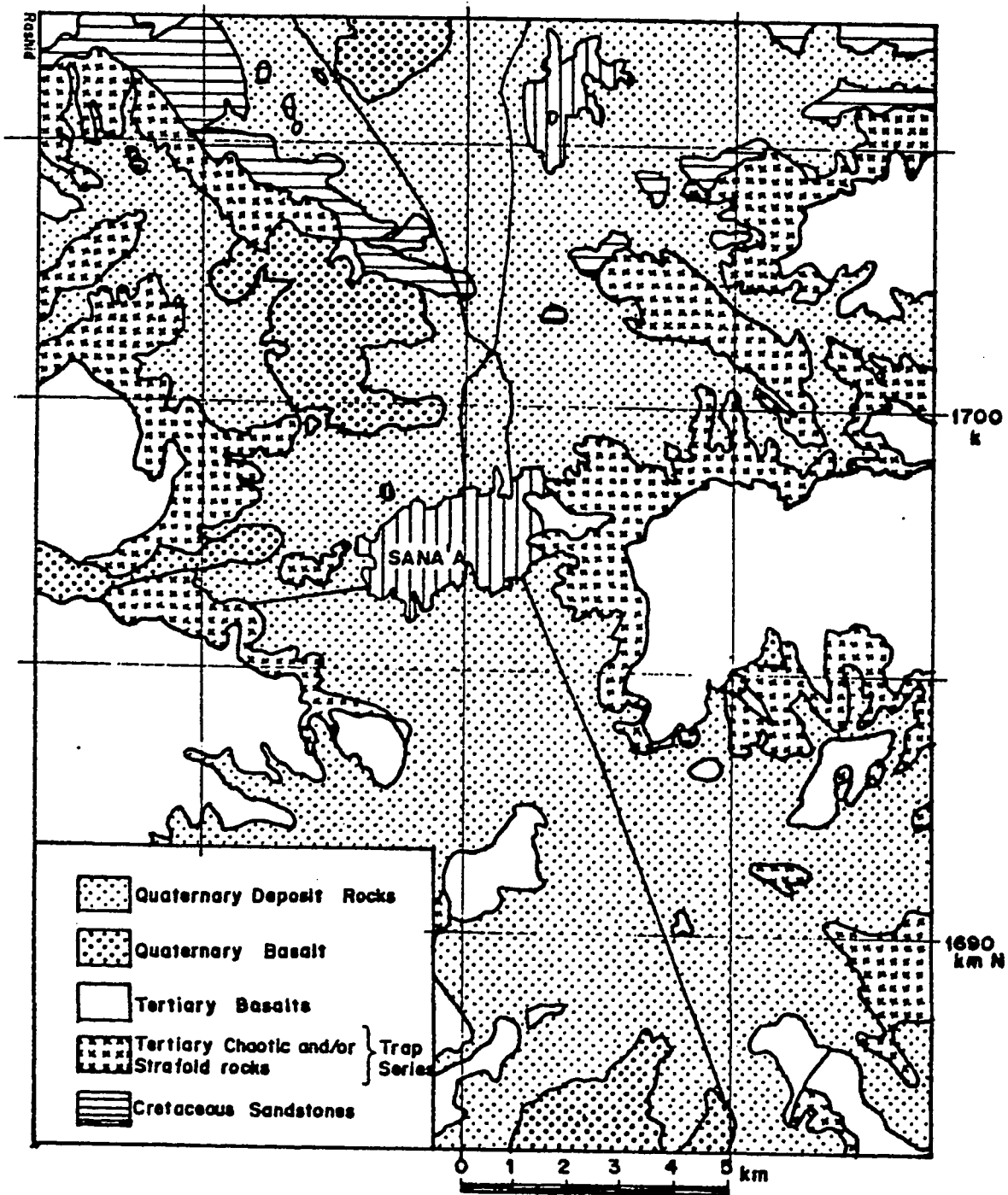


Fig. 2.3 : The geological map of Sana'a area and surrounding areas (adopted from Kruck, W., 1983).

overlain by gypsum, clay, marl, shale and sandstone. Amran formation, about 300m thick, is underlain by a thick layer of Jurassic sandstone (Khawlen formation).

- 2) *Cretaceous, Tawilah Formation (Tawilah Sandstone)*: Twailah formation is exposed north, east and west of Sana'a along the outer border of the Yemen Volcanics to east, Fig. (2.3). The total thickness reached about 370m underlain by the Jurassic-Lower Cretaceous shale formation. Geukens (1966) described Tawilah Formation as consisting of white coarse-grained containing conglomeratic layers of rounded or subangular quartz fragments and interbedded red sandstone. Hematite nodules are found where this formation is in contact with Trap Series (Yemen Volcanics). Layers of clay stone, silt stone and ironstone (2 - 3 m) are found in interbedded layers with coarse materials (Italconsult).
- 3) *Paleocene, Medj-zir Formation*: The Medj-zir formation as Tawilah Formation consists of sandstone with locally fossiliferous, calcareous sandstone and shale along the base while the upper part consists of sandstone locally rich in hematite. The separation between these two formations can not be achieved on the basis of stratigraphic relations or reflectance (Grollier and Overstreet 1978). This formation is exposed north-east and north-west of Sana'a and also north of Al-Rawdah north boundary of the study area.

### Group (2): Tertiary, Trap Volcanic Series (Yemen Volcanics)

This group covers almost one-quarter of the Y.A.R. "The Yemen Volcanics are bedded alkalic flows and pyroelastic rocks including rhyolite, comendite, pantellerite, andisite, basalt and ankaramite with interbedded lenticles of fluvitile and locustrine sand, clay and shell; locally contains fresh water oligocene-miocene fossils", (Glorier and Overstreet, 1978). The upper surfaces of many volcanic beds weathered to reddish paleosols; a few centimeters to a few meters thick. "The Yemen Volcanics are commonly altered to chlorite, calcite and zeolite" (El-Anbaawy, 1985).

Italconsult(1973) divided the Yemen Volcanics into two groups. the Basal Basalt and Stratoid Volcanics. The Basal Basalt exists in the study area with a maximum depth of about 220m and occurs as blocking greenish black dense basalt, frequent quartz geodes and scattered lenses and sheets of trachyte and rhyolite. The stratoid volcanic rock consists mainly of alkalic flows and pyroelastic rocks. They include rhyolite, comendite, pantellerite, trachyte, andesite, basalt and ankaramite besides a large variety of tuffs of different colors. They are exposed with a maximum thickness of about 300m around Sana'a, (Italconsult, 1973 and El-Anbaawy, 1985).

### Group (3): Quarternary Formations:

Various Quarternary rocks laid down over the formations discussed before. The Quarternary rocks are mainly of two types:

Quarternary sedimentaries and Quarternary basalt volcanic s.

**A) Quarternary Sedimentaries:**

Quarternary sedimentaries occur widely in Sana'a Basin covering whole study area. They occur in the form of valley-fill or raised terraces as they are in the southern part of Sana'a region. The Quarternary deposit which mostly covers the area under study is really the point of interest and the fundamental guidelines for the present study as a geological informations.

Quarternary alluvial deposits in Yemen are divided according to the transportation mode, into aeolian (wind-laid) and fluvial (water-laid). The aeolian deposits are either loess deposits or dunes deposits. The inter-mountain plains are subjected to the loess deposits which have been reworked by alluvial processes. The fluvial deposits are either alluvial fans, such as in the bottom of mountains, or alluvial plains as in case of flat area. Alluvial fans are characterized by coarse-grained material, while alluvial plains are characterized by finer sediments, (Kings, J. and Abu Ghanem, 1983).

The most recent Quarternary deposits, present in the flatter lying parts of Sana'a plain and the surrounding plateau, as well as on the man-made terraces, consists of loess-like light brown silts with thickness reaching several meters (Italconsult, 1973).

"The Quarternary sediments consists of an alternation of coarse and very fine horizons. The former are composed of silty sandy

gravel with boulders that range upward to 50 centimeter in diameter of light brown to light greenish white color. The layer thickness of individual coarse material can be 10-15 meters or more, while the interbedding of finer material - light brown silt or sandy silt - are only a few meter thick. Indeed, beds of clean sand and gravel are quite rare. Instead, clayey silty matrix is almost always present (Italconsult, 1973).

Kruck (1983) described the Quarternary deposits in the study area as Wadi-wash plain sand and basin alluvium, while Grolier and Overstreet (1978) described it as "alluvial gravel, sand and silt on the river terraces and fans adjacent to and higher than the flood plains of present-day streams; generally dark; may include colluvium at base of foothills".

The thickness of Quarternary deposits in the southern part of the study area varies from several meters to over 300 meters in the north boundaries. In some locations in the south, the bed rock exists without a cover of Quarternary deposit.

#### ***B) Quarternary Basalts:***

Basalts of Quarternary to subrecent age occur widely in the western and north western parts of the Sana'a Basin. Various photographic types have been recognized so far: basalt, augite basalt, nephetime basalt, veiscular basalt, scoriaceous basalt and basalt tuffs which occurs around eruption cones.

The thickness of the basalt is difficult to achieve especially in the place where volcanic activity has been greatest. However, the thickness may amount to a several hundred meters especially in the locations where the flows have filled earlier the morphologic depressions (Italconsult.1973).

Various generations of basalt flows are distinguishable from the degree of erosion point of view. Some flows are deeply incised by valleys, while no erosion at all can be recognized on some flows and cones. The latest flows cover the present surface of Sana'a Plain, particularly near the mountains. "The only sedimentary deposits which cover the Quarternary basalts are the loess-like silt", (Italconsult, 1973) and the notable alluvial deposits (gravel-sand-silt and clay). In some locations there is no cover at all and the surface of the flow basalt is rough and broken.

The earlier formations have greatly affected the deposits of the study area. The composition and mineralogy of the sub soil of Sana'a area are greatly related to the composition and mineralogy of these formations. The physical processes of weathering play a predominant role in this coincidence. Fig. (2.4) shows the summary of the previous formations and their thicknesses, geological age and their descriptions.

SYSTEM	SERIES	FORMATION	GEOHYDROLOGIC UNITS	LOG	APPROXIMATE THICKNESS	DESCRIPTION	WATER BEARING PROPERTIES	DRILLING AND CASING CONDITION
QUATERNARY	PLEISTOCENE-RECENT	BASALT	BASALT AQUIFERS		0 -> 300m	Loose. Sandy clay with gravel and boulders. Coarse terrace gravel. Basalt cones and lava flows	Water yielding. Usually low permeability. Only at scattered points good yield from alluvium. Good water yield from basalt in springs and wells due to fracturing.	In alluvium frequent boulders; casing particularly above water level. Requires screen but probably no gravel-pack. Clogging problems when drilling with mud.
		ALLUVIUM	VALLEY-FILL AQUIFER			Well stratified ignimbrites (?) and tuffs with some lava flows. Mostly rhyolitic (?)	From perched groundwater bodies locally water yielding. Springs emerging near the base, some with considerable discharge.	
TERTIARY	EOCENE TO MIOCENE	TRAP VOLCANICS						
		CHAOTIC AND STRATOID ROCKS			0 -> 500m	Black basalt and light-coloured rhyolite. Lava flows chaotically intermingled.	Not water yielding.	Formations not drilled.
		STRATOID ROCKS			0 -> 100m	Well stratified tan, red and green ignimbrites and tuffs with interbedded fluvio-lacustrine layers.		
		BASAL BASALTS	TRAP BASAL BASALTS		0 -> 300m	Greenish black basalt with a few trachytes (?) lenses. Frequent quartz geodes in some horizons.	Water yielding due to intense fracturing of the whole formation, permeability, however, is generally low.	Sometimes loss of circulation encountered. No casing and/or screens required.

Fig. 2.4: Generalized stratigraphic section of Sana'a Plain (Ital Consult, 1972).

IF UNCONSULT

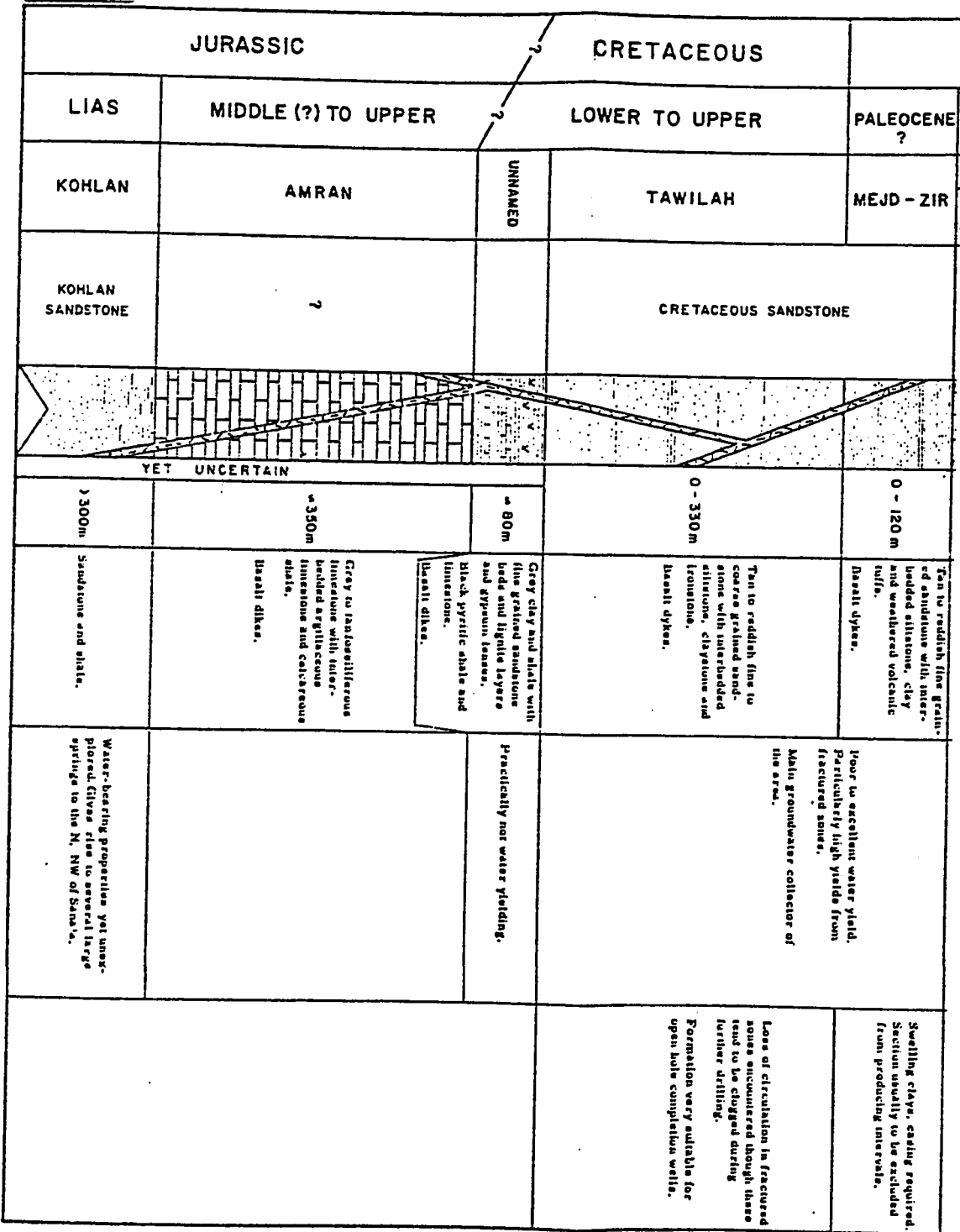


(Fig. 2.4 continued)

### 2.3.3 Structure

Structurally. Sana'a Basin has not been subjected to much upward ground movements. In spite of the notable intensity of the tectonic movements which started during the Paleogene and continued until the Quarternary, the movements are more of a regional nature involving few dislocations of a local character. The vertical movements on Sana'a Plain itself are of a minor magnitude with respect to those of the escarpments which onto the Red Sea (the western slope region). The structure of Sana'a Basin is of a local style which retains its tabular form. The dips acquired are always very low, 2° to 3° at maximum (Italconsult, 1973).

Concerning the most restricted area of Sana'a Basin, tectonic movements occurred in three forms: broad radius folding, dislocation along faults, and fracturing.

Within the study area a very gentle and broad radius folding is presumed to be a large anticline with MS axis along the main valley. On the other hand, faults are generally striking NNW, SSE. On the SW of the study area in Hada zone, one of the most important faults is recognizable. The maximum vertical throw is more than 200 meters, while the other faults are smaller ones. The last and the most important structural phenomenon is fracturing, particularly from the hydrological aspect. Fracturing is divided in a non-uniform manner. One of the most fracturing zones exists in NW from Dhahban to Wadi Dhahr, where the Cretaceous sandstones outcrop (Al-Anbaawy, 1985, Italconsult, 1973).

## Chapter 3

### METHODS OF INVESTIGATION

#### 3.1 General

The investigation program of the sub-soil of the study area included both field investigation and laboratory testing. The field investigation program includes exploration study, sampling, and in-situ testing, while the laboratory testing program includes classification tests, compressibility tests, shear strength tests and chemical analyses test. Fig. 3.1 shows a schematic diagram of the investigation program. The following sections in this chapter describe these methods of investigation.

#### 3.2 Field Investigation

The field investigation program started with studying the available information dealing with the study area involving the site observations. Then, thirty two (32) locations were selected within the study area for soil classification. Classification tests were carried out at the Ministry of Public Works laboratory in Sana'a. According to the obtained classification results, a horizontal and vertical soil distribution up to a maximum depth of about 6.0 meters was approximately achieved. Finally, based on these results and observations, eight extra representative locations were selected to run standard penetration test to obtain representative disturbed and undisturbed

INVESTIGATION PROGRAM

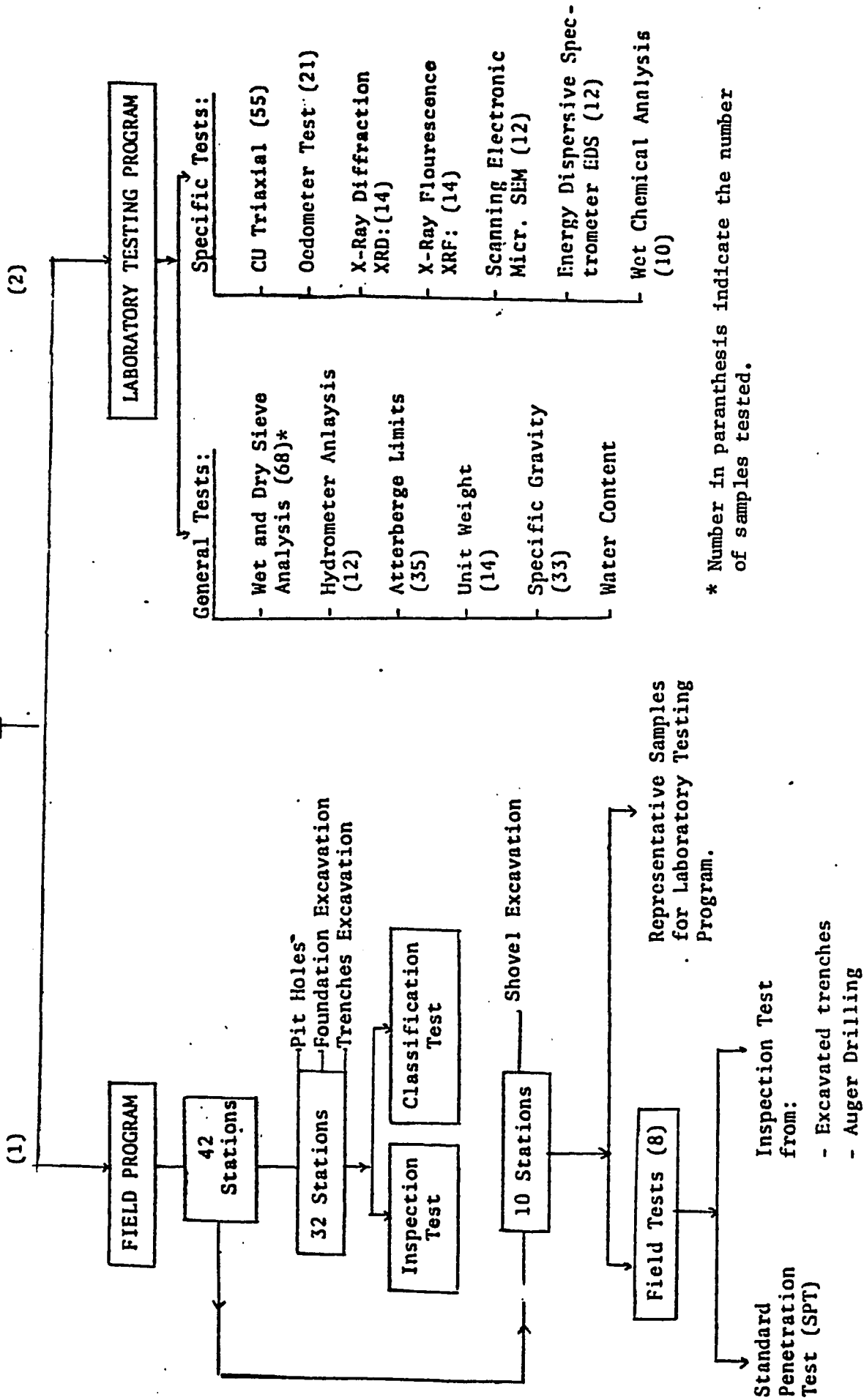


Fig. 3.1: Flow Diagram of Investigation Program

samples and to confirm the previously determined soil profiles. The details of all the above investigations are described in the following sections.

### *3.2.1 Exploration Study*

The first stage of the field investigation consisted of collecting existing data and informations about the study area and conducting site observations. Geological maps (W. Kruck, 1983), meteorological records (Italconsult, 1973), aerial photographs (Sana'a 1554 CI 1980), project reports from Ministry of Public Works were reviewed in this stage.

Both geological maps and aerial photographs were found to be the most helpful. The boundaries between the rocks and soil, the deposit types, rock types, different formations, faults and drainage patterns were obtained from the geological maps. Tracks of the flood streams, wadis, standing structures, the developed areas due to human-activities or disturbed ground and the geological features were easily identified on aerial photographs. The reports of some projects that had been conducted by the Ministry of Public Works and Italconsult described the soil in the study area in general terms as: silty sand soil, silty clay with sharp pebbles and some as gravelly sand with a clayey silt matrix. General cross sections showing the type of the subsoil and their distribution will be obtained based on the preceding observations. The hydrological and topographical reports did not contribute greatly to the desired geotechnical informations.

### 3.2.2 Sampling

The second stage of the field investigation consisted of sampling using test pits and trenches. "The pits are open excavation, large enough for a person to enter and study the soil in its undisturbed condition. They may be dug either by hand or power equipment" (Warrenk 1986). Thirty two test pits of about 2.0 meters diameter and long trenches were used to obtain 53 representative disturbed samples. The mean depth of these pits was about 8.0 meters with a maximum depth, in some cases, of over 20.0 meters. For undisturbed samples eight extra stations were selected and a shovel was used to excavate trenches with different levels up to a maximum depth of 6.0 meters. The distribution of those locations (pits and shovel excavations) is depicted later on in Fig. 4.3. More stations were located in the places around the north-south axis where more fine stratification occurs. More than one sample were obtained from those locations that have soil variation in the vertical direction.

**3.2.2.1 Disturbed Soil Samples:** Sixty representative disturbed soil samples were collected from different stations at different depths. Pits and shovel excavations were used for obtaining these samples. Each sample was placed in double nylon bag along with a label indicating the station number, the depth of the sample and the date of sampling. The natural water content for each soil sample was determined. The disturbed soil samples in this study will be described according to Hvorslev (1949) as:

"Representative samples contain all the mineral constituents of the strata from which they are taken and they have not been contaminated by material from other strata or by chemical changes, but the soil structure is seriously disturbed and the water content may be changed. These samples are suitable for general classification tests and positive identification of the materials, but they are not suitable for major laboratory tests and determination of the structural properties of the material insitu".

**3.2.2.2 Undisturbed Soil Samples:** Undisturbed soil samples may be defined after Hvorslev (1949) as:

"Samples in which the material has been subjected to so little disturbance that it is suitable for all laboratory tests and thereby for approximate determination of the strength, consolidation and permeability characteristics and other physical properties of the material insitu. The term is to some extent misleading since it is impossible to obtain a truly undisturbed sample, but it is firmly established in the engineering terminology and therefore been retained".

Eleven representative undisturbed soil samples were selected from the last eight stations at different depths. Excavations were conducted by using shovel making different berms at each different soil layer. Then undisturbed samples of a block type (hand carving) were taken from each berm.

### **3.2.2.3 Hand-Carved Undisturbed Soil Samples:**

**Application:** Test pits and trenches are the most reliable source of undisturbed soil samples. Undisturbed block samples can be hand-carved from these excavations. According to Peak and Terzaghi, (1967) "Samples obtained from such excavations are less disturbed than others". International Manual for the Sampling, 1981 described hand curving samples as follows:

"Sampling from pits or trenches is specially valuable in obtaining high quality samples. In addition to undisturbed samples, information of the soil stratification and discontinuities can be obtained by this method". "This method is often more expensive than other undisturbed sampling methods, but the greater value of the information obtained can offset the increase in cost".

**Excavation and Equipment:** Both mechanical power and hand-excavating tools were used in obtaining undisturbed block samples. A power shovel was used to make rough excavated trenches in the form that would allow obtaining one or more block sample from the same pit. Different berms or terraces were formed at different levels along one side of the trench with slope cut at the other side of the excavation to avoid the side's failure and the heave of the trenches bottom as shown in Plate 3.1. These terraces were made approximately at the top of different layers according to the stratification of the soil in the excavated trench. The power shovel was used for test pit excavation with a depth approximately 50 cm of

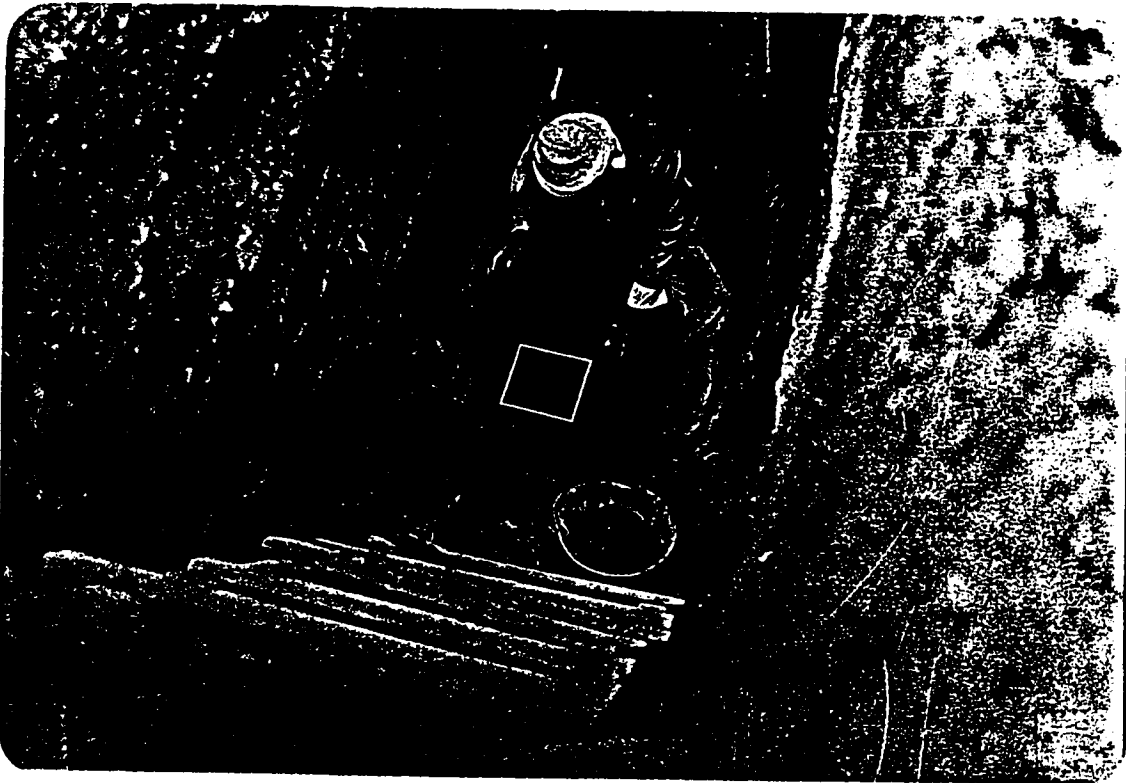


Plate 3.1: Block sampling from excavated trench having different levels in one of the sides while the other side was kept vertical. Sample was taken from 4.5m below the ground surface.

the top of the intended sample with 5 to 10 cm larger in each dimension, was left undisturbed. Hand-excavating tools for sample trimming included pick, saw, shovel, different sizes of knives and spatulas.

***Samplers and Sampling Procedures:*** A wooden box of clear internal dimensions of 20 x 20 x 20 cm was used as a soil sampler with a thickness of the sides of 0.9 cm. The top and bottom lids dimensions are 22 x 22 x 0.6 cm. Sides were fixed using halved joint connection system with glue as a binder agent along the internal side corners of the box so that the box could resist the lateral movement and give up the susceptibility of sample to disturbance due to handling and transporting.

Plates 3.1 and 3.2 shows a cubic block sample that was taken from Station # 38 at two different levels. Fig. 3.2 shows the procedures commonly used in hand-carving undisturbed soil samples. After the block of the soil had been trimmed to within several centimeters of the final size, the wooden sampling box with the base removed was used as a template to mark of the size of the soil block sample. The top and sides of the block then were carefully trimmed to the final dimensions using a sharp square mouth shovel and trimming sharp knives and trowel. The wooden sampling box was pushed down over the block noticing and removing the excess soil from the block sides, using hand-excavating tools. When the sampler box reached the desirable depth the top of the soil block

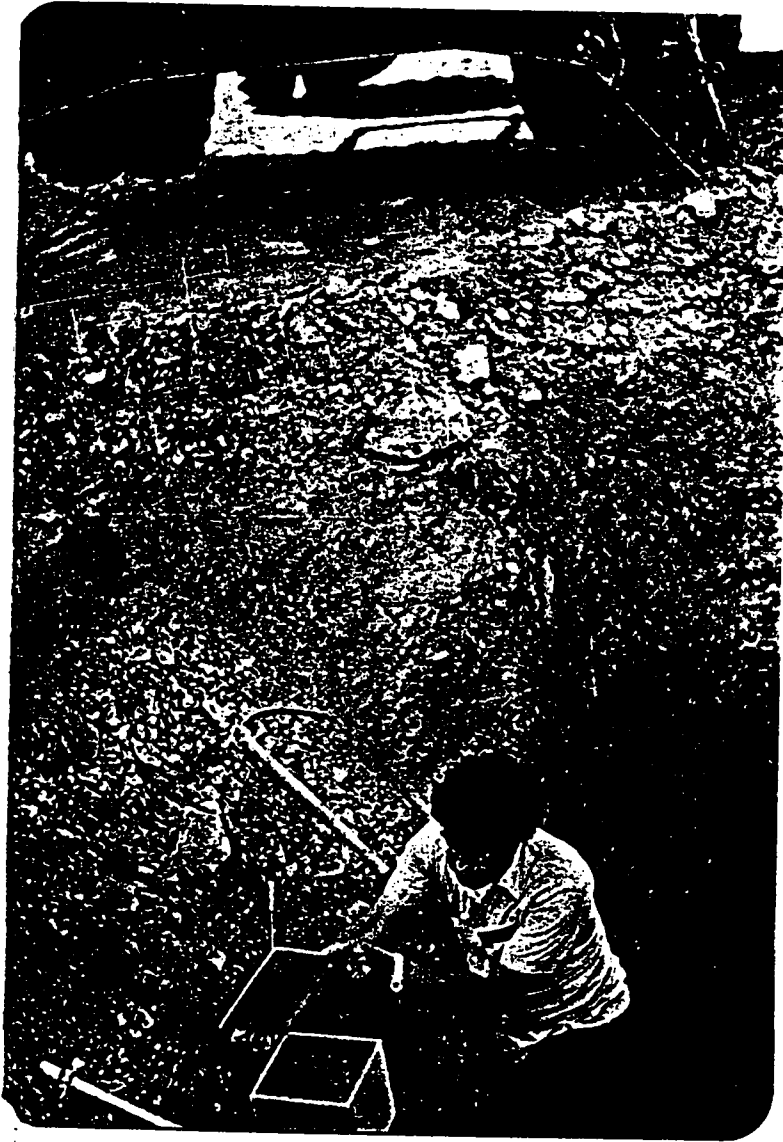
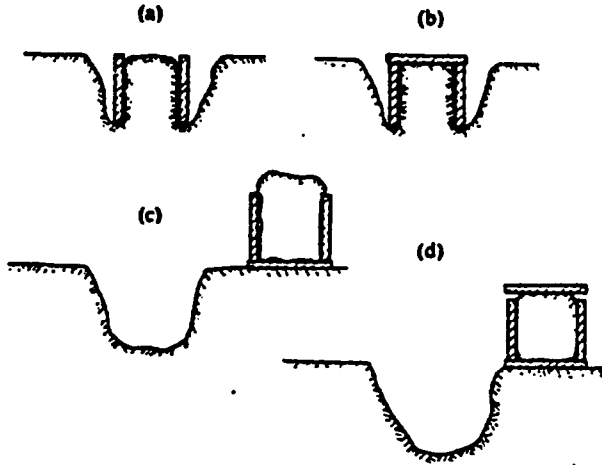
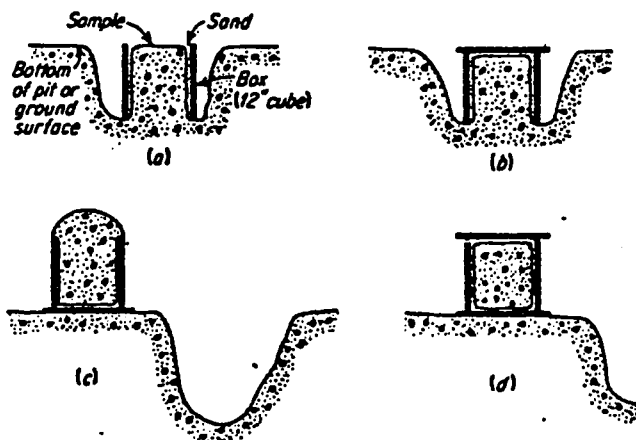


Plate 3.2: Block sampling from excavated trench at 1.8m depth, the level of the firts berm.



(a) Step by step procedure of hand-curved undisturbed sampling.



(b) Hand-curved undisturbed sampling.

Fig. 3.2: Hand-Curved Sampling (After Krynine, 1957)

was levelled off (Fig. 3.2a.a) and the top corner was fixed (Fig. 3.2a.b). The base of the soil block was then cut several inches below the bottom of the wooden box and the block with the box was lifted out (Fig. 3.2a.c). Removing the over size soil, levelling the surface and covering the base by the bottom wooden cover were the last sampling procedures (Fig. 3.2a.d).

Then the box was labeled and marked carefully, showing the top and the bottom directions, depth, location, number of sample and the date of sampling. Some samples that contained both cohesive and cohesionless soil (silty clay with gravel or pebbles) were difficult to obtain with final smooth sides; therefore, the final dimensions were under-sized approximately 4 mm smaller in each side. Fine sand or fine soil from the same location was used to fill these gaps between soil block and sampler's sides (Fig. 3.2b.a). A little tapping with flat thin knife was carefully done upon the filling soil in order to support the sample and prevent movement of the soil block inside the sampler during transportation and handling. The filling and sampling procedures in case of cohesive soil with gravelly material sampling are shown in Fig. 3.2b.

*Storage and Handling of Block Samples:* Samples were kept in a room under a wet blanket till they were transported carefully by airplane directly to the laboratory of Civil Engineering Department of King Fahd University of Petroleum and Minerals in Dhahran (KFUPM), Saudi Arabia. Great care was taken during handling

and transporting to avoid sample disturbance. Determination of the natural water content were taken in the field at the same time of sampling. As the water table is very low all the samples were partially saturated (about 45 - 60 %). The maximum loss in water content was about 3 %. This is not a significant point since those samples were tested under full saturation which is the most critical condition in this case.

### 3.3 Insitu Testing

#### 3.3.1 Types of Testing

Due to the limited resources available, the insitu testing was limited to the standard penetration test. The Ministry of Public Works contributed by running the standard penetration test over seven locations from which the undisturbed hand-curved samples were obtained. In fact, the standard penetration test was the most appropriate insitu test for the available soils. The layering system makes the using of plate load test unreliable, while the existence of boulders and gravelly soil among the fine soils was the difficulty in using the cone penetration test.

#### 3.3.2 Auger Drilling:

In order to carry out the standard penetration test at different levels suitable bore holes must be drilled. For advancing such bore holes the method of continuous flight augers was used. A



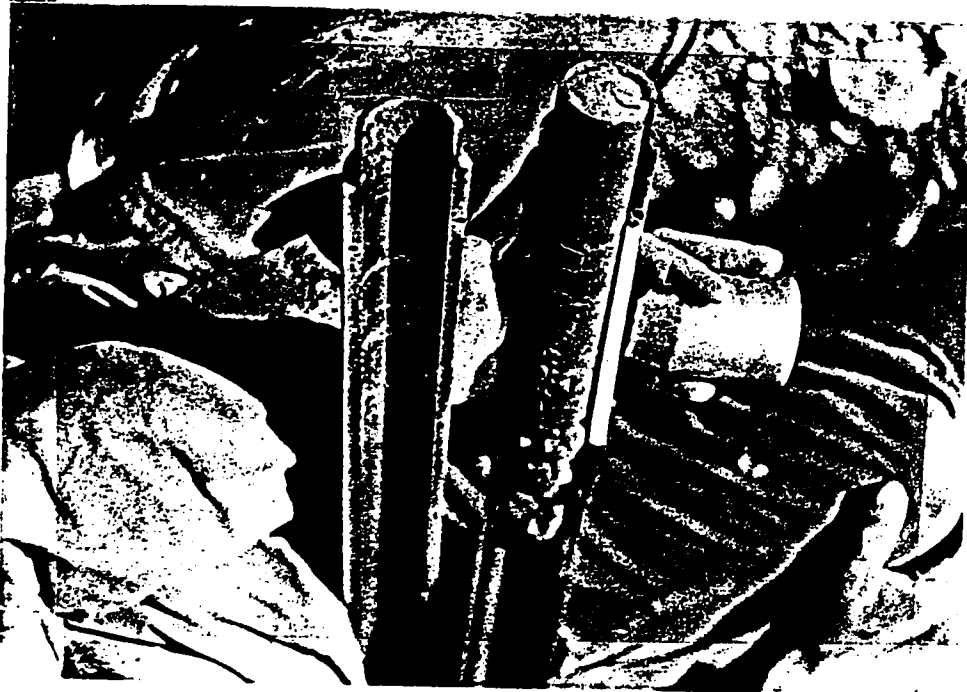
Plate 3.3 : Auger Drilling and SPT Testing  
by the Tractor-Mounted Rig.

tractor-mounted drilling rig of the Ministry of Public Works Plate (3.3) was used. Flight augers of a solid stem with an outer diameter of 152 mm were used in sections of 1.5 and 3.0 meters. In case of a cohesionless soil a metal pipe was used as a casing to prevent the soil from caving in.

In making a hole, a cutter head was attached to the tip of the auger. During the drilling operation, the rotary drill equipment applied a pressure against the cutter head and provided the rotation at a speed 75 revolution per minute. As the drill advanced, additional auger flights were added and the hole extended downward. In order to conduct the standard penetration test besides obtaining disturbed samples it was necessary to clean the bottom of the hole by keeping the auger rotating and reducing the applied pressure so that the disturbed soil would be brought to the surface either attached to the auger flights or spilled off the flights around the borehole. It was necessary to withdraw the auger at selected point in order to conduct the SPT test.

### ***3.3.3 Standard Penetration Test (SPT)***

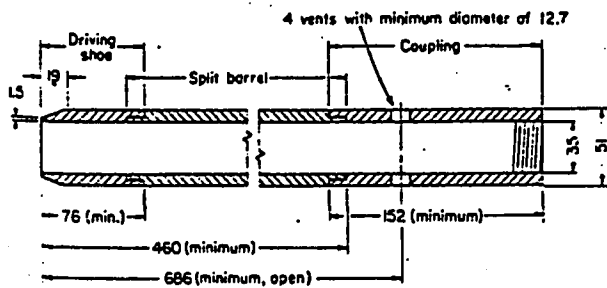
***3.3.3.1 Definition:*** The Standard Penetration Test (SPT) was the only field test that was carried out in this study. It consists of driving a standard split spoon sampler, as shown in Fig. 3.3, a distance of 46 cm (18 in) into undisturbed soil by using a 63.5 kg (140 lb) hammer falling freely from a height of 76 cm (30 in). The number of blows required to drive the split spoon the last 30.5 cm (12



a) Split spoon with the obtained disturbed sample



b) Split spoon assembled



(c) Dimensions (all in mm)

Fig. 3.3 : Used Split Spoon Sampler In Penetration Testing.

in) is recorded as the N-value (American Society for Testing and Materials, 1982, Designation D-1586-87). This depicted in Plate 3.3 during the performance of the SPT testing at Station No. 35.

### **3.3.3.2 Suitability and Validity of SPT:**

The limited availability of insitu testing equipments and the absence of highly skilled labour to operate them in Sana'a Area necessitated the use of the simplest piece of equipment, namely SPT. The SPT was the most suitable field test in this case because it suits practically almost all soils and weak rocks, besides its procedure is easy to execute and permits frequent tests. In addition, the equipment is available, relatively simple and the facility of obtaining disturbed samples are included. Furthermore, SPT provides several useful correlations such as relative density, unit weight and friction angle of cohesionless soil as shown later on. Such correlations were used in classification purpose and comparing some data results as indicated later on.

### **3.3.3.3 General Remarks on SPT Running:**

SPT testing was performed in seven locations down to a maximum depth of 7.0m. In a few locations during the drilling, water was added to simplify excavation and to help in getting out the disturbed soils. At some levels drilling was obstructed by boulders. To permit further penetrations, adding water, hammering and shafting techniques were used. In order to avoid both adding water and compaction effects in disturbing soils, SPT was carried out at a lower

depth, at least 0.5m, bellow the leval at which such procedures were applied.

The obtained samples of split spoon sampler were highly disturbed (Area ratio,  $Ar = 111\%$ ), but they were still representative ones. After removing the sampler from the string rods, the sampler unscrewed and the split spoon separated to display the recovered sample for inspection test in Fig. 3.3a. Most of cohesive samples, were tested using a pocket penetrometer to obtain the approximate values of their strength. Some of the samples were stored in labelled glasses and returned to the laboratory for classification tests purpose and for obtaining their natural water content.

### 3.4 Laboratory Tests

Laboratory testing included preliminary, general and specific tests. The general tests included classification tests, specific gravity, unit weight and water content tests. The specific tests were programmed to be sufficient to give properties of the strength, compressibility and mineralogy of soils under study. It included consolidated undrained triaxial, consolidation, x-ray diffraction, chemical and scanning electron microscope tests.

#### 3.4.1 *Inspection Tests*

The soil samples were preliminary inspected in the laboratory to detect their colour, smell, texture and to recognize the existance of the organic contents such as the remains of the plants. The con-

tents of the boulders, gravel, and sand along with their size and shape was identified by unaided eye. The silty sandy soil was distinguished from the silty clay soil by noticing the water adsorption of a sample of each type. In addition, they were distinguished by pressing a wet sample of each one between the hand balm and fingers and noticing both the friction in case of silty sand soil and the susceptibility to casting in case of silty clay soil. Such preliminary tests were greatly helpful in selecting the suitable laboratory testing program for the different soil types. The visual description of the soil was reported in this study as recommended by ASTM (D 2488-69).

#### *3.4.2 Classification and General Tests*

As a result of the variation in the horizontal and vertical distribution of the soil many representative disturbed samples for the classification purpose were needed. Classification tests were performed on fifty three samples, obtained from 32 stations, besides those disturbed samples obtained from the last eight stations during the preparation of the specimens for consolidation and triaxial tests. Classification tests included sieve analysis, hydrometer analysis and Atterberg limits (plastic limits and liquid limits). Classification tests to be performed on a sample, depends on its texture and grain size contents. Thus, samples appearing to be gravelly sandy soil were subjected to the dry sieve analysis and specific gravity tests, while those silty sand and gravelly silty sand samples were subjected to

the combined wet and dry sieve analysis test, along with the specific gravity tests. This combined sieving method was used due to the difficulty in breaking the fine soil into its individual particles even by using a rubber-tipped pestle. In this combined method (ASTM D 2217) the cementation between silty particles and granular particles was loosened by washing the soil sample through sieve # 100 and sieve # 200 into a deep container. The retained soil on # 200 was air-dried and then resieved through six to seven sieves according to ASTM (D 421). The silty and clayey soil samples were tested by using wet sieve analysis (by washing the sample through six sieves), hydrometer analysis, Atterberg limits and specific gravity tests. In the hydrometer analysis tests a 152H hydrometer was used according to ASTM (D 422). The liquid limit tests were carried out using the Casagrande apparatus (ASTM D 4318). The samples used in the classification tests were air dried as recommended by ASTM (D 421) and varied in weight for sieve analysis from 500 g in case of silty clayey soil to 2000 g and more in case of gravelly and sandy soil. The classification tests were performed as recommended by ASTM (D2487-69), (Bowles, J. E., 1986 and Wray, W. K., 1986).

The unit weight, specific gravity tests were performed on ten representative samples while the water content and classification tests were carried out on all soil samples. The average value of the specific gravity of three specimens for each soil sample was considered and similarly for the unit weight (ASTM D 854 and AASHTO T-87).

### **3.4.3 Laboratory Sampling and Specimens Preparation:**

Undisturbed block samples were used to prepare undisturbed triaxial, consolidation and scanning electronic microscope specimens. A great care was taken in preparing these specimens in order to reduce the disturbance especially in case of the existence of granular soil mixed with fines, or in the case of the weakly cemented fine soil.

#### **3.4.3.1 Consolidation Specimens:**

Rings of the consolidation apparatus of 70 mm and 63.5 mm in diameter with 20 mm and 18.2 mm in thicknesses respectively were used for cutting the consolidation specimens. Two specimens from each soil block sample were obtained. The ring was placed in the top of soil block and pressed into the soil. The ring containing the specimen was removed from the soil block after pushing the triaxial tube samplers into the block. The other specimen from the same block was obtained from the middle part by pushing the ring slowly, steadily and vertically using a cutter holder and trimming the surplus soil by hand from the front of the edge of the sharp part of the ring during the depression processes. The top and bottom faces of each specimen were levelled using a sharp blade and a flat glass plate, (Manual of Soil Laboratory Testing, 1981).

#### **3.4.3.2 Triaxial Specimens:**

A galvanized steel tube, made by Wykeham France (WF 30520), having an internal diameter of 38 mm and a height of 200 mm was used in resampling from the block samples. The area ratio of the

tube was about 14% which is in the acceptable limits as compared with recommended limits after Bhandari, (1980). The internal surface of the tube was oiled before sampling to reduce the friction between the tube and the soil. Two tubes were pressed slowly, steadily and vertically by using Versa-Tester compression machine made by Soil Test. They were compressed through holes made in three parallel horizontal plates, used as guides, placed over the wooden box (plate 3.4). A rigid steel strip was placed over the tubes to keep the penetration rate and the applied pressure equal during sampling.

After sampling, tubes were covered by a nylon sheet, waxed and kept in a humid room. Before testing, the samples were extruded from the tubes by means of a manual extruder. Soil specimens of diameter 38 mm and a length to diameter ratio of about 2:1 were prepared for the triaxial test. The top and bottom portions of the soil tube sample were removed to reduce the disturbance effect. Two specimens were usually obtained from each tube while in some cases only one sample from a tube was obtained because of the disturbance either due to jacking effect or due to the existence of gravelly soil. Plate 3.5 shows the jacking and trimming procedures.

#### **3.4.4 Consolidated Undrained Triaxial Compression Tests With Pore Water Measurements (CIU - Strength Tests):**

Consolidated undrained triaxial compression tests with pore water pressure measurements were carried out on a total of 55 specimens of the fine soil or fine with coarse soil. Specimens of 38 mm

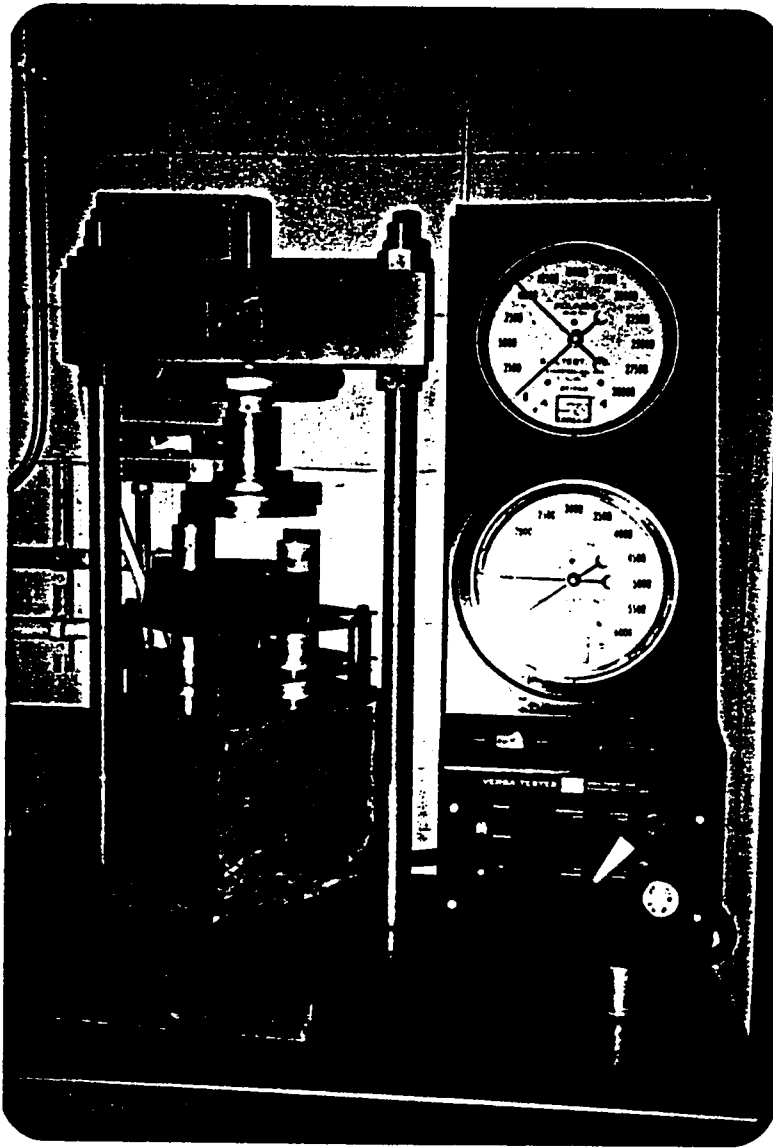


Plate 3.4 : Resampling from the block sample  
by thin tubes through guide plates.

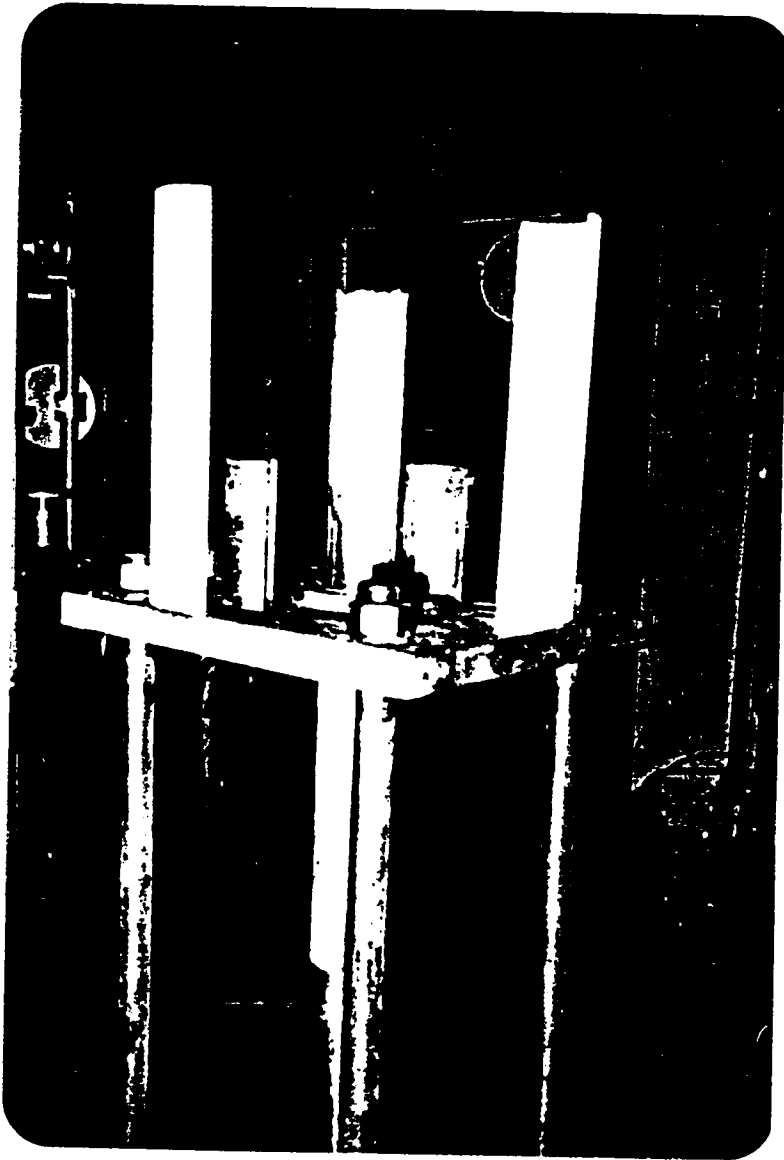


Plate 3.5 : Jacking and trimming process

diameter by 76 mm height were used in these tests. Each specimen was placed on the pedestal of the triaxial cell Fig. 3.4 and subjected to three major steps namely:

- 1) Saturation stage: consisting of applying a back pressure inside the sample. Both  $CO_2$  and distilled water were used in this stage. A vacuum pump was also used to accelerate the saturation.
- 2) Consolidation stage: consisting of application of confining pressure all round the specimen ( $\sigma_3$ ) during which drainage of water from the specimen was allowed and the volume change was measured, and
- 3) Shearing stage: consisting of applying deviatoric stress ( $\sigma_1 - \sigma_3$ ) during which no drainage from the specimen was allowed, no volume change took place and the developed pore water pressure was measured. Three specimens from each soil block were tested. Each specimen was tested under a different confining pressure till failure. Confining pressures of 10, 20 and 30 psi were used. The achieved degree of saturation was about (94 - 100%) under a maximum back pressure of 30 psi while in some soils the saturation was achieved under less back pressure. The test set-up and test procedures are shown in appendices A-1 and A-2 respectively. A computer program was used in calculating all samples. A representative print out of the calcu-

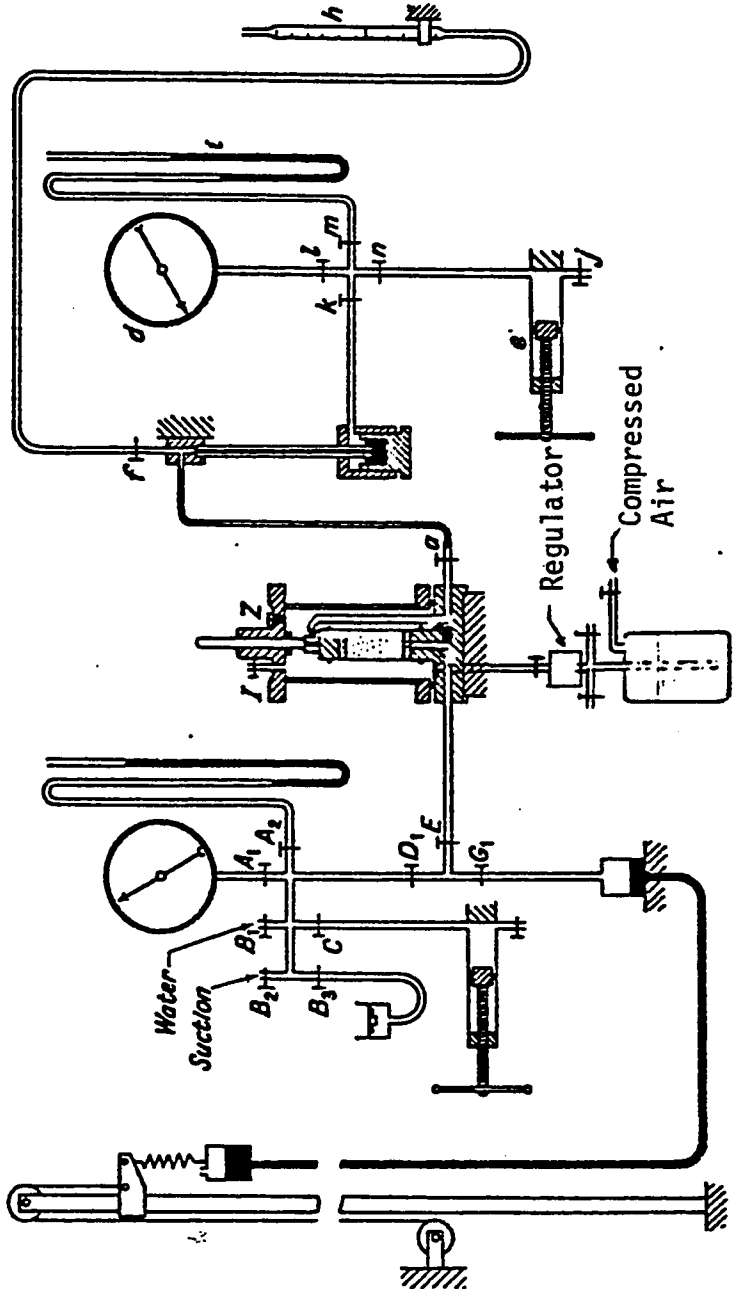


Fig. 3.4 : The layout of the apparatus for consolidated-undrained tests on 1½-in diameter samples: with measurement of pore pressure. (Adopted after Bishop and Hankel, 1962).

lated values of the triaxial results is shown in Appendix D-10.

### ***3.4.5 Oedometer Consolidation Tests***

The compressibility of fine soils of the study area were determined using the consolidation tests on undisturbed soil specimens of 70 mm and 63.5 mm diameter with 20 mm and 18.2 mm thickness respectively. The apparatus used were oedometers, front loading ones, the rear loading one, both from Wykeham Farrance Ltd. (WF 24001 and WF 24251). the procedure that was followed was in accordance to Method D 2435-70 of ASTM (1974) and BS 1377:1975. Procedures of the tests are described in appendix A-3.

### ***3.4.6 X-ray Diffraction Analysis***

***3.4.6.1 General:*** A Philips X-ray diffractometer model PW 1700 / 10 was used to produce a diffractogram of soil samples. Those diffractogram are used to identify the different minerals that exist within the tested specimens. The scanning speed was 0.01 degree per second and the interval of data collection was also 0.01 degree per second. The X-rays emitted was Ni Filter Cu. Radiation and a monochromator was used to reduce the background. The scanning angle range was  $5^{\circ}$ - $80^{\circ}$ .

The minerals were identified by comparing the above mentioned diffraction pattern with the diffraction pattern of different standard phases compiled by the International Center for Diffraction Data,

Swarthmore, Pennsylvania. This searching of the phases and matching with the standard diffraction pattern was assisted by PDP 11/23 Computer.

#### **3.4.6.2 Specimens preparation:**

##### ***Natural specimens preparation:***

X-ray diffraction analysis was performed on fourteen representative soil samples for the identification of the main mineral constituents. The tests are conducted in the Research Institute of King Fahd University of Petroleum and Minerals. The soil samples were grounded with the help of agate mortar and pestle to reduce the texture and preferred orientation and to make sure that it is homogeneous.

##### ***Oriented Specimens:***

Four representative specimens of fine soils were selected to be tested by X-ray diffractometer for clay minerals identification. They were prepared as follows:

- 1) 100 gm of unconsolidated and air dry specimen was taken and placed in cylinder containing 1000 ml distilled water (the water contains 4% of hexameta phosphate as a dispersive agent).
- 2) Allow sand and salt to settle down, taking the advantages of the hydrometer analysis that was known for the same soil. Settling of sand and salt was achieved by leaving

the cylinder a little longer than the required time for clay to settle.

- 3) After settling sand and silt in the above cylinder, the water suspension was centrifuged to separate clay from suspension.
- 4) Sufficient amount of the moist clay was placed on glass slide and allowed to dry at room temperature.
- 5) Glass slide was fixed on a circular metal disk which was placed in the X-ray diffractometer for analysis.
- 6) After the first run the specimen was taken and heated up to 575°C for one hour.
- 7) After one hour the specimen was placed in a desiccator for half an hour before the second run.
- 8) Both the first and the second resulted pattern were used in identifying the clay minerals as shown in Chapter 5.

#### *3.4.7 X-ray Fluorescence Spectrometer: (XRF)*

Fourteen specimens were selected from the study area and analyzed with XRF along with XRD. Moreover, extra ten specimens were analyzed also with XRF along with scanning electronic microscope. Quantitative evaluation in percent for the fourteen specimens was accurately obtained in terms of the mineral dioxide, while the analysis of the last ten gave only the identification of mineral types that exist in the soil specimens without quantitative evaluation. Each specimen had its own figure showing the different mineral contents.

The spectrometer, Philips PV 9500, is available at the Research Institute of the University.  $R_h$  target was used for the X-Rays and the operating conditions were 25 KV and 50 microamps. The spectrum was collected for 229 live seconds. No filter was used in the data collection and the specimen chamber was filled with the gas. To average out the microwhomogeneities, the spectrum was spined while collecting data. The quantitative analysis was carried out with the theoretical fundamental parameters which depend on the absorption of the element to the X-Ray and thus no standard was used.

#### *3.4.8 Scanning Electron Microscope:*

The scanning electron microscope (SEM) is widely used for the examination and analysis of the microstructure characteristics of material in a solid form. The SEM analysis performed in this study was carried out on JEOL JSM-840 available at the Research Institute of King Fahd University of Petroleum and minerals.

The JSM-840 enables morphological observations of a very fine structure and full elemental analysis using Energy Dispersive Spectrometer (EDS) system. In the secondary image, the JSM-840 has 4nm resolution and the magnification ranges from 10x to 300,000x. The JSM-840 can produce a very fine spot size (1 mm in diameter). This is very useful for EDS analysis and the spectrum can be viewed immediately on the screen.

The SEM analysis was necessary in this study to examine the

formation of fine and granular soil and the distribution of pores among the soil. In addition, the bonding between the fine particles such as clay and/or silt particle can also be examined. Ten soil samples were used for SEM analysis. Each sample was sectioned into 1.5 cm x 1.5 cm x 1.0 cm and mounted on a brass-mount by a double-sided tape keeping the surface under study relatively undisturbed. The specimen was then dried in an oven and then coated with a thin layer of gold (100 Å in thickness) prior to the examination. This gold layer acts as a conductive layer to avoid any build up of the absorbed electrons on the surface. This build up gives rise to an abnormal contrast, or charging effect, and greatly effects the electron beam. In order to avoid this effect, a small trail of silver was used to connect the gold layer to ground, in this case the brass-mount.

SEM analysis in this study involved the examination of the microstructure and elemental analysis by EDS at several areas. To fully understand the formation and distribution of the pores holes, several micrographs were taken at several areas in the transverse (horizontal) and longitudinal (vertical) section. The EDS analysis was obtained at respective microstructure. The analysis and results are discussed in chapter 5.

#### ***3.4.9 Soil Chemical Analysis***

Ten soil samples were chemically analyzed for the determination of chlorides, sulphate, pH and organic matter. Six fine samples were

used to obtain cation exchange capacity. Chemical constituents including  $Ca^{++}$ ,  $Mg^{++}$  and  $K^+$  were determined using the Atomic Absorption (Perking Elemer, Model 5000) that is available in the Environmental Laboratory of the Civil Engineering Department. Soil solution was extracted at 1:2 and 1:4, soil to water ratio, and the results were transferred to 1:1. Very brief description of the methods used in the above analysis, is as follows:

**3.4.9.1 pH Test:** A calibrated pH meter model made by Corning was used in this test. A sample of 20gm soil was added to 50 ml of distilled water. Stirring the solution for 30 minutes, then the pH electrode was dipped into the solution to read the pH directly.

**3.4.9.2 Organic Matter Test: (Hense, 1971):** Oxidizable organic carbon (Walkey-Black) method was used. 5gm of dry soil was placed in a flask. 10 ml of potassium dichromate ( $K_2Cr_2O_7$ ) and 20 ml of sulfuric acid ( $H_2SO_4$ ) were added to the flask which was then kept for 30 minutes. After that 200 ml of distilled water, 0.5 ml ferrion as indicator and 10 ml of orthophosphoric acid were added. Ferrous ammonia sulfate (FAS) was allowed to flow into the solution from standing graduated pipe starting from a reading x of FAS, keeping a continuous magnetic mixing till dark greenish colour was achieved at a reading y of FSA. The percentage of organic matter was calculated as follows:

$$\text{Organic Matter} = (x-y) \frac{0.003}{2W} 100 F$$

where:

x is blank titer

y is actual titer

w is soil weight in gm

F is transferring factor from organic carbon to organic matter. Practically it is found to be equal 1.724.

**3.4.9.3 Chloride Determination:** Mercurate Nitrate method was used in this test. 50 ml of extracted solution (w) was taken and 0.5 - 1.0 ml of potassium chromate was added as an indicator for chloride. Adding 0.5 ml of nitric acid gives a yellowish colour. Finally, mercurate nitrate ( $HgNO_3$ ) of known concentration (N), was continuously added till violet colour was achieved. The amount of mercurate nitrate added was recorded as R and the chloride was determined from the equation:

$$CL^- = R \times N \times \frac{35.54}{w/1000} \text{ mg/lit}$$

where N = 0.1492.

**3.4.9.4 Sulphate Determination:** 25 ml of extracted solution of the soil sample was added to 75 ml distilled water and 5 ml of conditioning reagent to give the final tested solution a certain viscosity. After stirring for one minute a small amount of the solution was

placed in a tube and then inserted into an electrical device (Spectronic 20) for four minutes. This equipment with 420 wave length manufactured by Baush and Lomb was used in determining the sulphate concentration in a solution. After four minutes the absorbance reading was achieved (R). From absorbance and concentration relationship a slope was defined as:  $\frac{\alpha}{0.00636}$ . The sulphate concentration was obtained from the equation:

$$SO_3 = \frac{\alpha}{0.00636} \times F \times R \text{ mg/lit}$$

where F is the dilution factor, F = 4.

**3.4.9.5 Cation Exchange Capacity Determination (CEC):** The method for determining CEC is after J. D. Rhoades, 1982). This method is valid for soil in arid area. Three main steps were carried out as follows:

- 1) 5 gm of oven dried sample was placed in a centrifuge tube. 33 ml saturation solution of 0.4 N sodium acetate [0.4N NaOAc] and 0.1 N sodium chloride ethanol (60%) [0.1N NaCl] was added. The tube was shaken for 5 minutes then centrifuged at 1000 rpm for another 5 minutes till liquid became clear. The supernatant liquid was decanted and discarded. This step was repeated three times by adding fresh saturated solution, shaking, centrifuging and discarding the clear liquid.

- 2) After the third discarding of pure liquid in the previous step, 33 ml of extraction solution 0.5N magnesium nitrate  $[0.5N Mg(NO_3)]$  was followed by shaking and centrifuging. At this stage, the clear liquid was collected in 100 ml volumetric flask. This second step was repeated two more times and clear liquid was made to volume (about 100 ml).
- 3) The last step was determining Na and Cl of saturated solution (NaOAc + NaCl) and  $(Na/Cl)_s$  ratio was calculated. Similarly  $Na_t$  and  $Cl_t$  in dilution of extracted solution of tested sample were determined. Finally, cation exchange capacity was calculated from the equation:

$$CEC = Na_t - (Cl_t)(Na/Cl)_s.$$

where CEC in meq/100 gm of dry sample.

## Chapter 4

### SOIL FORMATION AND SOIL DISTRIBUTION

#### 4.1 SOIL FORMATION AND SOIL DEPOSITION

##### 4.1.1. Introduction:

Formation and deposition of the soil within the study area are markedly affected by the environmental and topographical conditions. Sana'a area is arid to semi-arid region. Such regions are considered as an environment with little precipitation in which evaporation rates are considerably in excess of precipitation (Richard, 1983). The mountains bound the study area from west, east and partially from south. These mountains along with their steep slopes and the gentle slope of Sana'a plain effect the soil formation and the type of depositional system. Mountainous areas serve as the ultimate sediment source, besides they are the energy source, with respect to the running water by which rocks are weathered and sediments are transported. Moreover, these mountains act as a barrier to the wind which blows from east-north and north to southwest and south respectively. The soil of the study area is a transported soil from those weathered surrounded rocks.

#### 4.1.2 Depositional Systems :

Under the effects of the above features, there are two major and one minor weathering and sedimentological processes operating at various times on Sana'a plain:

- Alluvial processes act as a physical weathering and transporting mode in form of running water.
- Aeolian processes also act as a physical weathering and transporting agent, but in form of wind action.
- During the rainfall, the chemical precipitation may effect as a minor weathering agent in form of oxidation and leaching.

The latter two sedimentological processes operate for long periods of time between the few days associated with rainfall events. The soil formation in the vertical direction, soil profile, is greatly affected by the above three systems, while in case of the horizontal formation only the previous two sedimentological processes are the influence factors.

#### 4.1.3 Soil Deposits :

As a result of the different depositional systems different soil deposits have been developed. The study area is covered by alluvial deposits, wind deposits and chemical deposits

#### 4.1.3.1 Alluvial Deposits:

Alluvial deposits are the weathered sediments which are transported by the running water. In the study area, the source of this running water is the precipitation which occurs in the summer for few days and sometimes in the spring but with less amount. In case of high rates of rainfall, flash flood takes place. In May 1967 and August 1970 flood was reported in Sana'a city. Such floods contribute in forming recent alluvial deposits (Italconsult, 1971). The two major types of the alluvial deposits are: arid alluvial fans deposits and wadi deposits.

#### *Arid Alluvial Fans:*

The area is partially surrounded by mountains. These mountains with their sharp steep slopes and the gentle slope of the plain led to the development of alluvial fans. Fans were defined by Richard, 1983, as "A fan-shaped wedge of sediment which typically develops at the base of a rather steep mountain slope where there is an abrupt change to a flat or only slightly sloping area and where sediment loses its confinement from a high-relief valley. Alluvial fans are particularly numerous in tectonic regions where long fault blocks produce an extensive scarp" (Richard, 1983). Fans exist mainly on the eastern and western parts area extending towards the central wadi area.

Arid fans show a wide range in size from a few hundreds to a thousand square meters. They are generally subdivided into three

zones: the upper-fan near the apex, the mid-fan and the lower-fan. The upper-fan and the mid-fan are the predominant zones. The extension of the fans is related to the flood or the rainfall intensity. In case of heavy rainfall or high flood, continuous layer of gravely sand may cover most of the study area, including the wadi area as a water-laid deposit.

Alluvial fans deposit their sediments in form of four common sedimentation processes: debris flow, streams channel, sieve deposition and sheet-floods. The first three forms mostly deposit their loads in the upper-fan portion at the base of mountains, whereas sheet-floods and finer debris flow are mostly prevalent at the downstream ends of channels in the last portion of the fan. In some cases where the stream confinement ends the sheet-floods and finer debris deposit their loads in the lower portion of the mid-fan (Richard, 1983).

In fact, the study area may be affected by all or some of the above forms according to the flood or rainfall intensity. In case of moderate rainfall and no flood, loads of arid fans are deposited in areas restricted near mountains and stream channels. While in case of floods and high intensity rainfall, the deposits of the different fan forms, specially the sheet-floods, extend towards the Wadi area. This type of deposition may cause a sort of relative irregular soil distribution in vertical direction.

Fan sediments are coarse and poorly sorted as a result of short

transport from high relief sources. The grain size distribution has a general decrease from the apex to the distal portions of the fan and also a decrease from the base of the fan upward to the active surface. In the apex near the mountains base (Plate 4.1) boulders, coarse gravel and little or no material of sand size are the dominant deposits. These were sedimented by debris flow and sieve deposition. The channels deposits consist of sand and gravel with some grading; gravel layers are typically concentrated at the base of the channels (Plate 4.2), and cross-stratification of sand layers is found as shown in Plate 4.3 (Bull, 1972). Stratification in form of grading with fines and imbricated pebbles are common as shown in Plate 4.4 (Richard, 1983). The sheet-floods deposits consist of sand, with some silt and gravel, and are somewhat more common in the mid-fan than in another areas of water laid deposits in Wadi. In case of the normal flood and normal annual rainfall, sand and silt accumulations are very common as mid-fan deposits in the wadi areas. Fig. 4.1 shows a block diagram indicating the distribution of arid alluvial fans deposits, streams and wadi deposits.

#### **4.1.3.2 Wadi Deposits:**

The strip which occupies the middle part of the study area, with an average width of 3.0 km, extends gently from south to north along the plain axes at the terminus of fans. This area is defined as wadi with no permanent channels due to the lack of continuous water



Plate 4.1 : The Upper Fan Portion (Apex) at the base of Asser Mountain in the Western part of the Study Area.



Plate 4.2 : Bed Stream Deposits.

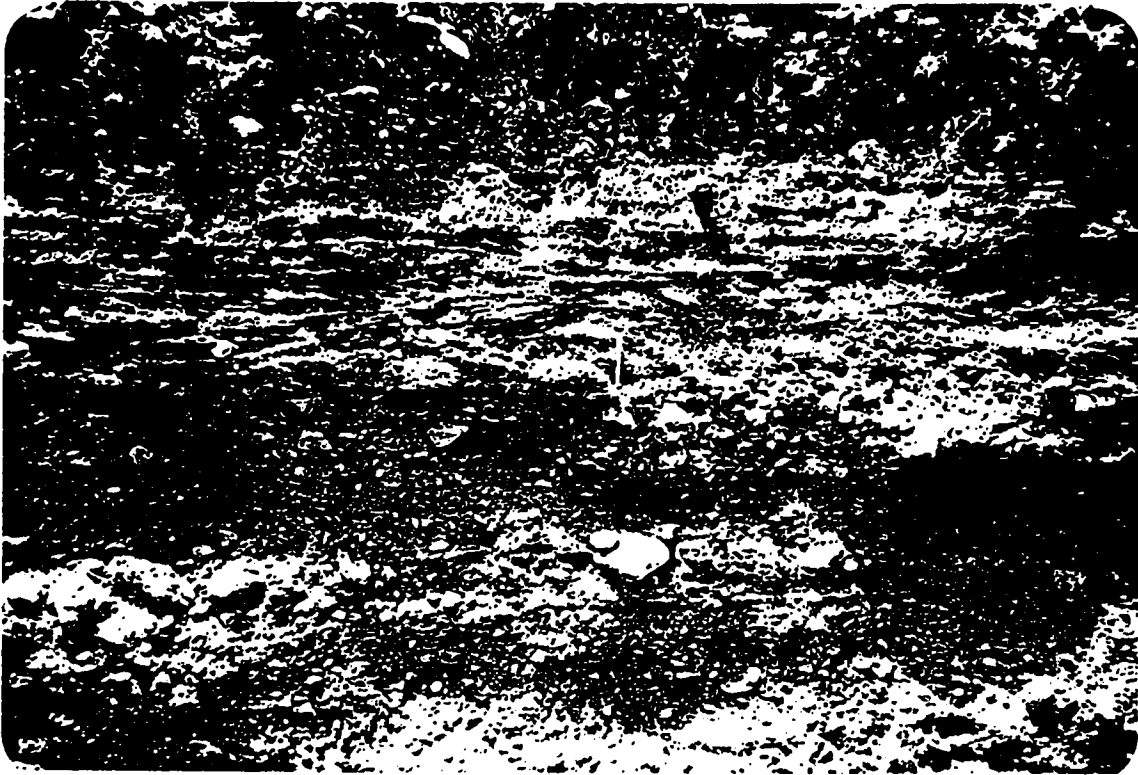


Plate 4.3 : Cross-Stratification of Water-laid  
Deposits.



Plate 4.4 : The Implicated Pebbles  
Formation in granular  
soils.

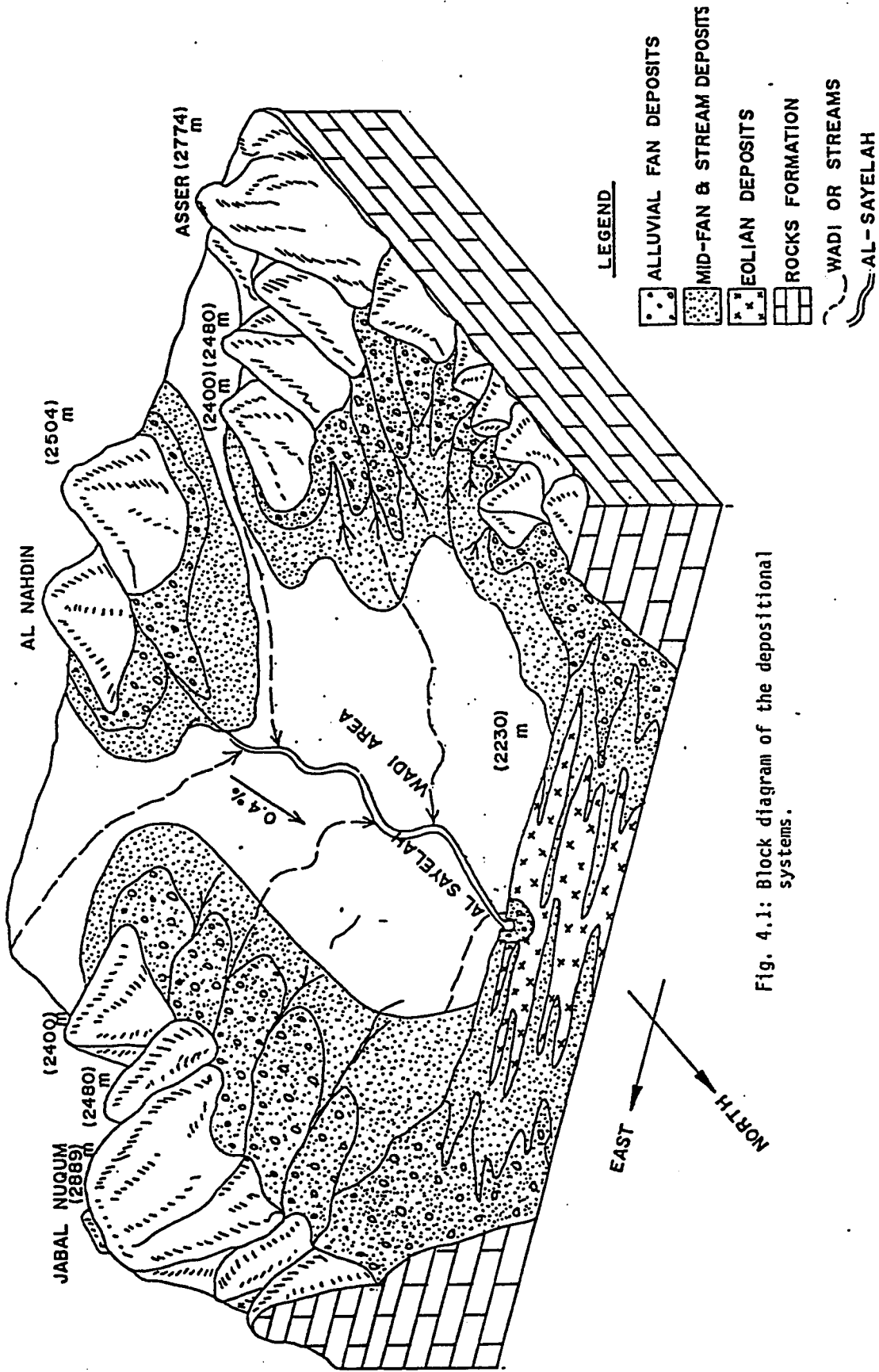


Fig. 4.1: Block diagram of the depositional systems.

flow (Glennie, 1970 and Richard, 1983).

The wadi deposits consists mainly of water-laid deposits and wind-laid deposits. The water laid deposits result from flash floods which are the common events of significant sediment mobilization on the wadi area, and the deposits of the stream channels which sedimented along the channels and vicinity areas to these streams in wadi area. The wind deposits are mainly in form of loess deposits. Some fines of the water deposits are reworked by wind and retransported from either the bars of channel or from the down streams of these floods. In contrast same loess deposits are reworked by water action forming modified loess deposits.

The floods result from the high rates of precipitation which takes place either in the study area and the surrounded mountains, as recorded in 1967 and 1970, or in the eastern-southern mountains (Khawlan Mountains) through Wadi As Sere. The resulting deposits from the surrounded mountains are commonly in a wide spread sheet of sand and fine gravel of poorly sorted with some silt (Bull, 1972). Such sheet may invade the wadi from both sides, east and west, or from one side according to the flood source. These floods from the sides flow with smooth curvature towards the north as a result of the combination of the mountain base slopes and the plain slope. The floods resulting from Khawlan Mountain display a braided pattern deposits extending through the southern part towards the north. Coarse gravel, sand with little pebbles and internal particles are

included. The sediments are characterized by smooth surfaces and well sorted due to long transportation effects. Graded bedding is common on the sand (plate 4.5), while some imbrication may be present in gravel as shown in Plates 4.4 and 4.6.

The stream channels, which spread out either from alluvial fans on the sides of the study area or from the braided streams on the south east, contribute in depositing sediments in the wadi areas as a water-laid deposits. They end to a main channel known locally as 'Al-Sayelah'. The stream pattern of this channel is slightly to moderately sinuous as shown in Plate 4.7. Such channel was defined by McGowen and Garner (1970) as a coarse-grained menderbelt. "The coarse-grained menderbelt is actually somewhat of a transition between typically braided systems and the classical mendering systems", (Richard, 1983). It passes through the wadi area alongside the axes of the Plain and extends to Al-Rawdah in the north boundary of the region.

The coarse-grained menderbelt displays sand and gravel with almost no mud accumulation on the southern part of the study area, while sand pebbles and predominantly silt are displayed in point bars. In the down stream of this channel most of finer materials such as silt, clay and fine sand are spread out. In case of high floods only fines such as silt and clay spreads along the channel sides forming levees. All fines silt, clay and fine sand are considered the major source for the wind deposits in form of loess.

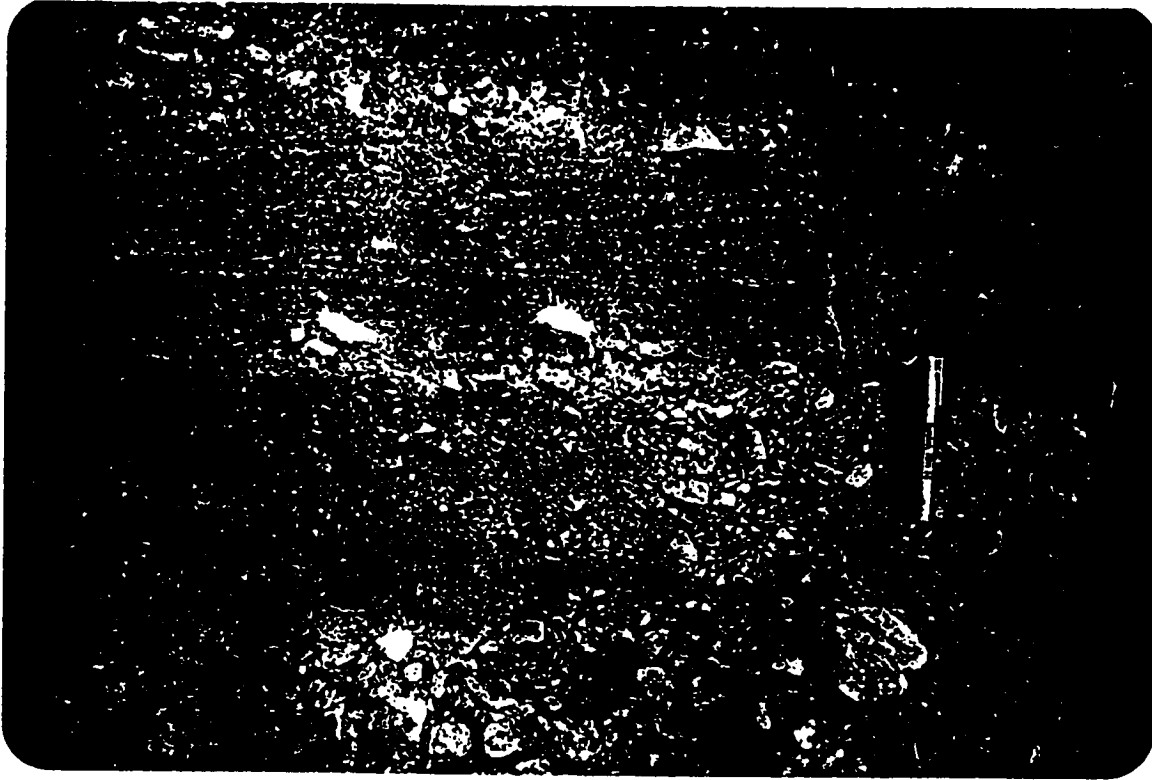
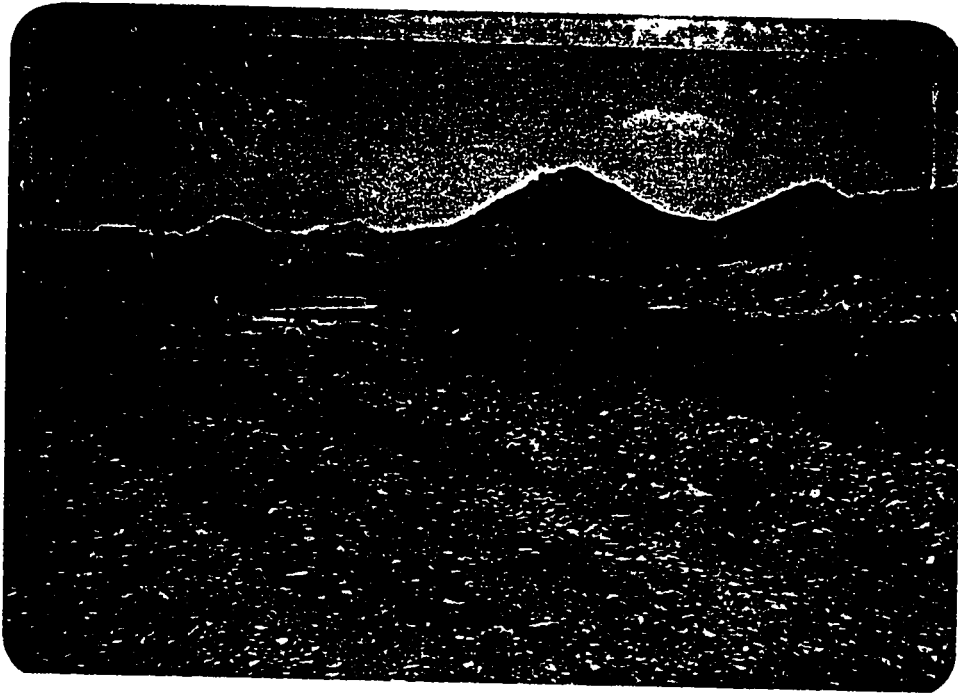


Plate 4.5 : Granular soil of graded bedding form. The gravelly soil in the bottom, while sandy soil is in the top. Indicated scale is 13 cm.



Plate 4.6 : The repeated layering system of water and wind-laid deposits as found in Wadi Area. Loess, wind-laid, interbedded by imprecator water laid deposit. Indicated scale is 13cm.

a)



b)



Plate 4.7.: Coarse-grained  
Minderbelt as shown  
in a) Southern part,  
and b) central part  
of the study area.

The study area is frequently subjected to moderate annual rainfall. In such condition, the water will not be sufficient to cause flash floods or even a fan, including its different zones. The coarse sediments are deposited in the upper fans portions only while sand and silt accumulations are deposited in most of the study area and more specifically the wadi area as indicated in the block diagram Fig.4.1. The recognition of water-laid deposits is shown in Table 4.1.

#### *4.1.3.3 Wind Deposits*

The study area is an arid to semi arid region which is characterized by the absence of moisture during the no rainfall period. This phenomena permits much eolian transport of sediment during the no rainfall period. Those sediments are dominated by eolian silt accumulation and evaporate deposits with some sand accumulations. These sediments are of well sorted particles and most grains are quartz.

The existance of the mountains in the east and west and partially in the southern part affects the prevalent blown wind. The wind often blows from north-east to south-west into the mountains which present a barrier to the wind, causing it to slow down and drop its sediment load as loess deposits. These loess deposits are either from the primary loess or secondary loess which are deposited

**Table 4.1: Recognition of Water-Laid Deposits**

Adopted after Glennie 1970

---

- a) Commonly calcite-cemented, or locally cemented by gypsum or anhydrite.
  - b) Many grains coated with hematite.
  - c) Conglomerates may be common, and sometimes with several cycles of deposition that lack a sand-size fraction at the top of the cycle (deflation of the sand and silt).
  - d) Presence of mud-flow conglomerates.
  - e) Sharp upward decrease in grain size (in case of graded bedding structure).
  - f) Common presence of imbricated pebbles and sand cross-stratification.
  - g) Great variation in bulky forms due to variation in transporting distance.
  - h) Common presence of different coloured particles due to variation in their parent rocks.
  - i) Clayey deposits are commonly stiff with no vertical holes and with low permeability.
-

mainly by wind and transported by water over a short distance (Krynine and Judd, 1957).

A wide spread of wind deposits is observed in the wadi area, consisting mainly of horizontal stratified loess. The wind laid deposits exist with a variable thickness with respect to the location in which it is deposited. Loess deposits are concentrated mainly in the wadi area while it may exist in a thinner thickness within or beyond the mountain base areas. The existence of slope, terraces and the long period between two successive rainfall or floods effect the occurrence of this fine soil in a specific location. Within the wadi area, the loess deposits accumulate in higher thicknesses more than the alluvial deposits due to the long period of time at which wind operates with no water deposits interrupting. Near the mountains the opposite is true, since little amount of water is sufficient to wash all the accumulated fines down to the wadi. Table.4.2 summarizes the general recognition of loess deposits. The block diagram(Fig.4.1) indicates the general repetitive nature of wind and alluvial deposits in the middle (Plate 4.6) and sides areas as will also be shown in the developed soil profiles in section 4.2.2.

#### **4.1.3.4 Chemical Deposits:**

The chemical effect on the available sediments is greatly restricted because of the relative dry status of both soil and atmosphere. The higher the water content the higher the chemical effect on deposits in form of leaching and oxidation. Oxidation has only a

**Table 4.2 : Recognition of a Wind-Laid  
Deposit as Loess Soil**

---

- Relative overall homogeneity of the sediment within a loess body.
  - Most of the grain are quartz, consisting of silt and silt-size particles of poorly graded distribution.
  - The grain size particles are rather uniformly sorted.
  - Fine sand and clay particles are present.
  - The cementation among the silt-size particles is related to a clay coating over these particles or due to the precipitation of chemicals leached by rain water.
  - The material is slightly or moderately plastic.
  - The permeability in the vertical direction is greater than in its horizontal direction due to the presence of long vertical tubes in the loess fabric as shown in Plate 4.8.
-



Plate 4.8 : Vertical root holes in the wind deposits,  
loess soil.

minor influence on arid fan sediments. In case of oxidation, such minerals as calcite is present as precipitation especially in wadi areas and lower parts of fans (Bull, 1972).

The precipitation of chemicals leached by rainfall causes adhesion between fines by hydrated cement, (calcite), while in case of quartz sands are slightly cemented by the presence of hematite. Fig. 4.2 shows the chemical deposits in form of calcite and iron oxide. Upon saturation this cementation is easily lost. Leaching can be recognized by looking at the increase in chemical cementation agent, such as calcium carbonate, with depth. In addition, leaching results in the formation of channels and sink holes in fine soil as depicted in loess deposits. Moreover, leaching can be recognized through the existence of aragonite with its needle forms as a calcium carbonate of surface up to 2.0m. When aragonite leaches downwards it changes to calcite which is known by its bulky form. In contrast, oxidation of surficial particles such as feldspathic rock fragments may be recognizable since such rock is easily weathered. Since the study area is arid to semi-arid region the accumulation of organic matter is of low level in soil horizon. The effect of chemical decomposition on the fine deposits is more than on the granular deposits, although it has generally a minor influence on deposits. This chemical influence may increase in case of high rate of rainfall or flood and when terraces are available because they reduce the run-off effect, subsequently increasing the leaching of the soil.

a)



b)

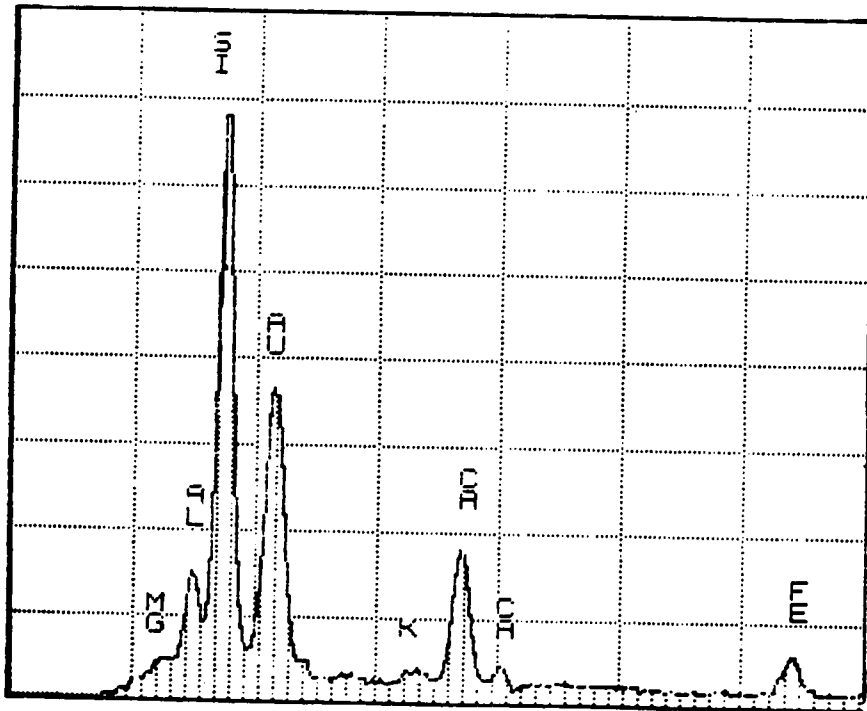


Fig. 4.2: Chemical deposits due to leaching as detected by a) SEM, and b) EDS.

## 4.2 SOIL DISTRIBUTION AND SOIL UNITS

### 4.2.1 General Definitions and Results:

The study area was divided into five regions in order to simplify the site investigation as shown in Fig. 4.3. Each region was investigated by inspection of the the following excavations: trenches (TE), foundations (FE) and pit holes (PH) which were found during the 4 monthes site exploration. Pit holes are mainly done by hand tool excavation for sewage disposal purpose (Plate 4.9). They have been excavated for new structures since there were no public sewage disposal system in the area. Each pit hole extends downward from 6m as a minimum depth up to more than 20m as a maximum depth. During the excavation of these pit holes, as well as other excavations, disturbed samples were obtained, the soil layers were inspected and the variations of layers thicknesses were recorded.

The above excavations were named stations. In each area selective stations were chosen . A total of 32 stations were chosen all over the five regions. From those selective stations 53 representative disturbed samples were obtained for classification purposes. Based on the above classification results, ten extra stations were chosen for obtaining final representative samples. These last stations were excavated by shovel which allowed for more inspection and comparison with the results of the previous classification analyses. The distribution of all the 42 stations is shown in Fig. 4.3. The final

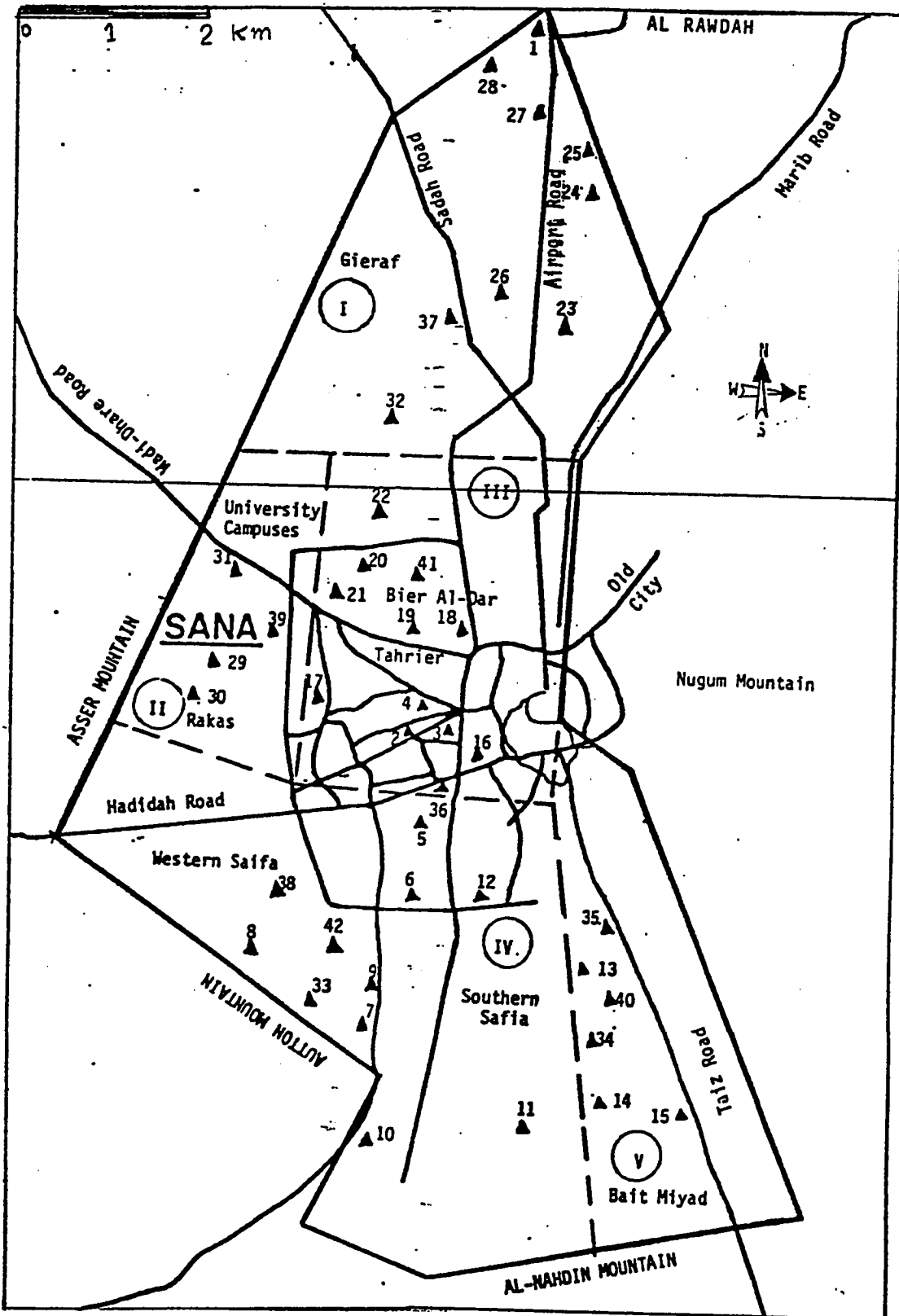


Fig. 4.3 : The regions and stations distribution

a)



b)



Plate 4.9 : The pithole station as depicted from:  
a) the ground surface showing the variety  
in the excavated soils.  
b) Inside the pithole showing the continuity  
of light brown sandy silt, loess.

representative samples were 11 undisturbed samples (US) of block type and 4 disturbed samples (DS). These samples were transported to King Fahd University of Petroleum and Minerals (KFUPM) where classification tests as well as other tests were carried out as indicated earlier in chapter three.

In the vicinity of seven stations out of the last ten stations the auger drilling tests were done and further inspections were carried out. The field standard penetration test (SPT) was carried out in these seven stations at different levels up to a maximum depth of 6.5m bellow the surface. One or two SPT were carried out in each area.

Table 4.3 indicates the locations of stations and the obtained samples from each station along with their depths. In addition, it indicates the index properties and soil classification of each sample. Both Unified Soil Classification System (USCS) and American Association of State Highway and Transportation Officials system (AASHTO) were used to classify the studied soils. Appendix B-1 through B-6 show the tables and figures used in the soil classification according to both systems. The USCS was used as a primary system in this present study. the geotechnical data results shown in the following chapters were arranged and organized according to the different soil units that were classified according to this system.

Table 4.3: Locations of the Obtained Samples and Their Classification

Area #	Station #	Location Description	Index Properties				Soil Classification		Layer Thickness (m)	General Comments
			Sample #	Depth (m)	Wc %	LL %	PL %	USCS		
I	1	Sewage line excavation along the airport road near Al-Mashriq House	1	1.5	10	--	--	SP	A-3(0)	Samples are disturbed (DS) obtained from trench excavation.
			2	3.0	8	--	--	SP	A-1-b(0)	
			3	4.0	12	20	16	SP-SM	A-1-b(0)	
23	Giraf, near Al-Madani House	10	3.5	10	--	--	MG	A-1-a(0)	DS obtained from pit hole (PH)	
		11	4.5	18	--	--	SC	A-7-6(6)		2.0
24	Giraf, near Abd Al-Kader's House	34	3.5	11	--	--	GM-GH	A-1-a(0)	>4.0	DS from PH
25	Giraf, beside Al-Hizami House	35	5.0	13	--	--	SP	A-1-a(0)	3.0	DS from PH
26	Giraf, the north side of Al-Thaura Garden	45	5.0	12	--	--	GM	A-1-a(0)	4.5	DS from PH
		46	1.5	13	--	--	GM	A-1-b(0)	0.8	
27	Giraf, west to Al-Shaif Mosque	47	1.5	10	--	--	GM	A-1-a(0)	>3.0	DS from PH
28	Giraf, south to Al-Thaura Football Yard	48	4.5	9	--	--	SM	A-1-b(0)	>1.0	DS from PH
32	Giraf, north to Yamaia Airlines	49	5.0	9	--	--	GM	A-1-a(0)	2.3	DS from PH
		50	2.0	11	29	24	ML	A-4(6)		
37	Giraf, in the Water Company Yard	61	2.0	11	28	22	ML	A-4(4)	1.2	SPT was carried out. DS+US were obtained and sent to KFUPM
		62	2.5	12	--	--	GM	A-1-a(0)		
29	Rakas Farm	16	1.8	16	62	25	CH	A-7-6(8)	2.0	DS from PH.
		18	3.9	5	--	--	GM	A-1-a(0)		
30	Rakas Farm	19	2.0	14	34	29	ML	A-4(5)	1.8	DS from PH
31	South to the University Fence	20	2.0	5	31	24	ML	A-4(4)	2.0	DS from FE
		21	4.0	--	--	--	GM	a-1-a(0)		
39	Rakas, west to the Secondary School	65	3.0	6	--	--	GM	A-1-a(0)	>2.5	Transported to KFUPM

(Table 4.3 continued)

2	Tahrir Center near Flag's position	4	2.5	8	--	--	GM	A-1-a(0)	>1.0	DS from ET of sewage line
		5	2.0	9	--	--	SP	A-1-b(0)	0.8	
3	Tahrir Center, west to sout of Al-Mehda School	8	3.2	8	--	--	GP-SP	A-1-b(0)	>1.5	DS from ET of sewage line
		9	2.0	7	--	--	SP	A-3(0)	2.0	
4	Tahrir Center, in front of Hajar's House	52	2.0	10	--	--	SM-GM	A-3(0)	2.0	DS from ET of sewage line
		53	3.0	9	27	22	ML	A-4(3)	>1.5	
16	Zubairi Street, in front of Al-Moori House (Al-Durthi)	42	2.5	10	--	--	SH	A-1-a(0)	1.5	DS from PH
17	West to Al-Zorra'a Street in front of Al-Hamdani House	31	3.0	9	29	25	ML	A-4(5)	2.5	DS from PH. Dark lean clay found at lower depth
		32	4.0	24	51	27	CH	A-7-7(17)	0.8	
		33	5.0	5	--	--	GH	A-1-a(0)	>2.5	
18	Beir Al Dar in front of Al-Ansie House	7	2.5	19	30	28	ML	A-4(8)	2.3	DS from PH
19	Bier Al Dar in front of Al-Brakani House	13	3.0	20	29	23	SM	A-4(2)	3.0	DS form PH
		17	4.0	5	--	--	GP	A-1-a(0)	>1.0	
20	Bier Al-Shaif	14	2.5	21	29	23	ML	A-4(6)	3.0	DS from PH
21	Bier Al-Shaif (Al-Arshad)	15	3.0	24	33	29	CL	A-6(9)	3.0	DS from PH
22	Bier Al-Shaif, near Al-Takwa Mosque	51	2.5	30	39	31	ML	A-4(6)	2.0	DS from PH
36	Safia, within Arwa School	59	1.10	16	51	26	CL	A-7-5(15)	1.3	SPT was done and US obtained and sent to KFUPM
		60	4.0	12	40	22	CL	A-6(10)	>2.0	
41	Bier Al Shaif, within Atesha's School	68	1.8	8	28	26	SC-SH	A-1-a(0)	1.2	SPT was done, US was obtained and sent to KFUPM.
5	West to Arwa's School in front of Al-Ansi's House	27	6.0	18	33	23	CL	A-6(8)	>2.5	DS from PH
6	Safia, in front of Abud Al-Malik Al-Ashhi's House	28	2.5	20	31	21	CL	A-4(5)	>4.0	DS from PH
		29	2.0	10	--	--	SM	A-3(0)	0.9	
		30	1.0	21	43	26	CL	A-6(11)	1.1	

IV

(Table 4-3 continued)

7	Safia, near to National Police	6	3.0	15	29	22	ML	A-4(4)	>2.0	DS from PH
8	Safia, east to Al-Aki Mosque	22	4.0	8	33	23	ML	A-4(6)	>3.5	DS from PH
9	Safia, beside Al-Girfa Embassy	23	3.0	9	32	26	ML	A-4(7)	1.3	DS from PH
10	Safia, Hada near Al-Kastimi House	36	5.0	7	--	--	GW	A-1-a(0)	4.0	DS from PH
11	Safia, near President House Gate	41	1.8	10	29	24	ML	A-4(6)	1.5	DS from PH
12	Safia, near Al-Gouth in front of Hydan House	24	2.0	11	28	22	ML	A-4(4)	1.3	DS from PH
		25	3.0	10	--	--	SP	A-1-b(0)	>1.8	DS from PH
33	Safia within Alawi's land near al-Gasous's land	54	0.7	14	45	25	CL	A-7	1.1	SPT was carried out and US obtained and transported to KFUPM
		55	1.8	21	29	27	ML	A-4(5)	1.2	
		56	4.0	10	30	27	ML	A-4(6)	>1.5	
38	Safia within Ghamthan's Land	63	2.0	15	25	20	ML	A-4(3)	2.0	SPT was carried out and US obtained and transported to KFUPM
12	Safia within Al-Ghalli's land	64	4.5	12	29	21	ML	A-4(4)	2.3	US from FE
		68	1.5	8	29	23	ML	A-4(4)	1.2	
13	Safia, behind Athban's Showroom (Al-Gawla)	37	5.0	4	--	--	GW	A-1-a(0)	5.0	DS from PH
14	Bayt Miyad, east to Tarqu's School	38	6.0	9	--	--	SW	A-1-b(0)	>2.5	DS from PH
		39	2.0	7	--	--	SP	A-1-b(0)	1.2	
15	Bayt Miyat in front of Bayt Miyad Mosuq	40	2.0	7	--	--	GW	A-1-a(0)	3.0	DS from PH
35	Tais Str. behind Nauman Mutails Bldg.	67	4.5	15	31	22	ML	A-4(7)	1.2	SPT was done, US was obtained and transported to KFUPM
34	Bier Aubaid, in front of Abud Alla Al-Ansi's House	57	2.5	6	--	--	SW	A-1-b(0)	0.6	SPT was done, US was obtained and transported to KFUPM
		58	3.0	5	--	--	GW	A-1-a(10)	1.5	US was obtained from ET and transported to KFUPM
40	Bier Aubaid, within Al-Haurash's School	66	2.5	7	31	--	ML	A-4(5)	0.8	

DS: Disturbed Samples

US: Undisturbed Block Sample

PH: Pit Hole

TE: Trench Excavation

FE: Foundation Excavation

SPT: Standard Penetration Test.

#### 4.2.2 Soil Profiles:

Fig. 4.4 shows the sections that are taken in different directions. The legend of the chosen profiles is shown in Fig. 4.5. The longitudinal section A-A was taken from south to north through the wadi area along the axis of the plain while B-B and C-C were chosen in a curved manner to follow the direction of water flow. Both curves B-B and C-C gave approximately the same profile, so only B-B is shown herein. The slope which causes the water flow is the component slope of both the plain slope from south to north and the extended slope of the mountain heels from west to east. The transfer cross sections 1-1 , 2-2 and 3-3 were chosen from west to east near the mountain bases and crossing the wadi region. Figs. 4.6 - 4.10 show these sections which define the soil profiles. "The term soil profile indicates a vertical section through the subsoil that shows the thickness and sequence of the individual strata. The term stratum is applied to a relatively well-defined layer of soil in contact with other layers of conspicuously different character. If the boundaries between strata are more or less parallel, the soil profile is said to be simple or regular. If the boundaries constitute a more or less irregular pattern, the soil profile is called erratic" (Terzaghi and Peak, 1967). In the shown profiles, the specified thicknesses of any soil layer were recorded as detected from each station. In between the stations the continuity of the layers were approximately interpolated. The shown profiles indicate certain features that may be generalized. A relatively regular layering profile is evident. Terzaghi and Peak (1976) indicated that the flood-plain and wind-plain deposits

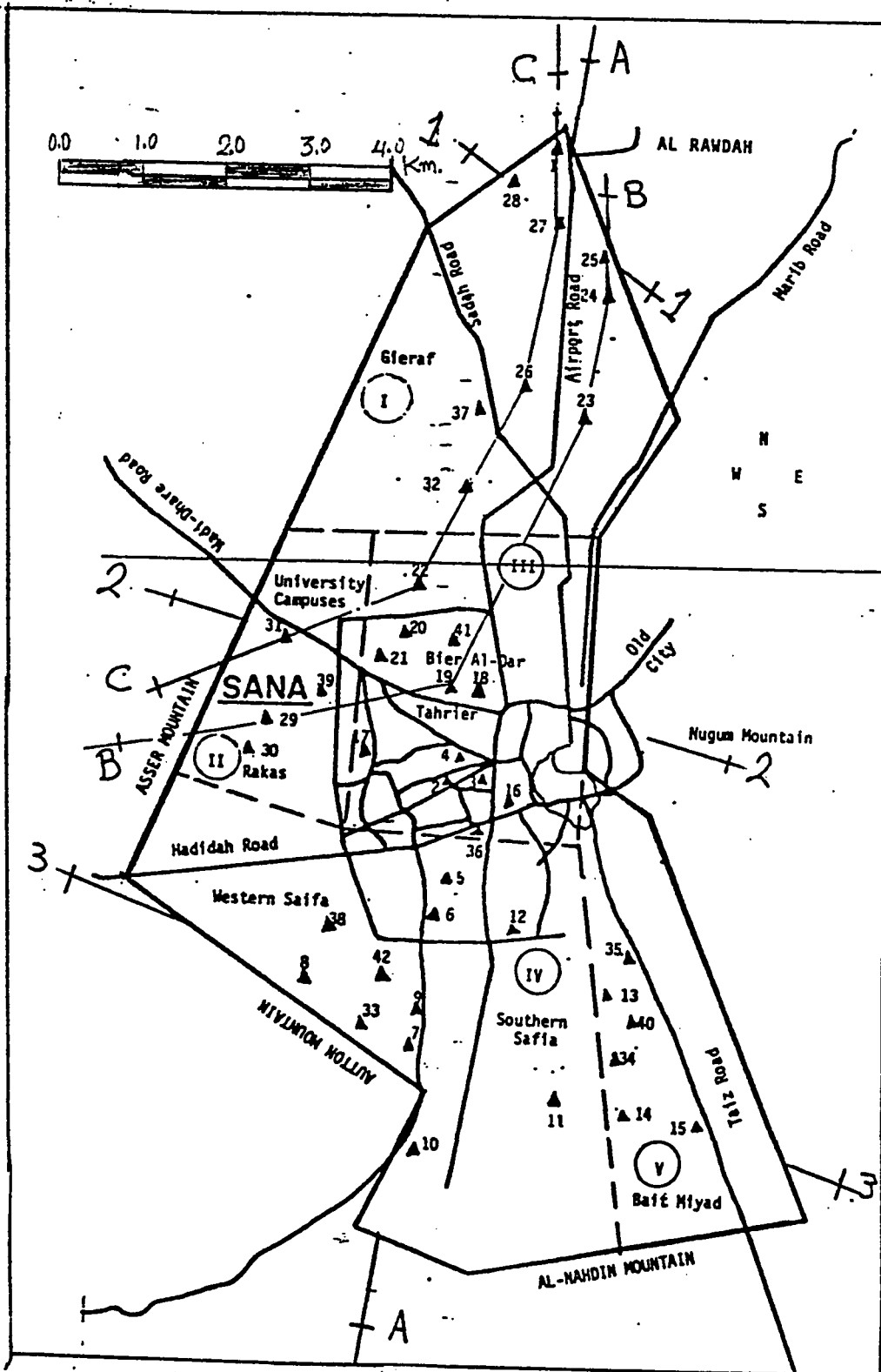


Fig. 4.4 : Longitudinal and transfer cross-sections.

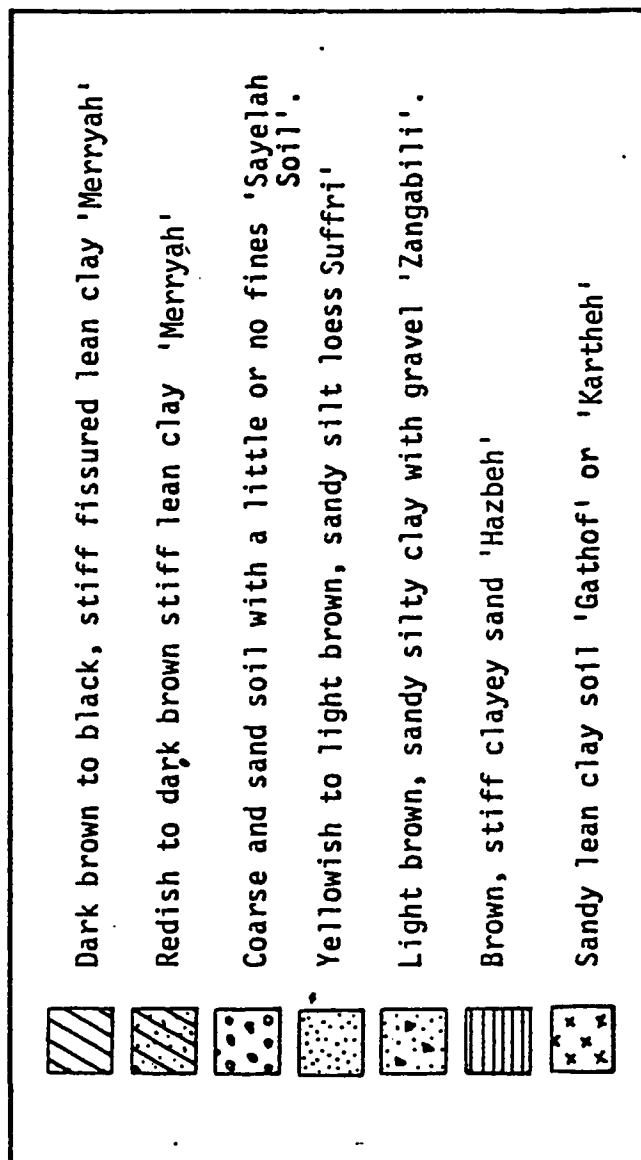


Fig. 4.5: Legend of the different soil profiles  
(Figs. 4.6 - 4.10).

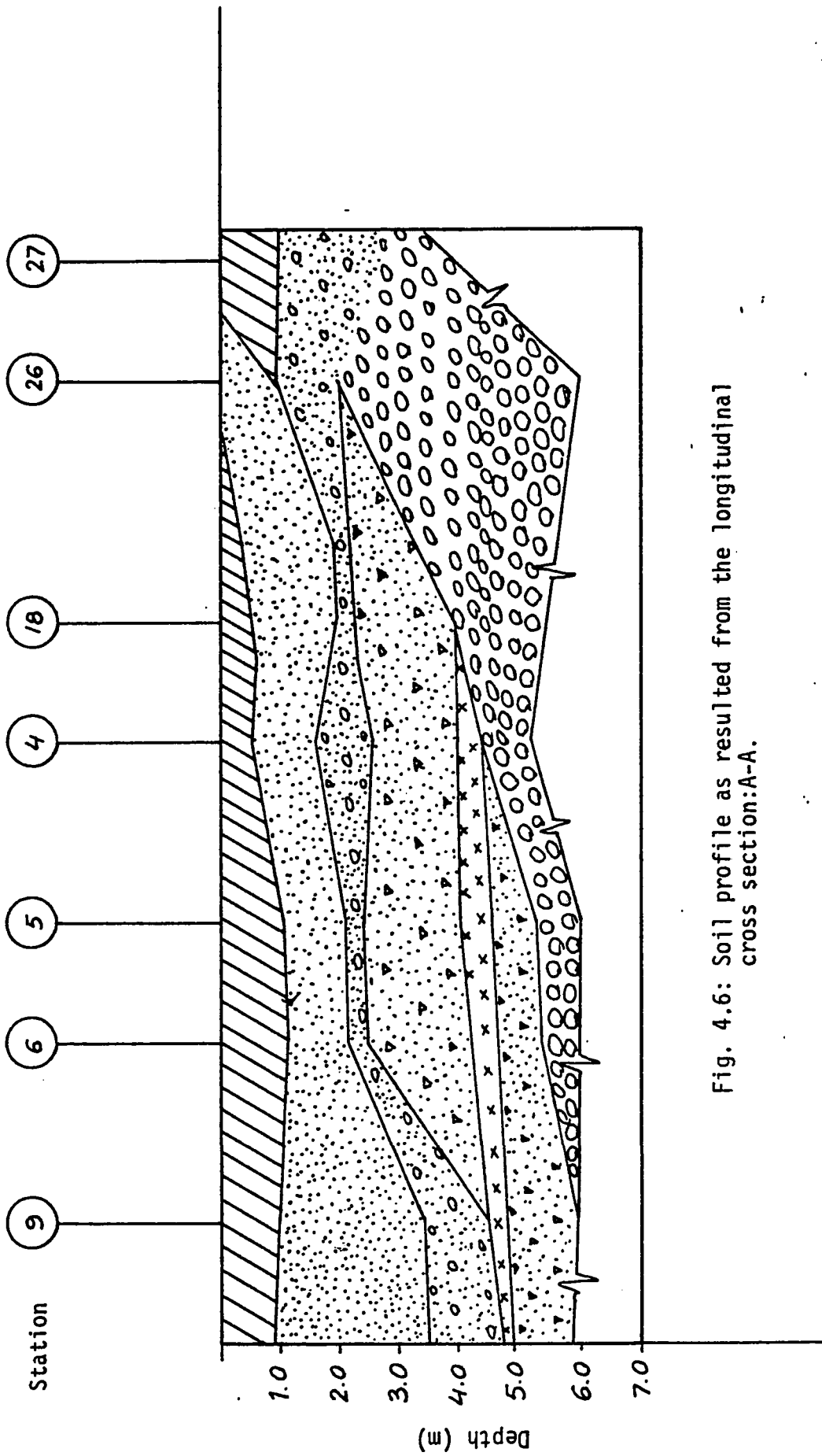


Fig. 4.6: Soil profile as resulted from the longitudinal cross section:A-A.

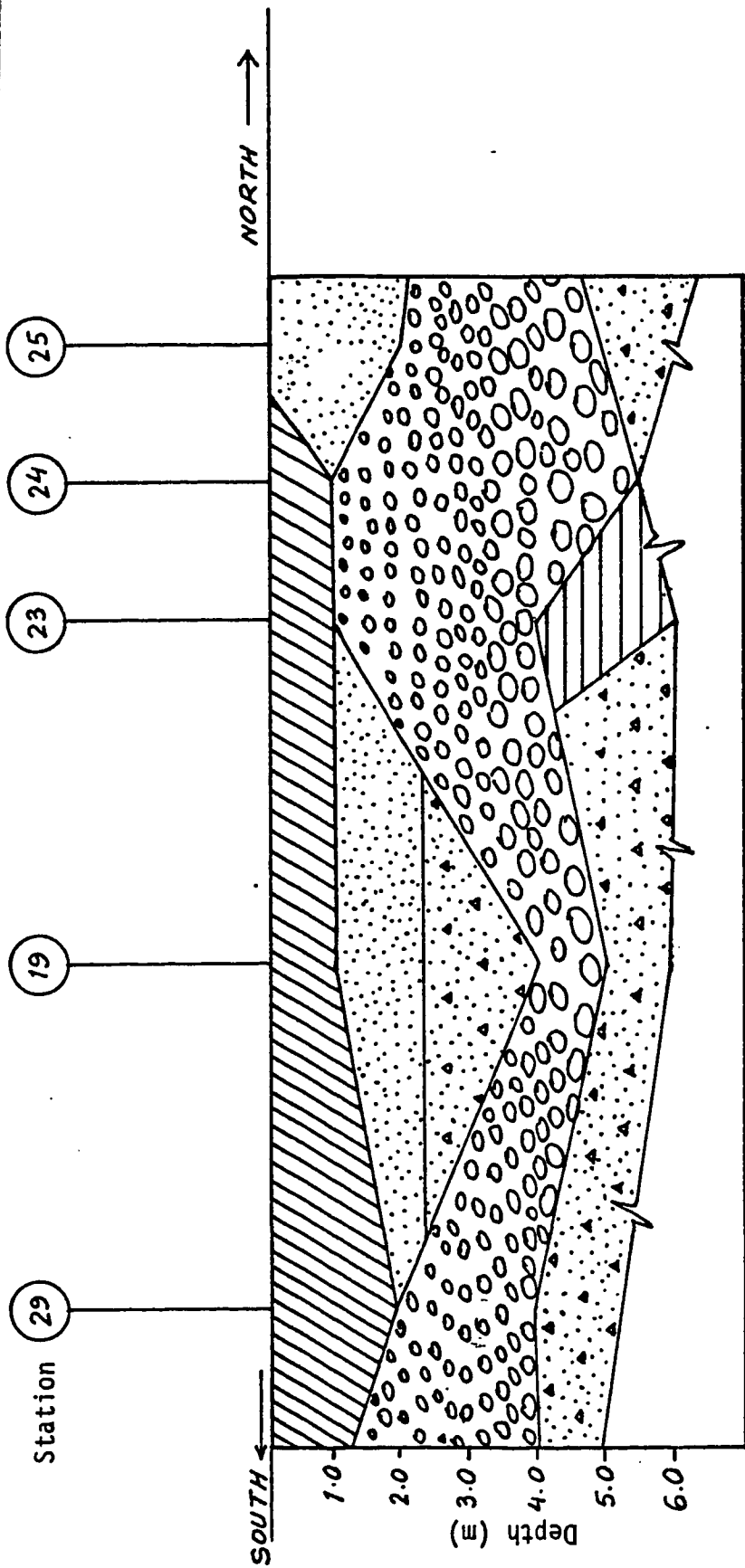


Fig. 4.7: Soil profile as resulted from the curved cross section: B-B.

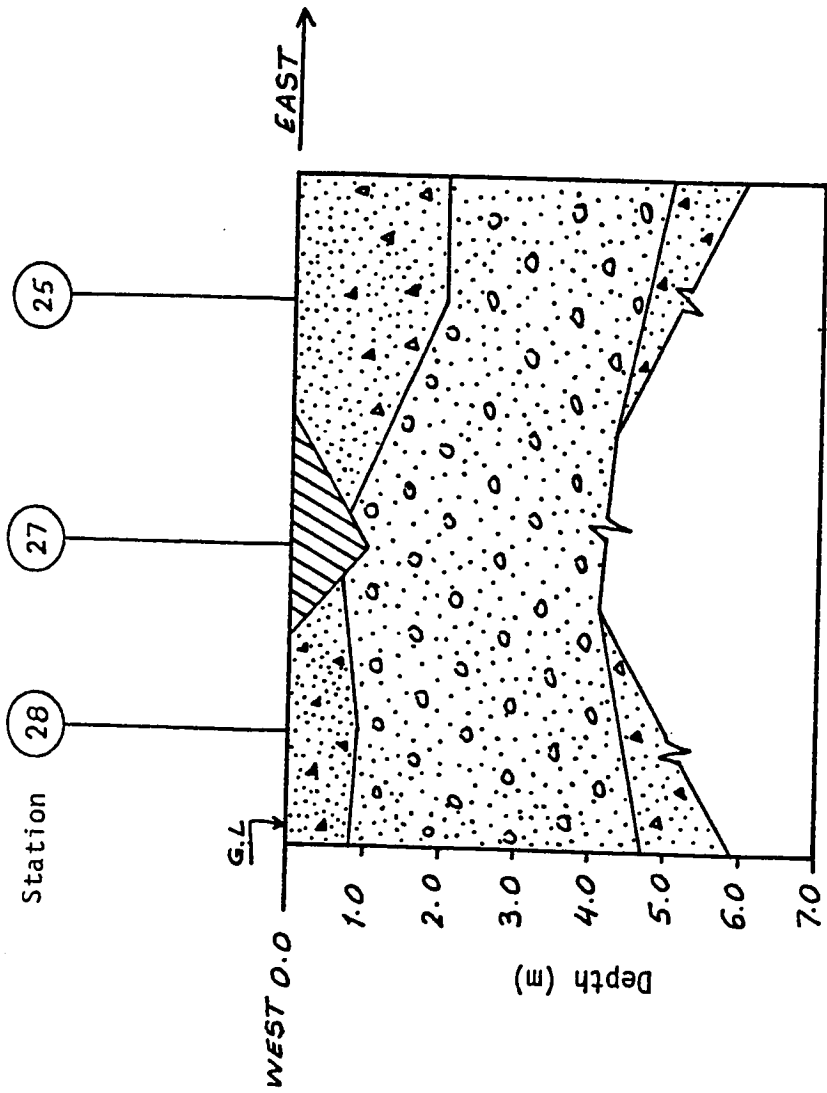


Fig. 4.8: Soil Profile as resulted from cross section: 1-1.

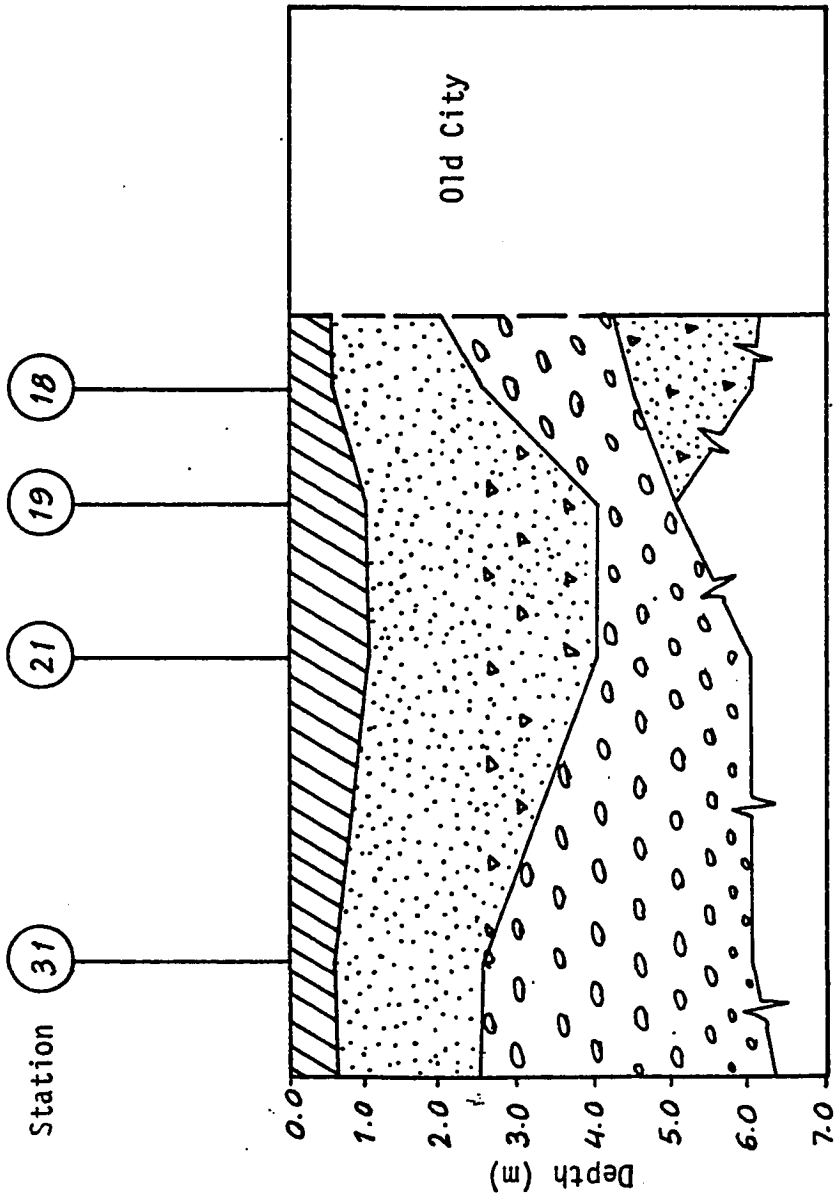


Fig. 4.9: Soil profile as resulted from cross-section: 2-2.

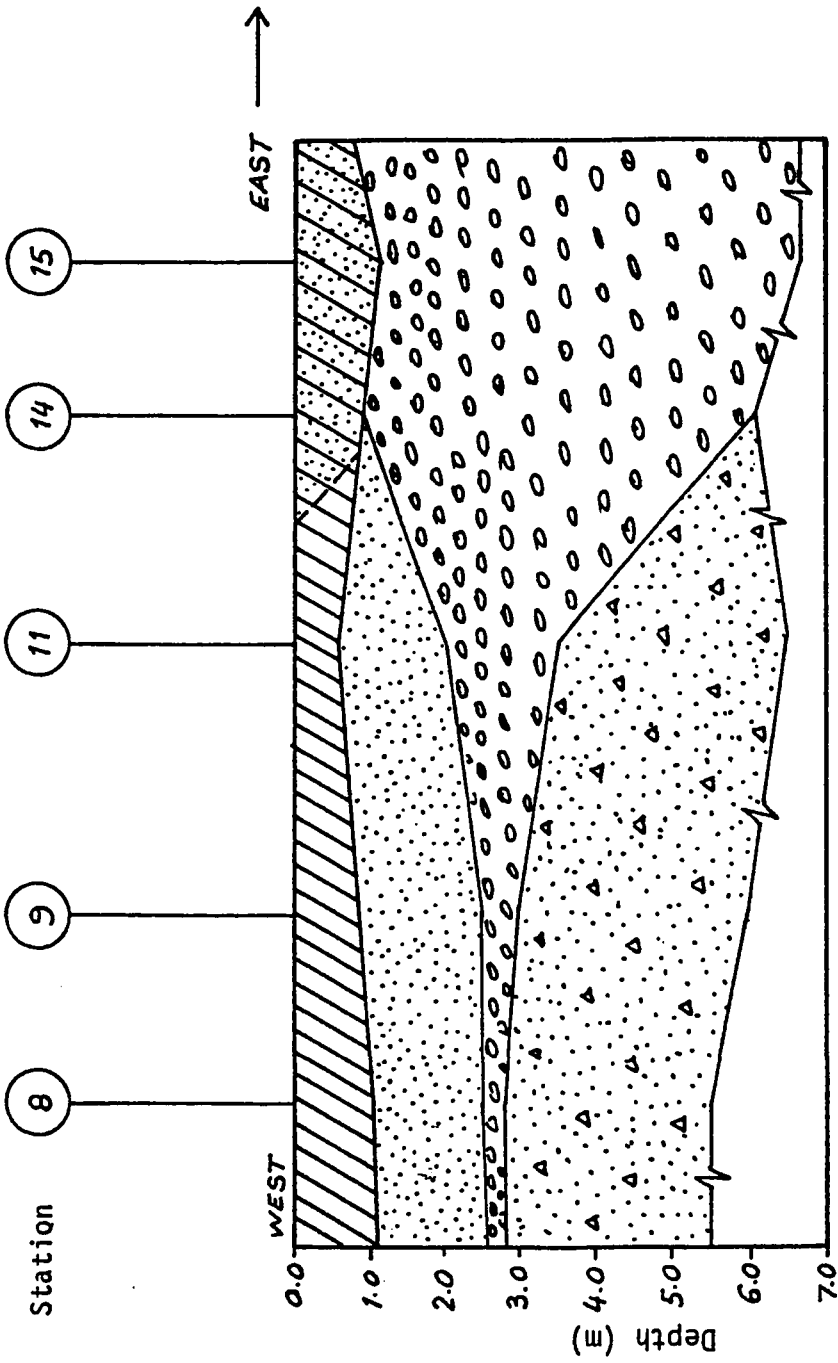


Fig. 4.10: Soil profile as resulted from the cross-section 3-3.

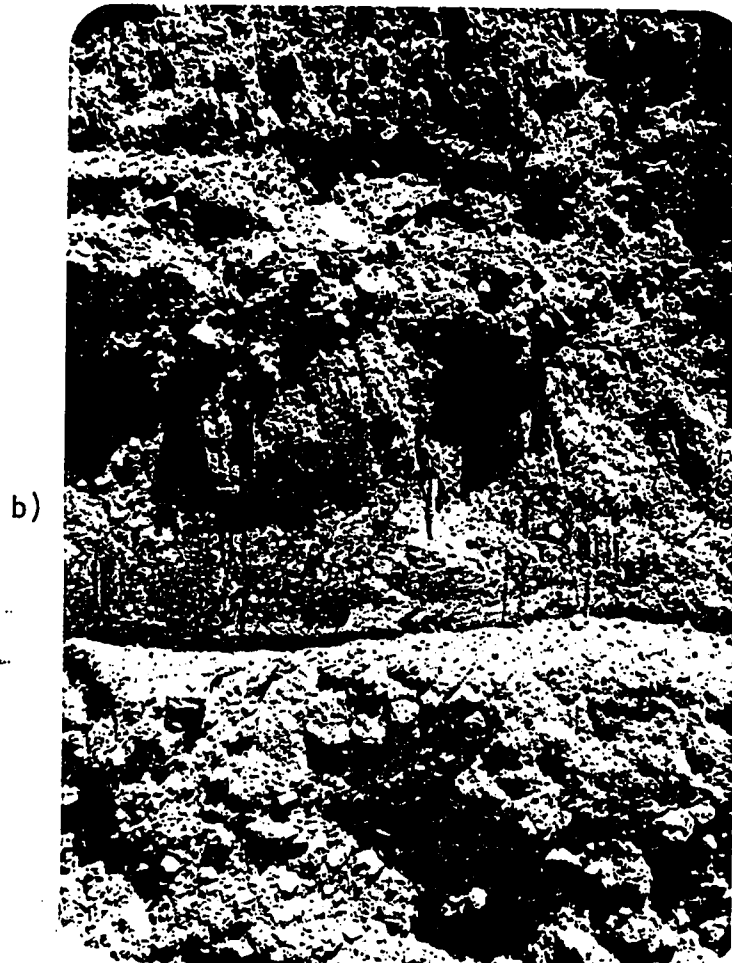
and those formed in large bodies of standing water are likely to have a fairly regular soil profiles. Considering the feature and topography of the study area, as a relatively flat plain subjected to both wind-laid deposits and water-laid deposits, the soil profile of the study area is expected to be relatively regular. Indeed, the observed soil profiles in some of the inspected stations were found to be fairly regular, as shown in Plates 4.7, 4.10. Unfortunately, this regular profile is not uniform all over the area and is affected by the area location. The observation and the results of the soil classification indicated also that there is no uniform layering system all over the area. For example the granular soil was commonly found to exist within the mountain's heel and near the streams (area I, II and V), while the fine materials occupy most of the central area (area III and IV) extending from the south to the north except the bed of streams that cross the central area. This distribution of soils are affected by many factors such as streams distribution, mountains and heels locations, faults, wind direction, man-made effect, etc. are the factors that contribute greatly in the soil formation and distribution in the vertical direction as well as in the horizontal direction.

Generally, down to 6.0m below the surface two different profiles are common. The first one consists of alluvial granular deposits in form of a layer of sandy gravel with a little or no fine material. Near the base of mountains this profile is over-laid by a clayey top layer. Boulders and rock fragments may be found within this



Plate 4.10 : Relative regular soil profile:

- a) longitudinal section
- b) vertical section



profile. Seldomly, the coarse layer may be separated into two layers by a thin layer of fine wind- deposit as shown in Fig. 4.6. The second profile is the most common within the wadi area. It consists of wind-laid deposits of light brown sandy silt and sandy silty clay layers. These layers are interbedded by one or two water-laid deposit layers in form of silty clayey sand with gravel as shown in Figs.4.6 and 4.10 and Plates 4.7 and 4.10. The wind deposits, loess, may reach 4.0m in thickness, while the granular layer may reach 1.0m. The appearance of wind-laid deposits layers interbedded by water-laid deposits was found to be repeated as going deeper within the wadi area as detected from some inspected deeper stations (down to 20.0m).

On the other hand, erratic profiles were observed in certain locations where the continuity of a certain stratum has been disturbed locally by channel fillings, man-made effect, existence of a depression filled by different deposits or any other bodies of foreign material as shown in Fig. 4.7 at station 23. In addition, the localized erratic stratum were also observed in some stations that were found along the boundaries between rock and soil or coarse and fine materials specially in area I, II and V.

#### 4.2.3 Soil Units:

A main objective of soil classification is to define similar soils into groups so that the complexity of the testing procedure to

characterize soil nature and behavior may be reduced or better directed. The classification data resulted from the representative samples shown in Table 4.3 indicated that different soil units are available in the study area including both fine and granular soils. Moreover, most of these samples were in dry state having different water content. The water content of the granular soil varies from 4 to 10 percent while it varies from 10 to 24 percent in case of fine soils. Most of the fine soil tends to absorb water. This tendency is due to the environmental conditions of the semi arid region of having an annual rainfall less than the rate of evaporation, and the very low water table which exists at about thirty meter below the ground surface. Generally based on the Unified Classification System, the soil in the study area are divided into the following units:

- i) Well to poorly graded gravel with sand 'Sayleh Soil'.
- ii) Well to poorly graded sand with gravel 'Sayelah Soil'
- iii) Silty clayey sand with gravel 'Hazbeh'
- iv) Sandy lean clay or lean clay with sand 'Karteh or Gathoef'
- v) Sandy silt 'Sauffri Soil'
- vi) Sandy silty clay with gravel 'Zanjabeli'
- vii) Lean clay 'Merryah'

The above soil units represent about 90 percent of the study area and the remaining 10 percent represents rare soils which were found in very few locations such as clayey sand, fly cemented ash

and others.

These different units show the complexity and the difficulty in defining the characteristics of each type. The existence of such soils in a wide range of variety is related to the variety in depositional system and the source of these soils. The granular soil is related to the alluvial deposits such as the alluvial fan and wadi alluvium deposits, while the fine soil is related to both alluvial deposits in the form of flood-plain and the wind deposits in the form of loess deposit. Some fine soils were deposited by water action and then reworked by wind action.

The relative density of the cohesionless and cohesive soils were determined based on Terzaghi and Peck (1967). Correlation with the N-values of standard penetration test and field identification are shown in Appendices B-7 and B-8.

1) *Light Grey, Well to Poorly Graded Gravel With Sand, Sayelah Soil:*

This soil unit exists commonly below the first two meters and extends downward varying in thickness from 0.6 meter in the the southern part of the study area to more than 4.0 meters especially in the northern and eastern area as shown in Fig. 4.6 and Fig. 4.10. In nondeveloped areas near the mountain it exists directly at the top surface.

The bulky shapes of the particles of this soil are rounded or subrounded with almost smooth surface due to the effect of weathering and transportation on these particles as observed mostly in area II and V at stations 14, 15, 34 and 39 (Fig. 4.10). In few locations some particles were found having subangular bulky forms. These granular particles were derived from the surrounded mountains and transported for short distance before deposition as found mostly in area I at station 25 and 26 (Fig. 4.6 and 4.7). The texture of this soil covered a wide range of grain size and substantial amounts of all intermediate particle size. The maximum size of the particle was found to have a diameter of about 25 centimeters. Plate 4.5 shows the variation in size of such soil indicating the smooth surfaces, maximum size, the bulky shapes and the existence of some fines.

The average standard penetration number for this soil stratum over a depth of four meters was 40 (station 34). According to this the soil will be in dense state. In few stations this soil unit was found to be very dense, having a greenish to dark grey colour and bulky shapes of subangular forms as appeared in station 16, 24 and 26. Fig. 4.11 gives the bore log for SPT that was carried out on station 34.

The gradation curves of four representative samples selected from four stations were plotted in Fig. 4.12. The percentages of sand and gravel vary from 26 to 45 percent, and from 52 to 69 percent respectively. Less than 5 % of the fine grained soil was found. The

Depth (m)	Soil Description	Wc %	SPT Blows per 15 cm			N
1	<input checked="" type="checkbox"/> Very stiff, dark brown to redish brown, lean clay	14	10	18	5	33
2	<input checked="" type="checkbox"/> Light grey, dense, poorly graded sand with gravel	8	8	15	20	35
3	<input checked="" type="checkbox"/> Light to bluish grey, dense well graded gravel with sand. Pebbles and boulders may be present.	7	15	20	29	49
4						
5						
6						
7						

 SPT

 Disturbed Sample

Fig. 4.11: Bore Log of Station # 34

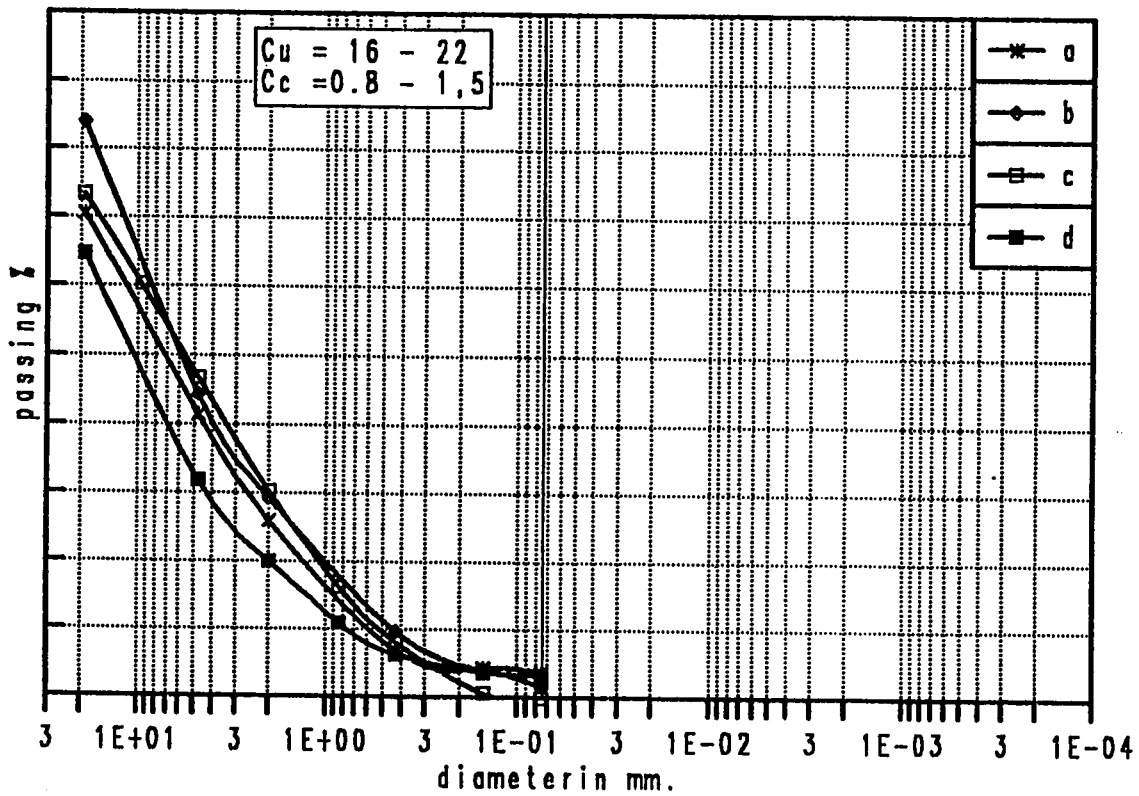


Fig. 4.12 : Gradation curves of well to poorly graded gravel with sand (Soil unit 1).

- a) Station # 13 at 5.0m.
- b) Station # 17 at 5.0m.
- c) Station # 34 at 3.0m.
- d) Station # 39 at 3.5m.

values of the coefficient of uniformity ( $C_u = D_{60}/D_{30}$ ) and the coefficient of curvature ( $C_c = (D_{30})^2/D_{60} \times D_{10}$ ) are shown in the figure.

The natural water content of this soil is very low because of the large voids among the coarse-grained particles and the small surface area of such soil. Moreover, the ground water table is very low at a depth of about 30.0 meters below the ground surface and the height of capillary rise is low due to the large voids between the solid particles. The natural water content of this soil unit varies from 3 to 9 percent. In case of the very dense granular soil (Station 26) it reached 12 percent.

The AASHTO classification for this soil is A-1-a(O). According to this system the soil consist predominantly of stone fragments, gravels and sand with or without a well graded binder fine material. This type of soil is excellent material as a subgrade and borrow material. In addition, it possesses high California Bearing Ratio (CBR), and subgrade modulus (k).

This type of granular material is locally named by Sayelah soil and characterized of being hard as individual particles, very good soil as foundation base and posses good drainage properties.

## 2) *Grey, Well to Poorly Graded Sand with Gravel 'Sayeleh Soil':*

This soil unit exists in a thin layer either above the gravelly soil (unit one) or in an individual layer having a thickness of about 0.3m to 0.8m as shown in Plate 4.5. The particles are smooth, hard

and rounded. The percentage of gravel exceeds 15 percent, while fines does not exceed 5 percent. The well graded sand with gravel has a wide range of grain size and substantial amounts of all intermediate particle sizes as found in stations 14 and 16 (Fig. 4.10), while in case of the poorly graded sand with gravel the texture is completely different. It has either a wide range of particles with some missing intermediate sizes or almost a uniform texture, having particles approximately of the same size as observed in Stations 1, 2, 3, 14 and 34. The maximum particale size was about 5 centimeters. Plate 4.5 shows the bulky form and size variation of the particales besides the graded bedding formation. The top part of the plate shows this soil unit as detected from station 34.

The common observed colour of this unit is light bluish grey. But, in some stations like stations 1 and 16 a dark grey to black sand was found. This variation in colour is related to the mineralogical composition of the sand itself. The bluish grey sand is rich with quartz while the blackish sand is rich with maghemite and augite.

The grain size distribution curves of some representative samples are plotted in Fig.4.13. The texture contents included 17 to 25 percent of gravel and 73 to 82 percent of sand. Most of this sand contents are of the medium and fine sand. As a result of that, the drainage condition of this soil unit is less than that of soil unit 1. But, this ability of holding water is still low. The detected natural

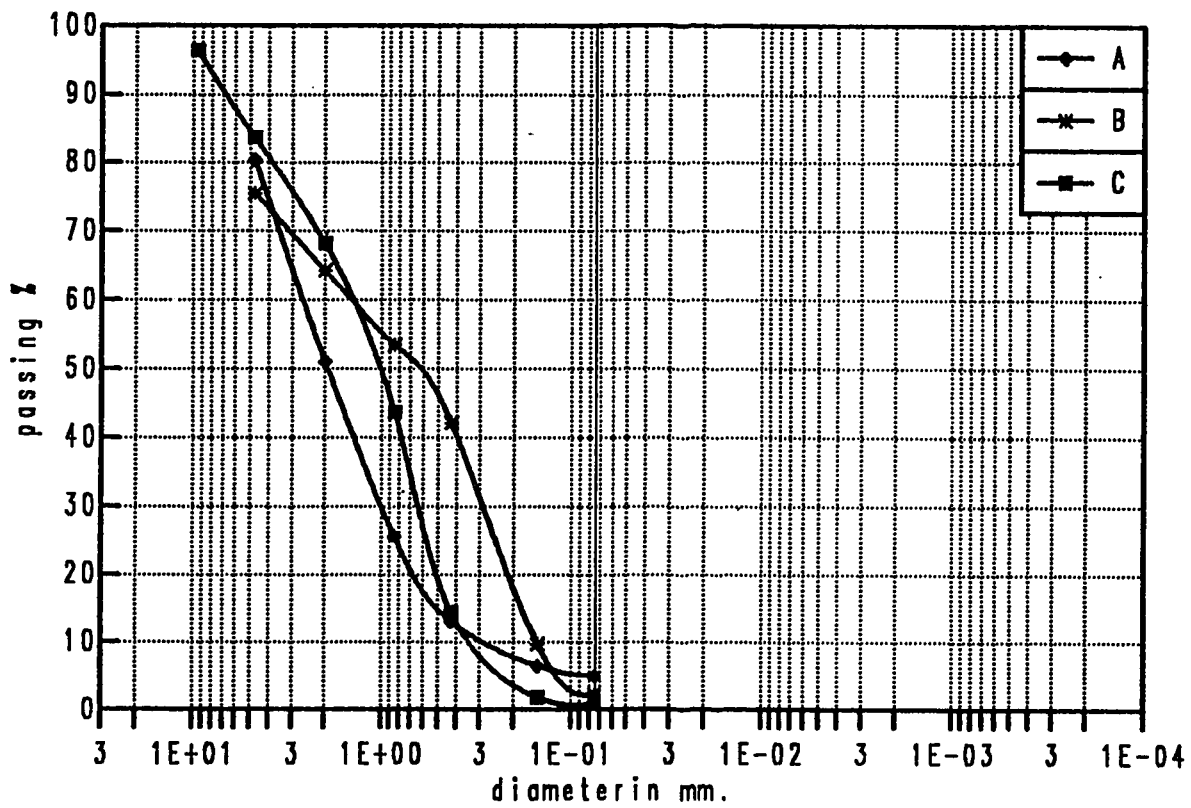


Fig. 4.13 : Gradation curves of well to poorly graded sand with gravel (Soil unit 2).  
 a) Station # 14 at 6.0m.  
 b) Station # 12 at 3.0m.  
 c) Station # 34 at 2.5m.

water content was a minimum of 5 percent and a maximum of 10 percent.

Reverting to Fig. 4.11, the recorded SPT value of this unit was about 35. This soil unit exists in a dense state according to correlation with SPT value. In fact this condition is valid for the well graded sand with gravel and the deeper poorly graded sand with gravel, while in case of the surficial poorly graded one, it is medium to dense.

According to AASHTO system this soil was classified as A-1-b (0). It consists predominantly of coarse sand with or without a well graded binder. It is good to excellent as a subgrade and borrow material. The CBR and subgrade modulus of this unit are high, but less than those of unit 1. Locally this type of soil is also known as Sayelah soil.

3) *Light Bluish Grey, Silty Clayey Sand with Gravel or Brown, Silty Clayey Gravel with Sand, 'Kartheh'*:

This third and last coarse-grained soil unit includes two types of soil according to the gravel and sand percent. They are grouped here under one unit because of the similarity in the group name with respect to the fine contents (silt, clay) and to simplify the identification of the coarse-graded soils. Moreover, the choice of the representative sample may affect the percentage of the coarse fractions due to the existence of the boulders and coarse gravel. The description of these two sub-units is as follows:

*i) The light Bluish, Grey, Silty Clayey Sand with Gravel:*

It exists widely in area IV at 1.5m to 3.0m below the ground surface having a thickness varying from 0.3m to 1.2m, as occurred in stations 4, 33 and 41 etc. It exists mostly between two layers of loess as shown in Plate 4.6 and Figs. 4.6 and 4.10 specially in area IV. The granular particles which are hard and almost rounded were coated by the fine soil causing a weak to moderate cementation throughout the total matrix. Plate 4.11 shows a scanning electronic photomicrograph of relatively undisturbed sample taken from Station 41. It indicates the distribution of fine particles among the smooth rounded granular particles and thus, approach conglomerates. The maximum particle size is about 3 cm.

*ii) Dark Brown, Silty Clayey Gravel with Sand:*

This second sub-unit was found at a depth of about 1.5m below the ground surface extending downward to a depth more than 6.0m in the most observed stations 16, 26, 27 and 37 especially at area I as shown in Fig. 4.6 and 4.8. The colour of the individual coarse particles vary from white, green, brown to light grey, etc. according to the geological origin of these particles. In spite of the great variation in colours of the individual particles, the dark brown colour relatively represents the colour of the total

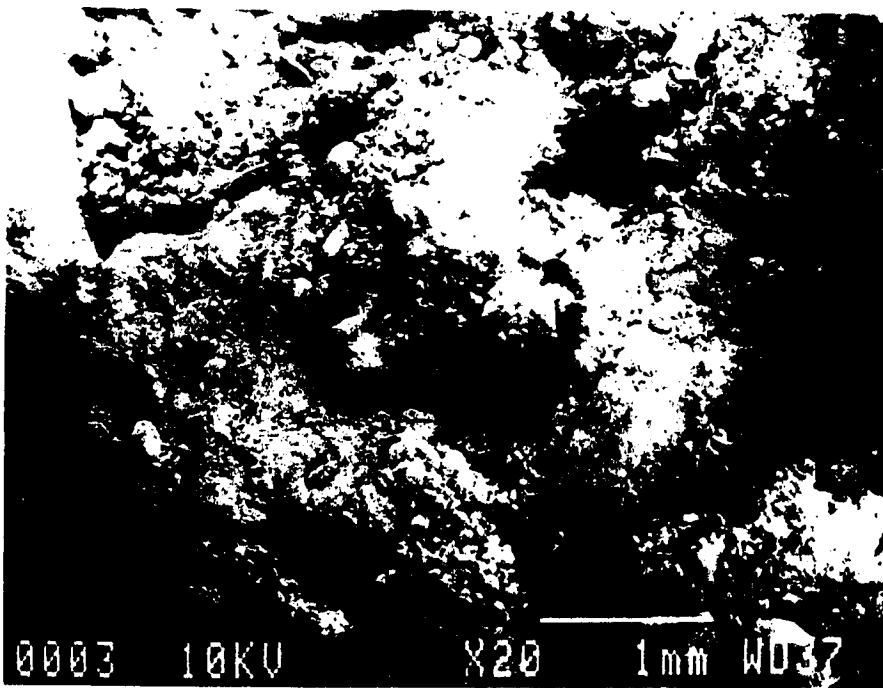


Plate 4.11: Conglomerates of sand, silt and fine particles interaction.

matrix of the coarse and fine contents. The bulky shapes of the coarse grained included both sub-rounded and sub-angular. The texture of this sub-unit contains boulders of a maximum size of about 25 cm.

The gradation curves of the previous two sub-units are plotted in Fig.4.14. Both exhibit a gap grade in fine sand zone. Coarse sand is predominant in the silty clayey sand with gravel soil as indicated from Curve a, meanwhile, the gravel content is predominant in the silty, clayey gravel with sand soil as shown from Curve b. In addition, Curve b exhibits more fine contents than Curve a.

The variation of the liquid limits and plastic limits of this unit are in the range of 28-32% and 25-27% respectively, while the natural water content varies from 5 to 15%. The existence of the silt and clay particles coating the coarse fraction of this unit besides its low natural water content enables it to adsorb water, whenever it is available, and holds it more than the previous two coarse soil units.

Figs.4.15 and 4.16 indicate the SPT values that were obtained from Station 41 and 37. The N value of the silty clayey sand with gravel (Sub-unit 1) is 30 while it is 60 for the silty clayey gravel with sand (Sub-unit 2). According to these values, the density of Sub-unit 1 is

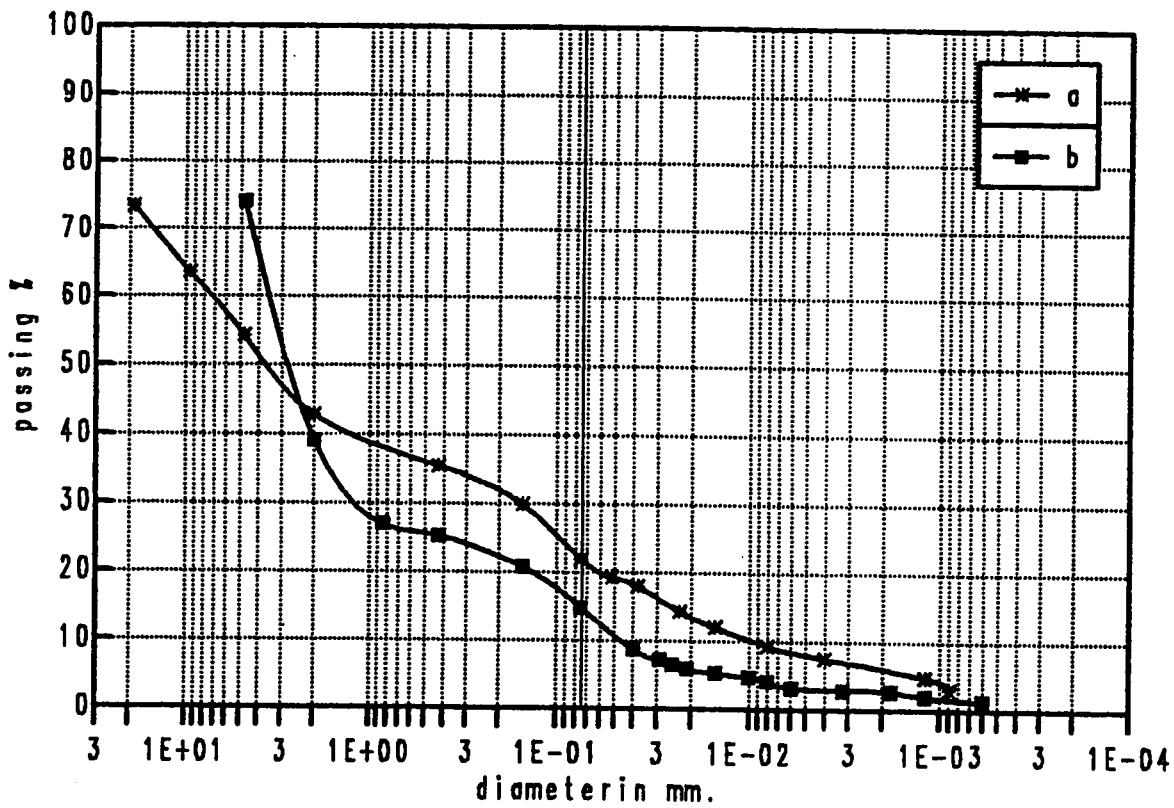


Fig. 4.14 : Gradation curves of sand and gravel with silty and clayey matrix (Soil unit 3).  
 a) Silty clayey gravel with sand, Station # 37 at 3.5m.  
 b) Silty clayey sand with gravel, Station # 41 at 2.0m.

Depth (m)	Soil Description	Wc %	SPT Blows per 15 cm			N
1	<input checked="" type="checkbox"/> Medium to stiff dark brown lean clay with odder	18	2	4	5	9
2	<input checked="" type="checkbox"/> Stiff light brown sandy silt soil	15	4	6	13	19
3	<input type="checkbox"/> Medium to dense, bluish grey, silty clayey sand with gravel	9	6	11	19	30
4	<input checked="" type="checkbox"/> Stiff light brown sandy silty clay with gravel	14	6	7	10	17
5						
6	<input checked="" type="checkbox"/> Very stiff sandy silty clay with gravel	12	6	20	15	35
7						

 SPT

 Undisturbed Sample

Fig.4.15: Bore Log of Station # 41

Depth (m)	Soil Description	Wc %	SPT Blows per 15 cm			N
	Fill soil	-	8	14	13	27
1	Yellowish sandy soil with gravel	11	27	27	-	54
2	Very dense, dark to greenish silty clayey gravel with sand and boulders, upto 25 cm in diameter.	12	25	29	31	60
3						
4						
5						
6						
7						

 SPT  
  Disturbed Sample  
  Undisturbed Sample

Fig. 4.16: Bore Log of Station # 37

medium to dense while it is very dense in case of Sub-Unit 2, where the water content affects greatly the density state specially the soil of Sub-unit 2.

The silty clayey sand with gravel was classified according to AASHTO system as A-1-a(0) but the silty clayey gravel with sand was classified as A-1-b(0), because of the higher fine contents of the later one. Both types are excellent soils as a subgrade and borrow materials. Such soils exhibit an excellent to good drain condition and high subgrade reaction modulus. This soil unit is locally named by 'Hazbeh'. It is known to be very stiff due to the rock fragments which it contains, that is why it is desirable to be the base of foundation for those moderately high buildings. The shear strength and the compressibility of the the silty clayey sand with gravel was studied in details, since this soil occurs widely and it is possible to get undisturbed sample for simulated stress strain and deformation tests.

#### 4) *Sandy Clay Soil 'Gathoef or Kartheh' :*

The USCS divided the soil in this unit into two types; sandy lean clay and lean clay with sand as indicated in Appendix B-6. These two sub-units are affected by the percentage of soil that is retained on No.200 sieve and the percentage of the sand and gravel. The description and index properties of the above two soils are as

follows:

*i) Stiff, Light Brown, Sandy Lean Clay :*

This soil is defined as sandy lean clay since percentage of the coarse fraction, retained on No.200 sieve, is equal or more than 30% and the percentage of sand is greater than gravel percent. This fine clay soil exists in a thin stiff layer having a thickness 0.4 - 0.8 m as shown in Fig. 4.6. It occurred in stations 4 and 36 at 3.0m - 4.0m below the ground surface, while in some locations such as Station 6, it was found at 1.0m below the ground surface. It may be a modified clayey loess deposit which were remolded by water. That is why it exists between loess deposits. This soil is a stiff according to its SPT value that was obtained from station 36 as indicated in Fig.4.17. This stiff consistency is related to the high cementation contents in form of calcite ( $\text{CaCo}_3$ ), and the densification due to the environmental conditions and the overburden pressure. This is why it exhibited a slightly overconsolidation stress history behavior.

The small fraction particles are strongly cemented forming particles with sharp edges and rough surfaces. These cemented particles are white limestone and yellowish brown sandstone of a light weight. The maximum size of the cemented particle is about 3.0 cm when the accumulated fines are washed away. The gradation curve of a representative sample obtained from station 36 at the depth 3.6m is shown in curve A in Fig.4.18.

Depth (m)	Soil Description	Wc %	SPT Blows per 15 cm			N
1	<input checked="" type="checkbox"/> Dark fill soil with gravel	13	7	12	8	20
2	<input checked="" type="checkbox"/> Light brown, dense, sandy silt	11	7	9	7	16
3	<input checked="" type="checkbox"/> Silty clay sand with gravel	9	-	-	-	-
4	<input checked="" type="checkbox"/> Sandy silty clay with gravel	12	6	7	10	17
4	<input checked="" type="checkbox"/> Stiff, light brown sandy lean clay	12	6	14	15	29
5						
6						
7						

 SPT Undisturbed Sample

Fig. 4.17: Bore Log of Station # 36

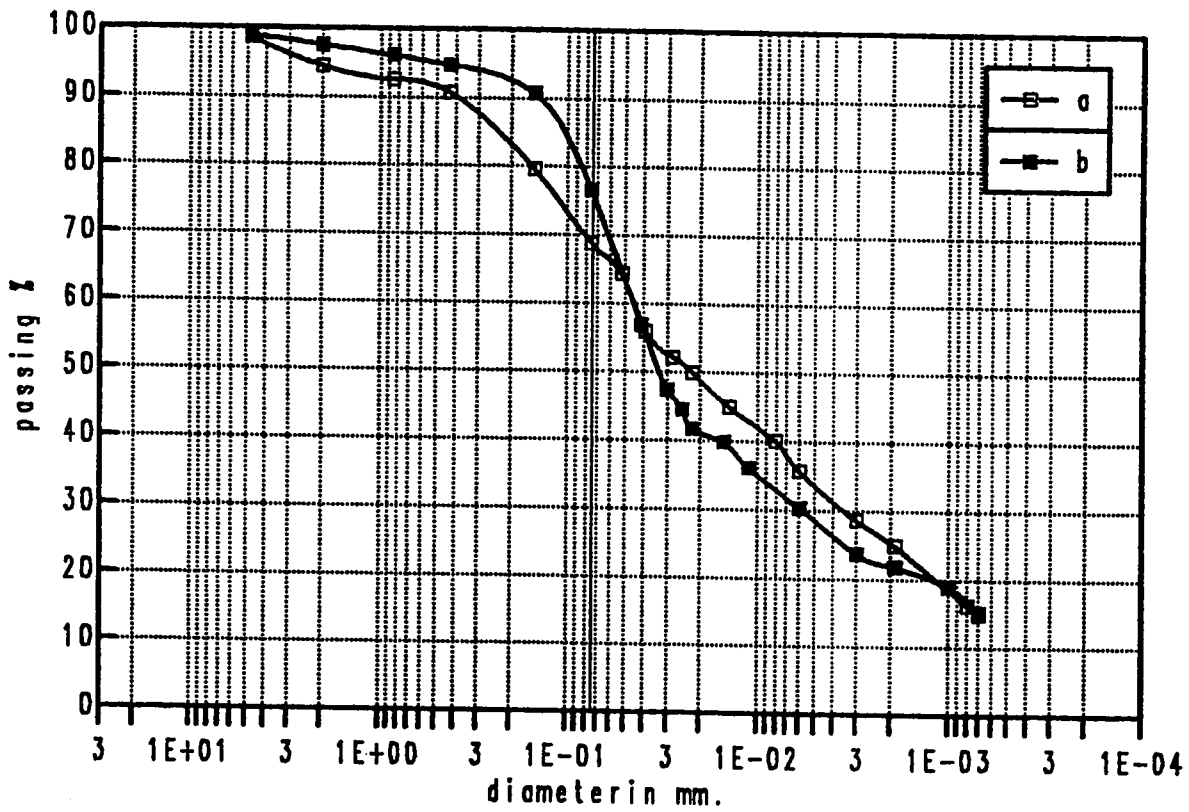


Fig. 4.18 : Gradation curves of sandy clay soils  
(Soil unit 4).  
a) Station # 36 at 4.5m.  
b) Station # 35 at 5.0m.

The soil gradation distribution curve shows a low percentage of the coarse sand contents. The percentages of the silt and clay are 42 and 26%, respectively, while the percentage of sand is about 30% of which 20% is fine sand.

The index property including the liquid limits and plastic limits are in the range of 40% - 43% and 22% - 26%, respectively. This sandy lean clay soil is a medium plasticity clay according to the plasticity chart shown in Appendix B-2. The natural water content varies from 13% to 24%. This relative high variation is related to the effect of environmental conditions, the depth at which this sub-unit exists, the soil stratification, etc. The soil is in solid state since the natural water content is mostly below the plastic limit.

This soil is classified as A-6(10) according to AASHTO System. Its group index is approximately in the range 8-12. The typical material of this group is plastic clay soil. The material of such type usually has high volume change between wet and dry states (Spangler and Handy, 1982). It is fair to poor as a borrow material or subgrade soil. This stiff sandy lean clay soil is locally named by 'Gathoef or Kartheh' which is known as a difficult soil to be excavated by hand tool due to its stiffness.

*ii) Medium to Stiff, Redish Brown, Lean Clay with Sand:*

This soil is defined as a lean clay with sand. It occurred in Stations 6, 8 and 35 at 2.0m to 3.0m below the surface,

varying in thickness from 1.5m to 4.0m. It exists in a medium to stiff state according to SPT values that obtained from Station 35. The consistency condition was affected by the existence of boulders within this layer and water content at the time of testing. The stress history of this soil has been found to be a normally consolidated one.

The index properties including the liquid limit and plastic limit are 31% - 33% and 21% - 23% respectively and the natural water content is in the range of 11% - 20%. This soil was plotted just a little above A-line in the plasticity chart. This soil has high silt content of about 55 %. The characteristic of this soil is similar to those silty loess.

AASHTO classification system classifies this soil as A-4(7) which typically consists of non or moderate plastic silty soil, 75% or more of which usually passes the No.200 sieve (Fig. 4.18).

**5) *Medium to stiff, Reddish to Light Brown Sandy Silt Soil 'Suffri':***

This soil unit, covers most of the middle part of the study area (III, IV and part of I). Mostly it appears at about 1.0m below the ground surface extending downward up to 4.0m as found in stations 12, 20, 19, 38 and 41. Fig. 4.7 and plate 4.9-b show the existence of this soil unit with a relatively big thickness ( 3.0 to 4.0m ). In some locations the vertical continuity of this soil was interrupted by 0.3m - 0.8m thick layer of a silty clayey sand with gravel as found

in stations 5, 6, 8, 9, 30, 40 and 42 as shown in Figs. 4.6 and 4.10. Plate 4.12 indicates this layering system which occurs widely along the south-north centerline axes of the study area. This soil is known as wind deposits, loess. In some locations it was found directly at the surface as found in stations 25, 26 and 28 in area I (Fig. 4.6 and 4.7).

This soil unit is a normally consolidated soil with a high voids ratio and low unit weight. The dry unit weight is in the range of 1.27 - 1.45 gm/cm<sup>3</sup>. The top part of this soil, commonly 1.0m below the surface, exhibits a medium consistency and a lower dry unit weight while the lower part exists at 2.5m and extending downward exhibits a stiff consistency and higher dry unit weight. The increase in the density of the soil with increasing depth is related to the overburden pressure, the available layering system and the environmental condition in terms of cyclic drying and wetting. These factors helped in leaching the fine contents from the top layers downward into the bottom layer of this soil. The layering system helped greatly in the leaching process due to the existence of the silty, clayey, sand with gravel layer that seeps the suspended fines in the water easily. Fig.4.19 gives the SPT values that were obtained from station 33 which included the discontinuous layer of this soil unit. The N values of the upper layer varies from 8 - 14 while it varies from 16 - 26 in the lower layer.

The texture of the sandy silt soil includes high fine sand, silt



Plate 4.12 : Light brown sandy silt layer interrupted by silty clayey sand with gravel. Indicated scale is 13 cm.

Depth (m)	Soil Description	Wc %	SPT Blows per 15 cm			N
1	<input type="checkbox"/> Very stiff, fissured, dark brown lean clay with white traces.	14	9	10	11	21
	<input checked="" type="checkbox"/>					
2	<input checked="" type="checkbox"/> Light brown, medium sandy silt with koot holes traces.	12	3	4	6	10
	<input type="checkbox"/>					
3	<input checked="" type="checkbox"/> Grey, dense, gravel with sand	8	12	14	18	32
4	<input checked="" type="checkbox"/> Stiff brown sandy	12	5	8	9	17
	<input type="checkbox"/> Silty clay with					
5	<input checked="" type="checkbox"/> calcareous gravel	11	6	10	9	19
6	<input checked="" type="checkbox"/>	10	5	9	14	23
7						

 SPT

 Undisturbed Sample

Fig. 4.19: Bore Log of Station # 33

and clay contents. A sign of very thin roots and a great number of small holes are visible. The grain size analysis was carried out on three selected samples obtained from Stations 33 and 40 as shown in fig. 4.20. Comparing curve a with c, as they were obtained from the same station, we note that the deeper the soil, the higher the clay contents due to the leaching process and also the higher the coarse fraction due to the effect of environmental condition and depositional system.

The liquid limits and plastic limits of this soil are 29% - 34% and 24% - 29%, respectively. The water content is below the plastic limit in the range approximately 12% - 21%. This low water content besides the low clay contents and high cementation agent contents cause this soil unit to be relatively highly compressible upon wetting, as known about the loess deposit, although the classification of this unit according to USCS describes it as low to moderate compressible silty soil (Appendix B2). The colour of this soil is yellowish to reddish brown in most cases with light brown in relative dry state.

According to the AASHTO system this soil is classified as A-4(5). It is described as a non-plastic to moderately plastic silty soil with 75% or more passes the No.200 sieve. The variation of the group index is in the range of 4 - 7. This soil is described as a fair to poor material as a subgrade soil or borrow material and it is susceptible to frost action. It is locally named Suffri Soil and known by its relative high compressibility and moderate.

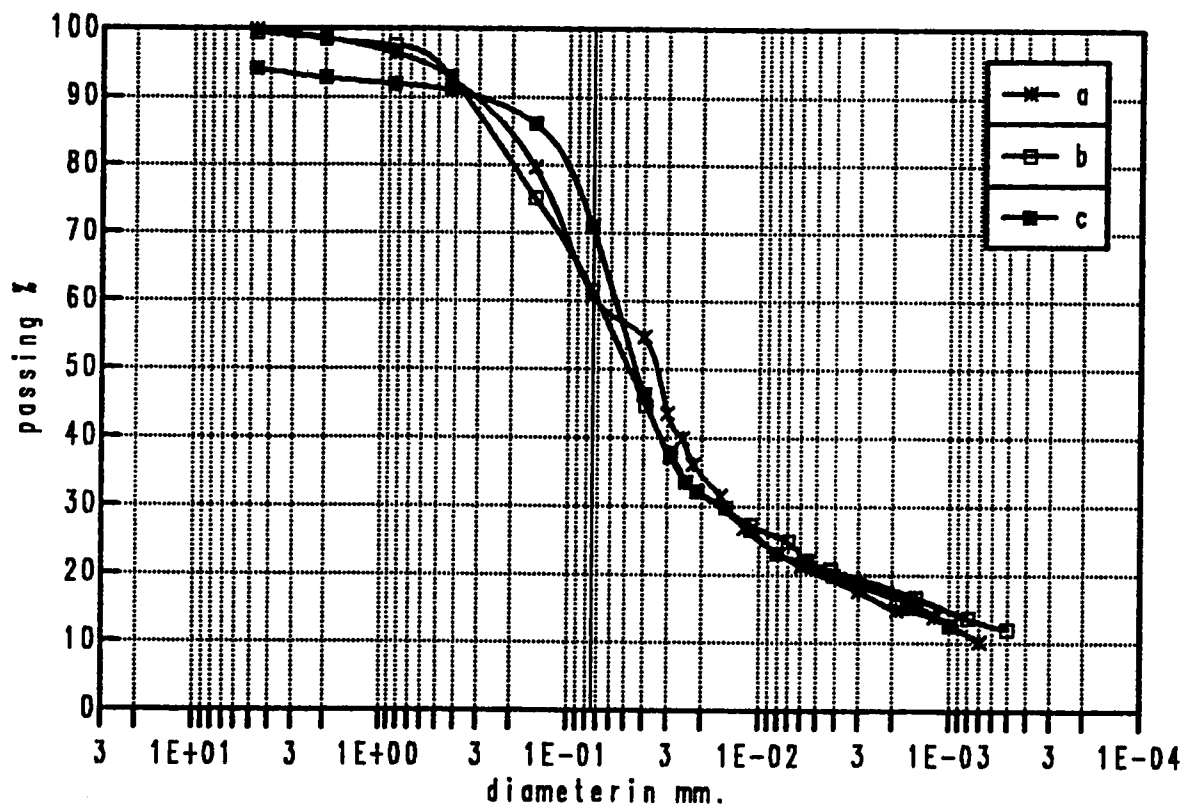


Fig. 4.20 : Gradation curves of sand silty soils ( Soil unit 5).

a) Station # 33 at 1.8m.

b) Station # 40 at 2.5m.

c) Station # 33 at 4.5m.

6) *Medium to Stiff, Light Brown Sandy Silty Clay with Gravel*

*'Zanjabeli':*

This soil unit is classified as a sandy silty clay soil with gravel since the percentages of the fines and gravel are greater than 30% and 15% respectively. It exists similar to Unit 5 at about 1.0m below the surface either in a continuous layer reaching 3.0m - 4.0m in thickness (Plate 4.9.b) or in a discontinuous layer interrupted by a thin granular layer as shown in Fig. 4.10. In some cases it may be found at the surface as found in station 28 as shown in Fig. 4.8.

There is a similarity between this soil unit and the previous one (Unit 5) not only in the location of the layers, but also in most of the features, properties and the depositional system.

The variation in the texture contents between this soil unit and Unit 5 led to a variation in the plasticity index and consistency state. The texture of the soil of this unit contains higher coarse fractions, specifically those well cemented sands in form of sandstone and limestone in the size of gravels with their rough surfaces and sharp edges to which the name Zanjabeli is related. Comparing the gradation curve of this soil unit, Fig.4.21, with Fig.4.20, this soil unit has a higher coarse fraction and a lower fine sand and silt contents. This reduction in fine contents resulted in reducing the plastic limit, 20% - 21%, with no significant change in the liquid limits, subsequently, the plastic index

increased to 5% - 7%. That is why this soil unit plots just above the A-line in the plasticity chart, subsequently it is classified as a clay soil according to USCS. The soils that plotted just a little above the A-line and deposited by wind action are identified to be silty loess soil as discussed by Gibbs and Holtz (1951).

Fine material plotted above A-line in the plasticity chart are classified as low compressible soil (CL). But, in fact, they are silty soils characterized of being sensitive to settlement when they are inundated. Such phenomenon was discussed and studied by Holtz and Gibbs (1951). They defined such soil to be a silty loess soil exactly similar to Nebraska loess soil. Fig.4.22 shows this sort of classification and identification that was used for sand, silt and clay of Nebraska loess soil. The gradation limits of each soil type and their zones are also indicated in the same figure.

The SPT values of this soil are higher than soil unit 5 by about 25 % which demonstrates the relative increase in the density of this soil as shown in Fig. 4.23. But, the consistency state of this soil is still medium in case of the upper layer and increases with depth from stiff state at 4.0m to hard at 5.5m below the surface.

The sandy silty clay with gravel soil, the sandy silt soil and the lean clay with sand soil are plotted in Fig.4.24 to compare them with other wind-deposited sediments after Peck, Hanson

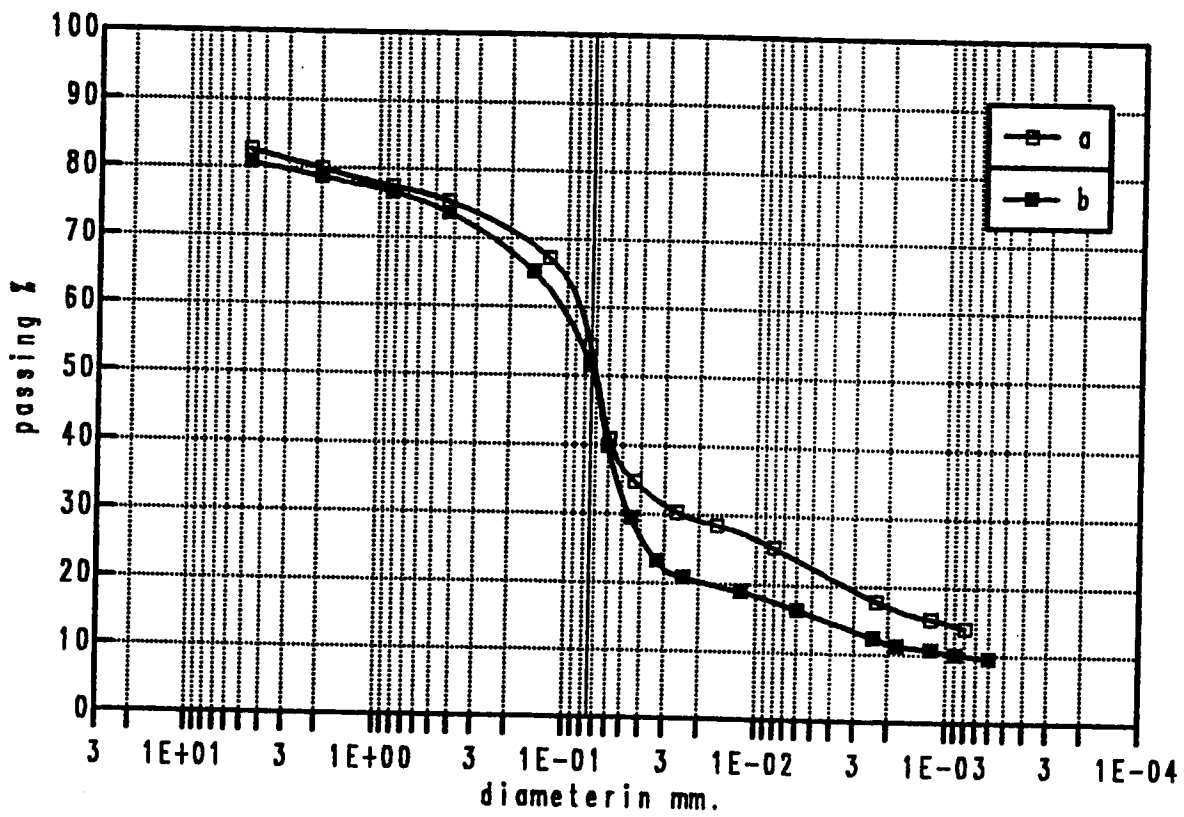


Fig. 4.21 : Gradation curves of sandy silty clay with gravel  
 ( Soil unit 6 )  
 a) Station # 36 at 4.5m.  
 b) Station # 35 at 5.0m.



and Thornburn, (1974). From this figure and the above discussion, these three soils are identified and classified as silty loess soils.

Following the AASHTO system this soil is defined as Unit 5 as A-4 (8), with no change in the description. Moreover, this soil unit is also known by the same local name as 'Suffri Soil' or by 'Zanjabieli' due to the existence of the sharp and rough gravelly particles.

7) *Very Stiff, Fissured Black, Lean Clay 'Merryah':*

This dark layer extends widely covering about 60% of the top part of the study area specially in agricultural regions. It extends downward from the surface mostly in a thin layer 0.4m - 1.2m thick at most stations as shown in Figs. 4.6 and 4.10 and the top part of Plate 4.7.b.

This soil is characterized by a black colour with considerable amount of white traces and fine roots as observed in most of the detected stations. In the southern eastern part, this soil has a dark brown colour either with little white traces and fine root or without as found in stations 14, 15, 34, 41, etc. as shown in Fig. 4.10. An earthy odour is noticeable in this soil due to the existence of roots.

Fissures and joints are predominant characters of this soil by which it can be identified besides its dark colour, white traces

Depth (m)	Soil Description	Wc %	SPT Blows per 15 cm			N
	<u>Dark, Stiff Fissured Lean Clay</u>	-	--	--	--	--
1	<input checked="" type="checkbox"/> Light brown to yellowish, medium to stiff sandy	15	3	5	7	12
2	<input type="checkbox"/> Silty Clay					
3	<input checked="" type="checkbox"/>		5	5	10	15
4	<input checked="" type="checkbox"/> Stiff, brown, sandy silty clay with calcareous gravel	10	12	10	12	22
5	<input type="checkbox"/>					
6	<input checked="" type="checkbox"/> Sand gravel with clayey silty matrix and some	8	12	16	26	42
7	<input checked="" type="checkbox"/> boulders		20	30	33	63

 SPT

 Undisturbed Sample

Fig. 4.23: Bore Log of Station # 38.

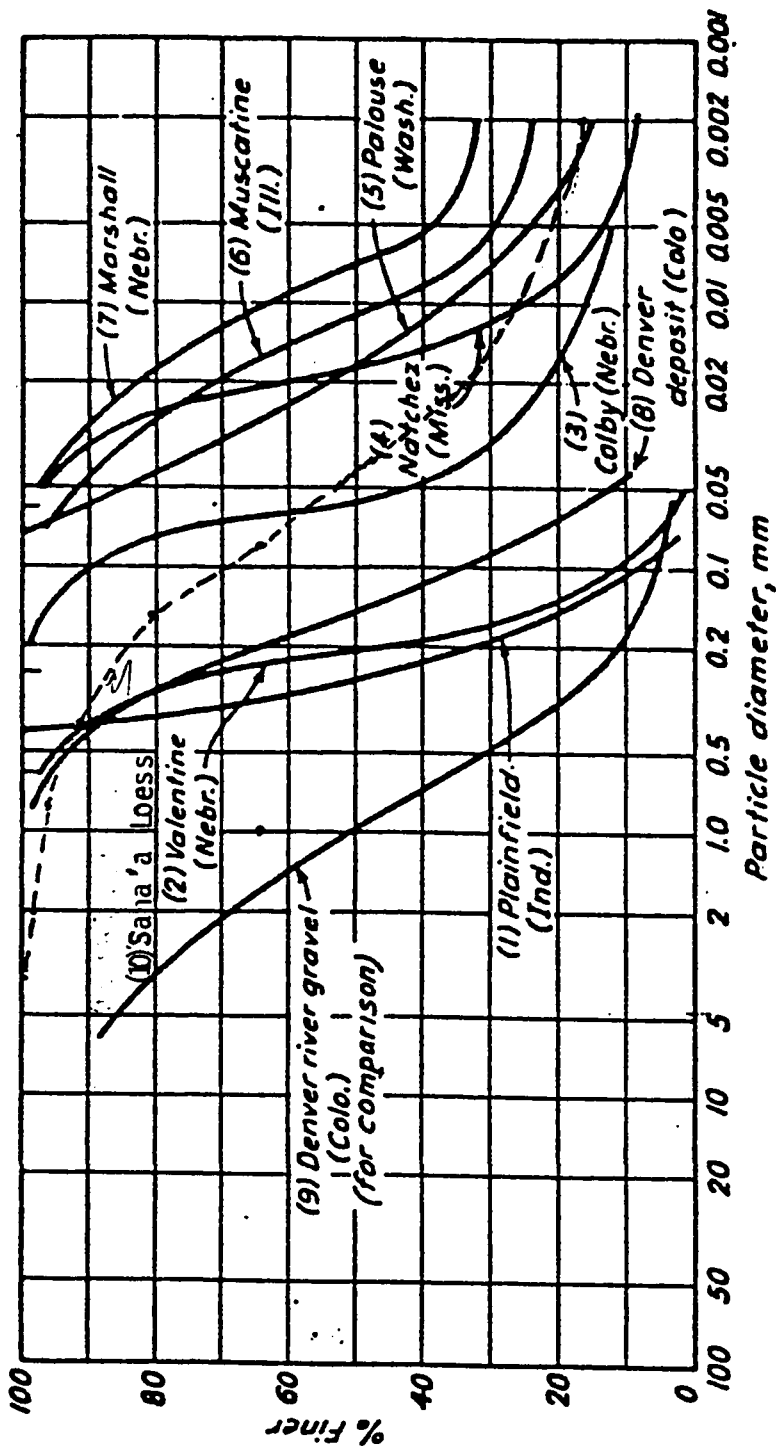


Fig. 4.24 : Particle-size distribution curves for wind-deposited sediments. Dune sand in northern Indiana (1), central Nebraska (2) Sandy loess in western Nebraska (3), Silty Loess in western Mississippi (4), southeastern Washington (5), Clayey loess in central Illinois (6), eastern Nebraska (7), Dune sand to loess transition in eastern Colorado (8), River gravel in eastern Colorado (9), for comparison (10), Sana'a loess, (After Peck, Hansen and Thurnborn, 1974).

and thin roots. Such characteristic of flood plain deposits were analyzed by Mitchell (1976). He indicated that "Some normally consolidated clays, almost all flood plain clays, and many preconsolidated clays are weakened by joints. Joints in flood plain clays result from deposition followed by cyclic expansion and contraction from wetting and drying". The fissures and cracks in some clays were related to the existence of trees and roots as indicated by Gillott (1987). These fissures and joints can be easily inspected if an excavation is carried out in this soil and exposed to sun for a while as indicated in Plate 4.13. The width of these fissures varies from fraction of mm up to few centimeters, while the extension of these fissures downward varies mostly from a discontinuous depth to a continuous one.

This soil in its natural state gives a high SPT value, of about 21 blows per foot, while a very low resistance was obtained, 9 blows per foot, when the same site was prewetted before testing. A correlation with SPT N values of the soil at natural state, indicates that this soil has a very stiff consistency as shown in Fig.4.19. When a stiff crumb of this soil is submerged in water, it loses its stiff state and is converted into a visco-liquid state. This loss of strength and stiffness is related to the particle arrangement and the interaction among them according to the chemical composition of the soil itself and the internal water tension between particles.

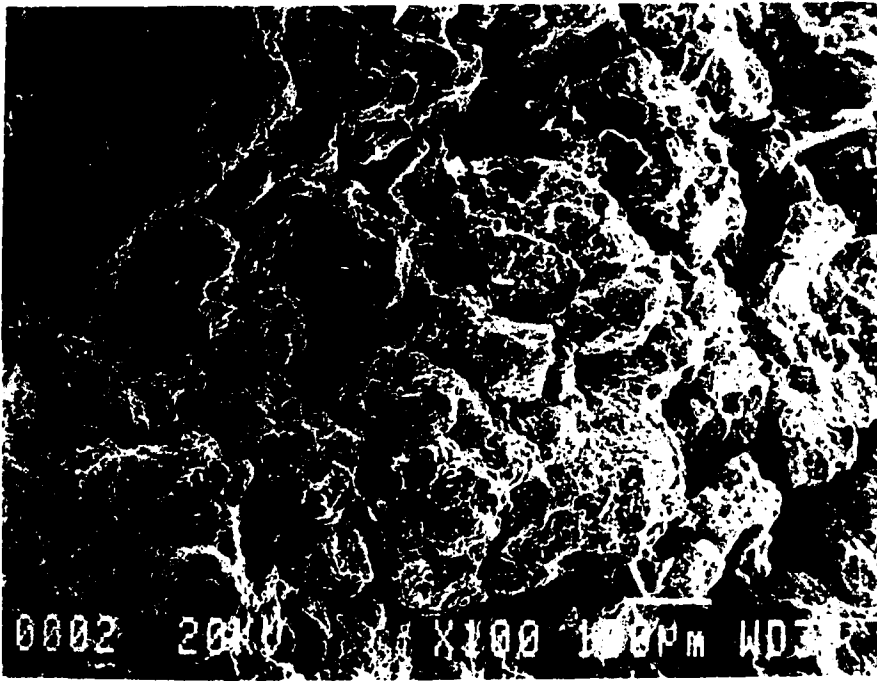


Plate 4.13 : Micro fissures and joints of lean clay soil.

The liquid and plastic limits of this soil are in the range of 42% - 53% and 24% - 26%, respectively, and the natural water content is about 12% - 16%. The liquid limit of the dark brown soil reaches 60%. Initially, due to the color of this soil the existence of roots and its dark colour, it was thought that this soil was an organic clay, but the chemical analysis and the ratio of the liquid limit of an oven specimen to the liquid limit of an air-dry specimen was found more than 75%, which ensures that this soil is inorganic clay. According to the plasticity chart, it is medium to high plastic inorganic clay.

The gradation curve depicted in Fig. 4.25 of a sample selected from station # 33 at a depth of 0.7m indicated the existence of high percentage of fines. The percentages of silt and clay are 58% and 32% respectively, and the percentage of fine sand is 8%. None or little coarse sand content was found. The high silt content may be a sign to identify this soil as a modified clayey loess soil.

AASHTO system classifies this soil as A-7-6(15). The group index (GI) varies in wide range 1 - 20. The higher GI the higher PI (LL - PL) and the lower the coarse material contents. This soil is described as clay with widely varying ranges of plasticity, cohesion, shrinkage and swelling properties and deformation characteristics. It is a poor soil for subgrade or borrow material, and it is not suitable as a foundation base. It

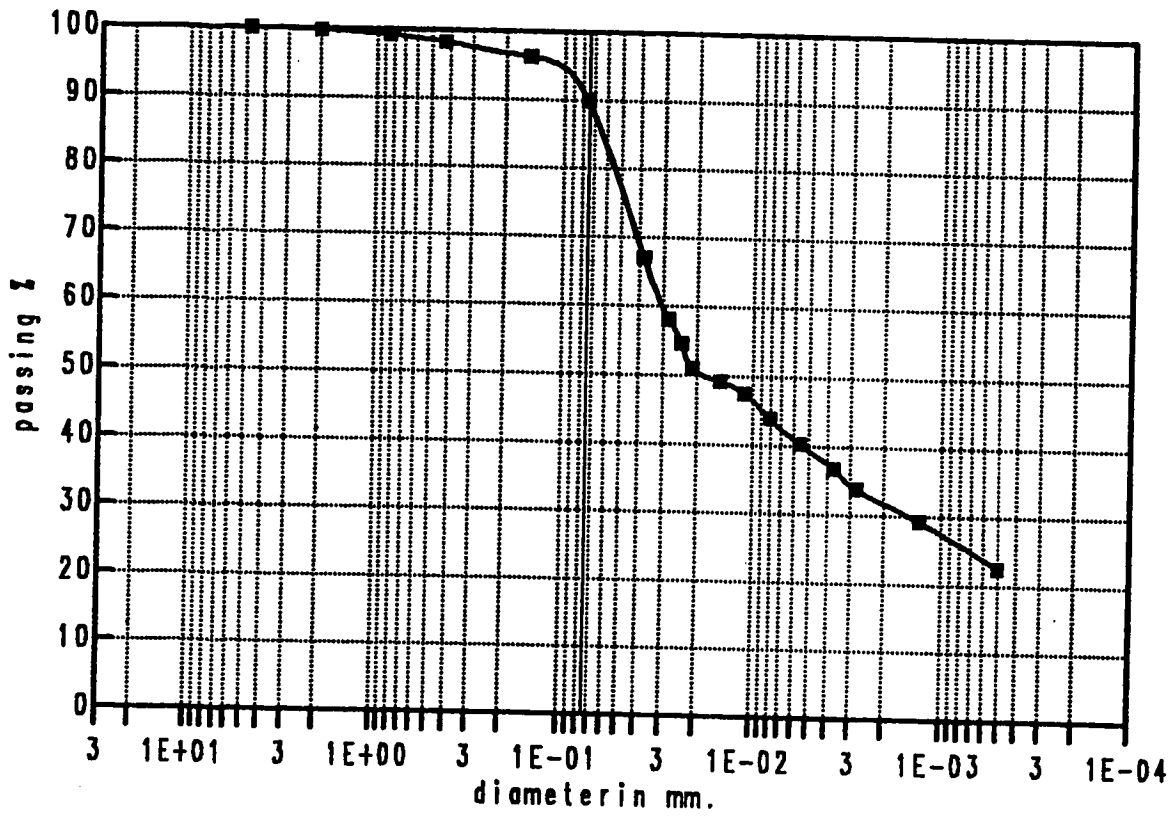


Fig. 4.25 : Gradation curve of lean Clay soil (Unit 7) selected from Station 33 at 0.7m.

is locally named 'Merryah'.

The previous soil units represent the most common existence soils as found from all the inspected stations. They represent about 90 to 95 percent of the all soils within the study area. Other different soils (5%-10%) are rarely present. Such soils are Brown, Stiff clayey Sand (5%), Reddish and greenish tuff volcanic soils (2%) and others. Fig.4.26 shows the gradation curve of the clayey sand soil which was found in station 23 at 4.0m bellow the surface as shown in Fig. 4.7. It extends downwards up to 6.0m. Plate 4.14 shows the reddish tuff volcanic soil which was observed at the surface in Hada area in the southern western part of the region. It exists with rock extending downward up to 3.0m. In some locations of the same area it occurred at 5.0m bellow the surface. These soils were not studied in detail as the other units due to their rare appearance and the difficulty in obtaining undisturbed samples of tuff volcanic soils. Table 4.4 shows the summery of the index properties of the different fine soils including the clayey sand soil. While Table 4.5 shows the properties of some wind deposits after Peck, Hanson and Thurnborn (1974) for comparing purpose. Plate 4.15 shows the variation in colour and some characteristics of the different soil units. Appendix B-9 gives a general summery of the engineering properties of the different soils after USCS.

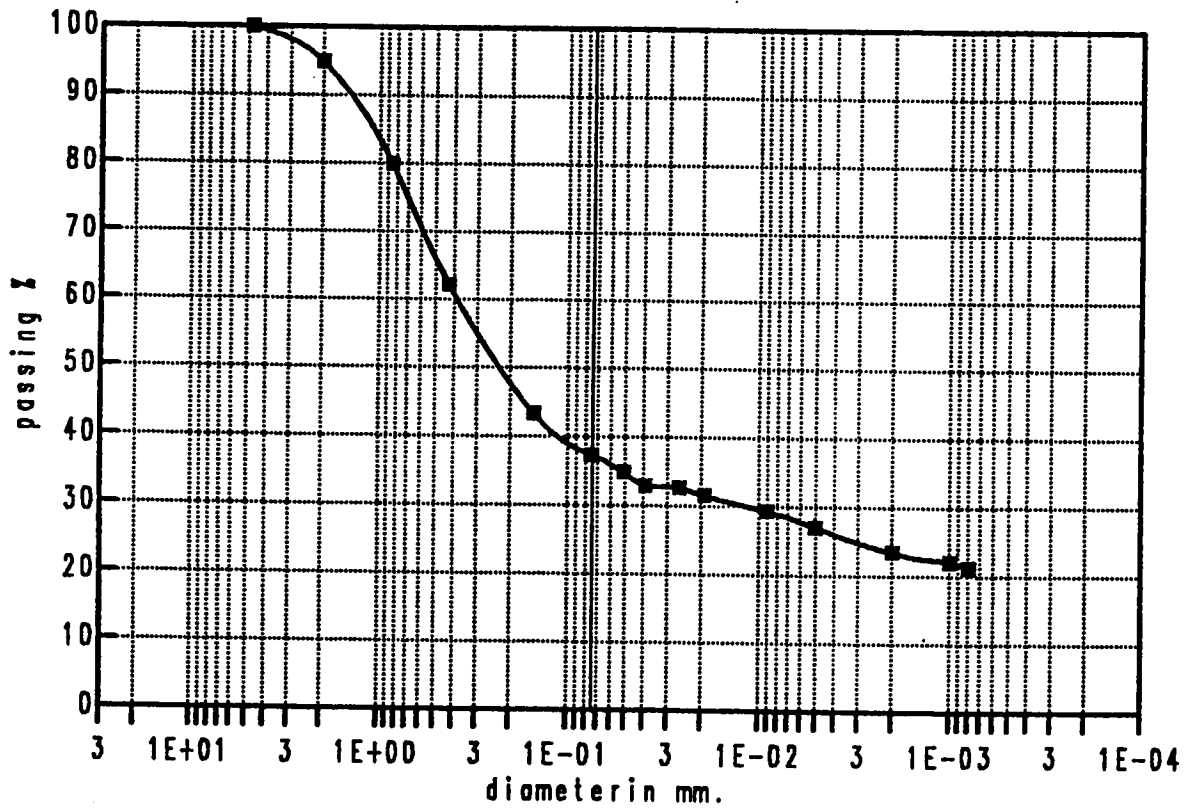


Fig. 4.26 : Gradation curve of the clayey sand soil selected from Station 23 at 4.5m (Rare soil existence).



Plate 4.14 : Occurance of the Tuff volcanic soil at surface in Hada Region.

Table 4.4 : Index Properties of the Fine Soils

Soil Unit	Soil Type	Station #	Depth (m)	W <sub>c</sub> %	P.L. %	L.L. %	PI	LI	Clay Content %	Activity A
7	Dark Stiff Lean Clay	33	0.7	14	25	45	20	-ve	32	0.62
5	Redish to Light Brown Sandy Silt	33	1.8	14	28	29	1	-ve	15	0.07
		33	4.5	12	27	29	2	-ve	17	0.10
		40	2.5	12	28	31	3	-ve	18	0.17
4	Light Brown Lean Clay with Sand	36	4.5	13	22	40	18	-ve	26	0.69
6	Light Brown Sandy Silty Clay with Gravel	38	2.0	15	20	25	5	-ve	12	0.41
		38	5.0	12	21	28	7	-ve	17	0.41

Table 4.5 : Index Properties and Engineering Classification  
of Representative Windblown Deposits.\*

Soil Type and Location	$w_L$	PI	$\gamma_{max}$ (lb/cu ft)	$w_{opt}$ (%)	AASHO Classification	Unified Classification
1. Plainfield fine sand, Pulaski Co., Ind.	—	NP*	107	10	A-3(0)	SP
2. Valentine fine sand, Hall Co., Neb.	—	NP	—	—	A-3(0)	SP-SM
3. Colby loam, Dundy Co., Neb.	24	3	—	—	A-4(1)	ML
4. Natchez silt loam, Claiborne Co., Miss.	27	4	108	16	A-4(3)	ML
5. Palouse silt loam, Walla Walla Co., Wash.	30	6	105	18	A-4(6)	ML
6. Muscatine silt loam, Livingston Co., Ill.	30	10	112	16	A-4(9)	CL
7. Marshall silty clay loam, Washington Co., Neb.	42	18	107	19	A-7-6(20)	CL

\*NP = Nonplastic.

\*(After Peck, Hansen and Thurnborn, 1974).

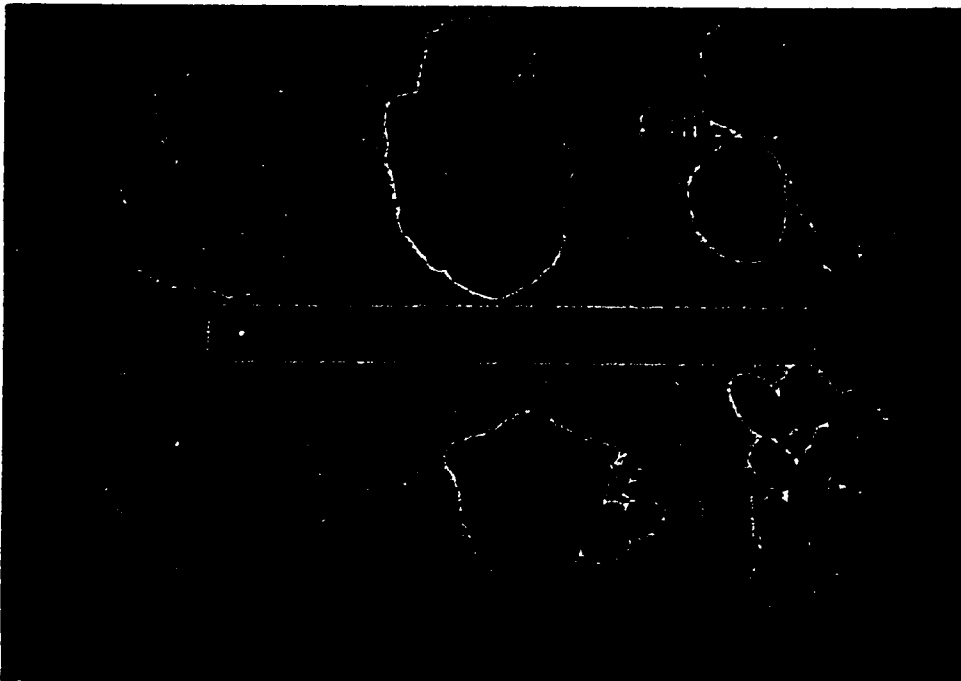


Plate 4.15 : Different studied soils

- a) Dark stiff lean clay
- b) Redish to light brown loess
- c) Cemented gravelly sand with silty matrix and pebbles
- d) Stiff brown sandy clay
- e) Sandy silty clay with sharp cemented gravel of sand stone.
- f) granular colour and form variations.

## Chapter 5

### SOIL COMPOSITION AND SOIL FABRIC

The properties of any soil rely directly on environmental effects, mineralogical and chemical composition, texture and soil fabric. In the present study the soil composition was analyzed by the following methods:

- 1) Grain size analysis as the most useful qualitative and semi-quantitative method as indicated in the previous chapter.
- 2) X-ray diffraction as a powerful tool in identifying both non-clay and clay minerals.
- 3) X-ray fluorescence spectrometer in order to find out the chemical composition in terms of mineral oxides.
- 4) Wet chemical analysis for determining cation exchange capacity, pH, organic matter, soluble salts, etc; and finally;
- 5) Scanning electron microscope study for identifying the microstructure of the soil.

The results of the soil composition and soil fabric are discussed in the following sections.

#### 5.1 Mineral Composition of Soil Samples from X-Ray diffraction (XRD) Analysis

Fig. 5.1 shows some of the standard X-ray diffraction diagrams

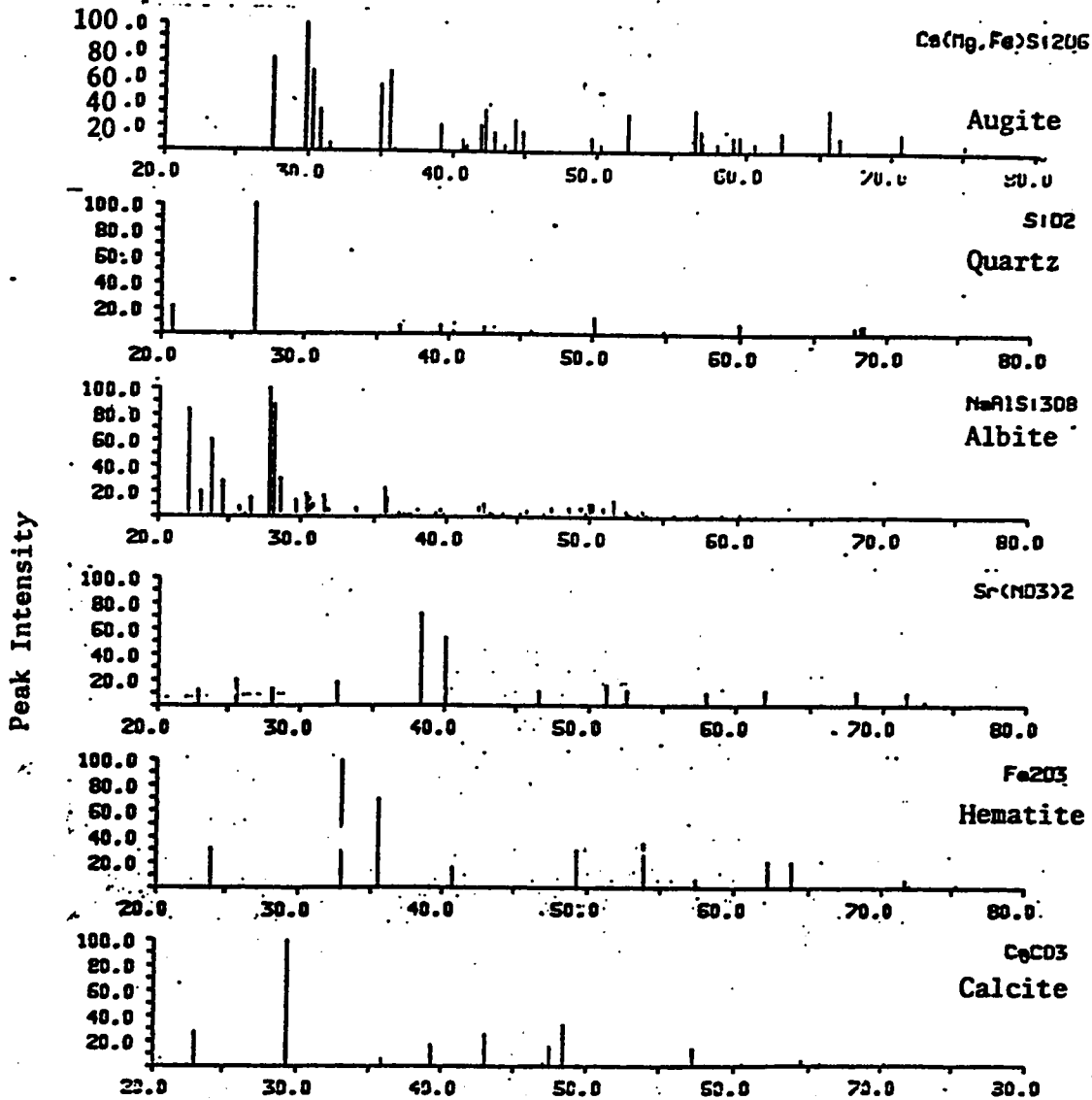


Fig. 5.1: Some standard X-Ray Diffraction Powder diagrams: Augite, Quartz, Albite, Sr(NO<sub>3</sub>)<sub>2</sub>, Hematite, Calcite.

which are used in analyzing the available minerals in the tested samples by comparing their X-ray diffraction patterns with these diagrams. This techniques is used in identifying both nonclay and clay minerals as follows:

### **5.1.1 NonClay Minerals:**

Figs. 5.2, 5.3, 5.4 and 5.5 show the X-ray diffraction patterns of the main natural mineral composition for the untreated powder samples. These figures showed that the predominant non-clay minerals of both coarse and fine soils are quartz, calcite, aragonite and albite. Augite, hematite and maghemite are found specially in the coarse soil. Fig. 5.6 shows how the standard diagrams of quartz, calcite and albite were used to identify the available minerals within the above indicated pattern. Quantitative analysis indicated the rare existance of some minerals within the granular samples such as judeite (6%) in station 39, and afwillit (4%) and cancrinite (3%) in station 34. A representative computer analysis print out of the sandy silty clay with gravel (station 38 at 4.5m) sample including peaks characteristics such as intensities of the peaks, basal spacing, the heights of the peaks, etc. is shown in Appendix C-1. This analysis technique gives an acceptable quantitative analysis with 95% accuracy.

Table 5.1 shows the quantitative analysis of nonclay minerals for the different types of soils. The table indicates an increase in the calcite with depth for the fine silty and clayey soils samples from

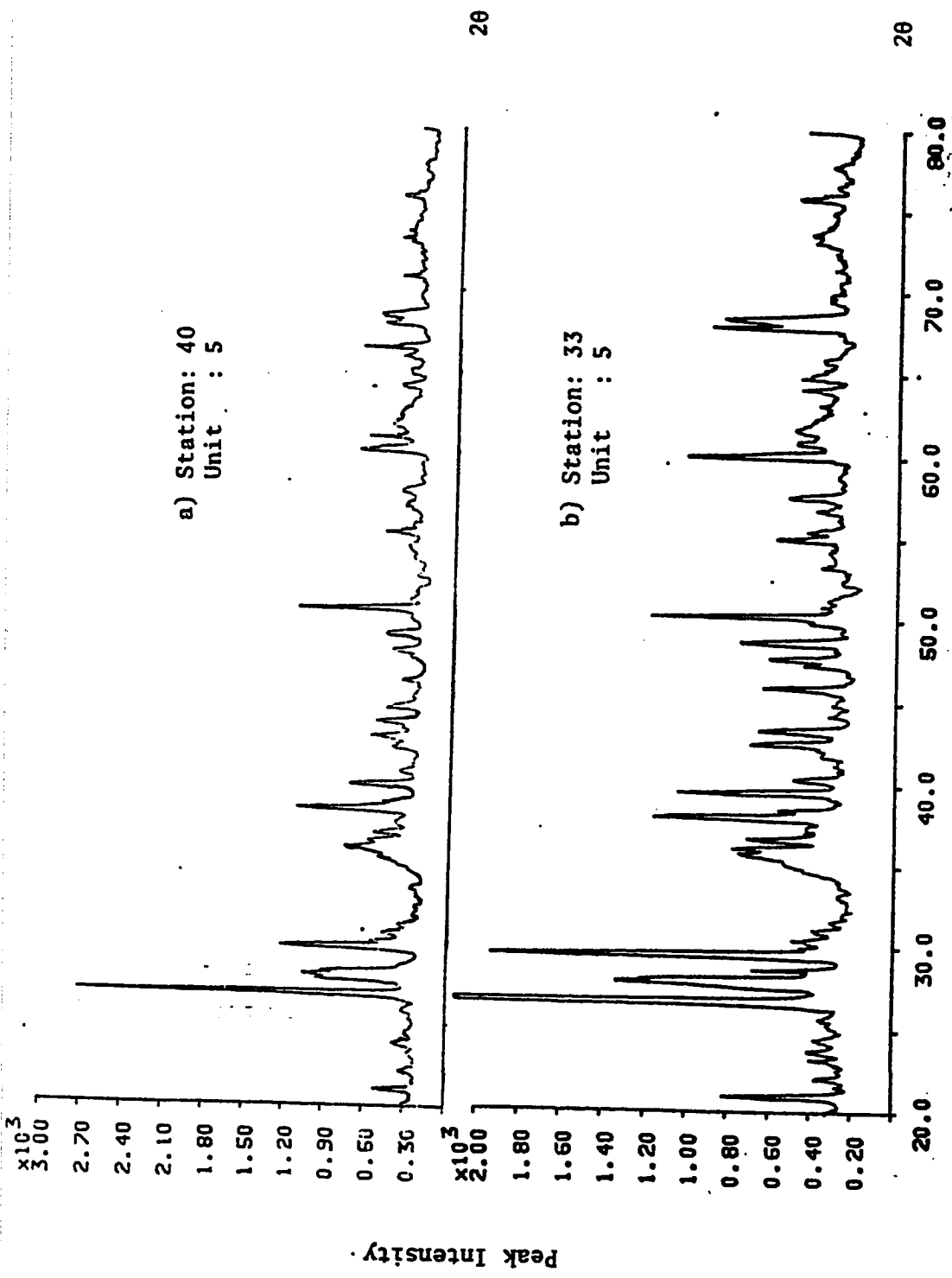


Fig. 5.2 : X-Ray patterns of nonclay minerals of:  
a) Sandy silt soil taken from 2.5m depth  
b) Sandy silt soil taken from 4.5m depth

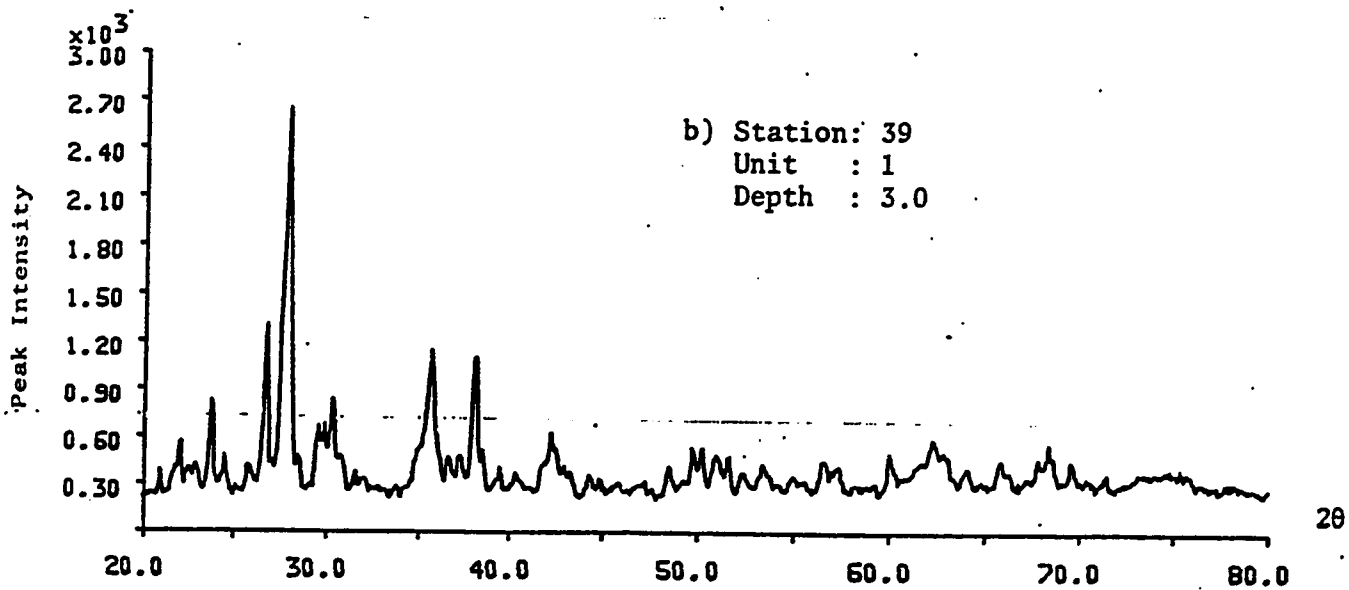
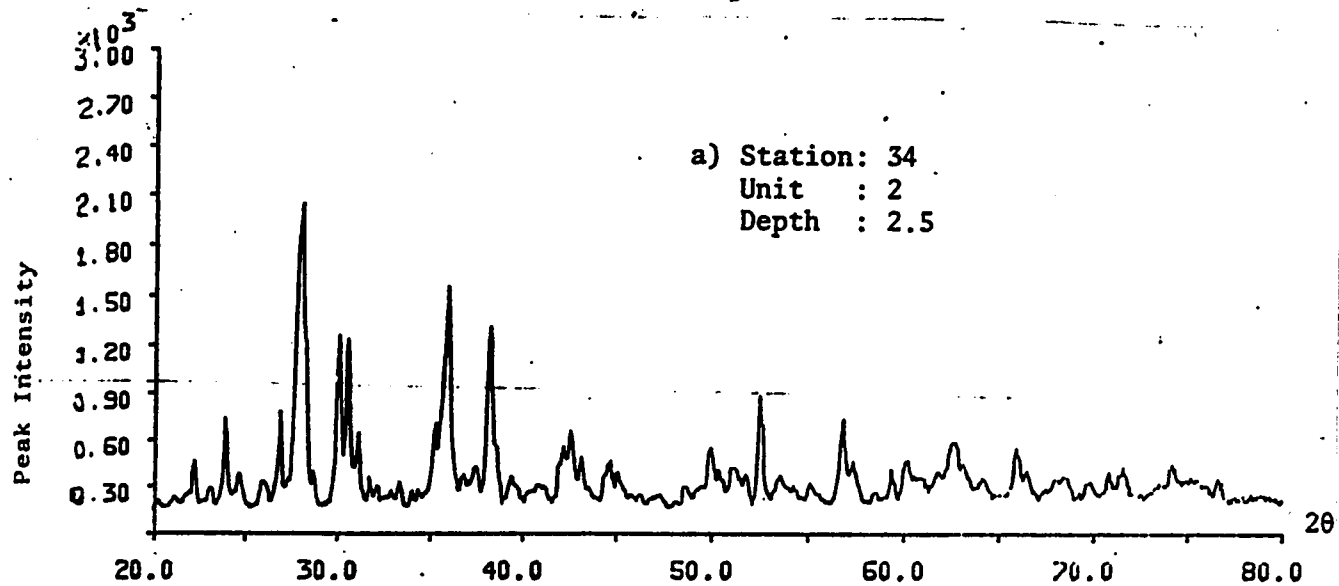


Fig. 5.3 : X-Ray patterns of nonclay minerals of:

- a) Well to poorly graded sand with gravel
- b) Well to poorly graded gravel with sand

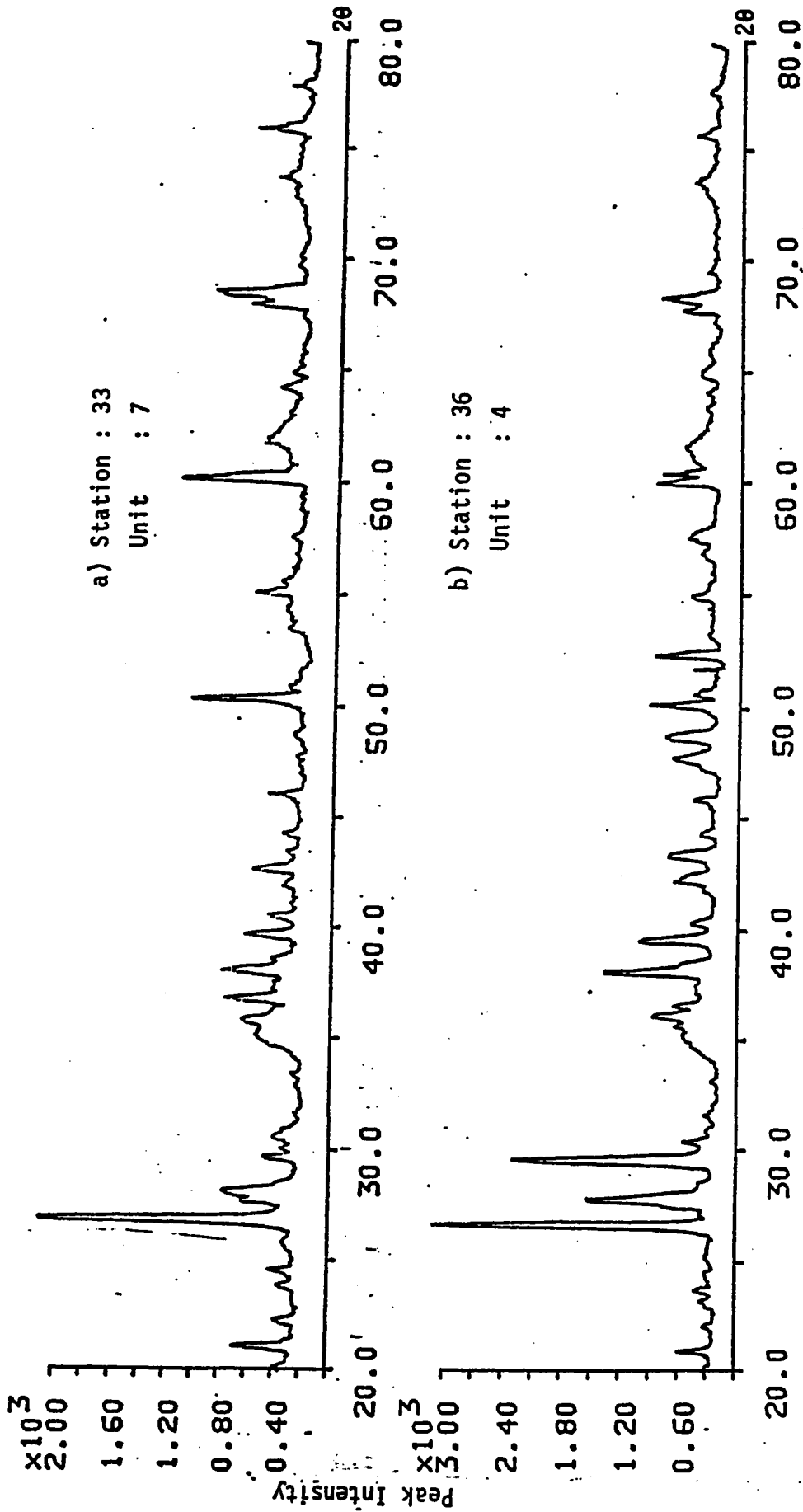


Fig. 5.4: X-ray patterns of nonclay minerals of:

- a) Lean clay taken from 0.7m
- b) Sandy lean clay taken from 4.0.

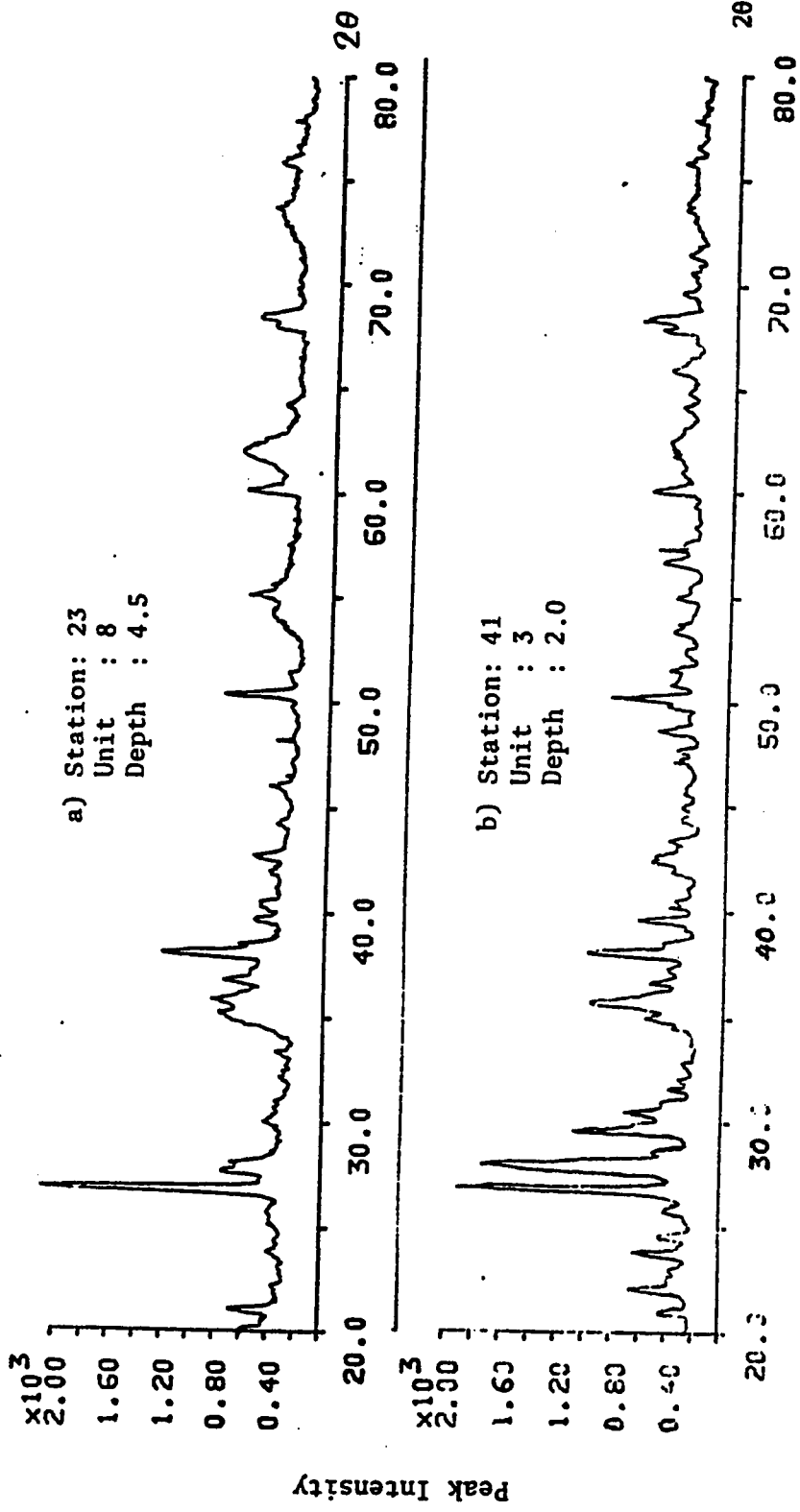


Fig. 5.5 : X-Ray patterns of montmorillonite minerals of  
 a) Clayey sand soil  
 b) Silty clayey sand with gravel

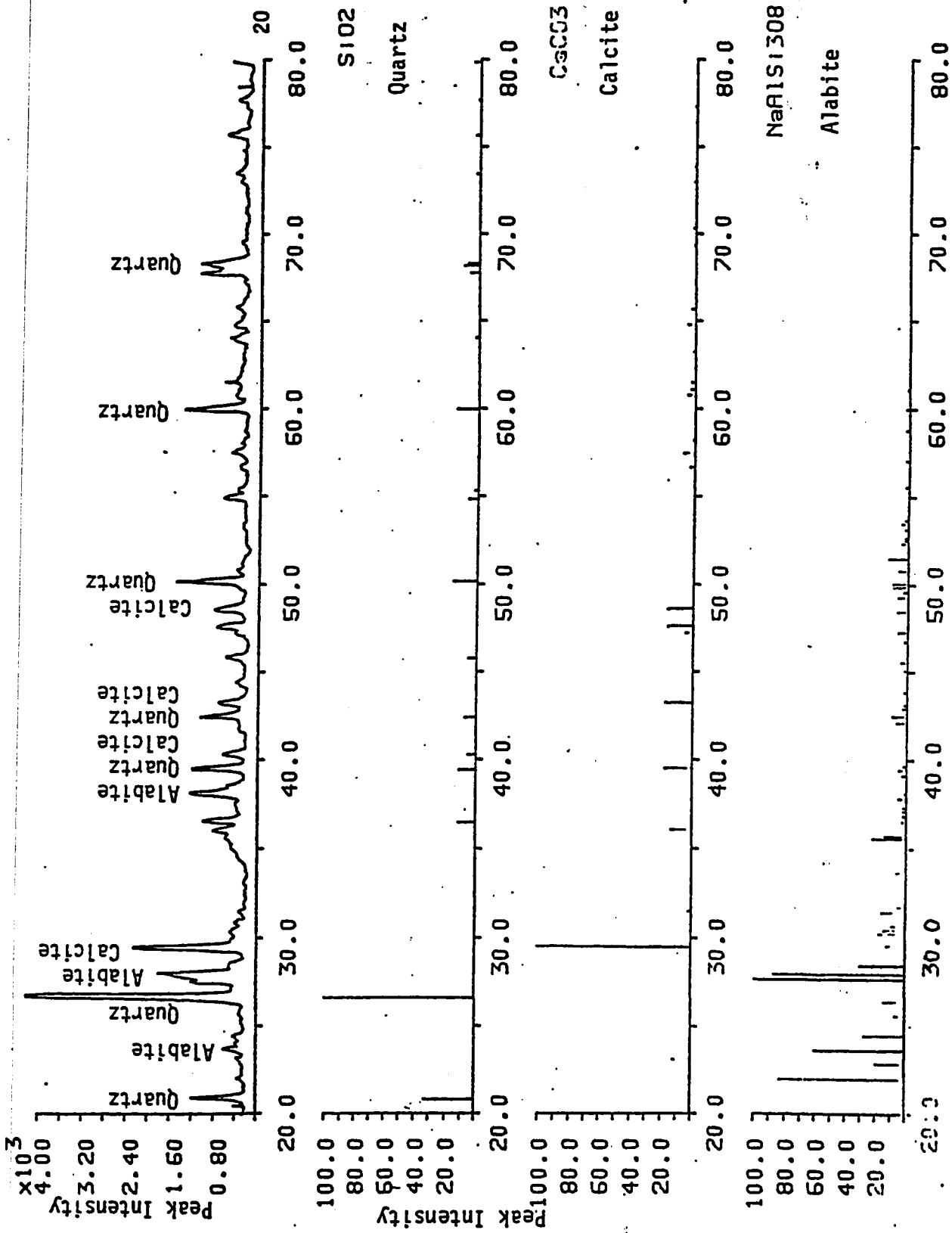
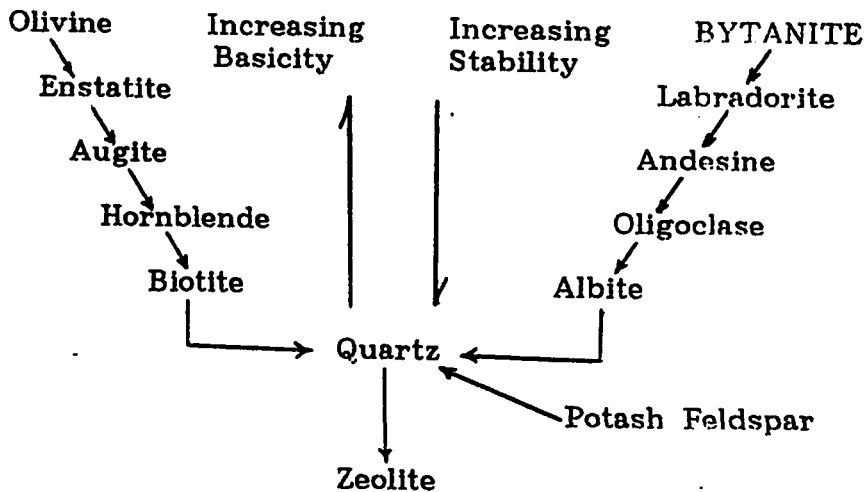


Fig. 5.6: X-Ray Pattern and Standard powdered diagrams of silty clay with gravel Station 38 at 20m.

Table 5.1: Quantitative Analysis of Non-Clay Minerals  
by X-ray Diffraction

Soil Unit	Station #	Depth (m).	Quartz SiO <sub>2</sub> %	Alabite NaAl Si <sub>3</sub> O <sub>8</sub> %	Calcite CaCO <sub>3</sub> %	Augite Ca(Mg, Fe) Si <sub>2</sub> O <sub>6</sub> %	Magnetite γ-Fe <sub>2</sub> O <sub>3</sub> %	Other Minerals
7	33	0.7	71	25	4	-	-	-
5	33	1.8	55	15	15	4	12	4
6	38	2.0	57	14	28	-	-	-
4	36	4.5	59	12	30	-	-	-
3	41	2.0	63	22	15	-	-	-
2	39	4.0	38	30	-	12	13	6
1	34	3.0	30	29	-	35	-	7

stations 33. In case of granular soil with fines less than 5%, calcite is not found as shown from samples of stations 34 and 39. In contrast, the albite exists in the granular soil more than the in fine soil. Furthermore, it decreases with depth in fine soils regardless the fine soil type as shown in the table. This is because the deeper the soil the longer weathering time the soil is subjected to. Augite is also common in granular soil rather than in fine soil. This is related to the stability of the minerals and their resistance to weathering and decomposition. The more basic is the mineral, the less stability of the mineral is. Bear (1964) gives the order of crystallization and stability of soil minerals as shown below.



Bear (1964) indicated that the stability of the minerals to weathering and to decomposition is found to be as: quartz > albite > augite. Augite and albite are less stable than quartz because of the

decrease in the linkage of the tetrahedrons in case of the augite, while in case of albite it is due to an increase in the number of alumina tetrahedrons (Bear, 1964).

The following sub sections describe quartz, calcite and albite, the common nonclay minerals within the study area soil.

**5.1.1.1 Quartz  $SiO_2$ :** Quartz is composed of a silica tetrahedral grouped in a spiral form. The silica tetrahedral structure has a high stability. Moreover, the spiral form results in a structure without cleavage planes. Quartz is already an oxide, so there is no weakly bonded ions in the structure, and it has a high hardness. All these factors account for the high stability of quartz as a non-clay fraction of soils (Mitchell, 1976). Quartz is inherited mainly from sandstone, basalt, granite, etc. as shown in Table 5.2. Quartz in powder form can be less than  $2 \mu m$ , clay size, and this accounts for its appearance along with calcite within the quantitative analysis of clay minerals. "Quartz is common in the clay size grade and is sometimes fine enough to have colloidal particles" (Gillott, J., 1987).

**5.1.1.2 Calcite ( $CaCO_3$ ):** The most abundant carbonate mineral of soils is calcite, which forms in sub-humid and more arid regions. Calcite is inherited mainly from limestone, marl and chalk rocks as well as from marble parent materials. Since limestone has an average 43% of calcium, it is mostly the main source of calcite. Limestone formation which spreads widely in the northern part of the study

area, Amran Formation, represents the main source for calcium carbonate. Calcite is found in the form of bulky particles, or shells. Specimens viewed by scanning electron microscope exhibited the needle form of aragonite and the bulky particle of calcite coating or precipitating on silt and coarse particles as shown in Fig.5.7. Aragonite is found in the surficial samples up to 2.0m below the surface while calcite exists at any depth.

During precipitation, the leaching results in depletion of  $CaCO_3$  from the more highly leached soils, while during evaporation of water calcite precipitates in the lower layers. Indeed, calcite was found to increase with depth as observed at station 33. At certain depths, calcareous soils contain as high as 20 to 50 percent  $CaCO_3$ . The proportion of these to other constituents are greatly affected by the chemical weathering and leaching (Bear, 1964). The hardness of calcite is low and the cleavage planes appear in three directions.

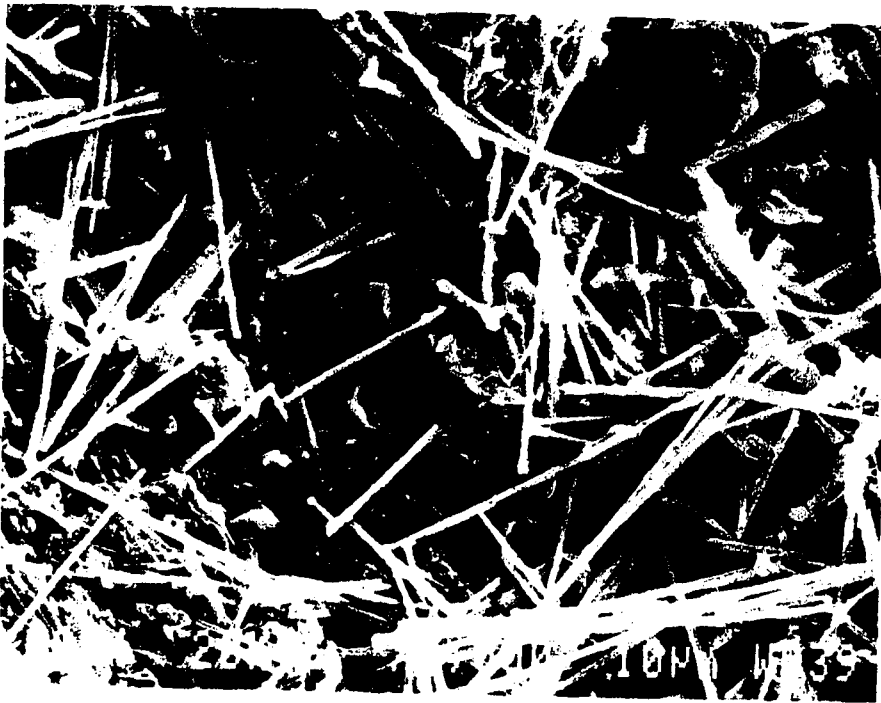
The existence of calcite within the soil plays a very important role in profile formation, cementation and decementation. Removal of calcite from soil causes slight consolidation. In addition, calcite dissolves in water, so it contributes in gaining or losing clay particles and it is one of the main reasons which controls the collapsing mechanism in loess soil.

Table 5.2 : Common Nonclay Minerals (Mitchell, 1976)

Mineral Name	Composition	Rock Occurrences
Quartz	$\text{SiO}_2$	Granite, sandstone, shale, etc.
Orthoclase feldspar	$\text{KAlSi}_3\text{O}_8$	Granite, sandstone, shale, etc.
Plagioclase feldspar	$\text{NaAlSi}_3\text{O}_8 - \text{CaAl}_2\text{Si}_2\text{O}_8$	Granite, sandstone, shale, basalt
Muscovite (mica)	$\text{KAl}_2(\text{Si}_2\text{Al})\text{O}_{10}(\text{OH})_2$	Granite, sandstone, shale, schist
Calcite	$\text{CaCO}_3$	Limestone
Dolomite	$\text{Ca} \cdot \text{Mg}(\text{CO}_3)_2$	Dolomite
Gypsum	$\text{CaSO}_4 \cdot 2\text{H}_2\text{O}$	Gypsum, shale
Amphiboles and pyroxenes	Variable	The heavy dark minerals in granite, basalt, etc.



(a)



(b)

Fig. 5.7 : Cementation agents of calcium carbonate in form of  
a) Calcite with bulky form, Station 40 at 2.5m and  
b) Aragonite with needle form, Station 41 at 2.0m.

**5.1.1.3 Albite ( $NaAlSi_3O_8$ ):** Albite is one of the plagioclas feldspars series. It is common in pigmatites and metamorphic rocks, but does occur in granite and some igneous rocks. Its weathering rate is slow and occurs commonly in the temperate climatic zones. The crystal structure of albite as any plagioclas feldspar, consists of a three dimensional framework of silicate minerals. Some of the silicon are replaced by aluminum resulting in excess negative charge, which is compensated by sodium cation. The higher the cation compensation, the lower the stability of structure unit because of the formation of an open structure with low bond stress between units. As a sequence, there are cleavage planes in two directions, the hardness is moderate and albite as feldspar is relatively easily broken down. Therefore, the appearance of feldspar minerals in soil is lacking comparing to their existance in igneous rocks (representing 60% by weight of igneous rocks), (Mitchell, 1976).

**5.1.2 Clay Minerals:** According to Bell (1981) "Clay deposits are principally composed of fine quartz and clay minerals The latter represents the commonest breakdown products of most of the chief rock forming silicate minerals". Clay minerals of the study area were identified by X-ray diffraction analysis. In addition, some properties of the clay minerals were indirectly used to ensure the identification. Some of these properties are: Cation Exchange Capacity (CEC), activity , and the change in X-ray pattern after subjecting the mineral to heating up to a certain degree.

**5.1.2.1 Clay Minerals Identification:** X-ray diffraction analysis were carried out upon four oriented samples (as described in Chapter 3). Figure 5.8 shows the X-ray patterns of two fine oriented samples. The quantitative analysis of the samples is shown in Table 5.3. From the computer analysis of these patterns, kaolinite is found to be the predominant clay mineral. Quartz and calcite appeared among clay minerals although they are nonclay minerals. In fact this is related to the possibility of quartz and calcite to exist in clay fraction size, less than 2  $\mu\text{m}$ .

The crystalline structure of kaolinite changes to amorphous at 550 - 600°C. Taking the advantages of this property for further identification, two samples out of the above four were chosen to satisfy this property. They were heated upto 575°C and retested by X-ray diffraction. The resulted pattern was imbricated upon the previous pattern of the same sample as shown in Fig. 5.9. At 2 $\theta$  equals 12.0 a reduction in the intensity of kaolinite peak is noticeable due to the transference of kaolinite to amorphous. This confirms the exitance of kaolinite as a clay mineral in the tested soil.

One of the most important properties of clay minerals is the exchangeable cations required to balance the charge deficiency of clay. This property is termed the "Cation Exchange Capacity" (CEC) and is usually expressed as milliequivalents per 100 grams of dry clay (Mitchell, 1976). Table 5.4 shows the values of CEC of different clay minerals. The cation exchange capacity was utilized for

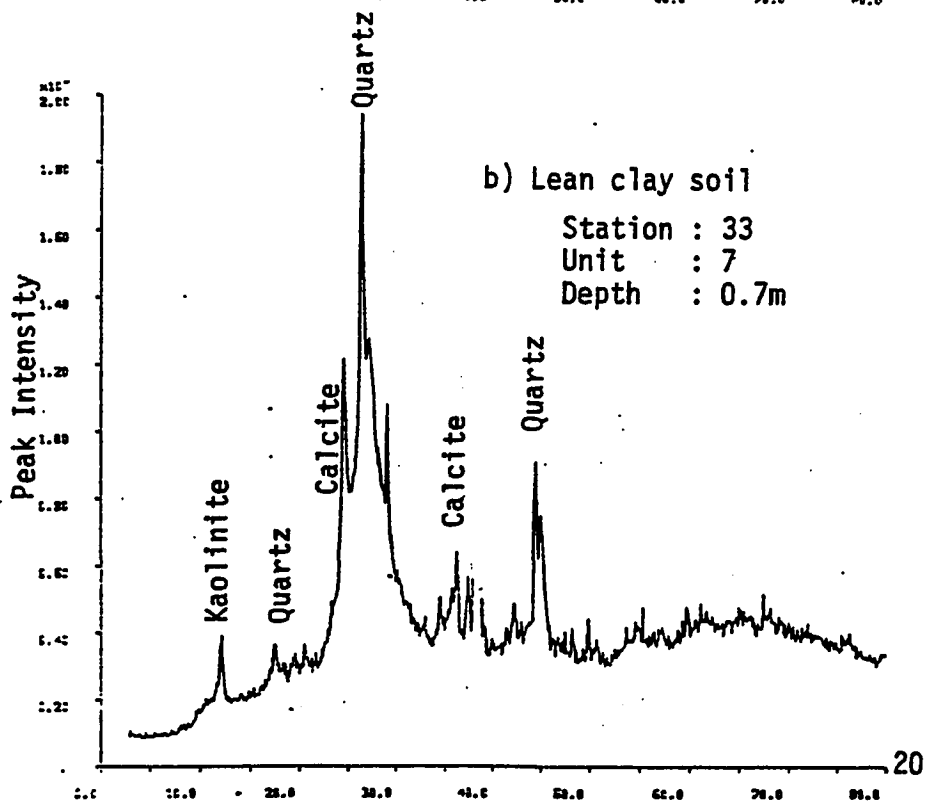
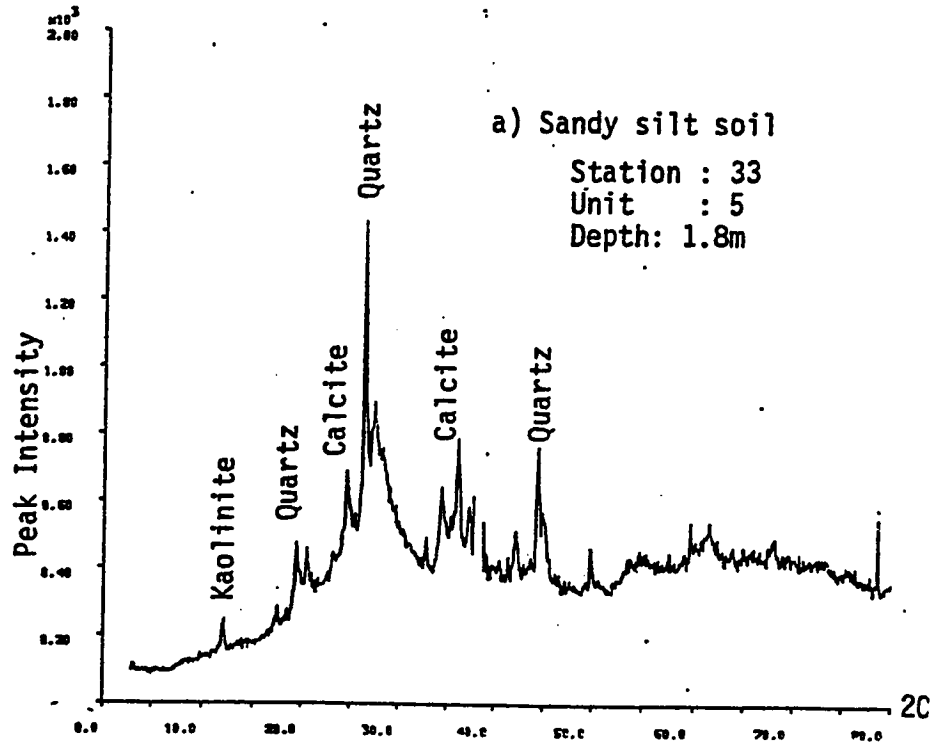


Fig. 5.8: X-Ray patterns of clay minerals

Table 5.3: Quantitative Analysis of Clay Minerals  
by X-ray Diffraction

Soil Unit	Soil Type	Station #	Depth (m)	Quartz SiO <sub>2</sub> %	Calcite CaCO <sub>3</sub> %	Kaolinite Al <sub>2</sub> Si <sub>2</sub> O <sub>5</sub> (OH) <sub>4</sub>
7	Lean Clay	33	0.7	37	23	39
5	Sandy Silt	33	1.8	81	--	19
6	Sandy Silt Clay with Gravel	38	4.5	22	53	25
3	Silty Clayey Sand with Gravel	41	2.0	17	51	33

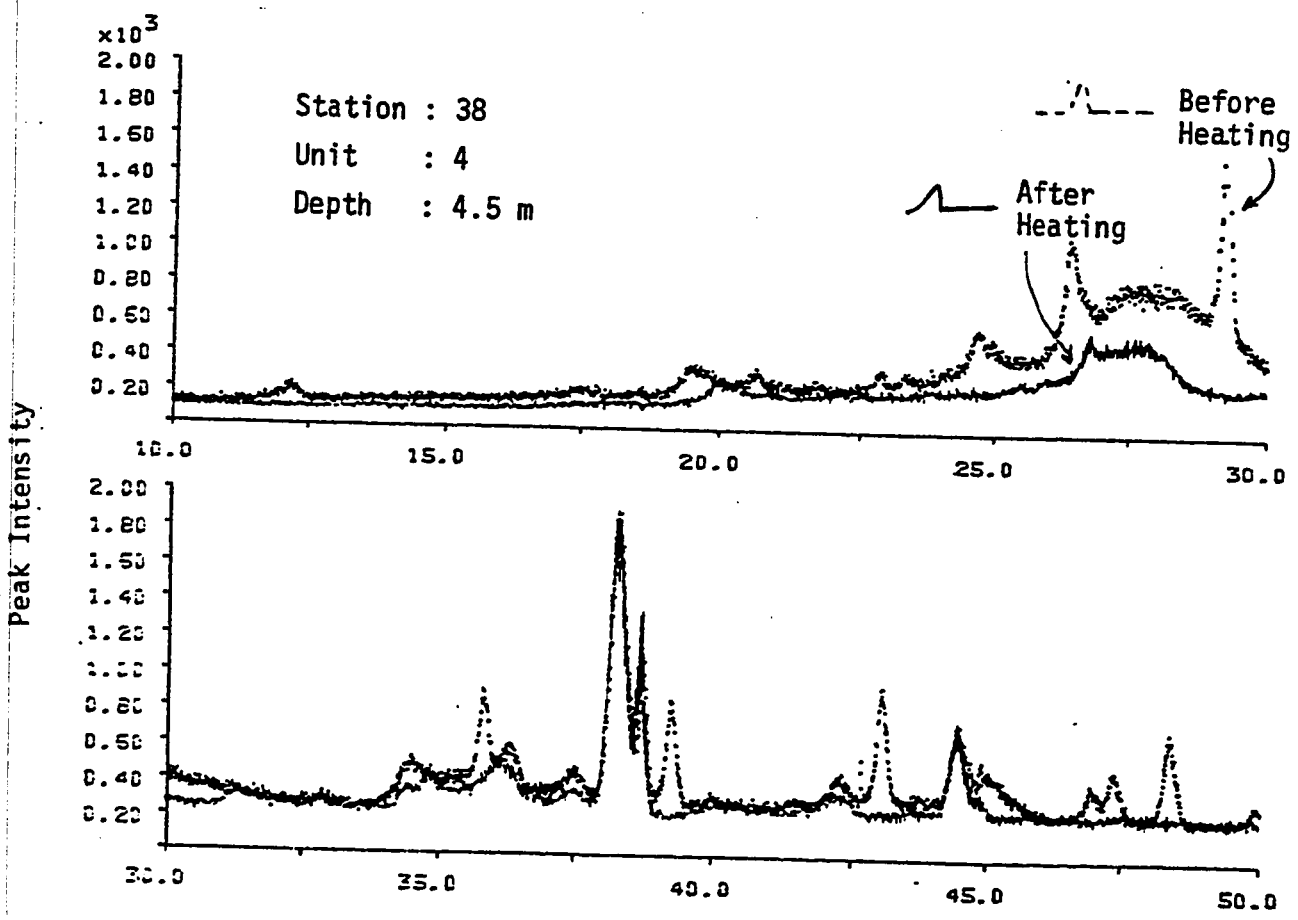


Fig. 5.9: Heating effects on clay minerals identification.

identifying the clay minerals of the soil within the study area. The wet chemical analysis and the CEC values are presented in Table (5.9). All the CEC values are almost in the range of 6 - 16 meq/100 gm, which is almost the same range of kaolinite (3- 15 meq/100 gm).

Another indirect identification method is by making use of the activity of the soil, which is the ratio of the plasticity index to the amount of the clay fraction (percentage by weight of particles finer than  $2\mu\text{m}$ ). Tables 5.5 gives values for the activities of different clay minerals. The activities of some soil samples from the study area are listed in Table 4.4. Comparing the values in both tables indicates the following:

- The soil of the study area is inactive soil as indicated in Table 5.5.b after Gillott and et al. (1987). This means the effect of clay on the properties of the soil is not that much. "The higher the activity of a soil, the more important the influence of the clay fraction on properties" (Mitchell, 1976).
- The activities of the soil of the study area are mostly in the range of the activity of kaolinite(0.5). This identification coincides with the X-ray diffraction and CEC identifications, except for the dark stiff fissured lean clay, top layer, which has an activity of 0.64 greater than 0.5. This means it may contain some illite(0.5-1.0), which does not coincide with the other identification methods.
- Finally, the existance of montomorillonite has not been shown

Table 5.4 : Cation Exchange Capacity of Clay Minerals  
(After Joseph E. Powels, 1984).

Clay	Exchange capacity, meq 100 g
Kaolinite	3-15
Halloysite (4H <sub>2</sub> O)	10-40
Illite	10-40
Vermiculite	100-150
Montmorillonite	80-150

Table 5.5: Clay & Clay Mineral Activities

a: Activities of Various Minerals  
(After Mitchell, 1976).

Mineral	Activity*
Smectites	1-7
Illite	0.5-1
Kaolinite	0.5
Halloysite (2H <sub>2</sub> O)	0.5
Halloysite (4H <sub>2</sub> O)	0.1
Attapulgit	0.5-1.2
Allophane	0.5-1.2

$$* \text{Activity, } A = \frac{\text{Plasticity Index}}{\% < 2 \mu\text{m}}$$

b: Classification of Clays in terms of Activity ( After Gillote and et al. 1987).

Description of clay	Activity
Inactive	< 0.75
Normal	0.75-1.25
Active	> 1.25

by comparing the activities values method as well as by the other methods.

#### 5.1.2.2 Kaolinite $\text{OH}_8\text{Si}_4\text{Al}_4\text{O}_{10}$ :

Kaolinite mineral is the most important clay mineral. It is principally formed as an alteration product of feldspars, feldspathoids and muscovite as a result of weathering. Kaolinite mineral is composed of 1:1 alternating silica and octahedral sheets as indicated diagrammatically in Fig 5.10. Its appearance in soil is very common in successive layers pattern, strongly bonded by both Van der Waals forces and hydrogen bond as shown in the Figure. That is why kaolinite does not exhibit an inter-layer swelling. The shown chemical composition gives an indicator to the different available components within the shown picture. The heights of peaks in Fig. 5.10.c are proportional to each other. The higher the peak the predominant the element is. The peak under symbol AU represents the gold which was used in coating the specimen which is not original mineral within the sample.

The type of absorbed cations influences the behavior of the soil. The greater their valency, the better the mechanical properties. The higher bonding between layers and the high Al content reduce the adsorption of water. The cation exchange capacity (CEC) of kaolinite is in the range of 3 - 15 meq/100 gm which is very low value comparing with the other clay minerals. As the cation



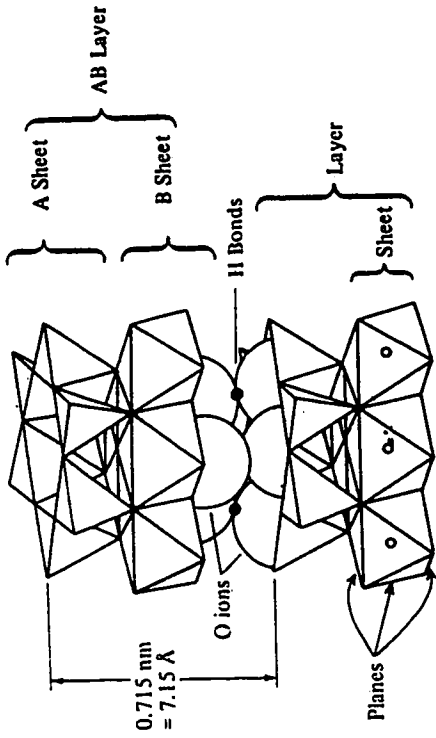
(a)

Fig. 5.9 : Kaolinit Composition

a) SEM of Kaolinit of air-dried specimen of sandy silty clay with gravel, vertical fracture section.

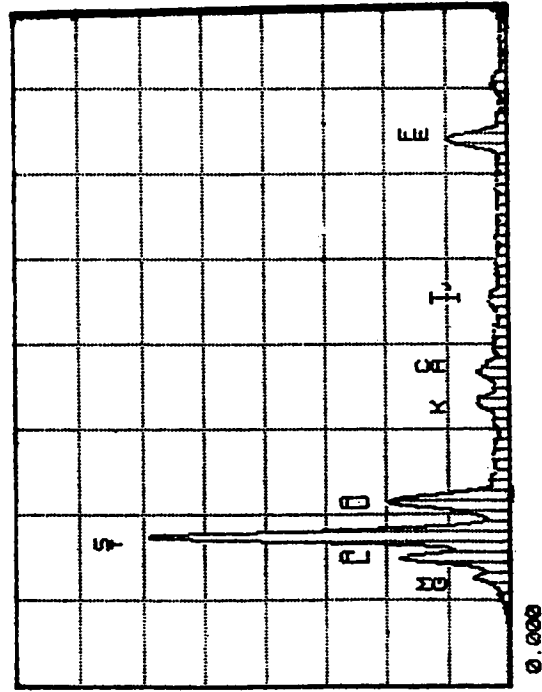
b) Schematic of kaolinit structure

c) EDS-composition



KAOLINITE

(b)



(c)

exchange capacity of a cohesive soil decreases so does its plasticity index. The lower the plasticity index and the tendency, the lower the compressibility and the higher the strength. The CEC values of the study area soils varies from 6 - 16 meq/100 gm. It is in the high range because of the alkalinity of the soil (pH > 7). The specific gravity of kaolinite is about 2.6 - 2.68, while its specific area is 10 - 20  $m^2/gm$ .

## 5.2. Soil Chemical Analysis

Soil chemical analysis was done by X-ray fluorescence (XRF) , energy dispersive spectrum (EDS) and wet chemical analysis as described in the following sections.

### 5.2.1 Soil Chemistry by Energy Dispersive Spectrum & X-ray Fluorescence:

Fig. 5.11 shows some representative patterns of the available elements, Ca, Ti, K, Mn, Fe, etc. within the studied soils as they detected by EDS . The figure shows also some of the scanning electron microscope (SEM) of the minerals which contain those elements. The intensity of peaks in the EDS patterns give an idea of the element concentration with respect to other elements. Fig. 5.11.a shows the calcium carbonate in the needle form of aragonite. EDS analysis of the same figure shows the relative high calcium contents(Ca). Fig. 5.11.b shows the existance of titanium which

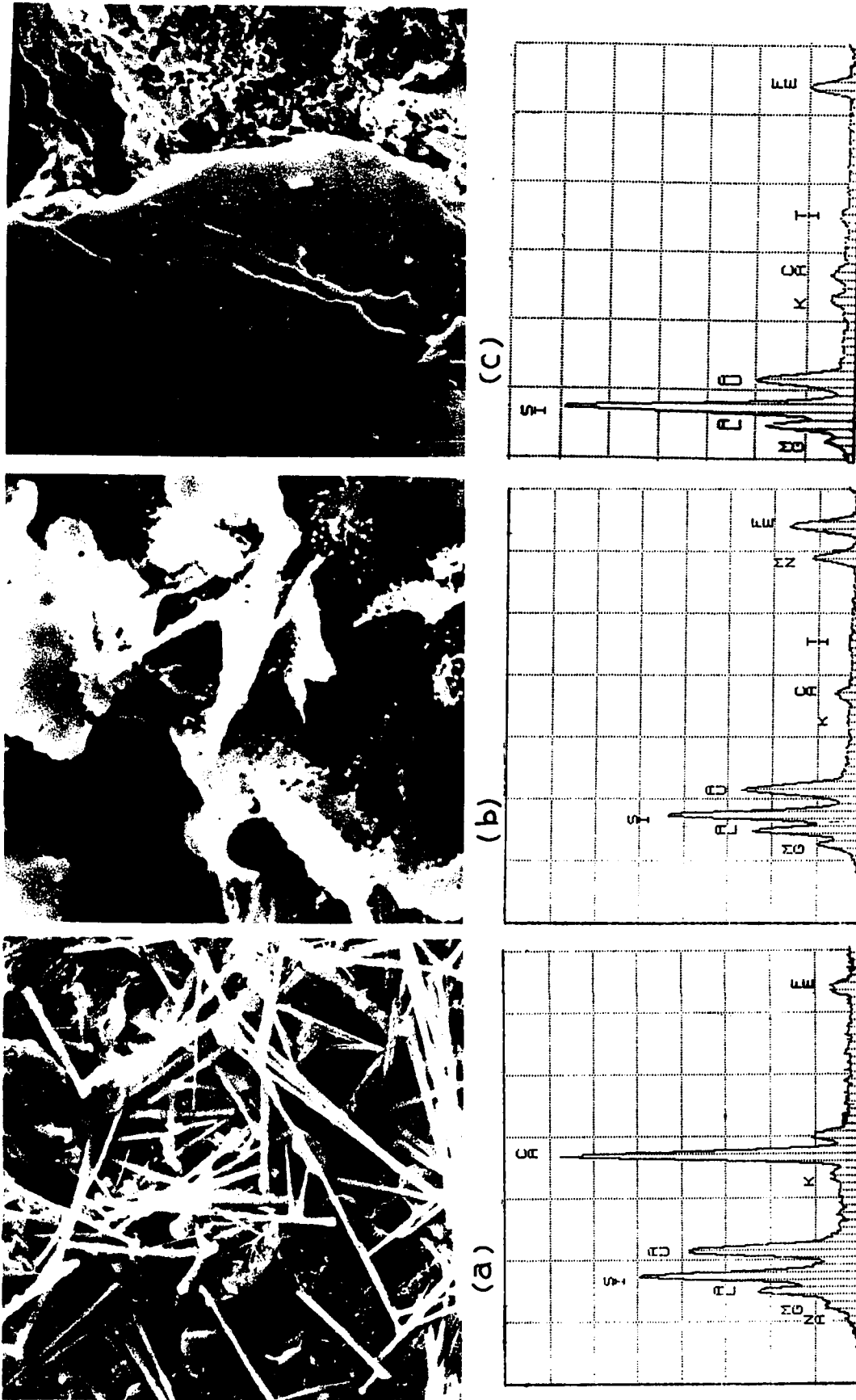


Fig. 5.11: Different forms of some chemical elements along with their EDS,  
 a) calcium, b) manganese, and c) iron oxide.

occures primerly in a coarse- grained crystals of free  $TiO_2$  such as rutile, antase or ilmanite (Bear, 1964). EDS pattern of the same figure indicates also the manganese existance which was found in the dark rounded particales attracted to the clay particales as shown in the SEM figure (Fig. 5.11.b). Fig. 5.11.c. shows the iron oxide covering a platy sheet as detected by SEM.

Tables 5.6 and 5.7 show the chemical composition of granular and fine soils in terms of element oxides percentages. Comparing the composition of the different soils of the study area with the natural average chemical composition of the earth's crust, as shown in Appendix C-2 (Bear, 1964), the following can be stated.

- All soils contain high calcium oxide content (17% - 31%) with respect to the natural calcium content (5.1%) . Consequently, the higher the calcium in the soil, the higher the calcium carbonate content (calcite or aragonite). The high calcium carbonate in form of calcite has been resulted from the albitic plagioclase (feldspar), igneous rock, metamorphic rocks and mostly from limestone. Bear, (1964) indicated that "As the weathering intensity and time factors increase, the calcium supply can progressively be obtained from the more albitic plagioclase".
- The soils of the study area contain higher values of  $Fe_2O_3$  (6.6% - 22.7%) than natural values (3.7%). High stability of soil aggregates and high soil porosity are usually associated with high iron oxide contents (Bear, 1964). Iron oxides are inherited from

Table 5.6 : Chemical Composition of Granular Soil by X-ray Fluorescence Spectrometer

Soil Unit	Soil Type	Station #	Depth (m)	SiO <sub>2</sub> %	Al <sub>2</sub> O <sub>3</sub> %	K <sub>2</sub> O %	CaO %	TiO <sub>2</sub> %	V <sub>2</sub> O <sub>5</sub> %	MnO %	Fe <sub>2</sub> O <sub>3</sub> %	SO <sub>3</sub> %	Total %
1	Well to Poorly graded gravel with sand	34	3.2	57.35	6.75	3.51	17.95	4.54	0.06	0.67	9.13	0.04	100
		39	3.0	65.12	7.05	3.69	18.46	3.75	0.07	0.64	9.08	1.14	100
2	Well to Poorly graded sand with gravel	33	2.5	53.07	6.53	3.53	18.62	5.38	0.13	0.81	10.74	1.19	100
3	Silty Clayey sand with gravel	41	2.0	47.56	5.22	2.89	26.76	4.48	0.06	0.69	10.95	1.40	100

Silicon Oxide : SiO<sub>2</sub>

Aluminum Oxide : Al<sub>2</sub>O<sub>3</sub>

Potassium Oxide : K<sub>2</sub>O

Calcium Oxide : CaO

Titanium Oxide : TiO<sub>2</sub>

Vanadium Oxide : V<sub>2</sub>O<sub>5</sub>

Manganese Oxide : MnO

Iron Oxide : Fe<sub>2</sub>O<sub>3</sub>

Strontium Oxide : SO<sub>3</sub>

Table 5.7 : Chemical Composition of Fine Soil By X-ray  
Flourescence Spectrometer

Soil Unit	Soil Type	Station #	Depth (m)	SiO <sub>2</sub> %	Al <sub>2</sub> O <sub>3</sub> %	K <sub>2</sub> O %	CaO %	TiO %	V <sub>2</sub> O <sub>5</sub> %	MnO %	Fe <sub>2</sub> O <sub>3</sub> %	SO <sub>3</sub> %	Total %
5	Sandy Silt	33	1.9	55.88	6.26	3.63	17.59	4.11	0.08	0.68	10.51	1.26	100
		33	4.5	47.01	5.84	3.62	24.96	4.35	0.08	0.78	11.89	1.47	100
		4D	2.5	43.64	5.97	3.02	27.68	5.06	0.08	0.73	12.22	1.60	100
6	Sandy Silt Clay with Gravel	38	2.0	49.17	5.04	3.13	31.62	2.85	0.04	0.48	6.65	1.02	100
4	Sandy Lean Clay	36	4.5	46.09	5.77	3.39	28.45	3.59	0.05	0.36	11.09	1.22	100.01
7	Lean Clay	33	0.7	51.44	6.73	3.70	20.76	4.00	0.04	0.69	11.62	1.02	100
--	Clayey Sand	23	4.5	47.94	5.41	5.72	8.46	6.00	0.13	1.76	22.67	1.92	100.01

parent rock, sedimentary and igneous rocks.

- All soils within the study area exhibited higher values of  $TiO_2$  with an average value of 4% than the natural values (1%) .
- Finally, all the other elements oxides of the different soils are in the range of the average values, except MnO of the clayey sand soil.

### 5.2.2 Wet Chemical Analysis

Table 5.8 shows the cations or anions concentrations of the chemical elements of the different soils expressed in mg per liter. These concentrations were obtained from extracted solutions of 1:4 or 1:2 (soil to water). The tabulated values were converted to 1:1 soil to water.

As can be observed from table 5.8 most of the study area soils contain high percentage of calcium carbonate. The sulphate content ranges between a maximum of about 352 mg/lit within the sandy silt soil to a minimum of about 25 mg/lit within the poorly to well graded gravel with sand. The maximum sulphate content of the silty soil of the study area can be expressed as almost 18  $SO_3$  parts per  $10^{-5}$  of 1:2 water to soil extraction. After M. J. Tomlinson (1980) this value is less than 30  $SO_3$  per  $10^{-5}$  , so normal portland cement ( type I) can be used and no need for high sulphate resistant cement (type V).

Table 5.8: Wet Chemical Analysis of 1:1 Extraction

Soil Unit	Soil Type	Station #	Depth (m)	Ca <sup>++</sup> mg/lit	Mg <sup>++</sup> mg/lit	K <sup>+</sup> mg/lit	Na <sup>+</sup> mg/lit	Cl <sup>-</sup> mg/lit	SO <sub>4</sub> mg/lit
7	Lean Clay	33	0.7	828	264	7	188	3064	75.5
5	Sandy Silt	33	1.8	1368	532	4	128	3892	35.2
6	Sandy Silt Clay with Gravel	38	2.0	502	273	3	144	2242	50.3
-	Clayey Sand	23	4.0	1806	776	36	472	11128	251.6
3	Silty Clayey Sand with Gravel	41	2.0	626	416	14	344	3808	166.1
2	Well to Poorly Graded Sand With Gravel	34	3.0	449	277	8	276	2834	50.3
1	Well to Poorly Graded Gravel With Sand	39	4.0	305	237	11	160	1582	25.2

Table 5.9 : Chemical Engineering Properties

Soil Unit	Soil Type	Station #	Depth m	pH	Organic Matter %	CEC meq/100gm	TDS* meq/lit	Na <sup>+</sup> %	SAR	ESP
7	Lean Clay	33	0.7	8.1	0.62	9.3	39.9	20.5	2.05	2.03
5	Sandy Silt	33	1.8	8.1	0.113	15.0	61.8	9.0	1.05	0.6
6	Sandy Silty Clay with Gravel	38	2.0	8.5	0.176	13.0	30.1	21.0	1.81	1.7
-	Clayey Sand	23	4.0	7.65	0.21	----	98.5	21.0	3.3	3.8
3	Silty Clayey Sand with Gravel	41	2.0	8.65	0.155	16.0	48.0	31.0	3.7	4.4
2	Well to Poorly Graded Sand With Gravel	34	3.0	8.2	0.015	---	34.8	34.0	3.6	4.2
1	Well to Poorly Graded Gravel With Sand	39	4.5	8.35	0.01	---	24.3	28.5	2.6	2.8

Table 5.9 gives some of the chemical engineering properties which were obtained either by direct chemical analysis such as pH, organic matter and cation exchange capacity (CEC), or by applying certain formulae such as sodium adsorption ratio (SAR), exchangeable sodium ratio (ESP) and total dissolve salts (TDS). TDS can be obtained by direct chemical methods, but for the identification of dispersion phenomena purpose it is derived using the following formula:

$$TDS = [Ca^{++} + Mg^{++} + Na^+ + K^+]$$

where concentrations are in milliequivalents per liter (meq/lit). The sodium adsorption ratio is equal to:

$$SAR = \frac{Na^+}{\left(\frac{Ca^{++} + mg^{++}}{2}\right)^{1/2}}$$

The exchangeable sodium ratio is defined by

$$ESP = \frac{100 \left[ -0.0126 + 0.01475(SAR) \right]}{1 + \left[ -0.0126 + 0.01475(SAR) \right]}$$

Since the values of pH greater than 7, the soils under the study are alkaline soils. The value of pH effects the CEC values. The higher the pH, the higher the CEC. As shown in the table the organic matter percents are very low so it has no significant effect on soil behavior.

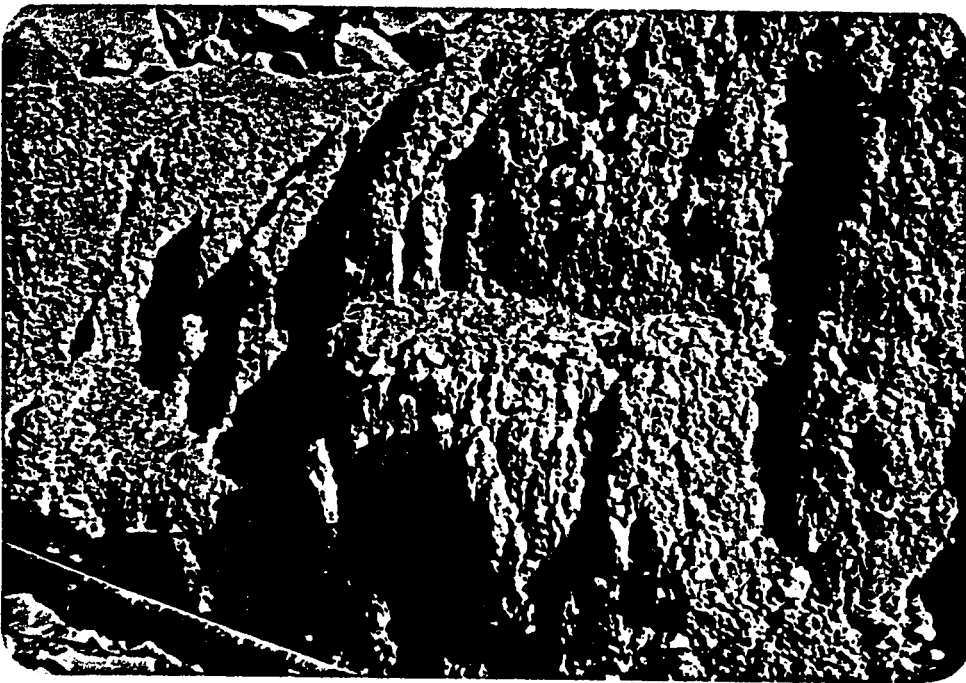


Plate 5.1 : Inspected erosion of top surface layers of an open excavation.

### 5.2.3 Dispersive Soil

Plate 5.1 shows a surficial erosion due to rainfall effect on an open and vertical excavated side in sandy silt soil. Erosion of fines from the soil structure upon wetting has a significant effect on the soil fabric and its cohesion. This will be discussed in the following section.

Dispersive soils are defined as soils which are structurally unstable and have high susceptibility to erosion. Dispersive soils are mostly clayey soils. The repulsion forces between particles exceed attraction forces which cause colloidal particles on the outer surface of a soil mass to spring out into suspension (Sherard and Dekker, 1976 and Spangler and Handy, 1984). The leaching of fine particles in this way may cause a collapse in the fabric of the soil as discussed in next section.

The principal difference between dispersive soils and the non-dispersive soils is the nature of the cation in the pore water. Dispersive soils have higher content of sodium, while ordinary soils have higher content of calcium and magnesium cations in the pore water. Taking the advantages of these characteristics, simple tests can be used directly to identify dispersive soils.

- The first simple identification test is the crumb test (Rallings, R. A., 1966). In this test a small crumb of soil at natural water content is dropped into a beaker of water (150 ml) and the dispersion is observed directly by observing the tendency of the clay particles to go into colloidal suspension after 5 - 10 minutes of immer-

sion. The presence of these colloidal clouds indicates the tendency of dispersion. In fact all fine soils within the study area exhibited this cloudy colloidal forms upon immersion, but this way of identification interferes with the way of identifying the collapsing soils. In other words, this colloidal clouds may be due to dispersion or collapsing. So the following identification systems are more reliable than the previous one.

- Exchangeable sodium ratio (ESP) is a good indicator of particles dispersion. Different studies showed that soils with ESP greater than 2% are susceptible to dispersion, and clays with ESP greater than 10-15% will disperse instantly, (Mitchel, 1976 and Sherard and Deker, 1976). Considering the ESP of the study area soils in Table 5.9, the following results can be derived: All fine soils are not susceptible to dispersion, but the fine portions within the granular soils are susceptible to dispersion as they were deposited by leaching and evaporating. These fine contents exist within clayey sand, silty clayey sand with gravel and within well to poorly graded soil having ESP values greater than 2.0 (table 5.9); finally:

- Soluble salts in pore water test is a standard test of agricultural soil scientists. In this test the percent sodium is used as an indicator to dispersion. It is defined as:

$$\text{Percent Sodium} = \frac{Na^+ \times 100}{TDS} = \frac{Na^+ \times 100}{(Ca^{++} + Mg^{++} + Na^+ K^+)}$$

where concentrations are in meq/lit. The higher the percent sodium, the more the tendency of the soil to dispersion.

- Sherard and Decker (1976), constructed a relationship between percent sodium, sodium exchangeable ratio and total dissolved salts. Different zones were used to identify the susceptibility to colloidal erosion as shown in Fig. 5.12. The required parameter of the different soils were calculated and plotted in the figure as shown. All soils plotted in zone B which means that all soils within the study area are nondispersive soils. This means that they are not highly erodeable according to the dispersion definition, but they still have the tendency to erode at low rates as detected from the fabric and shear strength analysis. The clay and colloids act as a cementation agent to other particles. The analysis indicated the softening of cementation upon wetting is associated with slow rate of eroding. These softening and erosion are the main reasons for collapsing and losing strength upon saturation which have been proved by laboratory testing as will be shown latter. For further studies, in future, of the dispersion phenomenon, pinhole tests should be done (Sherard and Decker, 1976).

### 5.3 Soil Fabric

#### 5.3.1 General

The fabric sometimes decisively affects the engineering properties of soils such as sensitive clay deposits, loess deposits, etc. According to Bates and Jackson, 1980, fabric is defined as "the

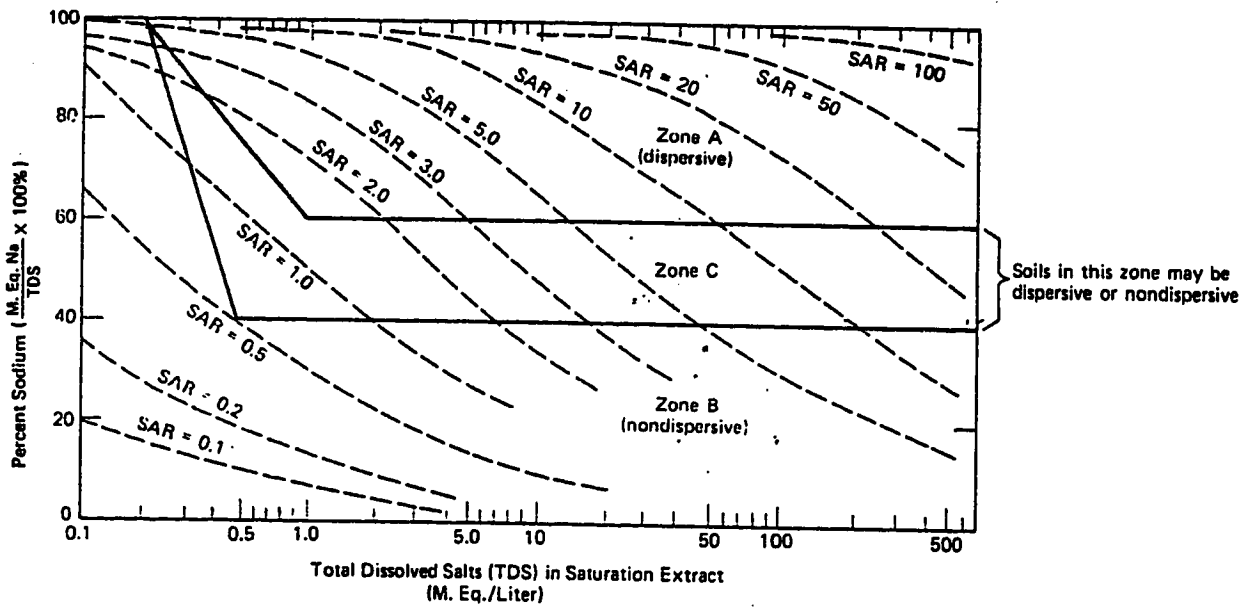
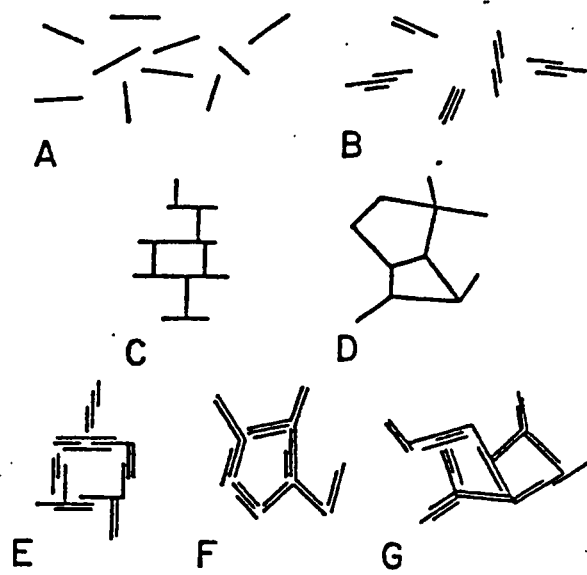


Fig. 5.12: Relationship between dispersibility (susceptibility to colloidal erosion) and dissolved pore water salts based on pinhole tests and experience with erosion in nature. From Sherard, Dunningan, and Decker, 1976b.  $SAR = \frac{Na}{\sqrt{0.5(Ca + Mg)}}$ , all in m. eq./liter. Note: Relationship shown is valid only when eroding water is relatively pure. (Mitchell, 1976).

physical nature of a soil according to the special arrangement of its particles and voids". Primary fabric forms develop on deposition time , while secondary fabric forms develop later on due to the effect of deformation-consolidation and shear, crystal growth, moisture movements, etc. The term "structure" has a broader meaning of the combined effects of fabric, composition, and inter-particle forces. The term "microstructure" is often used to show the effect of interparticle forces as well as fabric on soil properties.

Many scientists and authors have given different descriptions and expressions for the soil fabric. At an early time, Terzaghi suggested that some soils were composed of individual grains of silt and flocculated clay arranged in an arching skeleton enclosing large voids. This arrangement has been termed honey-combed by Casagrande (1932). Lamb and Martine (1953) predicted parallel type of arrangement of clay particles for fresh water deposits. In recent work it has been suggested that clay minerals are more often deposited as aggregates than as single crystals (Gillott, 1987).

In this study the microstructures of soils were identified according to the descriptions depicted in Fig. 5.13a given by Van Olphen (1977). This type of fabric depends on the inter-particle repulsive and attractive forces, and commonly used to describe the clay fabric. In case of loess deposits, the fabric is shown in Fig.



(a) Modes of particle association in clay suspensions, and terminology.

(After Gillute, 1978).

(A) "Dispersed" and "deflocculated."

(B) "Aggregated" but "deflocculated" (face-to-face association, or parallel or oriented aggregation).

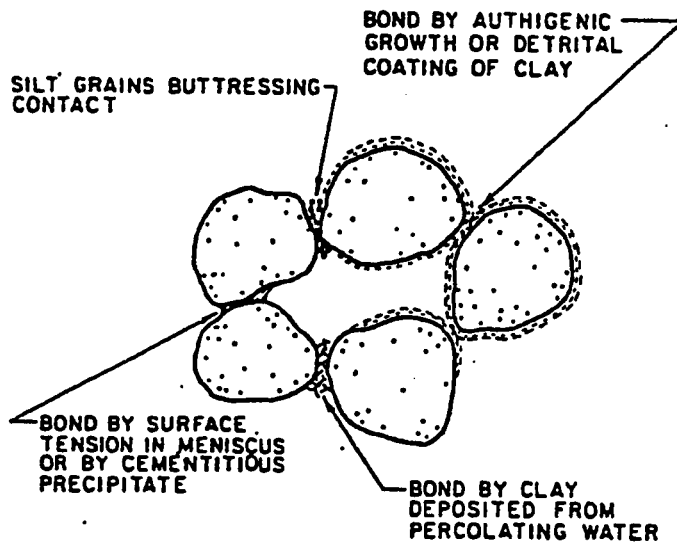
(C) Edge-to-face flocculated but "dispersed."

(D) Edge-to-edge flocculated but "dispersed."

(E) Edge-to-face flocculated and "aggregated."

(F) Edge-to-edge flocculated and "aggregated."

(G) Edge-to-face and edge-to-edge flocculated and "aggregated."



(b) Schematic of collapsing soil (Adapted from Dudley, 1970; Barden et al., 1973), after Gillute, 1978).

Fig. 5.13: Soil fabric

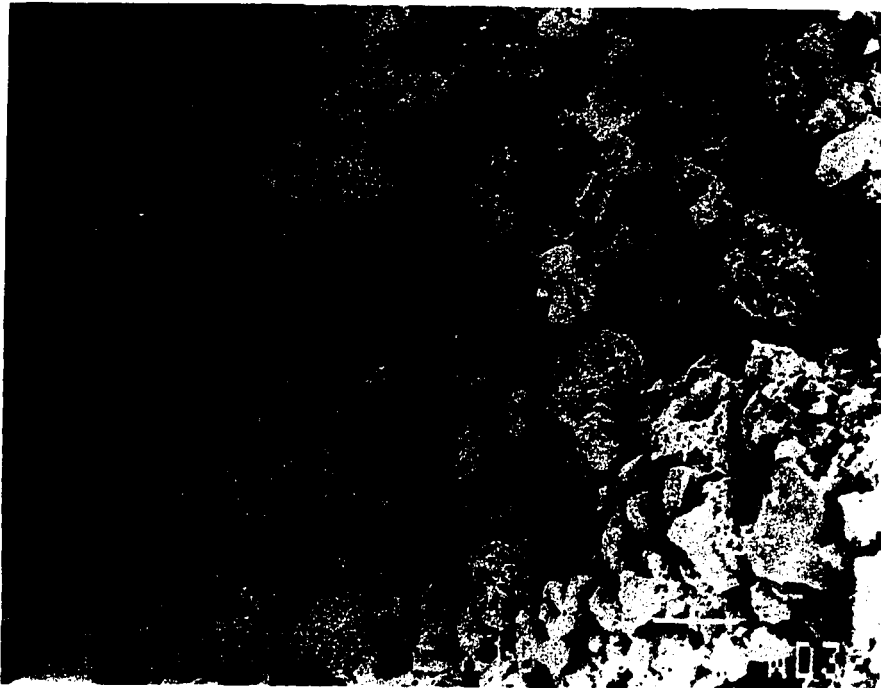
5.13.b after Dudley (1970) and Barden et al (1973).

### 5.3.2 *Fabric of Studied Soils*

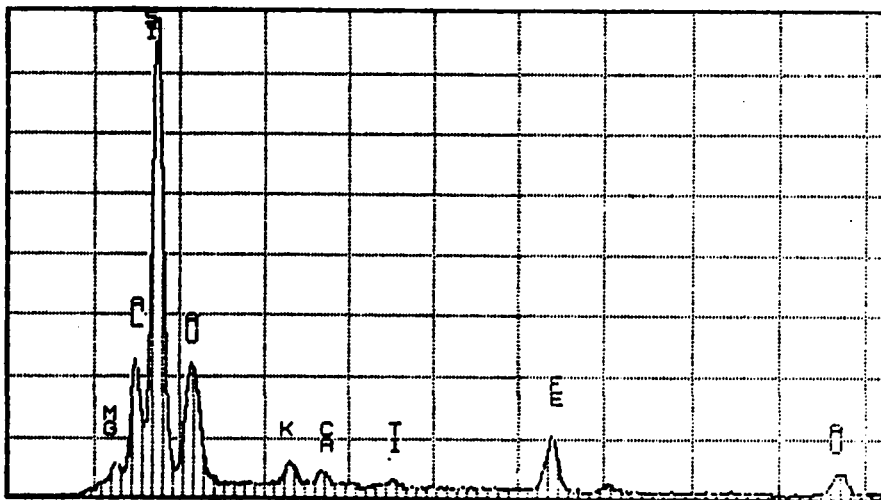
The fabric or microstructure of the study area soils included sandy silty soil, sandy silty clay with gravel soil (loess deposits), lean clay and lean clay with sand soil. The loessial soils exhibit a metastable structure, while lean clay soils exhibited a preferably oriented fabric. The microstructures shown in this section were selected out of sixty pictures in order to present the predominant and representative fabric.

**5.3.2.1 *Metastable Fabric (Collapsing Soils)*:** "Metastable fabric or collapsing soils are defined as any unsaturated soil that goes through a radical rearrangement of particles and great loss of volume upon wetting with or without additional loading" (Clemence and Finber, 1981). Soils with collapsible grain structures may be residual, water deposited, or aeolian (Dudley, 1970). Water and wind deposited collapsing soils are usually found in arid and semi-arid regions (Mitchel, 1976).

The collapsing soils within the study area are mainly of loess soils. Fans, mud flow, volcanic tuff and alluvial flood plain deposits may produce collapsible soils (Gillott, 1987). The natural structure of aeolian deposits contain clay cement binder. Upon saturation this clay binder loses its strength causing structure collapse. Figs. 5.14 and 5.15 show the microstructure of the loess

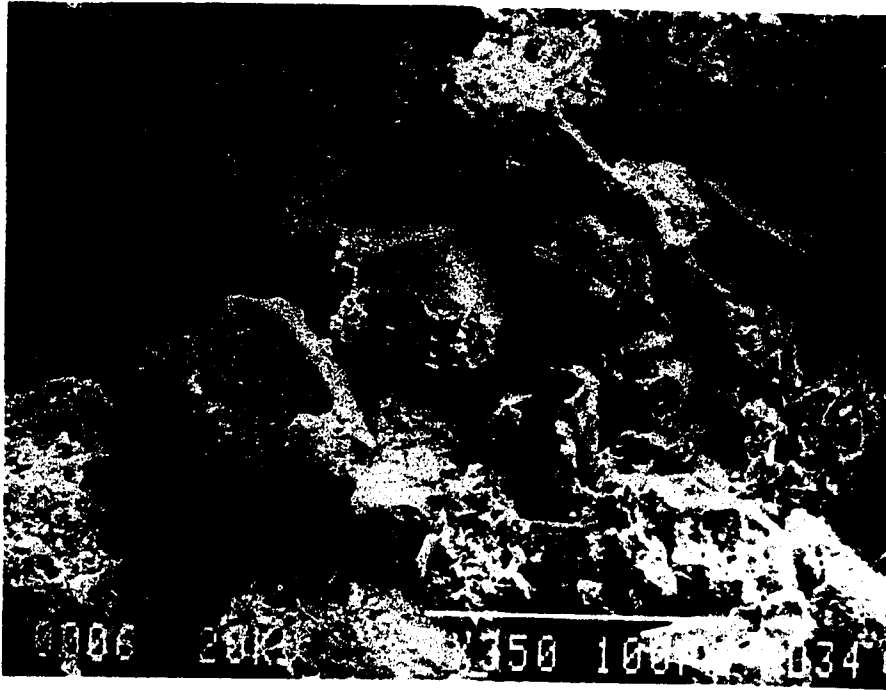


(a)

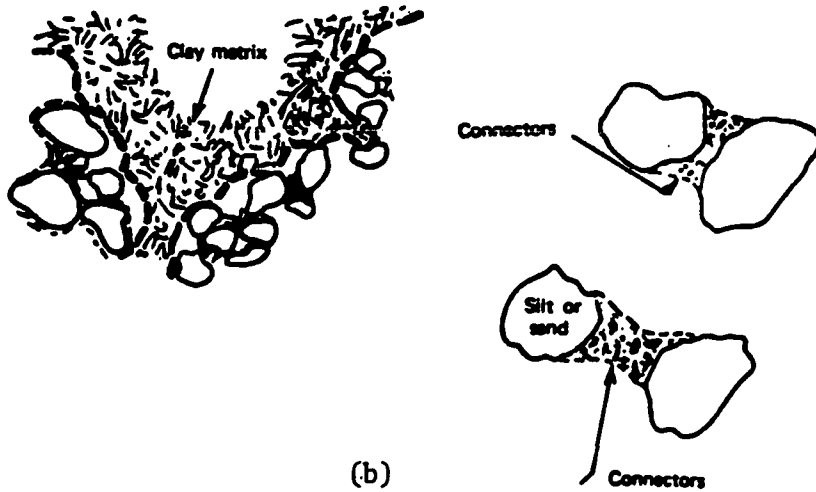


(b)

Fig. 5.14 : a) Loess microstructure of air-dried, vertical section, sandy silt. Station 33 at 1.8m.  
b) ED -spectrum of the loess specimen shown in (a).



(a)



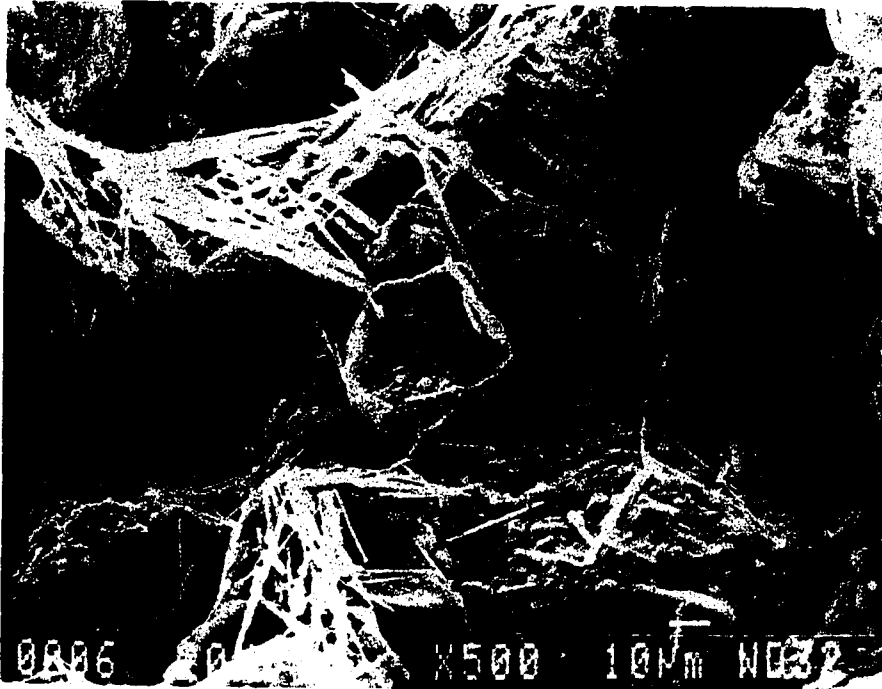
(b)

Fig. 5.15: a) Metastable fabric of sandy silt, loess soil, (Station 33, at 1.8m.)  
 b) Schematic representation of particle assemblages (Collins and McGown, 1974).

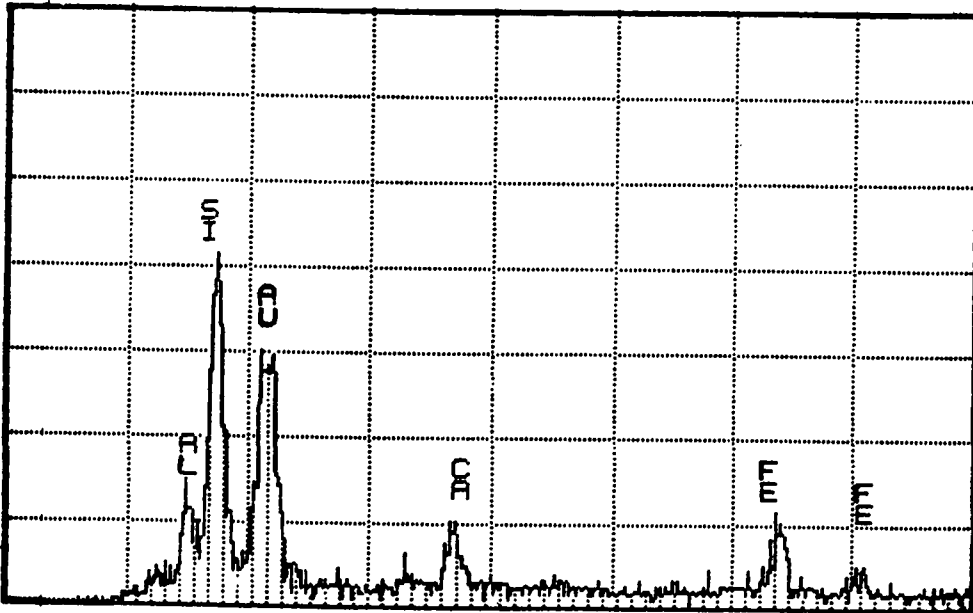
collapsing soil of sand silty soil type taken from 1.8 m below the ground surface at station # 33. These figures indicate the large voids and its distribution among the soil fabric either in the form of pores within the agglomerations or interparticle pores between individual particles and agglomerations. In addition, the energy dispersive spectrum (EDS) (Fig. 5.14.b) shows the existence of binder agents such as calcite and iron oxides. These open fabric and cementation binders, besides the higher silt contents (55%) and lower clay percentage (15%), led to a metastable structure that tends to collapse easily upon wetting.

The basic concept of collapsing phenomena is of an open fabric of bulky shaped grains, often in the silt to fine sand size range, held together by some bonding materials or forces. Different types of bond may be available such as flocculated clay buttress, capillary forces in case of silt-silt and silt-sand bonds, chemical precipitations and clay bridges (Fig.5.13.b) and clothed by clay interaction. A certain fabric may possess one or more of these bonding systems. The following microstructure figures show the metastable fabric with different types of bond.

Fig 5.16 shows the clay assemblaged, clothed silt and sand particle and inter assemblage pores. Aragonite, as a cementation agent, appears in needle forms. This figure represents the open clothed granular interaction of the sand silty soil from station # 33. Fig. 5.17 represents the same fabric of sandy silty clay with

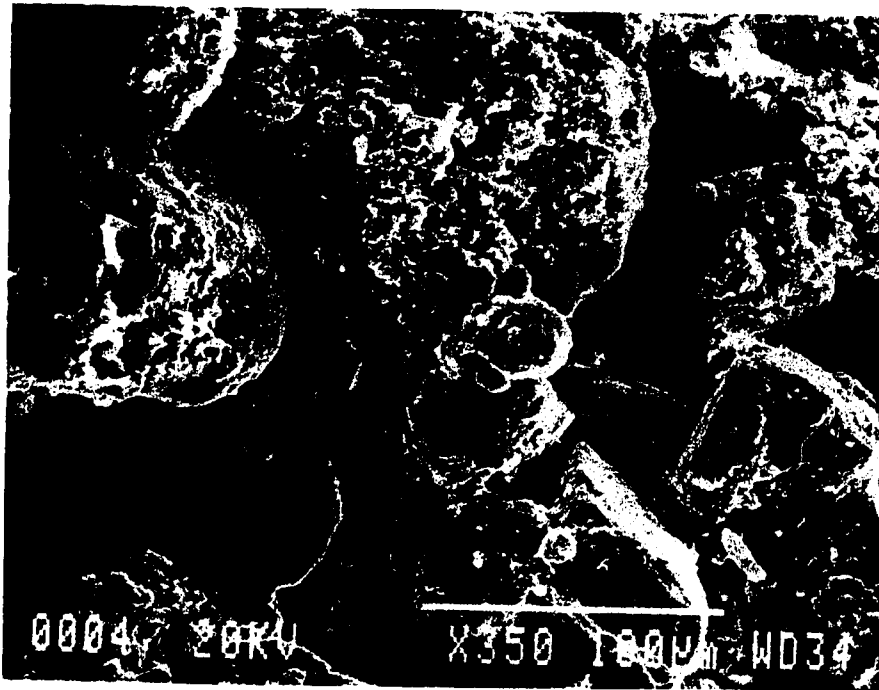


(a)

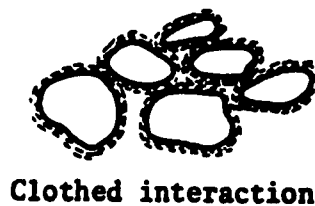
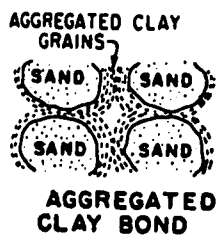


(b)

Fig. 5.16 : a) Microstructure of clothed silt and sand particles of undisturbed sample, air-dried and vertical section.  
 b) ED-spectrum, Station # 33 at 1.8 m.



(a)



(b)

Fig. 5.17 : Open fabric of clothed granular interaction type.  
 a) Microstructure of vertical undisturbed sample, air-dried, b) schematic representation for the above fabric, (after Collins and McGown, 1974) and Bradle, 1970.

gravel from station 31. The cementation agent, calcite, in Fig.5.17 is found in a bulky white form, compared with the needle form of aragonite in Fig. 5.16. Upon saturation the grains slide over one another, moving into vacant spaces. Moreover, during the sliding mechanism the clay coating represents a lubrication agent by which grain to grain friction is reduced and excessive collapsing takes place.

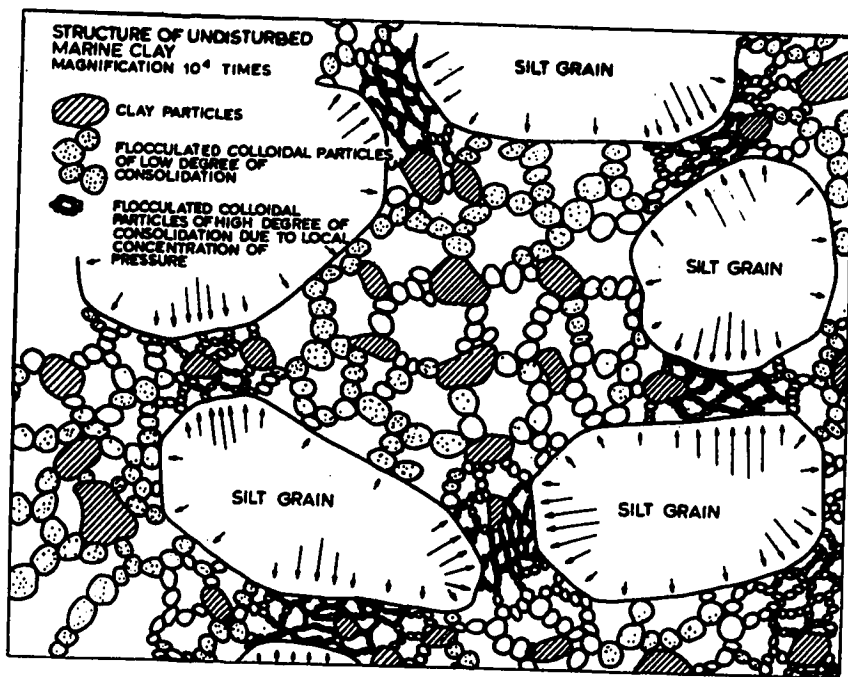
Fig.5.18 shows another open fabric known as honeycombed structure. The honeycombed is the main type of the metastable fabrics. Clay precipitation represents the connectors between sand, silt and clay assemblage. The particles and assemblages are sustained stable by calcite, iron oxides and aggregated clay bond. Upon saturation the fabric collapses.

Another open fabric is formed by keeping the silt and sand grains in positions without grain to grain contact by supports or bridges as shown in Fig.5.19. These bridges consist of clay having high calcium carbonate (calcite) and iron oxide contents as shown from the X-ray spectrum figure. The percentage of calcite of the same soil, sandy silty clay with gravel from station # 38, reached 28% as detected by X-ray diffraction (Table 5.3). Upon wetting the softening bridges govern the collapse of the structure into the open cavities.

The relatively high rate of chemical precipitations as shown in the microstructure figures (5.17.a, 5.18.a, 5.19.a, 5.20.a etc.)



(a)



(b)

Fig. 5.18 : a) Honeycombed open fabric structure of sand silts, loess deposit (Station # 33).  
 b) Structure of open fabric after Casagrande (1932) and Mitchell (1976).

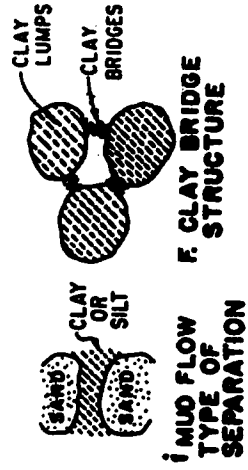
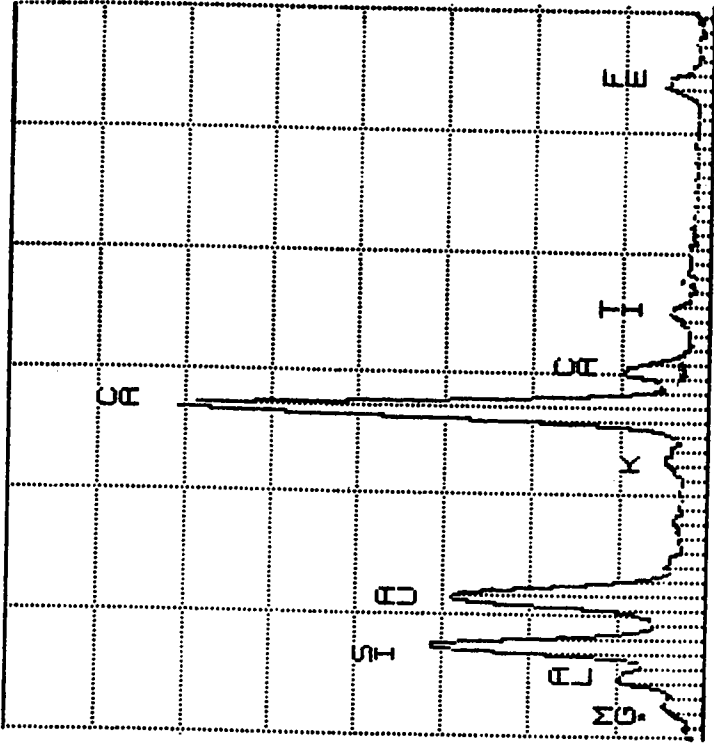
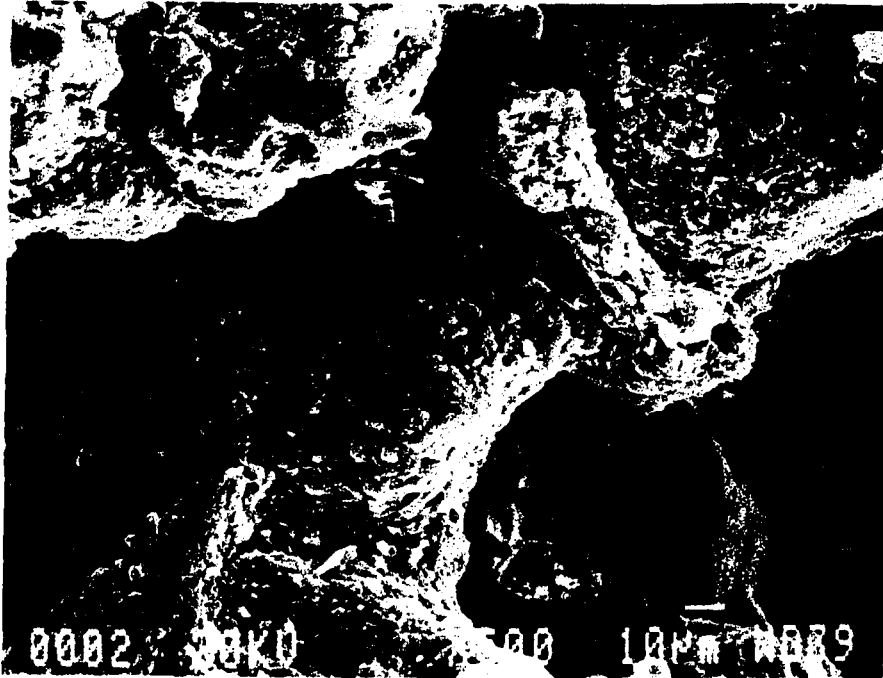


Fig. 5.19 : a) Microstructure of sand and silt particles supported by clay bridges of vertical section, air-dried.  
 b) EDS of clay bridge precipitation  
 c) Schematic of the structures after Dudley, 1971, et al.

may be due to the effect of high rates of evaporation and leaching in the region due to drying and wetting which permit high chemical precipitation. This cyclic weathering process of drying and wetting may cause little collapse within the initial fabric results in forming a secondary fabric form. This secondary fabric form has the tendency to collapse upon saturation and loading.

Fig. 5.20 shows the precipitation of flocculated clay on the cusp buttressed of grains. This picture gives another collapsing mechanism; upon wetting of this metastable structure (Gillott, 1987). Fig. 5.21 shows the flocculated clay that is rich in calcite as a predominant cementing agent within loess soils. The clay particles itself consist of face to face aggregated and flocculated. The collapse mechanism will take place not only in the cusp buttress, but also in the flocculated microstructure itself. The dissolving of the cementation agents will contribute to this collapse but in a slow rate compared to the collapsing of grain due to sliding into vacant voids.

**5.3.2.2 Oriented Fabric of Lean Clay Soils:** Oriented fabric is very common in water deposits. Stiff dark lean clay and stiff brown sandy lean clay are the soils which exhibited such fabric. The microstructure fabric of these soils is characterized by close-packed arrangement and close-packed face to face aggregation with less pores, both inter-assemblage pores and interparticle pores, as shown in Fig.5.22.



(a)

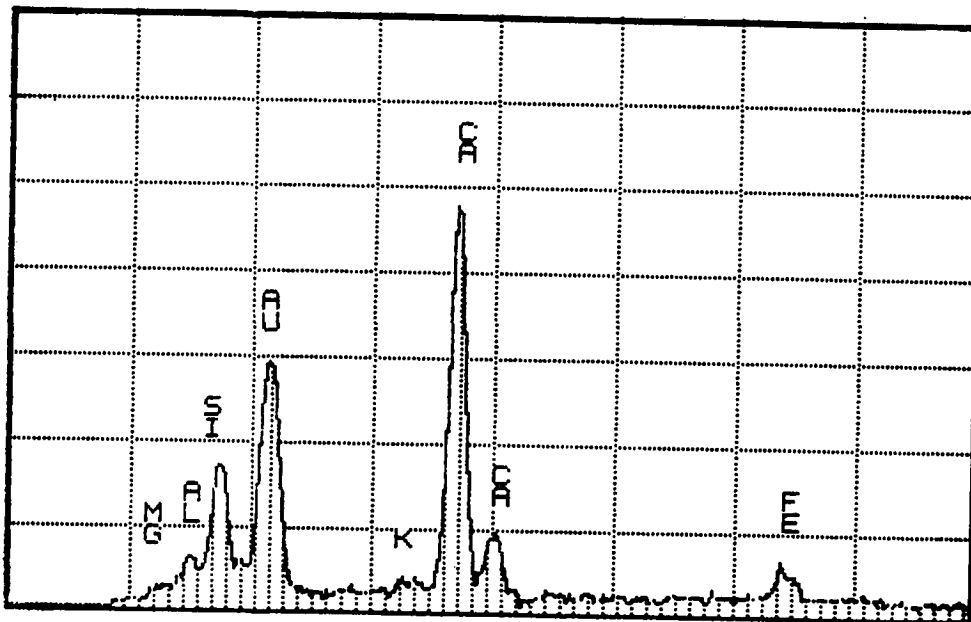


(b)

Fig. 5.20 : a) Microstructure of clay buttres selected from Station 36 at 2.0m.  
 b) Schematic of the fabric after Dudely, 1970 and others.



(a)



(b)

Fig. 5.21 : a) Scanning Electronic Microscope of Flocculated face to face clay structure.

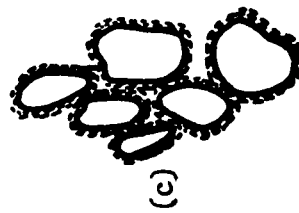
b) EGS of flocculated clay bonded by calcite and kaolinite.



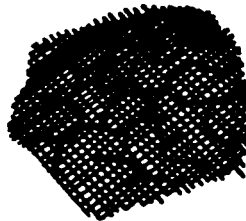
(a)



(b)

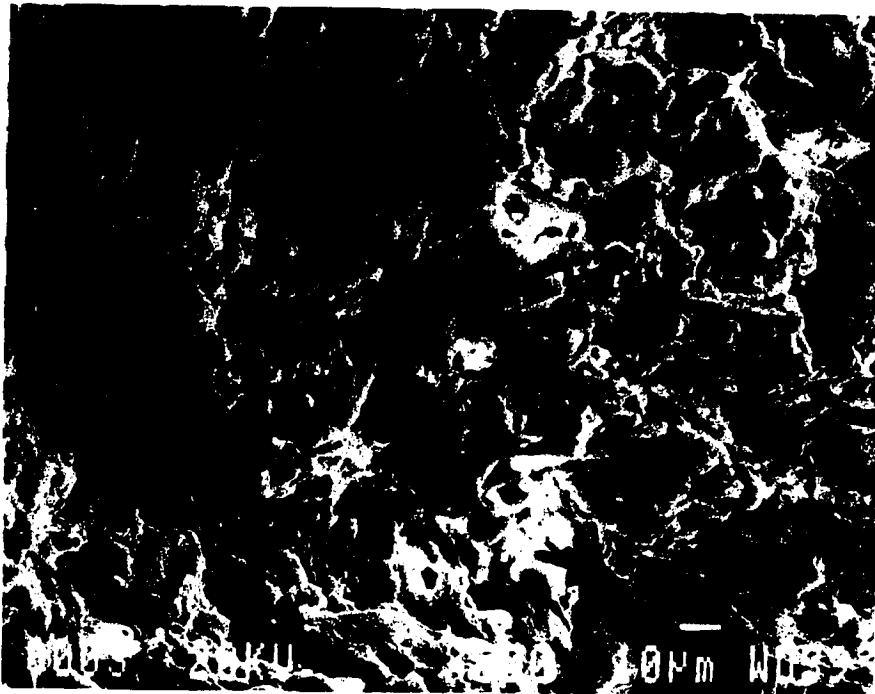


(c)

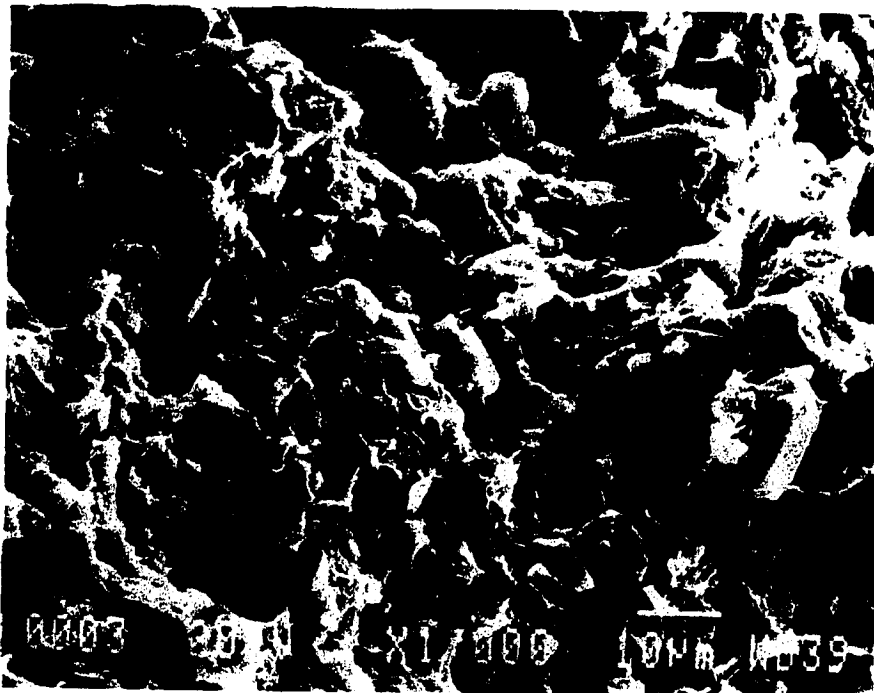


(d)

Fig. 5.22: Oriented structure, close-packed of lean soils: a) structure of sandy lean clay soil, b) structure of lean clay soil, c) clothed silt or sand particles interaction, d) partly visible interaction (after Collins and McGown, 1974).



(a)



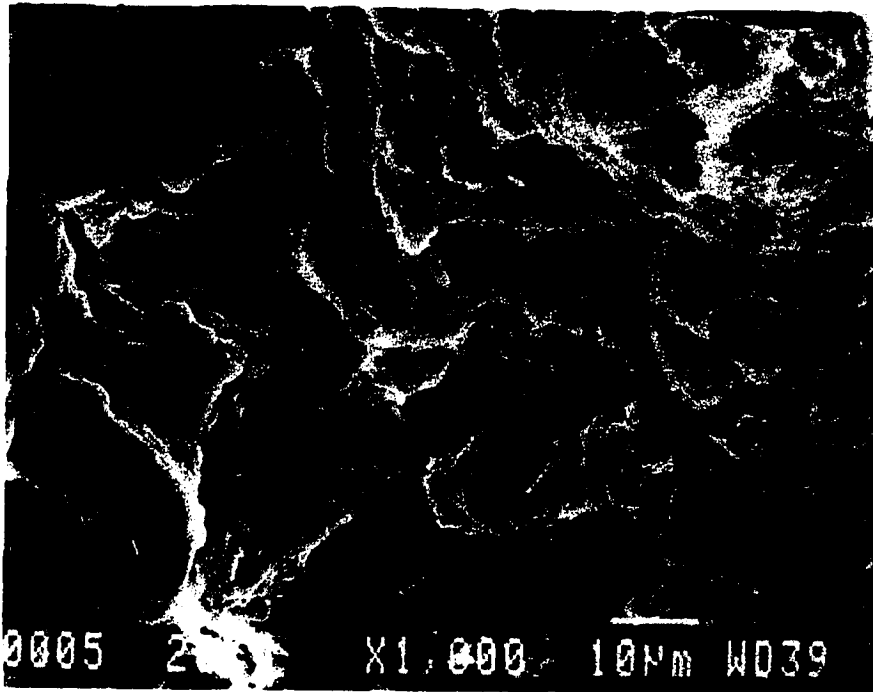
(b)

Fig. 5.23: High clay precipitation within silt particles of  
a) Sandy lean clay, and b) lean clay, Station 36  
at 4.0m and Station 33 at 0.7m. respectively.

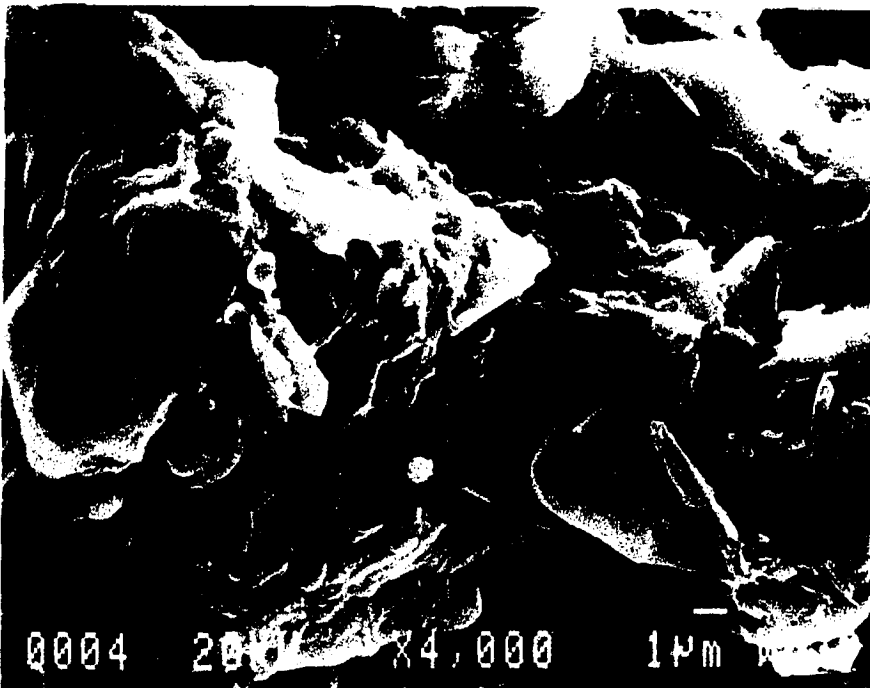
Fig. 5.23 shows the granular close-packed arrangement with high chemical and clay precipitation, and less interparticle voids. These precipitations are rich in calcite in case of sandy lean clay (30%) and rich in kaolinite in case of lean clay (39%), (Table 5.3). Ironoxide, potassium oxide and titanium oxide as chemical precipitation were also found in both soils as detected by X-ray spectrum. These chemical precipitations, which are the main source of bonding and cementation, give a complete clothed particle interaction fabric.

Fig. 5.24 shows the clay fabric of both soils. Edge to edge of the face to face aggregation is the common fabric. Smalley and Caberera (1969) described such arrangement by stepped face to face aggregation (Gillott, 1987). This pattern possesses an open structure and uneven edges. Sometimes edge to edge arrangement is not clear due to clay coating with chemical melting of calcite, iron oxide, etc. Sandy lean clay exhibited better orientation because it is located at larger depth which reduces the effect of weathering.

Freezing and thawing, wetting and drying and pressure effects are thought responsible for development of cracks, cleavage and fissures. Since the lean clay soil is the top soil, it is subjected to weathering processes more than other layers. In addition, this layer acts as a crust protection for those layers beneath it. Moreover, it preserves the natural structures of the



(a)



(b)

Fig. 5.24 : a) Well oriented face to face aggregation with edge to edge of sandy lean clay soil, Station 38 at 4.5m.  
 b) Layering in face to face aggregation bonded by chemical precipitation of lean clay. Station 33 at 0.7m.

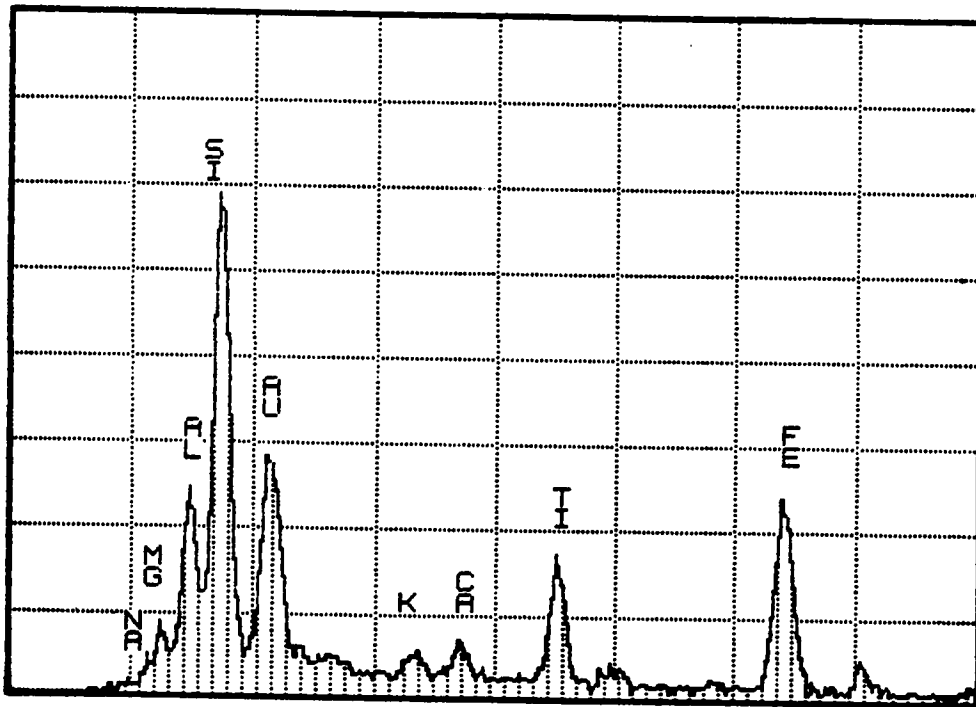
layers beyond it by stopping the seepage of large quantities of water. The weathering effects on particles of this top layer are very clear as can be seen in Fig 5.23.b. The cloudy shape represents the edges of the weathered particles. Comparing this with the microstructure of sandy lean clay in Fig. 5.23.a, the weathering effect is very minimum. This is because the sandy lean clay layer is at depth of 4.5m which is far away from the seasonal weathering effect.

The cloudy fabric, of the top lean clay soil, depicted in Fig. 23.b , is similar to the fabric of swelling soils which possess smectite (montmorillonite). This top soil exhibits a small swelling characteristic especially under low pressure, although the X-ra diffraction of this soil did not show any smectite minerals.

Fig.5.25 shows also the fabric of lean clay soil. A cloudy form with stepped face to face aggregation can also be seen. This may be due to weathering effects of swelling and shrinking. This swelling is related to the slightly over-consolidation property which this soil has. It is also related to the relative high clay content (32%), low natural water content (14%) and low calcite content (4%). These factors cause a swelling within the soil mass upon wetting and not within the intercrystal structures (octahedral and silica sheets) as smectite minerals do. The effects of these factors on swelling were discussed by, Altschaeffl (1982), Bull (1964) and (Gillott, 1987). The figure (5.25.b) shows the lower portion of



(a)



(b)

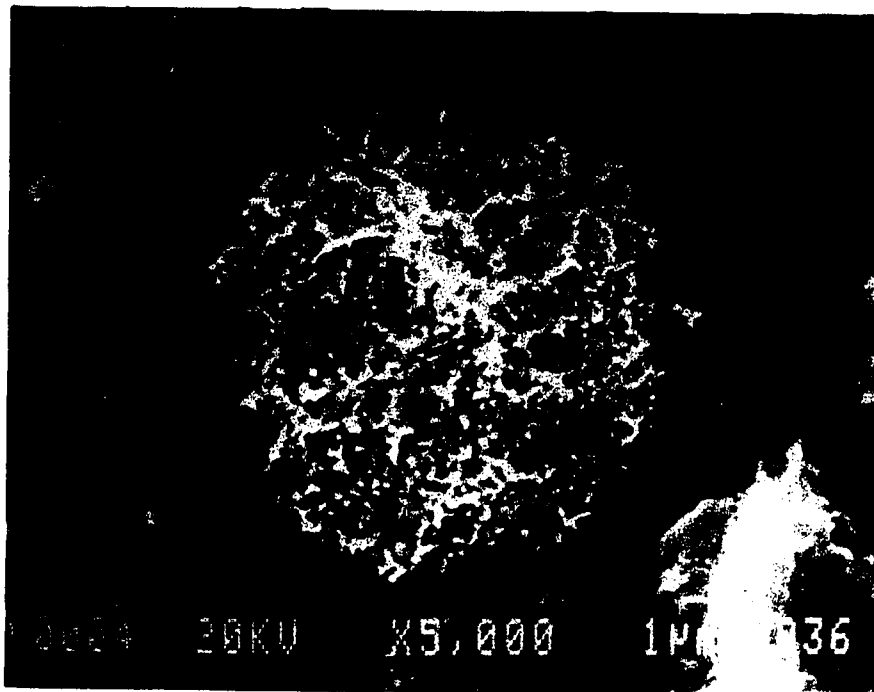
Fig. 5.25: Structure fabric of lean clay, Station 33 at 0.7m.  
a) Scanning Electronic Microscope of air-dried undisturbed sample.  
b) EDS of lean clay soil.

calcium as cementation agent and the higher of iron oxides and titanium oxides in the lean clay soil as detected by EDS.

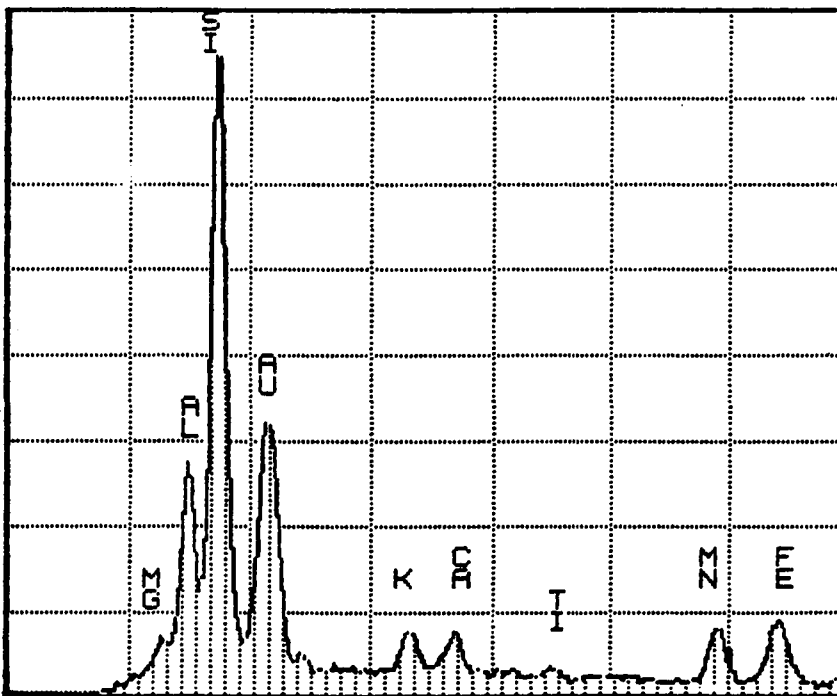
**5.3.2.3 Clayey Sand Fabric:** This soil was found in a very limited area. It was found at station # 23 and it may be found in levees zones on the sides of streams. It exhibited not only different chemical composition, but also different microstructure characteristics. Fig.5.26 shows the fissures, sand and silt particles as shown in white, and clay matrix as indicated in black. This fabric is greatly similar to the fabric of Cazenga clay (Angola) which was detected by Silva, J. A. (1971). This clayey sand soil may exhibit swelling characteristics and further study is advised to find its distribution and formation, and its shear strength and deformation characteristics. In this present study, mineralogy, composition, fabric and classification and index properties of this soil were studied.

### **5.3.3 Cementation**

Many soils such as sandstone, shales, loess are essentially cemented soil material. Such soils are most widely occur in semi-arid and arid region and in humid regions (Bear, 1964). The soils of the study area are either loess or alluvial soils containing mainly calcite, silica, aluminum and iron oxide, in form of hematite and maghemite, as cementation materials. Removal of this cementation material results in disaggregation of material as known by dis cementation.

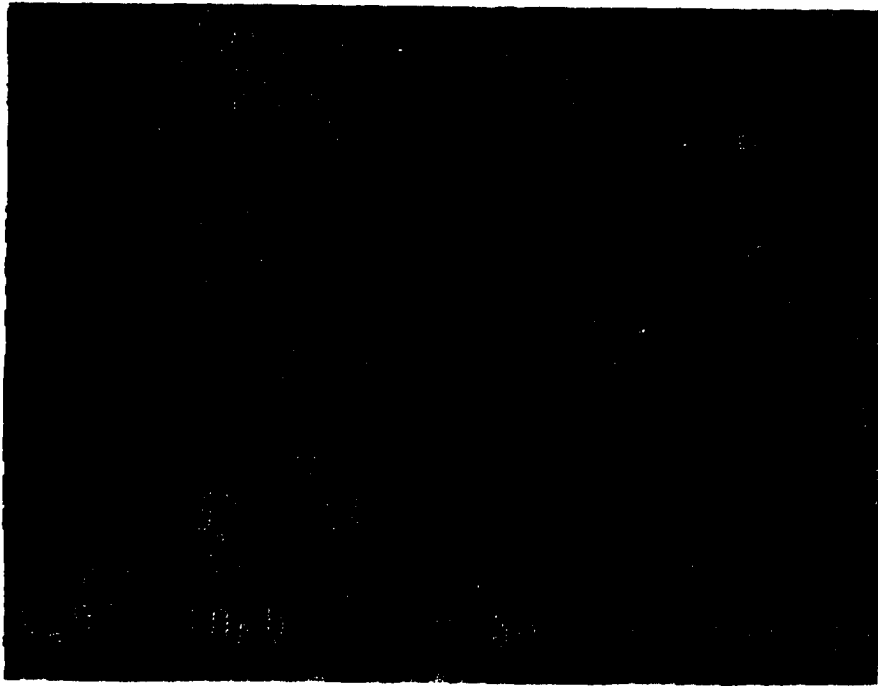


(a)

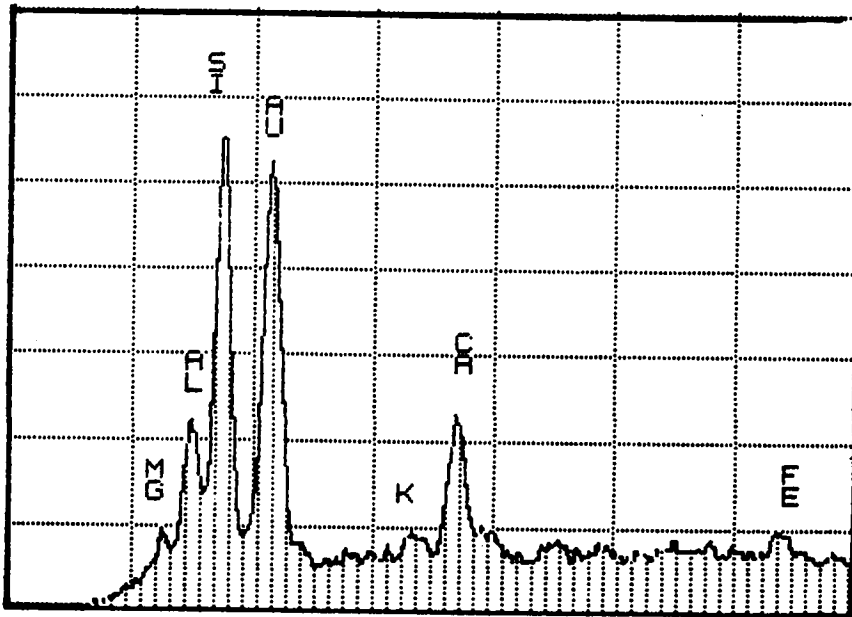


(b)

Fig. 5.26: Microstructure of clayey sand, Station 23 at 4.5m  
 a) SEM of air-dried, vertical section of undisturbed sample.  
 b) EDS of clayey sand.



(a)



(b)

Fig. 5.27: a) SEM of well cemented sand and silt particles by cementation agents.  
b) EDS of cementation agents. Station 38 at 4.5m.

Fig.5.27 shows the microstructure of the cemented particles. The cementation is in the form of a thin film coating the particles of silt and sand and joining them through contact points or in the form of platy particles interaction.

Cementation has important effects on the behavior of many soils. Cementation may result in an apparent over-consolidation. If the pre-consolidation is greater than the true applied pressure, a marked reduction in cohesion is observed (Mitchel, 1976). That is why some soils of the study area exhibited a slightly over-consolidated behavior. Upon saturation the soil loses its cohesion property. A noticeable volume decrease is measured due to weaken the cementation by wetting. In contrast, the cohesion is higher and the deformation is less in case of undisturbed unsaturated cemented soils. For cemented soils the lower the water content, the greater the bond strength (Clemence, 1981). The rate of losing cementation effectiveness relays upon the amount of incoming water and the applied stress. The higher the saturation and the higher the applied stress, the higher the rate of lossing the cementation (Gillott, 1987).

The most common soil fabric types including metastable fabric, well oriented fabric and the conglomeratic fabric of the cemented sandy gravelly soil are all summerized in table 5.10. The table also indicates the different forms of each soil fabric as well as the cementation agents.

Table 5.10: Summary of the Most Common Soil Fabric

Unit	Soil Classification	Station #	Depth (m)	SOIL FABRIC		
				Type	Description	Bonding Agent and Remarks
7	Lean Clay	33	0.7	Well oriented	Face to face aggregation with edge to edge and partially visible interaction	High clay precipitation between granular particles, Figs. 5.23 and 5.24b
4	Sandy lean clay	36	4.0	Well oriented	Face to face aggregation to edge and clothed silt or sand of close packed arrangement	High clay and chemical precipitation (calcite), Figs. 22.a, 22.b and 24.a
6	Sandy silt clay with gravel	38	2.0	Metastable	Clothed particles separated by clay bridges and clay buttress	Clay and chemical precipitations such as calcite, Fig. 5.19 and Fig. 5.20
5	Sandy silt	33	1.8	Metastable	Honeycombed open fabric Open fabric of loess	Flocculated clay and chemical precipitation, Fig. 5.18 Less cementation with high voids with low degree of consolidation, Figs. 5.14 and 5.15.
4		35	4.5	Metastable	Open clothed granular interaction	Clay and chemical film coating, Fig. 5.17.
3	Silty clayey sand	41	2.0	Conglomerates	Weakly cemented granular	Clay and chemical precipitation, Plate 4.11.

## Chapter 6

### SOIL DEFORMATION & SHEAR STRENGTH CHARACTERISTICS

#### 6.1 General

This chapter deals with the compressibility and deformation properties, obtained from one dimensional consolidation tests and the shear strength and stress strain behavior, obtained from consolidated undrained triaxial tests. The results will be shown in both conventional and critical state model forms.

#### 6.2 Consolidation and Collapsing Properties

##### 6.2.1 Results of Consolidation Tests:

Twenty one one-dimensional compression tests were performed on representative specimens from different fine soils selected from different depths. Figs. 6.1-6.3 show  $e-\log \sigma'_v$  curves of some selected soils. The rest of the curves are shown in Appendices D1 to D3. Appendix D-4 shows the computer program which was used in calculating  $e$  and  $\sigma'_v$  values. The figures (6.1-6.3 and D1-D3) show different patterns according to the soil type and its stress history. The natural water content ( $W_c$ ), the specific gravity ( $G_s$ ) and the initial void ratio ( $e_o$ ) are also shown in the figures. The pre-consoli-

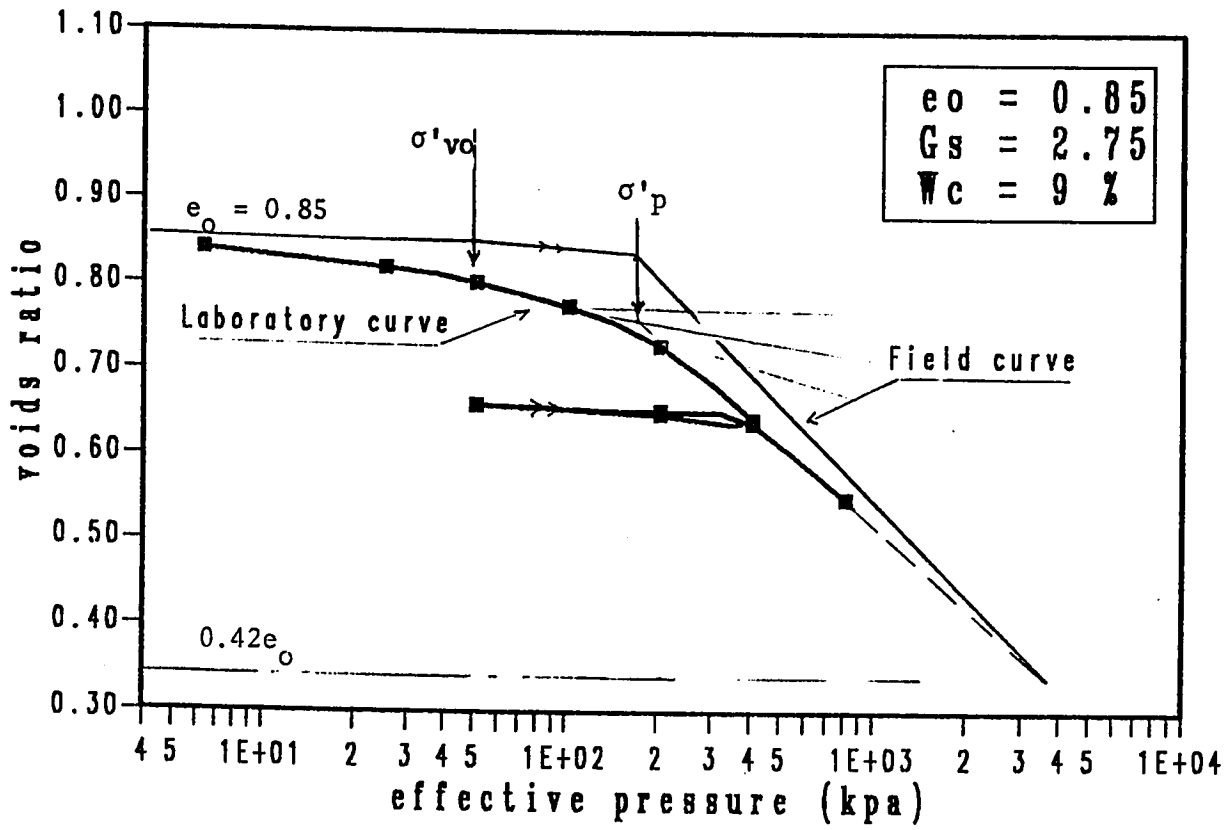


Fig. 6.1:  $e$ -Log  $\sigma'_v$  curve of sandy silt soil selected from station 40 at 2.5m.

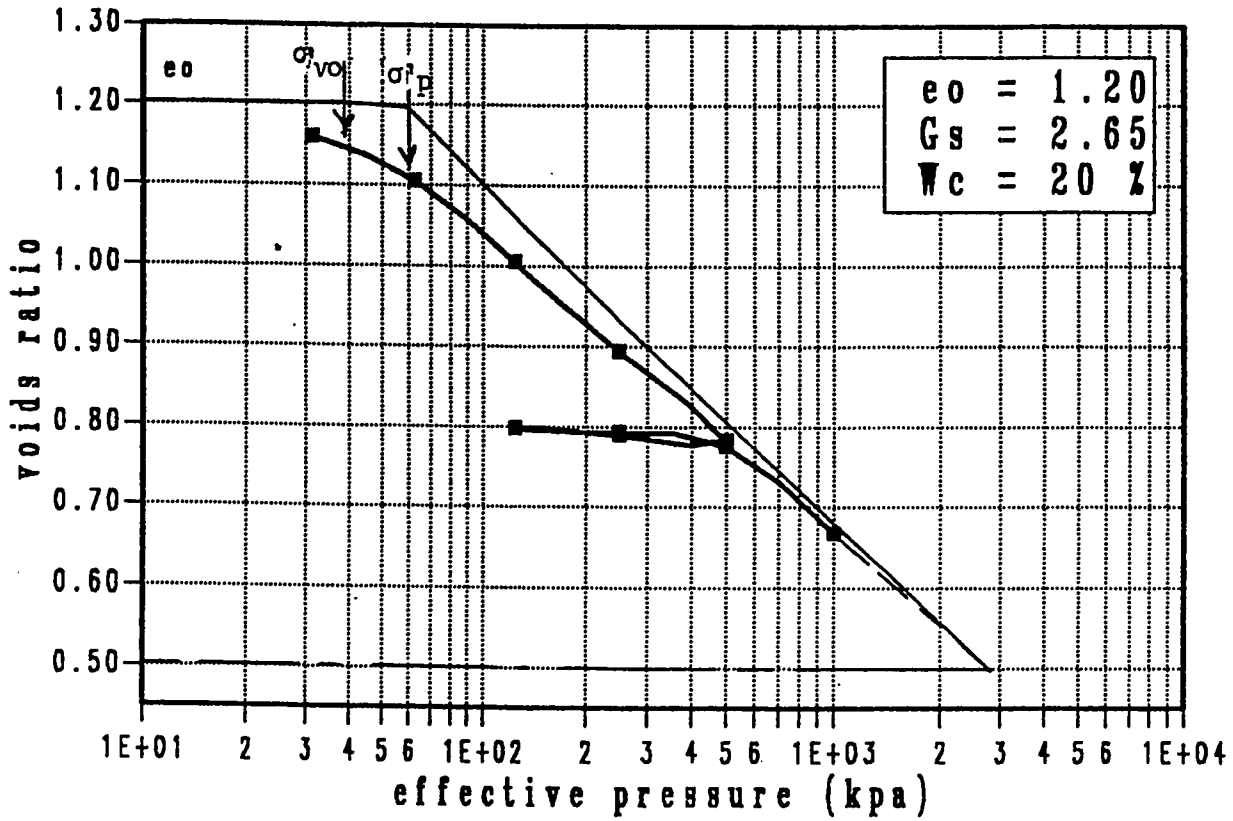


Fig. 6.2:  $e$ -log  $\sigma'_v$  curve of sandy silty clay with gravel selected from station 38 at 2.0m.

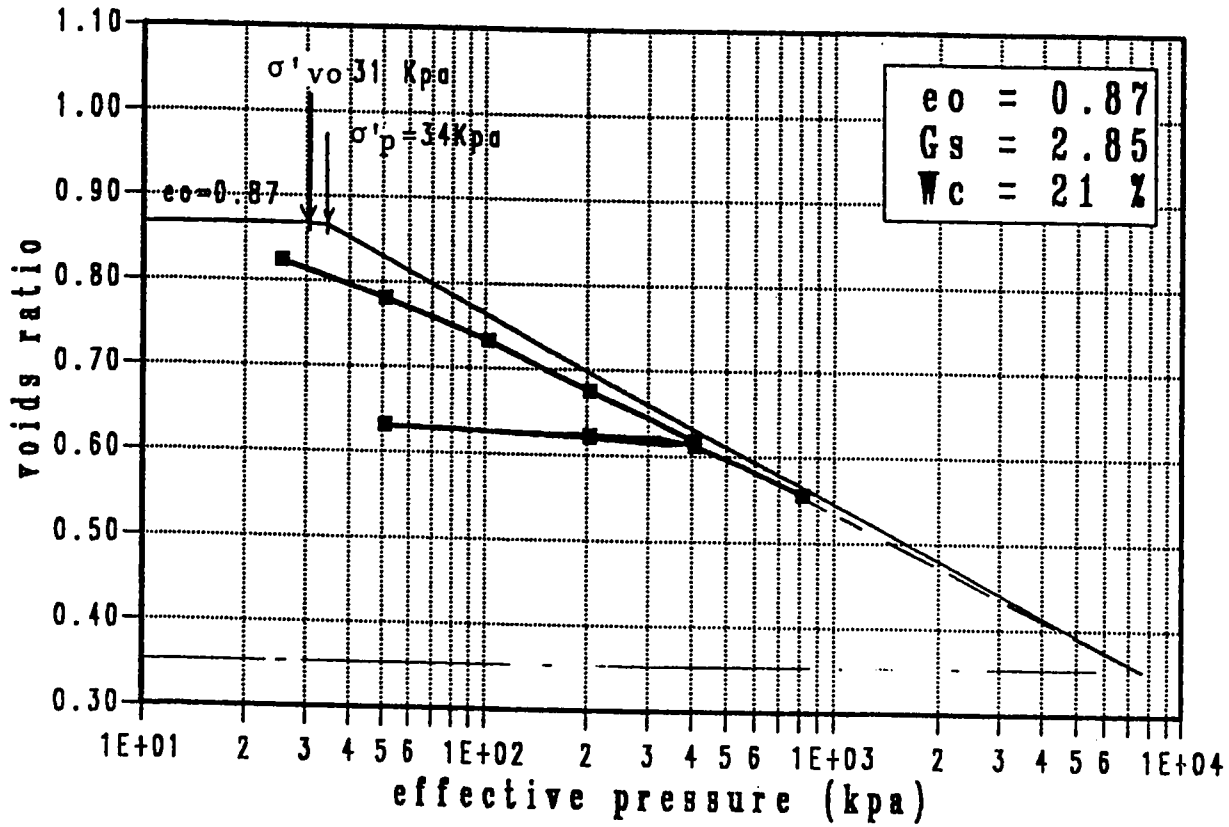


Fig. 6.3:  $e$ -Log  $\sigma'_v$  curve of silty clayey sand with gravel selected from station 41 at 2.0m.

dation pressure  $\sigma_p$  were determined by using Casagrande's method. The field curve was drawn for each sample using Schmertmann graphical method. The compression index  $C_c$  was determined from the slope of the straight portion of the laboratory curve. The coefficient of volume compressibility  $m_v$  was evaluated from the change in voids ratio corresponding to a pressure increase of about  $150 \text{ KN/m}^2$  from the first  $50 \text{ KN/m}^2$  loading of the lab curve. The swelling index,  $C_s$  was determined from the average slope of the unloading reloading curve. The values of these parameters are shown in Table 6.1. The table shows also the values of the coefficient of consolidation  $C_v$  which is determined by the square root of time method. The average value of  $C_v$ , of the following load increment (25, 50, 101, 203 and 407 KN), was considered. The overburden pressure  $\sigma'_{vo}$  was calculated according to the natural in-situ state. The values of over consolidation ratio (O.C.R) defined as  $\frac{\sigma_p}{\sigma'_{vo}}$  are also shown in

Table 6.1.

The different parameters of compressibility from laboratory tests can either be approximately evaluated by applying certain formulae or corrected by using certain suggested methods. The field values of the compressive index  $C_c'$  and the coefficient of volume compressibility  $m_v'$  were obtained using the field curve. These values

Table 6.1: Summary of Results from One-Dimensional Consolidation Test

Soil Unit	Soil Type	Station #	Depth (m)	$\gamma_n$ kN/m <sup>3</sup>	$\sigma'_{vo}$ KPa	$\sigma'_p$ KPa	O.C.R.	$C_c$	$C_s$	$m_v \times 10^{-4}$ m <sup>2</sup> /kN	$C_v \times 10^{-7}$ m <sup>2</sup> /sec
7	Lean Clay	33	0.7	18.2	13	130	10	0.26	0.042	2.42	4.20
4	Sandy Lean Clay	36	4.0	16.2	79	220	2.8	0.395	0.02	1.67	3.80
6	Sandy Silty Clay With Gravel	38	2.0	16.7	39	60	1.5	0.359	0.023	5.10	2.70
			4.5	17.2	76	77	1.0	0.254	0.021	5.10	3.13
5	Sandy Silt	33	1.8	14.2	28	33	1.2	0.332	0.04	4.43	1.60
			2.5	16.5	45	160	3.5	0.31	0.022	2.60	2.56
			4.0	15.7	62	78	1.3	0.345	0.021	4.71	3.76
			4.5	14.8	78	100	1.3	0.42	0.021	4.57	2.28
4*											
3	Silty Clayey Sand With Gravel	41	2.0	20.0	31	43	1.4	0.18	0.016	3.70	3.18

\*This soil was classified as lean clay with sand (Unit 4-ii) after USCS, but it has the characteristics of the sandy silt soil (Unit 5) as also identified after Holtz and Gibbs (1960).

are shown in Table 6.2. Comparing the laboratory and the field values, the following remarks are driven:

- A maximum approximation of about 17% results in case of using the following suggested relation by Terzaghi and Peck (1967):

$$C_c' = 1.3 C_c$$

where  $C_c'$  : is the compression index results from the field virgin.

The empirical relation:

$$C_c' = 0.009 (LL - 10)$$

after Terzaghi and Peck (1967) is applicable for clay soils such as lean clay in this study, while a difference of about 50 % was noted in case of using this relation for the silty soil (loess).

The coefficient of permeability was calculated from one-dimensional consolidation results by using two different methods. A third empirical relation was also used. In the first method the following relation was used:

$$K = C_v m_v \gamma_w \quad \text{m/sec}$$

where  $\gamma_w = 9.8 \text{ KN/m}^3$  and  $C_v$  is the coefficient of consolidation.

The computed values of K are shown in table 6.2 as  $K_1$ . In the sec-

Table 6.2: Interrelated Results of One-Dimensional Consolidation Test

SOIL TYPE	Station #	Depth (m)	$C_c'$	$m_v'$ $m^2/kNv$	$K_1$ m /sec	$K_2$ m /sec	$K_3$ m /sec
Lean Clay	33	0.7	0.29	$2 \times 10^{-4}$	$9.97 \times 10^{-10}$	$7 \times 10^{-10}$	$1.0 \times 10^{-10}$
Sandy Lean Clay	36	4.0	0.44	$1.69 \times 10^{-4}$	$6.2 \times 10^{-10}$	$1.8 \times 10^{-10}$	$1.6 \times 10^{-9}$
Sandy Silty Clay with Gravel	38	2.6	0.4	$2 \times 10^{-4}$	$1.35 \times 10^{-9}$	$7.80 \times 10^{-10}$	$3.6 \times 10^{-9}$
		4.5	0.33	$2.4 \times 10^{-4}$	$1.6 \times 10^{-10}$	$5 \times 10^{-10}$	$9 \times 10^{-10}$
Sandy Silt	33	1.8	0.4	$2.6 \times 10^{-4}$	$6.9 \times 10^{-9}$	$7.0 \times 10^{-10}$	$4.9 \times 10^{-9}$
		2.5	0.4	$2.6 \times 10^{-4}$	$6.5 \times 10^{-10}$	$7.84 \times 10^{-10}$	$9 \times 10^{-10}$
		4.0	0.41	$2.88 \times 10^{-4}$	$1.74 \times 10^{-9}$	$8.8 \times 10^{-10}$	$4.9 \times 10^{-10}$
		4.5	0.47	$2.5 \times 10^{-4}$	$1.02 \times 10^{-9}$	$3 \times 10^{-10}$	$1.6 \times 10^{-9}$
Silty Clayey Sand with gravel	41	2.0	0.25	$2.18 \times 10^{-4}$	$1.15 \times 10^{-9}$	$9 \times 10^{-10}$	$8.5 \times 10^{-6}$

ond method the square root of time depicted in Fig.6.4 was used to get the coefficient of permeability,  $K_2$  in Table 6.2 (Young, R. N. and Townsend, F. C. 1986). Different values were obtained corresponding to different load increments. The average values were considered. In order to compare the obtained values of the coefficient of permeability from oedometer test to other values, the Hazen relation was used as follows:

$$K = C(D_{10})^2 \quad \text{cm/sec}$$

where  $C = 100$  as an average value, since it depends on the soil type and  $D_{10}$  is the effective diameter in cm. This method is more suitable for sands. The computed values of  $K$  using Hazen relation are shown as  $K_3$  in Table 6.2.

### 6.2.2: Critical State Results:

To compute the critical state parameters, one need to calculate the mean effective pressure  $p'$  as

$$p. = \frac{1}{3} (\sigma'_v + 2\sigma'_h)$$

where:  $\sigma'_v$  = the effective vertical stress and  $\sigma'_h$  is the effective horizontal stress. Hence, the effective horizontal stress ( $\sigma'_h$ ) needs to be estimated, because it is not measured in the usual one dimensional test. The horizontal effective stress  $\sigma'_h$  is related to the

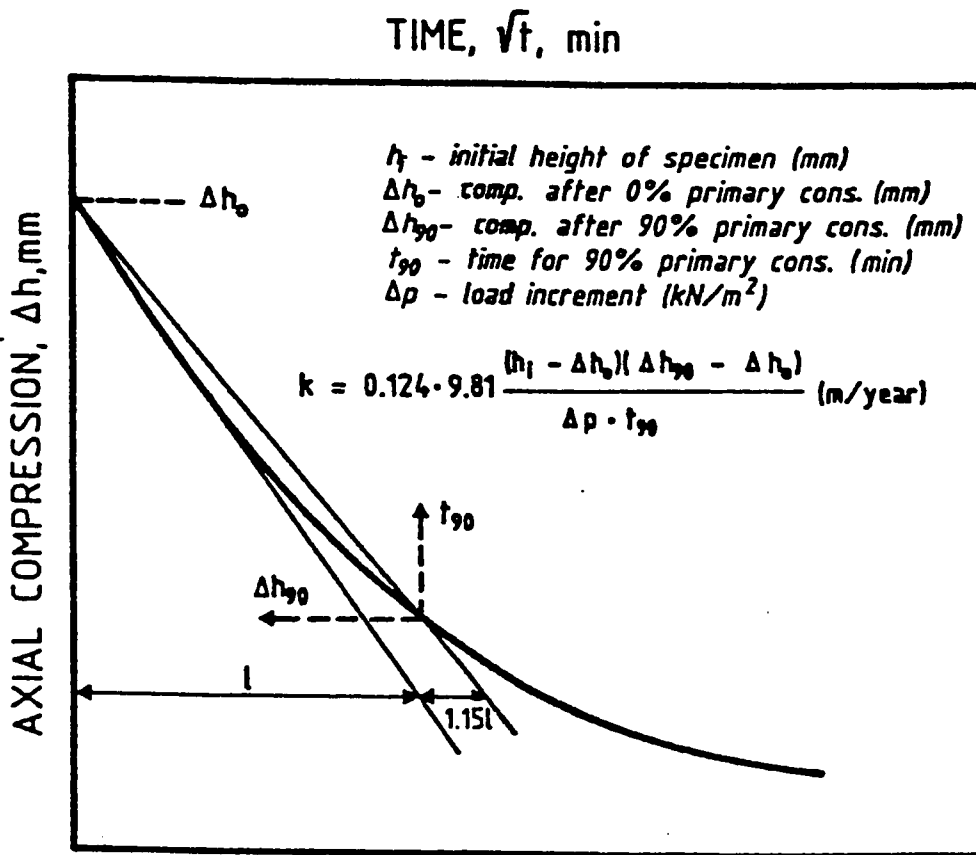


Fig. 6.4 : Coefficient of permeability  $k$  from time-compression curve.  
 (After Young, R.N. and Townsend, F.C., 1986).

effective vertical stress by

$$\sigma'_h = k \sigma'_v$$

where  $k$  is the coefficient of lateral earth pressure (Atkinson, J. H. and Bransby, P. L. , 1978). The coefficient at which no lateral movement in soil mass is called the coefficient of earth pressure at rest  $k_o$ . This relies upon the soil characteristics at natural condition which is very difficult to assess. So, two different empirical relationships were used to evaluate an average value of  $k_o$ . The first relationship,  $k_{o1}$  depends on the internal friction angle ( $\varphi$ ) of normally consolidated clays (Bowles, 1982). It is defined as:

$$k_{o1} = 0.95 - \text{Sin}\varphi$$

The second relation ( Bowles, 1982) depends on the plasticity index PI is defined as:

$$k_{o2} = 0.19 + 0.233 \log \text{PI}.$$

An average value of  $k_{o1}$  and  $k_{o2}$  were considered in calculating  $k_{ave}$ .

The critical state parameters for each soil type were obtained according to the following steps:

- For each vertical load increment of the odometer test, the final void ratio  $e$  is recorded.
- The horizontal stress is computed as:

$$\sigma'_h = (k_o)_{ave} \sigma'_v$$

- The critical state parameters required the calculation of the mean pressure  $p'$  as:

$$p' = \frac{1}{3}(\sigma'_v + 2\sigma'_h)$$

- For each void ratio  $e$ , the specific volume  $v$  is calculated as

$$v = 1 + e$$

- The data are plotted in  $v \ln p'$  space and the following critical state parameters can be obtained:

$\lambda$  = slope of the normal consolidated line

$\kappa$  = slope of the swelling line

$v_o$  = initial specific volume =  $1 + e_o$

$N_o$  = specific volume at  $p' = 1.0$  kpa

The previous steps were repeated for all soils. Table 6.3 shows an example of how to obtain these parameters for the sandy lean clay soil (Station # 36 at 4.0m). Figs. 6.5 - 6.6 show the  $v - \ln p'$  plots of some soils and the rest of the plots are shown in Appendices D-5 and D-6.

For one dimensional consolidation test the following relations were used to get  $C_c$ ,  $C_s$  and  $m_v$  from  $\lambda$  and  $\kappa$  as follows:

Table 6.3: Critical State Model Results of Sandy Lean Clay  
 Calculated from Oedometer Test Results.

Vertical Stress ( $\sigma_v$ ) kN/m <sup>2</sup>	$k_{av}$	Horizontal Stress ( $\bar{\sigma}_h$ ) kN/m <sup>2</sup>	Settlement $\Delta H$ mm	Specific Volume $V$	$P'$ kN/m <sup>2</sup>	$l_{np}'$
25	0.43	10.689	0.177	1.902	15.46	2.74
50.9	0.43	21.88	0.306	1.889	31.55	3.45
101.9	0.43	43.77	0.504	1.869	63.18	4.14
203.7	0.43	87.55	0.806	1.839	87.59	4.42
407.5	0.43	175	1.544	1.764	252.65	5.53
203.7	0.43	87.55	1.488	1.77	87.59	4.47
50.9	0.43	21.88	1.362	1.782	31.55	3.45
203.7	0.43	87.55	1.46	1.773	87.59	4.47
407.5	0.43	175	1.602	1.758	252.65	5.53
815	0.43	350	2.776	1.641	505.3	313.3

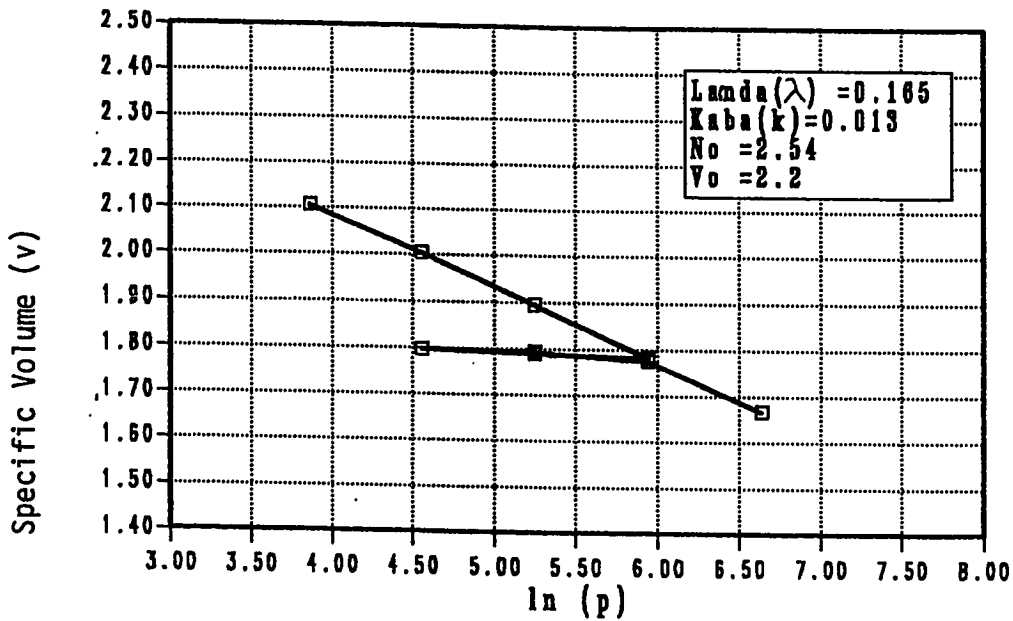


Fig. 6.5 :  $v$ - $\ln p$  space of the sandy silty clay with gravel (station 38 a 2.0m)

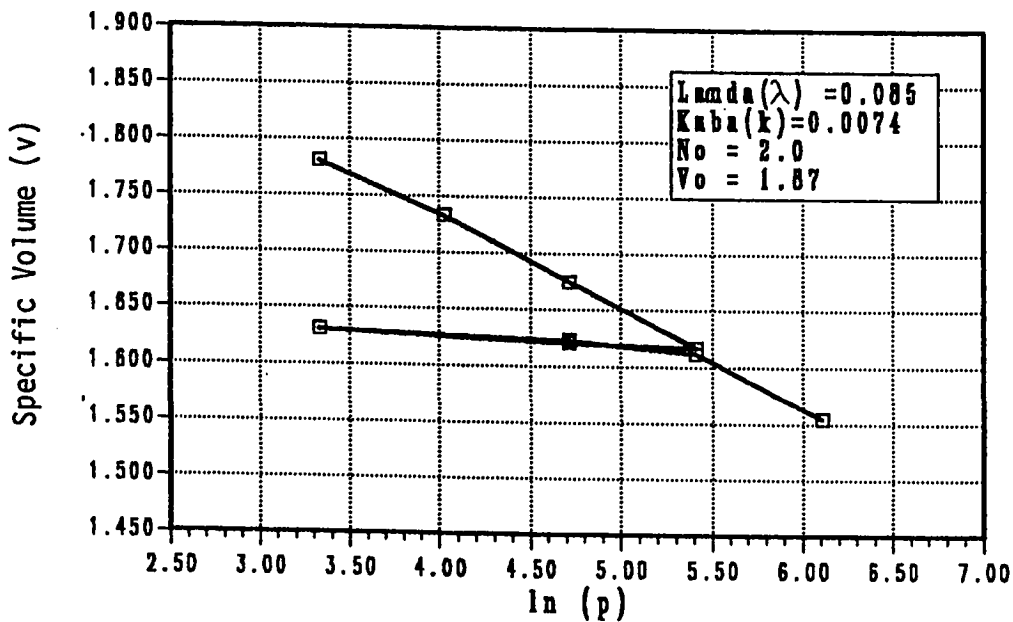


Fig. 6.6 :  $v$ - $\ln p$  space of the silty clayey sand with gravel (station 41 at 2.0m)

$$C_c = 2.303 \lambda$$

$$C_s = 2.303 \kappa$$

$$m_v = \frac{\lambda}{(\sigma'_v \times v)}$$

The coefficient of volume change  $m_v$  was calculated at specific volume corresponding to different vertical stresses. The vertical stress equals 203 kip gave the average values of  $m_v$ . All the above data results are summarized in Table 6.4

### 6.2.3 Analysis of Results:

Volume change in soils either compression or expansion have a great effect on changes of soil strength and deformation. Generally, changes in volume may result from changes in pressure, temperature and chemical environment. Since the study area is arid region, the volume changes of the study area soils are greatly effected by the chemical and environmental factors. Referring to Table 6.1, the stress-history of the clayey soils is predominantly normally to slightly overconsolidated except for the top layer soil, lean clay which exhibited a relatively high O.C.R. =10 .

The slightly overconsolidated soils within the study area (O.C.R. = 1.5 - 3.5) have been predominantly influenced by fluctuation in ground water table and soil composition. The water table was known to be about 2.0 to 4.0m below the ground surface twenty-five

Table 6.4: Oedometer Test Results in Form of Critical State Model

Soil Unit	Station #	Depth m	$\phi^o$	PI %	$K_{O1}$	$K_{O2}$	$K_{Oav.}$	$\lambda$	$\kappa$	$V_o$	$N_o$	$C_c$	$C_s$	$\frac{M_v}{m^2kN}$	$\mu$
7	33	0.7	32	20	0.42	0.49	0.45	0.124	0.0166	1.85	2.26	0.29	0.038	$3.4 \times 10^{-4}$	0.31
4	36	4.0	35	18	0.37	0.48	0.43	0.176	0.009	1.93	2.56	0.4	0.02	$4.7 \times 10^{-4}$	0.3
6	38	2.0	36	5	0.320	0.32	0.32	.165	0.013	2.2	2.54	0.38	0.029	$3.5 \times 10^{-4}$	0.24
		4.5	31	7	0.43	0.38	0.41	0.104	0.01	1.86	2.0	0.24	0.023	$3.2 \times 10^{-4}$	0.29
5	40	1.8	32	2	0.42	0.26	0.34	0.148	0.0198	2.44	2.59	0.341	0.045	$2.95 \times 10^{-4}$	0.25
		2.5	26	3	0.51	0.29	0.4	0.139	0.008	1.85	2.2	0.32	0.02	$3.9 \times 10^{-4}$	0.29
		4.0	38	3	0.33	0.31	0.32	0.156	0.01	2.14	2.48	0.36	0.023	$4.0 \times 10^{-4}$	0.24
4	35	4.5	35	0	0.37	0.41	0.39	0.184	0.01	2.04	2.54	0.42	$4.9 \times 10^{-4}$	0.28	
3	41	2.0	39	4	0.32	0.32	0.32	0.085	0.0074	1.87	2.0	0.196	0.017	$2.49 \times 10^{-4}$	0.24

years ago, while it is now about twenty meters below the surface. This movement of the water table led to densification or hydroconsolidation of the soil (Mitchell, 1976). The second significant and predominant factor is the chemical and environmental effect. The leaching and precipitation of chemical, clay and colloidal materials resulted in forming certain structures with high chemical precipitations as cementation agents, as shown earlier in chapter 5. This cementation may result in an apparent preconsolidation pressure. Removal of iron compounds, the cementation agents, from sensitive clays led to a decrease in apparent preconsolidation pressure of  $30 \text{ ton/m}^2$  (Mitchell, 1976). The cementation effect was also noted by Bjerrum (Mitchell, 1976). This preconsolidation could be a quasi-preconsolidation effect similar to the one noted by some investigators (Fadlul, 1982).

According to the above it is clear that most of the studied soils, below the dark top layer, are normally consolidated soils. The appearance of lightly preconsolidation of some soils are mainly related to soil composition.

The stiff fissured lean clay, top layer, exhibited relatively high overconsolidation ratio (O.C.R. = 10), as shown in Fig. 6.7. This is greatly related to the cycle of swelling and shrinkage which this layer has been subjected to as a result of wetting and drying. This layer preserves the layer beneath it against the weathering effects. Since this layer is a surficial layer, a dynamic loading effect may be considered as another factor which causes preconsolidation. The

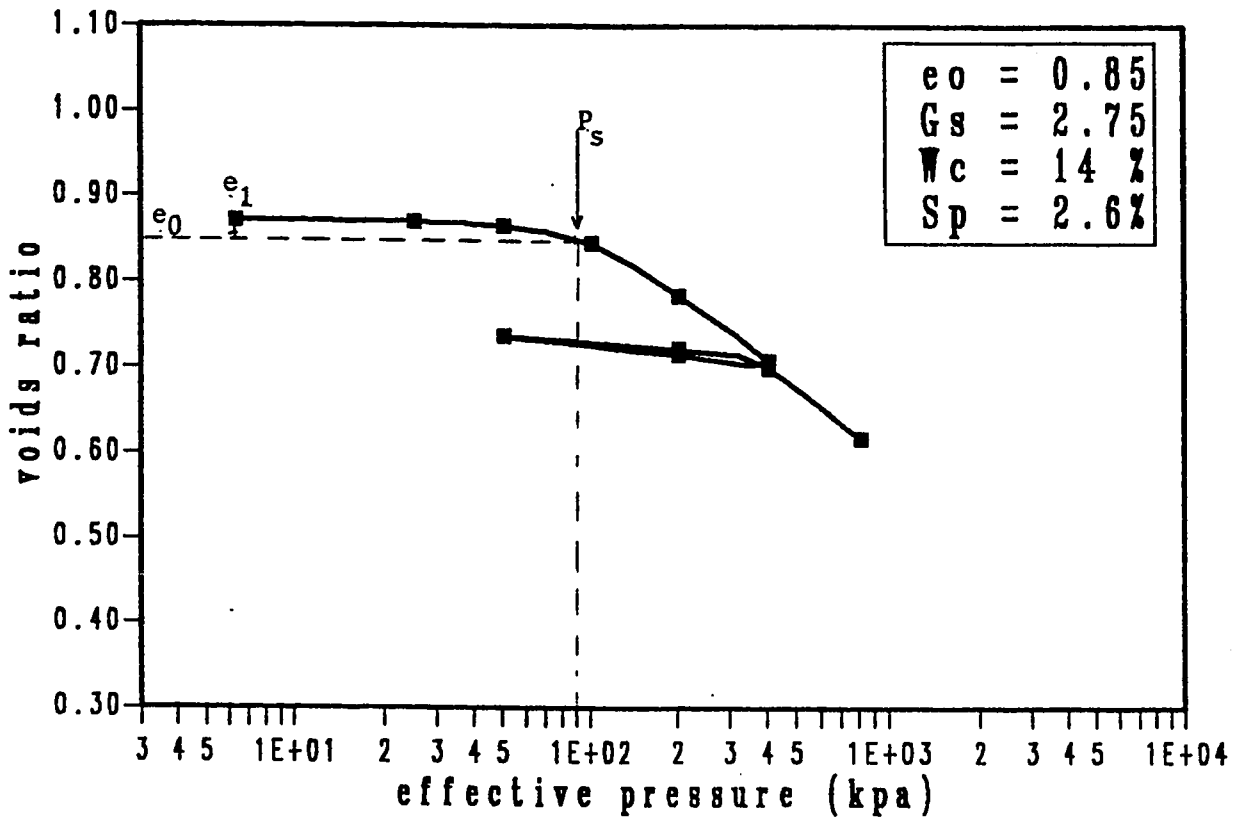


Fig. 6.7:  $e$ -log  $\sigma'_v$  curve of lean clay soil selected from station 33 at 0.7m.

overconsolidation of this layer may also be related to the internal water tension between particles or more specifically referred as the soil moisture tension. This soil is characterized by its cracks and joints which, in time, may be filled with debris and are no longer obvious. Such clay soil is known as desiccated clay. Upon wetting, this soil relaxes leading to a release of the internal tension between particles, subsequently, an expansion to a certain limit occurs. The expansion or compression of this soil is a function of the initial water content, the applied pressure and the swelling pressure of the soil (Spanglar and Handy, 1982).

The coefficients of volume compressibility  $m_v$  of the soil units are in the range 0.17 to 0.51  $m^2/MN$ . According to Tomlinson (1980), the lean clay and sandy lean clay identified as medium compressible soil ( $m_v = 0.1 - 0.3 m^2/MN$ ), while the other soils were described as highly compressible soils ( $m_v = 0.3 - 1.5 m^2/MN$ ). Something has to be noted in the identification of the compressibility between this system and the plasticity chart identification, Appendix B2. Both systems gave the same result in case of lean clay and sandy lean clay soils, while different identifications were obtained in case of loess and sandy soils. Since soils were tested in saturated condition, high compressibility is expected, specially from loess soils. Consequently, the identification of the compressibility of loess is low when they are partially saturated, but upon saturation high compressibility in form

of collapsing is expected. The collapsing of loess soil will be described later.

The compressibility of any saturated soils having different clay minerals increases in the order kaolinite < illite < montmorillonite (Mitchell, 1976). The values of the compressibility index  $C_c$ , the coefficient of volume change  $C_v$  and the swelling index  $C_s$  of the different clay minerals have been reported by Cornell University, 1951, as shown in Table 6.5 (adopted from Mitchell, 1976). The soil composition can be identified indirectly by using these parameters. "Since compressibility and hydraulic conductivity are strongly functions of soil composition, the coefficient of consolidation  $C_v$  should also be related to soil composition, because  $C_v$  is directly proportional to hydraulic conductivity  $K$  and inversely proportional to  $C_c$ " (Mitchell, 1976). The values of the compressibility index  $C_c$ , the coefficient of volume change  $C_v$  and the swelling index  $C_s$  of the studied soils (table 6.1) are within the range of kaolinite values. The kaolinite was directly identified by using the X-ray diffraction method as discussed in section 5.1.2.1.

The average values of the coefficient of permeability  $K$ , Table 6.2, are in the ranges of  $6.0 \times 10^{-9}$  m/sec  $1.0 \times 10^{-9}$  m/sec for silty, sand and clayey matrix and  $7.0 \times 10^{-10}$  m/sec  $1.0 \times 10^{-10}$  m for clayey soils. Low values of  $k$  are observed in comparison with the ranges

Table 6.5: Values of  $C_c$  and  $C_v$  of Clay Minerals\*

Clay Mineral	$C_c$	$C_v$ $\times 10^{-4} \text{ cm}^2/\text{sec}$	$C_s$
Kaolinite	0.19 - 0.28	12 - 90	0.05 - 0.08
Montmorillonite	0.50 - 1.10	0.03 - 2.4	0.31 - 0.37
Illite	1.00 - 2.60	0.06 - 0.3	0.34 - 1.53

Table 6.6: Order-of-magnitude values for permeability  $k$ , based on description of soil and by Unified Classification, m/s

$10^0$	$10^{-2}$	$10^{-5}$	$10^{-9}$	$10^{-11}$
Clean gravel GW, GP	Clean gravel and sand mixtures GW, GP SW, SP GM	Sand-silt mixtures SM, SL, SC	Clays	

of  $k$  in Table 6.6 after Unified Classification (Bowles, 1982). These low values of  $k$  reflect the influence of clay and colloidal particles which exist coating the granular particles. The clay contents influence the soil behaviour even if it exists in a smaller percentage compared with the other percentages of the soil (Mitchel 1976).

The soils exhibited a low tendency to swelling, except the stiff fissured lean clay soil as shown in Fig. 6.7. The average values of the swelling index  $C_s$  is about 0.022 for almost all the soils tested except for the lean clay soil, which  $C_s$  is 0.042. Under low stress this soil exhibited a swelling potential. When a specimen of this soil was loaded by about one psi then saturated (using ASSHTO Procedure) it exhibited a swelling potential. Further identification was done by using plasticity index, activity and clay content of the soil. Referring to Table 4.4, the stiff fissured lean clay is classified as a swelling soil with medium swelling potential (2.6%), as shown in Fig. 6.8. Table 6.7 shows the approximate ranges of the swelling potential and total expansion according to the plasticity index of the soil.

The swelling characteristics of the stiff fissured lean clay is mainly due to the climatic and environmental effects rather than to the existence of any swelling mineral, such as smectite. Altschaeffl (1982) indicated that swelling occurs under low pressures upon wetting the specimen. Many investigators (Seed and Chan, 1959; Mitchell, 1976) indicated that some soils which exhibit swelling behaviour due to factors such as stress history, low natural water content,

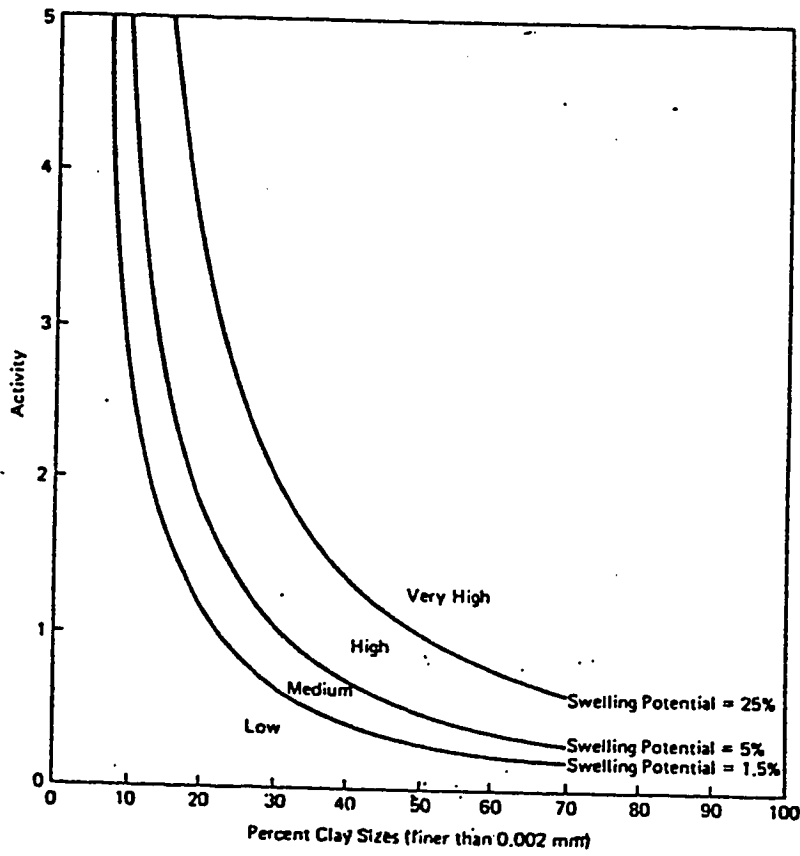


Fig. 6.8 : Classification chart for swelling potential (Mitchell, 1976).

Table 6.7 : Approximate relationship between total expansion, swelling potential, and plasticity index, (Mitchell, 1976).

Plasticity Index (%)	Swelling Potential (%)	Total Expansion (%)
10	0.4- 1.5	4.5-10.0
20	2.2- 3.8	13.5-18.7
30	5.7-12.2	21.4-18.0
40	11.8-25.0	28.0-35.0
50	20.1-42.6	33.0-40.0

\* For samples compacted at optimum water content using the standard AASHO procedure and allowed to swell under a surcharge of 1 psi.

† Air dry to saturation under 1 psi surcharge.

fabric, chemical and organic environment, shearing resistance, etc., are not necessary to contain expansive minerals in their crystals structure. The suction which is defined as the internal water tension between particals is the main factor that contribute to the swelling behaviour. Upon wetting this tension forces relax causing expansion.

Although the sandy lean clay possesses the same plasticity index, activity and clay content, as lean clay soil, it did not show any swelling behavior as the lean clay soil. This in fact reflects the effect of the stress history and the seasonal variation or climatic effect. The sandy lean clay has lower O.C.R. and it exists at a depth of 4.0 m, at which the soil is not subjected to the seasonal variation effect.

The studied stiff fissured lean clay has no expanding minerals as detected before. The swelling index  $C_s$  was used indirectly in identifying the clay minerals as shown in Table 6.5 (adopted after Mitchell, 1976). The values of  $C_s$  of this stiff fissured lean clay soil is in the range of the kaolinite values as shown in Tables 6.1.

The swelling pressure of the lean clay soil is about 90 kpa as calculated from Fig. 6.7. This swelling pressure may cause a damage for basement and floors of structures. Furthermore it may cause also damage to one or two-storey houses, as can be seen in Plate 6.1 which shows cracks in a house having a foundation of a bearing wall

type placed at 0.5 m. The indicated cracks are within the boundary zone of the minimum and maximum stress on the soil.

The computed values of Poisson's ratio  $\mu$  from the relation defined by the coefficient of earth pressure at rest,  $k_{ave}$  in Table 6.4, are in the range of the typical values of the different soils (Bowles 1982) as can be seen in Table 6.8.

Table 6.8 : Typical range of values for Poisson's ratio  $\mu$  (Bowles, 1982)

Type of soil	$\mu$
Clay, saturated	0.4-0.5
Clay, unsaturated	0.1-0.3
Sandy clay	0.2-0.3
Silt	0.3-0.35
Sand (dense)	0.2-0.4
Coarse (void ratio = 0.4-0.7)	0.15
Fine-grained (void ratio = 0.4-0.7)	0.25
Rock	0.1-0.4 (depends somewhat on type of rock)
Loess	0.1-0.3
Ice	0.36
Concrete	0.15



Plate 6.1 : Failures on masonry bearing wall of one floor building resting on the expanding lean clay, 'Merriah'.

#### 6.2.4 *Collapsing soils*

6.2.4.1 *General:* The sandy silt and sandy silty clay with gravel soils were classified earlier as loess deposits. In their natural conditions, low moisture content, these deposits possess high apparent shear strength; however, it is susceptible to large reduction in void ratio (collapse) upon wetting. This reduction in voids can occur at fairly low levels of stress. In contrast to consolidation, where the reduction in void ratio is the result of the time-dependent due to expulsion of pore water, the settlement of a collapsing soil is more or less immediate and coincides with the intake of moisture by the soil.

Shrinkage, swelling and collapsing are influenced by the fabric and structure of the soil. The loess deposits and the silty clayey sand with gravel, the alluvial deposits of the study area, are having metastable structures as explained in the previous chapter. Such fabric identifies the collapsing soils that undergo large volume change upon saturation. Further identification of the collapsing behavior was carried out upon the different types of soils using the void ratio relationships at natural density and liquid limit. In addition, laboratory testing on a representative samples was carried out to detect the soil susceptibility to collapse as discussed in the next section.

#### 6.2.4.2 Qualitative and Quantitative Methods for Predicting Soil Collapse:

Many investigators have suggested different qualitative methods to predict the soil susceptibility to collapse. Some of these methods (Denisov, 1951; Gibbs and Bora, 1967) which employ the void ratio relationships at natural density and liquid limit for predicting the qualitative susceptibility to collapse, the first and the second methods in this section. The third method is a laboratory testing, suggested by Jennings and Knight (1975), was used to get a quantitative prediction of soil collapse (ASTM, 1978; Spanglur and Handy 1982).

##### *Qualitative Methods:*

First Method (Gibbs and Bara, 1967): This method is a reliable and convenient method to detect collapsible loess. It relies upon the basis of liquid limit and bulk density of the soil. If the moisture content at saturation of any soil, having a certain bulk density, is more than the liquid limit, the soil is considered as collapsible. This water content at saturation is defined by the following relation:

$$W_c = \frac{V_s \gamma_w 1.0}{\gamma_d} = \frac{\gamma_w G_s - \gamma_d}{\gamma_d G_s} \quad (1)$$

where

$V_s$  : volume of solids

$\gamma_w$  : unit weight of water =  $9.8 \text{ kn/m}^3$

$G_s$  : specific gravity of the soil

$\gamma_d$  : in-situ dry density of the soil

$W_c$  : water content at saturation

To prove the previous relation, let the total volume (V) of the representative prism of the soil is ( $V = 1 \text{ m}^3$ ), then

$$e = \frac{V_v}{V_s} = \frac{V - V_v}{V_s}$$

where  $e$  = the void ratio

$V_v$  = the volume of water at saturation

therefore,

$$V_s = \frac{1.0}{1 + e} \quad (2)$$

since

$$\gamma_d = \frac{\gamma_w G_s}{1 + e}$$

then

$$1.0 \times \gamma_d = \gamma_w G_s \cdot V_s \quad \text{or} \quad V_s = \frac{\gamma_d \times 1.0}{\gamma_w G_s} \quad (3)$$

$$\text{at saturation: } W_c = \frac{e \times 1.0}{G_s} = \frac{1 - V_s}{G_s}$$

$$= 1 - \frac{\frac{\gamma_d \gamma_w G_s}{\gamma_w G_s G_s}}{\gamma_w G_s G_s} = \frac{(\gamma_w G_s - \gamma_d) \gamma_w}{\gamma_w G_s \cdot \gamma_d}$$

$$W_c = \frac{\gamma_w G_s - \gamma_d}{G_s \gamma_d}$$

If  $W_c$  is greater than LL (liquid limit), then soil is most likely collapsible, but if  $W_c$  is less than LL (liquid limit) then soil is not. The following example indicates the identification of the sandy silt soil, Station # 33 at 1.8 m (Spanglur and Handy, 1982).

The in-situ dry unit weight of the sandy silt is  $12.6 \text{ kN/m}^3$  and the liquid limit is 28.  $G_s = 2.73$ , then

$$W_c = \frac{9.8 \times 2.73 - 12.7}{12.7 \times 2.73} \times 100 = 41$$

Since  $W_c$  is greater than LL, then the soil is most likely collapsible.

The other soils were analyzed in the same way. The results are summarized in Table 6.9. This method is presented in a diagram as shown in Fig.6.9, (after Clemence, 1981).

The Second Method: It relies upon the voids ratio relationship (Denisov, 1951). In this method a subsidence factor  $K_c$  is defined as:

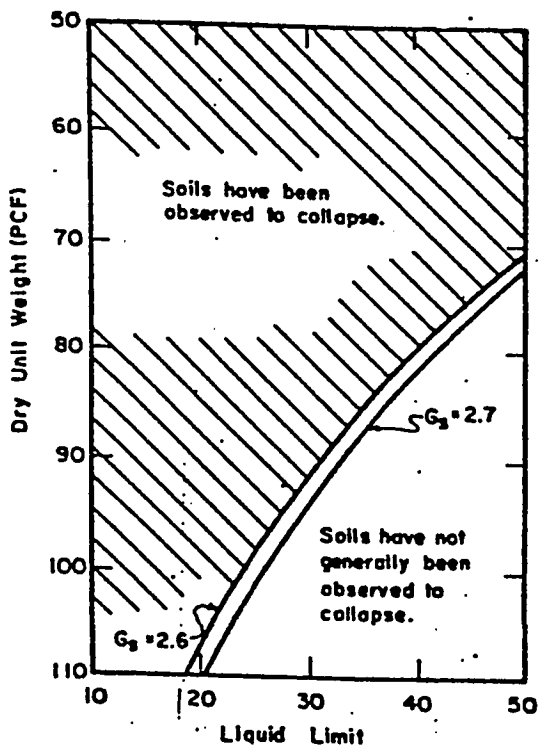


Fig.6.9 : Collapsible and Noncollapsible Loess (Clemence, 1981).

Table 6.9 : Collapsing Identification of the Different Soils of the Study Area

Soil Unit	Soil Type	Station #	Depth (m)	Densioiv's (1951) Method				Gibbs and Bara (1967) Method				
				$e_o$	$e_{L_c}$	$K_c$	Status	$G_s$	$\gamma_d$ $kN/m^3$	LL %	$W_c$ %	Status
7	Lean Clay	33	0.7	0.85	1.32	1.55	N.C.	2.75	16.0	48	25	N.C.
4	Sandy Lean Clay	36	4.0	0.93	1.12	1.2	N.C.	2.79	14.4	40	32	N.C.
6	Sandy Silty Clay with Gravel	38	2.5	1.2	0.66	0.55	H.C.	2.65	14.9	25	28	L.C.
			4.5	0.85	0.73	0.84	N.C.	2.69	15.6	27	26	N.C.
5	Sandy Silt	33	1.8	1.37	0.76	0.55	H.C.	2.73	12.5	29	42	M.L.C.
			2.5	0.92	0.85	0.93	N.C.	2.75	14.9	31	29	N.C.
			4.0	1.14	0.83	0.72	H.C.	2.75	14.0	30	34	L.C.
4		35	4.5	1.06	0.83	0.78	~H.C.	2.68	12.9	31	39	M.L.C.

N.C. : Non-Collapsing

H.C. : Highly Collapsing

L.C. : Likely Collapsing

M.L.C. : Most Likely Collapsing

$$K_c = \frac{e_L}{e_0}$$

where

$e_L$  is the void ratio at liquid limit, and  $e_0$  is the natural voids ratio.

$K_c = 0.5-0.75$ : Highly collapsible soil

$K_c = 1.0$  : Non-collapsible loams.

$K_c = 1.5-2.0$  : Non-collapsible soils.

In order to compare the limits of  $K_c$  with the values of  $K_c$  of the studied soils, the loams have to be identified. Terzaghi and Peck, (1967) defined loess loam as a type of the modified loess, which lost its characteristic due to chemical and other factors. "Through chemical decomposition produces loess loams, characterized by greater plasticity than other form of modified loess" (Terzaghi and Peck, 1967). The surficial studied loess soils still possess their natural characteristics. Modification by chemical changes, temporary saturation, erosion, etc., as discussed by Terzaghi and Peck (1967) may coincide on lean clayey soils in station 33 and 36. Since no loess loam was observed, the subsidence  $K$  for collapsing soils is in the range 0.5-0.75, while the non-collapsible soils have the value of  $K$  above this range.

The following example clarifies the identification of collapsibility of the sandy silt soil of the previous example. The initial voids ratio  $e_0$  is 1.37.

At saturation  $S = 1.0$

$$e = G_s \times W_c$$

For  $LL = 28\%$

$$e_L = G_s + LL = 2.73 \times 0.28 = 0.76$$

$$K_c = \frac{e_L}{e_0} = \frac{0.76}{1.37} = 0.56 \text{ (between 0.5-0.75)}$$

Since the value of  $K_c$  in the range 0.5 - 0.75, the sandy silt soil is highly collapsible as defined also by the first method. The values of  $e_0$ ,  $e_L$  and  $K_c$  for all the fine soils of the study area are shown in Table 6.9. The table shows that both methods give the same identification.

*Quantitative Methods* - The third method (Jennings and Knight, 1975):

This method is a laboratory experimental method by which the quantitative collapsing potential of a soil can be obtained. An undisturbed specimen, preferably a block specimen cut by hand, is cut to fit in the odometer ring and loads are applied progressively each 24 hour, until 200 kpa is reached. At the end of loading, water is added and left for a day. The consolidation test is then carried on till its maximum loading limit. The resulting curve of a tested specimen from the sandy silt soil selected from Station # 42 at 1.3 m, is shown in Fig. 6.10. The collapsing potential is defined as:

$$C_p = \frac{e_2 - e_1}{1 + e_0} \times 100 = 7.2$$

in which  $e_1$  and  $e_2$  are the void ratios before and after wetting; and  $e_0$  is the initial void ratio. Jennings and Knight (1975) have suggested some values for collapse potential shown in Table 6.10 (Das, B., 1984). According to the results of the tested soil, Fig. 6.10:

$$C_p = \frac{1.03 - 0.88}{1 + 1.08} \times 100 = 7.2$$

Referring to the above table this sandy silt soil, loess soil, has trouble collapse potential.

The previous three different methods gave the same results in identifying the collapse potential of the surficial sandy silt. Table 6.9 shows the collapsing identification of all the soils according to the first two methods.

**6.2.4.3 Mechanism and Settlement of Collapsing Soil:** The collapsing mechanism is greatly affected by the soil fabric, natural moisture, cementation and applied stress. The interparticle bond help to maintain the metastable structure. Upon wetting and loading the bond is weakened and the grains may assume a more closely packed arrangement with decrease in the bulk volume of the soil. This volume decrease may result from moisture uptake since on saturation interparticle tension disappears and hence there is a decrease in overall

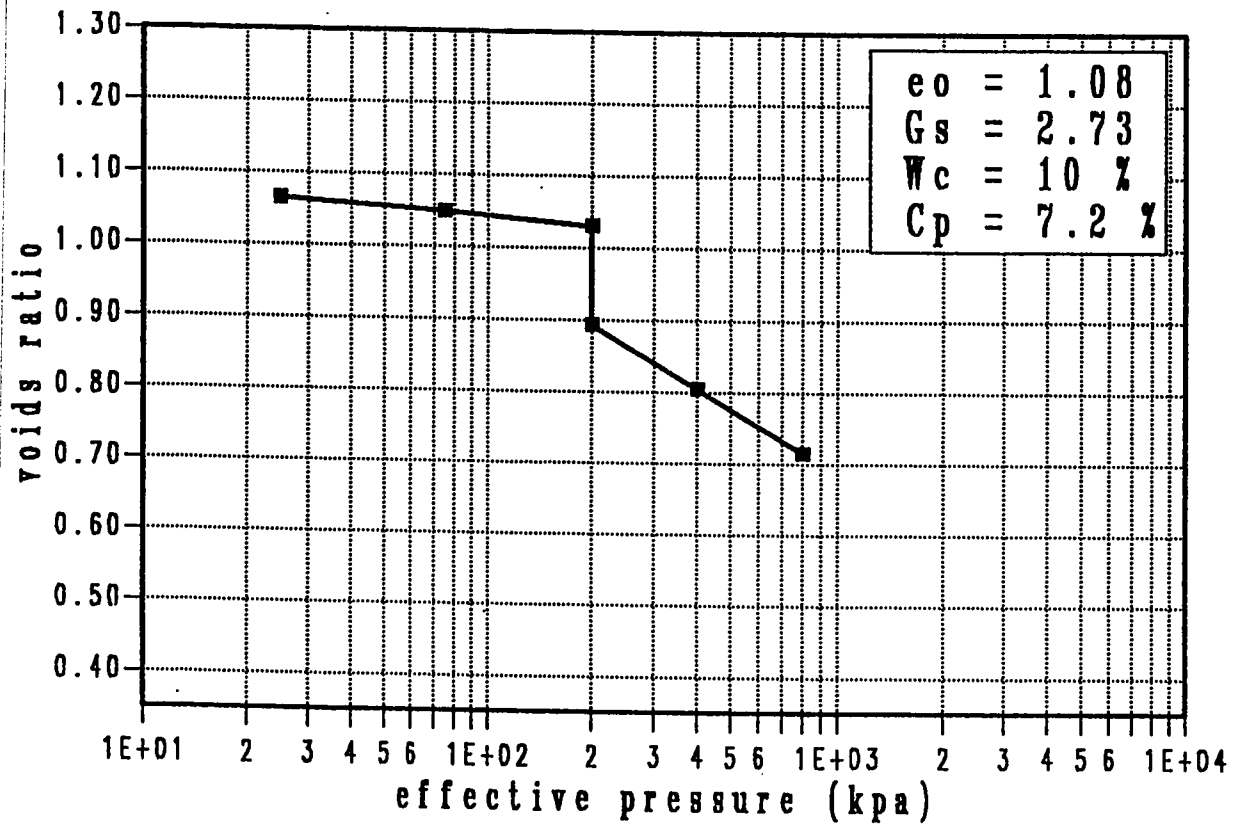


Fig. 6.10 : Collapsing potential as resulted from the oadometer test ( sandy silt station 42 at 1.3m)

Table 6.10 : Relation of Collapse Potention to the Severity of Foundation Problems (after Clemence and Finbarr (1981).

$C_p$ (%)	Severity of problem
0-1	No problem
1-5	Moderate trouble
5-10	Trouble
10-20	Severe trouble
20	Very severe trouble

contribution to bonding. Bonds due to clay or cementation agents may be weakened due to the removal of these materials by water uptake. Plate 6.2 shows the collapse in the bonding agents of the sandy silt soil (Station # 40 at 2.5m), as resulted from the odometer test and detected by SEM. Moisture uptake by clay lumps with softening and distortion has been considered a factor in the hydroconsolidation of partly saturated soils by Dusseault et al; (1985).

According to Silva, J., (1971) "the collapsing settlement should not be regarded as a consolidation settlement, since it does not follow the consolidation theory and should rather be considered a microshear-strength problem, which degenerates afterwards in volume change". Palka, J. and Naborczyk, J. (1985) indicated that the considerable part of settlement takes place during time of construction in the first period of exploitation, and the increase in consolidation settlement does not end even after the 30-year period. Most specimens of the study area soils exhibited an increase in weight after consolidation test compared to the weights of specimens before tests due to the intake of water, since they were at low moisture before the test. This intake of water caused a rapid or immediate settlement directly after applying the load. Such phenomena was indicated by Houston et al, (1988), who related the settlement of collapsing soil to be more or less immediate and caused by the intake of moisture by the soil.

The analysis of the time-compression data of the different soils

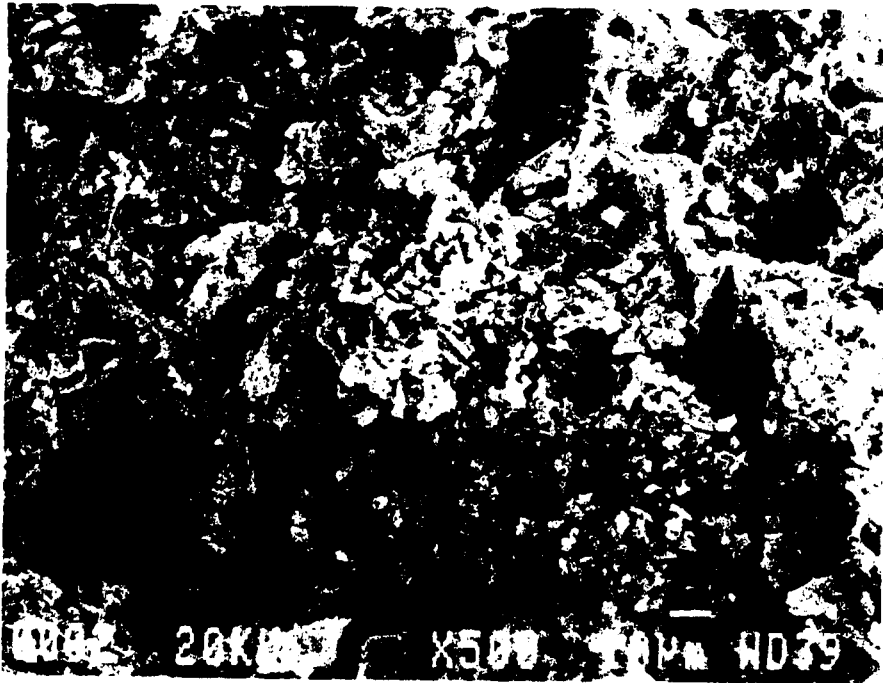


Plate 6.2: Collapsing in cementation agent of the sandy silt, loess as detected from oedometer test by SEM.

of the study area indicates that from the total consolidation, 50 to 65 per cent is initial (reading after one minute), 25-35 percent is primary (reading up to two hours), and 10-15 percent is of a secondary nature (reading up to 24 hours). These ranges are within the average values of all the fine soils of the study area over all the stress ranges (25 kpa - 320 kpa), except for the lean clay soil. It exhibited a swelling at a lower stress. Reconsolidation of this soil gave a lower rate of initial settlement (25%) and a higher primary consolidation (60%).

According to the above analysis, the settlement of the collapsing soils has to be calculated in a different way than the conventional consolidation method. The following method explains the procedures of obtaining the settlement of collapsible soils. Sandy silt soil selected from Station # 42 at 1.3 m deep was chosen as an example to calculate the settlement of normally consolidated soil ( $\sigma'_p/\sigma'_{vo} = 3$ ).

#### *Procedure for Calculation of Collapse Settlement*

Das, B. M. (1984) have used the following laboratory procedure to determine the settlement of structures on collapsing soil due to saturation.

- 1) Obtain two undisturbed soil specimens for tests in a standard consolidation test apparatus (odometer).
- 2) Place the two specimens under  $1 \text{ kN/ m}^2$  pressure for 24 hours.

- 3) After 24 hours, saturate one specimen by flooding. The other specimen is kept at natural moisture content.
- 4) After 24 hours of flooding, resume the consolidation test for both specimens by doubling the loads (same procedure as the standard consolidation test) to the desired pressure level.
- 5) Plot the  $e$  vs.  $\log \sigma'_v$  graphs for both of the specimens (Figs. 6.11.a and 6.11.b).
- 6) Calculate the in-situ effective pressure,  $\sigma'_{vo}$ . Draw a vertical line corresponding to the pressure  $\sigma'_{vo}$ .
- 7) From the  $e$  vs.  $\log \sigma'_v$  curve of the soaked sample, determine the preconsolidation pressure,  $\sigma'_p$ . If  $\sigma'_p / \sigma'_{vo} = 0.8-1.5$ , the soil is normally consolidated; however if  $\sigma'_p / \sigma'_{vo} > 1.5$ , it is preconsolidated.
- 8) Determine  $e_o$  corresponding to  $\sigma'_{vo}$  from the  $e$  vs.  $\log \sigma'_v$  curve of the soaked sample.
- 9) Through the point  $\sigma'_{vo}$ ,  $e_o$  draw a curve that is similar to the  $e$  vs.  $\log \sigma'_v$  curve obtained from the specimen tested at natural moisture content.
- 10) Determine the incremental pressure,  $\Delta \sigma'_p$  on the soil caused by the construction of the foundation. Draw a vertical line corresponding to the pressure of  $\sigma'_{vo} + \Delta \sigma'_p$ .

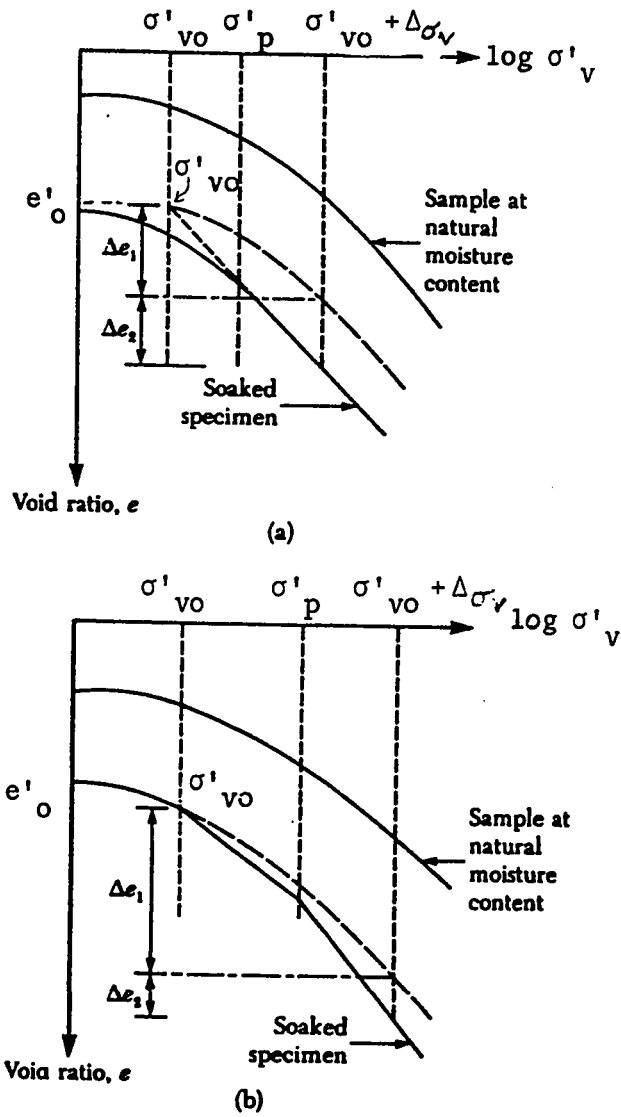


Fig. 6.11 : Settlement calculation from double oedometer test; (a) normally consolidated soil; (b) overconsolidated soil (Clemence, 1981).

in the  $e$  vs.  $\log \sigma'_v$  curve.

- 11) Now, determine  $\Delta e_1$  and  $\Delta e_2$ . The settlement of soil without change in the natural moisture content is

$$S_1 = \frac{\Delta e_1}{1 + e'_o} (H)$$

Also, the settlement caused by collapse in the soil structure

$$S_2 = \frac{\Delta e_2}{1 + e'_o} (H)$$

where  $H$  = thickness of soil susceptible to collapse.

Using the above procedure, two samples of sandy silt loess were tested by odometer as shown in Fig. 6.12. The figure indicates the tendency to collapsing. The collapsing potential value,  $C_p$ , can be evaluated from the figure at any loading stage. The collapsing potential is 8.6% for specimen with 6% initial water content. Fig. 6.13 shows the evaluation of  $S_1$  and  $S_2$  according to Fig. 6.10.a (normally consolidated state). For an average thickness of 1.0m these values are as follows:

$$\Delta e_1 = 0.04$$

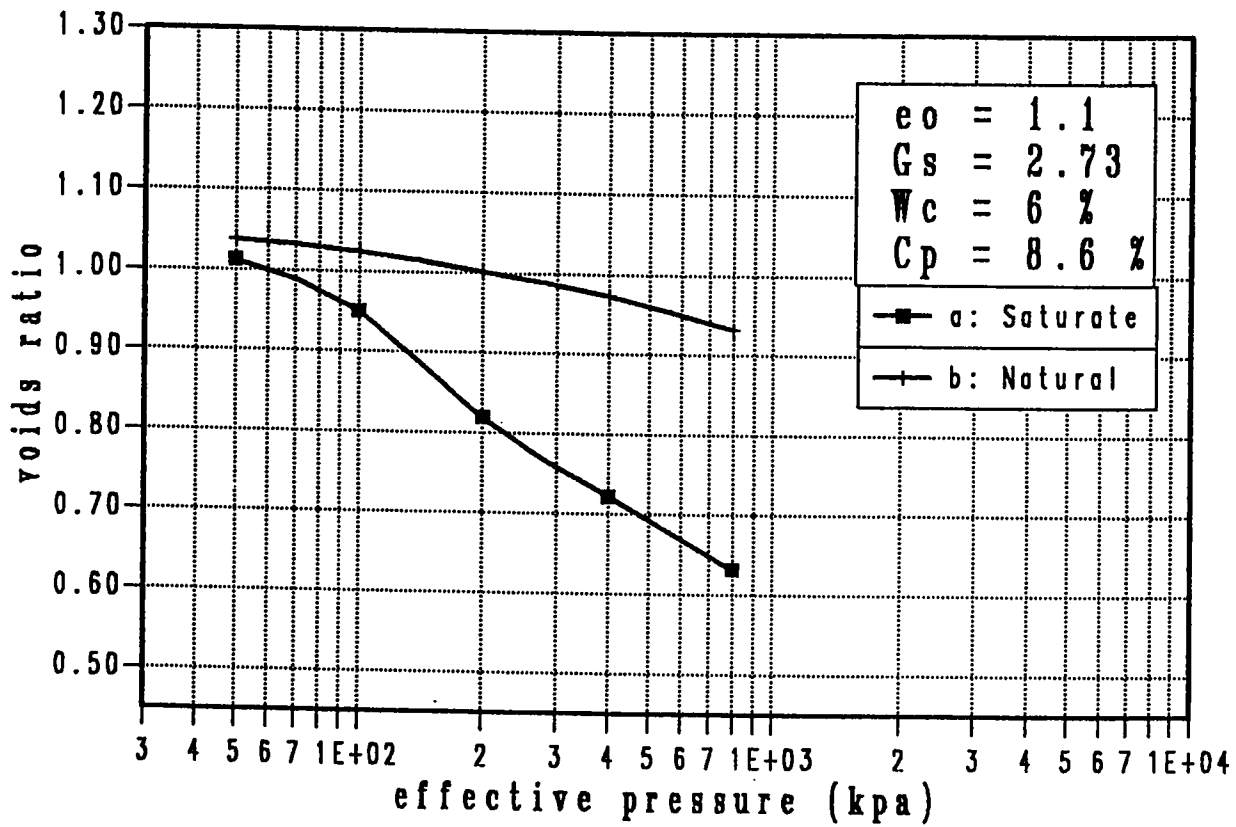


Fig. 6.12 : Double Oedometer Test of Sandy Silt Soil (Station 42 at 1.3m ).

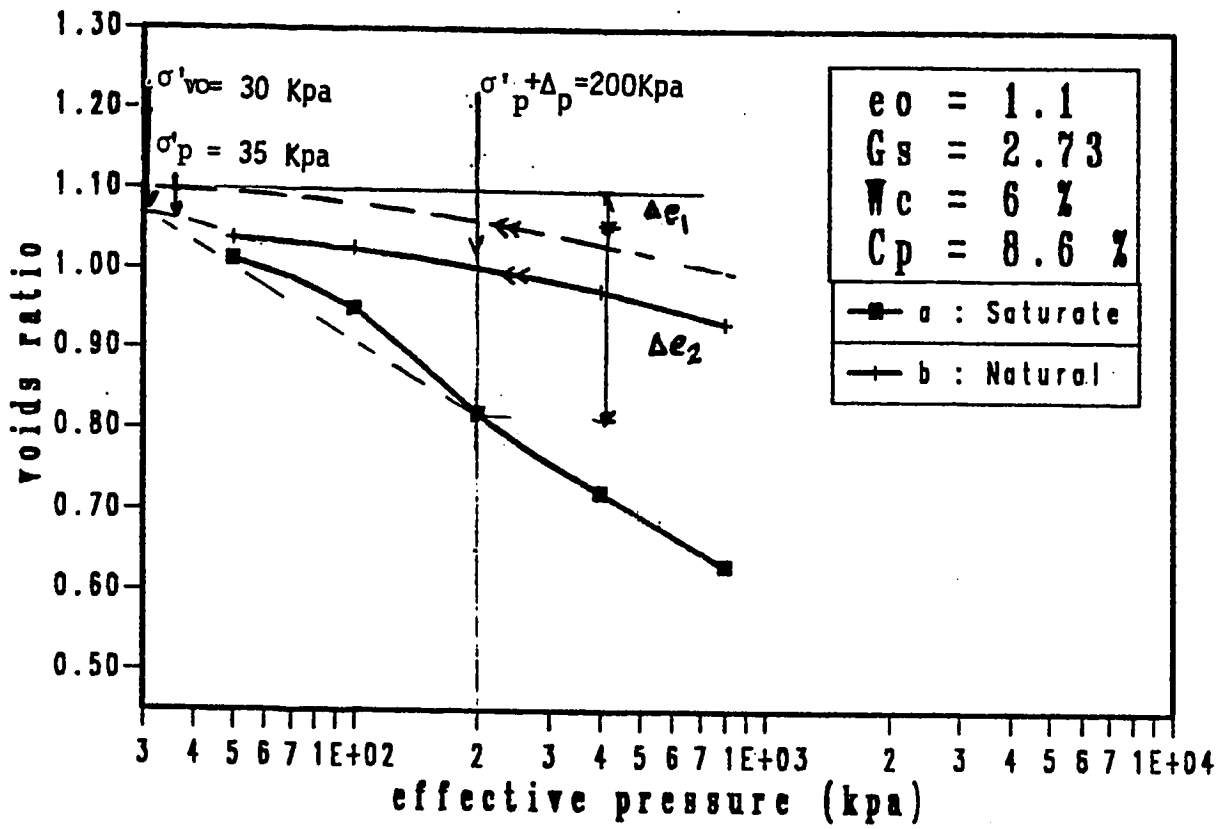


Fig. 6.13 : Calculation of Collapsing Settlement By Using Double Oedometer Test.

$$\Delta e_2 = 0.24$$

Therefore :

$$S_1 = \frac{0.04}{(1 + 1.1)} \times 1.0 \times 100 = 1.9 \text{ cm.}$$

$$S_2 = \frac{0.24}{(1 + 1.1)} \times 1.0 \times 100 = 11.42 \text{ cm.}$$

According to the above example, it is noticeable that the amount of settlement due to collapsing by saturation,  $S_2$ , is six times the settlement at natural moisture content,  $S_1$ , under the same load. The expected amount of collapsing can be estimated by using field odometer simulation which is a valuable tool for assessing the amount of collapse to be expected (Jones, D., and Van Olphen, G., 1980).

## 6.3 Strength Properties

### 6.3.1 Introduction

The deposits of the study area, an arid region, are characterized by having low natural moisture content. Such deposits show the tendency of changing their mechanical properties upon saturation due to changes in water table or seepage condition. In order to have the best simulation of the strength characteristics of these deposits, two conditions have to be considered

- The actual field condition at the natural moisture, and
- The worst possible condition at the full saturation state.

To satisfy the above conditions, the soils specimens were subjected to consolidated undrained triaxial tests on both remolded partially saturated samples and undisturbed saturated samples. The test results along with their analysis and correlations are discussed in the following sections.

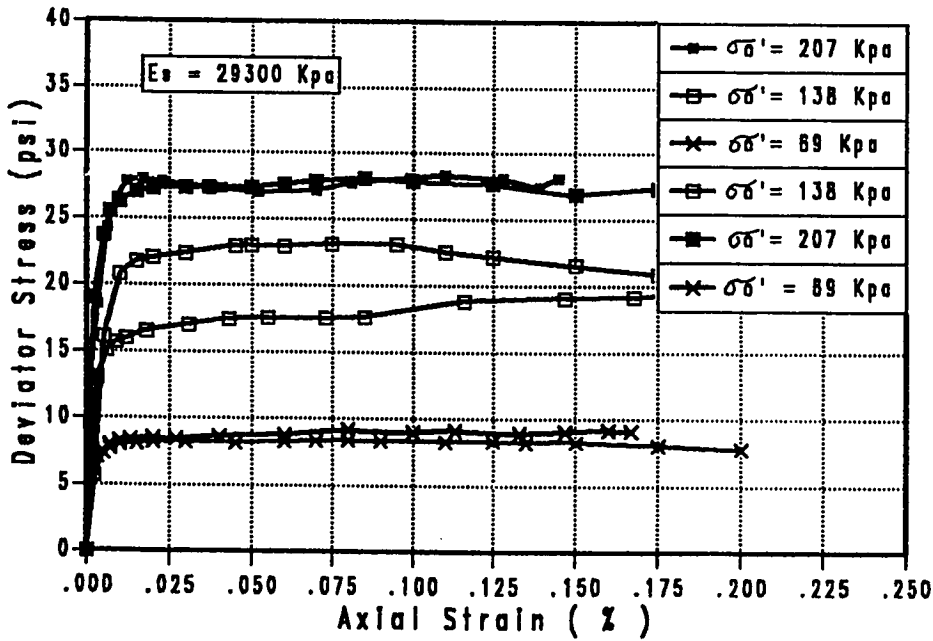
### 6.3.2 Results

The saturated and partially saturated samples of each soil type were tested under different confining pressures. The total confining pressures ( $\sigma_c$ ) of the saturated specimens were 50, 40 and 30 psi. The corresponding internal back water pressure was almost kept constant to give a net initial confining pressures ( $\sigma_3 = \sigma'_3$ ) of 30, 20 and

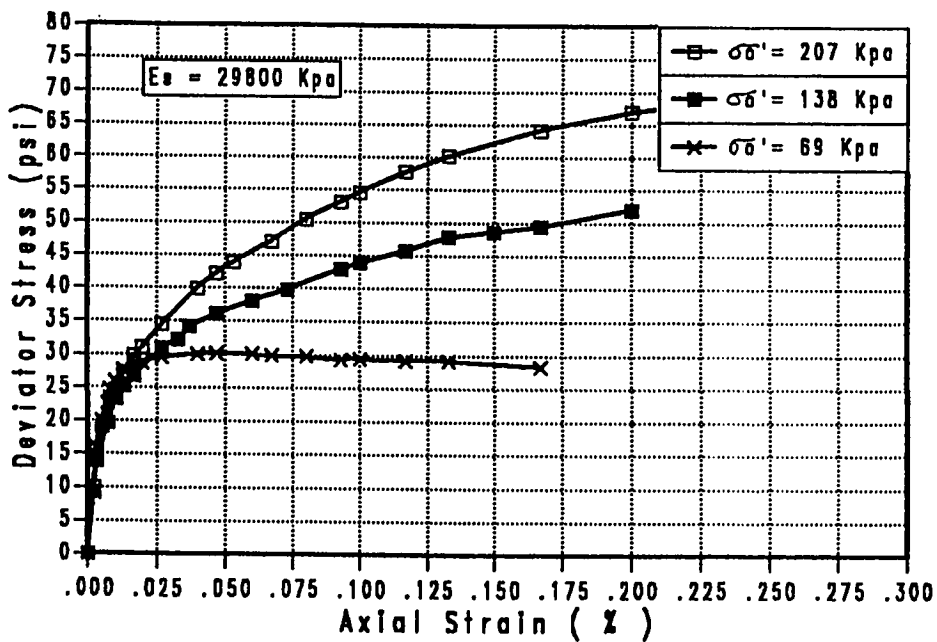
10 psi (207, 138 and 69 kpa) respectively. The back pressure was sometimes raised up to 30 psi with rising the confining pressure in order to achieve a higher degree of saturation almost 94 to 100 per cent.

Fig. 6.14 shows representative stress-strain relationships of the sandy silty clay with gravel for both saturated and partially saturated conditions. Three undisturbed and three disturbed samples were tested as shown in Fig. 6.14a which indicates no great difference between those two types of samples. The slope of elasticity was found using the initial modulus of the stress-strain curve (Bowles, 1982). Since  $E_s$  may be affected by the stress history, density, water content, confining pressure etc.; average values of  $E_s$  were obtained from the best fit for the initial tangent of the different curves as shown in the figure. In case of saturated samples the values  $E_s$  of clay (unit 4 and 7), sand (unit 3) and silty loessial soils (unit 5 and 6) are in the ranges 16.5 to 44 Mpa, 13.0 to 31.3 Mpa and 18.2 to 31.0 Mpa respectively. In case of partially saturated samples, the same ranges of  $E_s$  were 63 to 97.3 Mpa 20.1 to 476 Mpa and 40.0 to 74.7 Mpa respectively.

For fully saturated tests, the strain at failure varies from almost 4% to about 13% with an average of 7%. While, the partially saturated samples showed strain at failure reaching values beyond 20% as can be seen in Fig. 6.14. The rest of the stress strain curves of



a) Saturated condition



b) Partially saturated condition

Fig. 6.14 : Stress strain relation of the sandy silty clay with gravel (Station 38 at 4.0m).

(1 psi = 6.9 Kpa)

different soils are shown in Appendices D-7 and D-8. The values of  $E_s$  for saturated soils are shown in Table 6.11 while the values of partially saturated soils are shown in Table 6.12.

Fig. 6.15 shows the pore water pressure versus the axial strain along with stress-strain of the saturated sandy lean clay specimen (station No.36 at 4.0m depth). Since no water dissipation (no volume change) was allowed during the shearing stage, a considerable positive pore water pressure was developed as shown in the figure. The final pore water pressure  $U_f$  is a function of the confined pressure, initial pore water pressure  $U_o$ , stress history etc. The increase in the final pore water pressure  $\Delta U_f$  were 44.8, 100 and 141 kpa corresponding to the net confining pressures 69, 139 and 207 kpa respectively. The coefficient of pore water pressure at failure was defined after Skempton, 1954, as

$$A_f = \frac{\Delta U_f}{\Delta (\sigma_1 - \sigma_3)_f}$$

The values for the sandy lean clay soil was found to be in the range 0.57 - 0.62 which is in the range of slightly over consolidated soil (O.C.R = 2.7) as detected before. The values of  $\Delta U_f$ ,  $A_f$  are shown in Table 6.13.

Fig. 6.16 shows the effective stress path (E) and total stress path (T) of the lean clay soil (Station # 33, depth 0.7 m) in term of

Table 6.11: Critical state Model Parameters of the Different Soils

Soil Unit	Soil Type	Station #	Depth (m)	$v_f$ %	$\lambda$	N %	$q_f$ kpa	$P_f'$ kpa	M kpa	$\Gamma$	$\phi'_{cn}$	$E_s$ kpa
7	Lean Clay	33	0.7	1.88	0.214	2.49	138	105	1.3	2.22	32	19900
4	Sandy Lean Clay	36	4.0	1.81	0.176	2.66	130.0	81.22	1.6	2.24	39	44100
6	Sandy Silty Clay With Gravel	38	2.0	1.95	0.165	2.76	263	161	1.64	2.55	40	31400
			4.5	1.67	0.104	2.18	120.0	81.0	1.47	2.08	34	29300
5	Sandy Silt	33	1.8	2.065	0.148	2.79	92.0	70.00	1.32	2.4	32	21200
			2.5	1.875	0.139	2.56	125	94.0	1.33	2.24	32	27800
			4.0	1.984	1.156	2.55	128.0	89.0	1.43	2.38	35	18200
4*		35	4.5	1.895	0.184	2.8	97.0	61.5	1.58	2.3	38	23400
3	Silty Clayey Sand With Gravel	41	2.0	1.73	0.085	2.15	322	200	1.61	2.02	40	31300

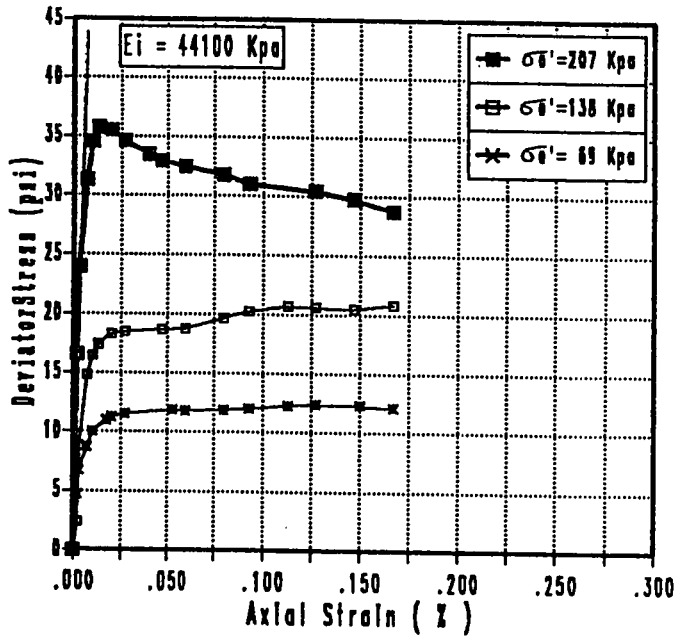
\*See Table 6.1.

Table 6.12: Summary of the consolidated undrained triaxial results of partially saturated soils.

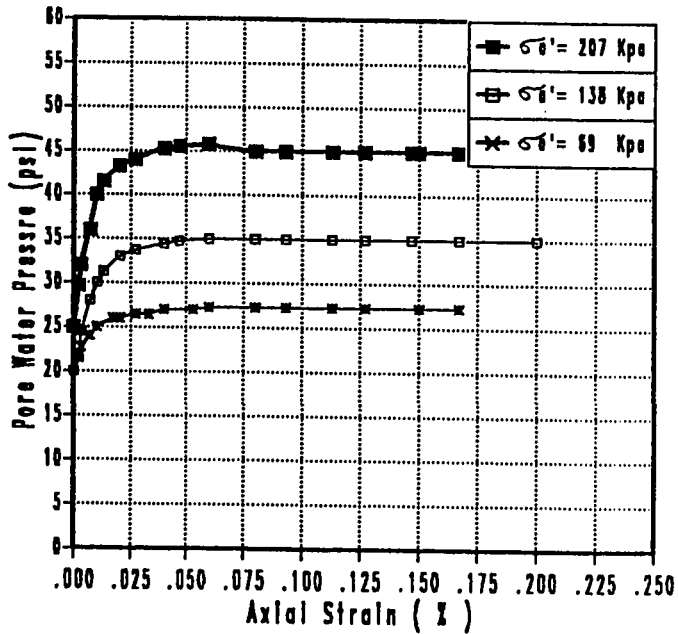
Soil Unit	Station #	Depth m	w <sub>C</sub> %	S %	γ <sub>n</sub> KPa	σ <sub>3</sub> KPa	(σ <sub>1</sub> - σ <sub>3</sub> ) <sub>max</sub> KPa	C KPa	φ Deg.	E <sub>s</sub> KPa
7	33	0.7	13	46	17.3	68.9 137.9	848 1061	155	37	97350
4	36	4.0	14	40	15.9	68.9 137.9 206.8	565 627 758	137	25	63600
6	38	2.0	16	52	16.7	68.9 137.9 206.8	234 309 484	27	28	23800
5	33	4.5	15	49	16.7	68.9 137.9 206.8	207 359 462	20	28	29800
5	33	1.8	13	31	14.2	68.9 137.9 206.8	179 328 453	7	30	20150
5	33	4.0	11	33	15.5	68.9 137.9 206.8	335 418 458	103	18	47600
4	35	4.5	15	39	14.8	68.9 137.9 206.8	228 358 440	41	25	28000
3	41	2.0	10	57	20.5	68.9 137.9 206.8	348 358 803	24	42	52400

Table 6.13: Summary of the consolidated undrained triaxial results of the saturated soils.

Soil Unit	Station	Depth (m)	Gravel	Sand	Silt	Clay	$\sigma_c$ KPa	$\sigma_s'$ KPa	$\sigma_1'$ KPa	$\Delta U_f$ KPa	$A_f$	C KPa	$\phi_{cu}^o$	C' KPa	$\phi_{cu}^{i,o}$
7	33	0.7	0.0	10	58	32	207	69	82.7	44.8	0.54	24.1	12	10.3	32
							276	138	138	86.2	0.63				
							345	207	157.9	156.8	0.99				
4	36	4.0	1.5	29.5	43.5	25.5	207	69	78.9	44.8	0.57	10.3	18	10.3	35
							276	138	129.6	100	0.77				
							379	207	227.5	141.3	0.62				
6	38	2.0	19	29	40	12	207	69	127.5	96.5	0.76	10.3	28	13.8	36
							276	138	263.4	75.2	0.30				
							345	207	380.6	148.2	0.39				
		4.5	17	28	38	17	207	69	63.4	43.4	0.68	0.0	18	0.0	36
							276	138	121.3	96.5	0.80				
							345	207	188.2	139.6	0.75				
5	33	1.8	0.0	40	45	15	207	69	48.3	55.1	1.14	6.9	11	6.9	32
							276	138	91.7	98.6	1.08				
							345	207	111.7	160.6	1.43				
5	40	2.5	1.0	37	44	18	207	69	53.8	46.5	0.85	10.3	10	0.0	32
							276	138	129.1	89.6	0.69				
							345	207	144.7	146.5	1.01				
5	33	4.0	6.0	23	54	17	138	69	72.4	41.4	0.57	22.5	8	0.0	39
							276	138	99	91.7	0.92				
							345	207	120.6	165	1.87				
4	35	4.5	1.0	22	55	22	207	69	59.3	50.3	0.85	0	22	0.0	36
							276	138	91.7	112	1.22				
							345	207	225.4	134	0.6				
3	41	2.0	26	59	8	7	207	69	158.6	20.7	0.13	27.6	21	0.0	39
							276	138	262.	62.0	0.24				
							345	307	291.6	124.0	0.42				



a) Stress strain



b) Pore water pressure vs. strain

Fig. 6.15: Stress Strain relations of the sandy lean clay soil (station 36 at 4.0m) (1 psi = 6.9 kpa).

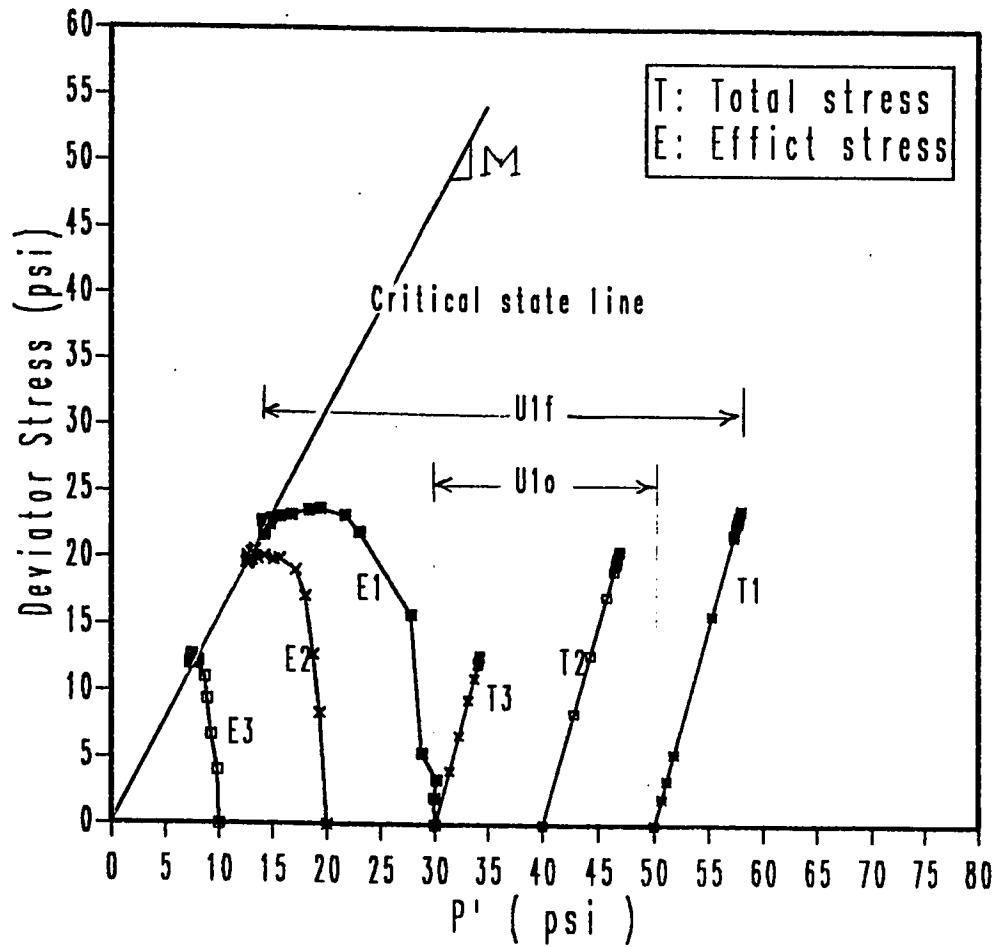


Fig. 6.16 : Stress path of the lean clay soil (Station 33 at 0.7m)

the p-q and p'-q' space, where q and p coordinates are defined according to Atkinson, J. H. and Bransby, P. L. (1978) as:

$$q = \sigma_1 - \sigma_3$$

$$p = \frac{(\sigma_1 + 2\sigma_3)}{3}$$

$$q' = q$$

$$p' = p - u$$

where u is the pore water pressure.

The figure indicates the developed pore water pressures and the stress variation in soil during shearing. The total stress paths rise at a constant slope of 3 to 1 while effective stress paths are shifted along the horizontal axis by the magnitude of the developed pore pressure.

The computer program used in calculating the different parameters resulted from the triaxial tests is shown in Appendix D-9. Appendix D-10 shows a representative output for the lean clay soil shown in Fig. 6.16.

The straight line that passes through the failure points of the effective stress paths is the critical state line, CSL. This line is defined by its unique slope M as a boundary line on which the soil fails under any stress combination (Atkinson, J. H. and Bransby, P. L., 1978). The slope is defined by:

$$M = q'_f / p'_f$$

where  $q'_f$  is the deviatoric effective stress at failure and  $p'_f$  is the mean effective stress at failure.

The behavior in  $q'$ - $p'$  and  $v$ - $p'$  spaces for each soil was required in order to determine the critical state model parameters of each soil. Since  $\lambda$  is a constant,  $v$  of each specimen is a constant in the undrained shearing stage ( $\lambda$  and  $v$  were defined in section 6.2.2) and the values of  $q'_f$  and  $p'_f$  of each specimen are known, then the intercept of the CSL in  $v \ln p'$  space with the reference vertical line at  $p' = 1.0$  kpa can be obtained as follows:

$$v_o = v_f$$

$$v_f = \Gamma - \lambda \ln p'_f$$

where  $\Gamma$  is the slope of CSL in  $v$ - $\ln p$  space.

Similarly the intercepts  $N$  of the normal consolidation line NCL with the same reference line at  $p' = 1.0$  kpa is defined as

$$v = N - \lambda \ln p'$$

The values of  $N$  of the different soils were evaluated at  $p' = 138$  kpa. Fig. 6.17 shows a representative plot including the NCL, CSL along with the effective stress paths in both  $q'$ - $p'$  and  $v - p'$  spaces as resulted from an undrained triaxial test.

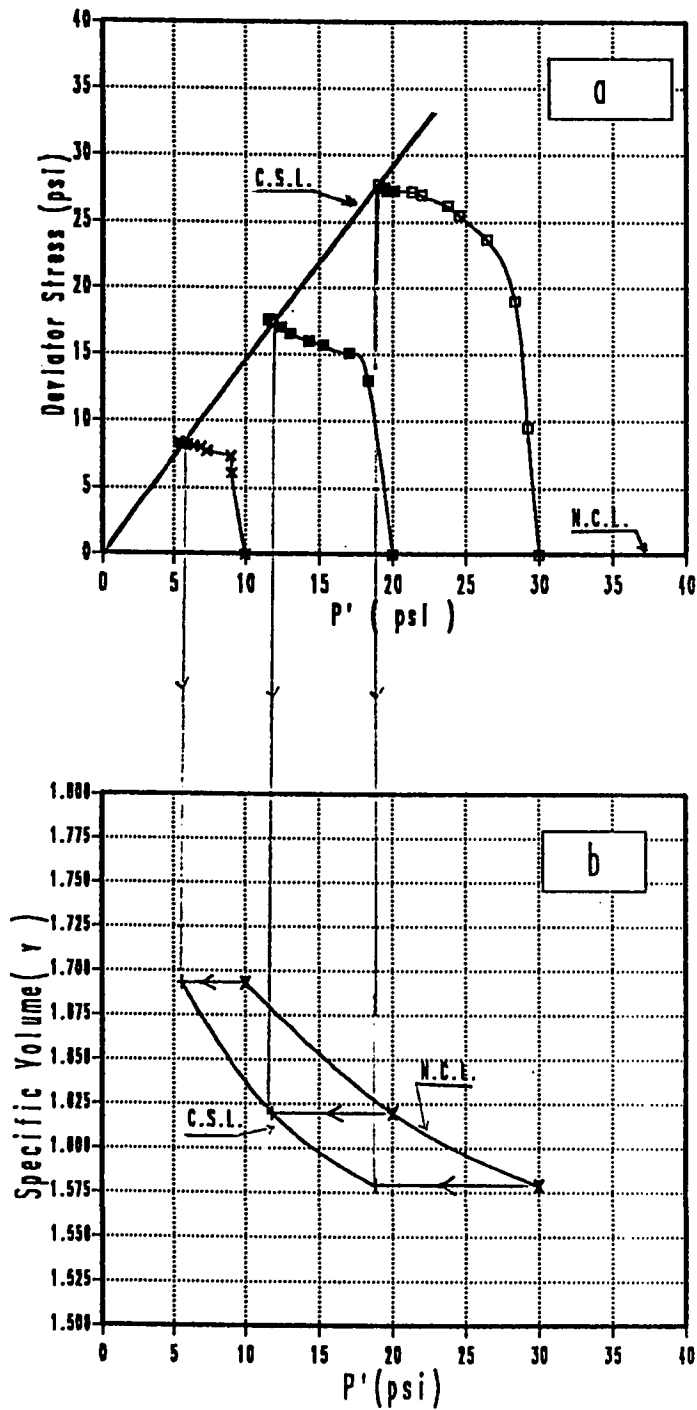


Fig. 6.17 : Stress path of sandy silty clay soil with gravel (Sta.38 at 4.5m) in term of  
 a )  $q'$  vs.  $p'$  , and  
 b )  $v$  vs.  $p'$  .

The previously mentioned parameters of the critical state model of the different soils under study are summarized in Table 6.11. The indicated values of the internal friction angles in the table were obtained according to the following relation:

$$\phi' = \text{Sin}^{-1} \left( \frac{3M}{6 + M} \right)$$

where  $M$  is the slope of CSL in  $q'$ ,  $p'$  space, (Atkinson, J. H. and Bransby, P. L., 1978).

Each fine soil of the investigated area exhibited its own shear strength characteristics. The variation in these characteristics of each soil formed upper and lower Mohr envelopes as boundaries. Fig. 6.18 shows a representative plot of Mohr circles in terms of both total and effective stresses. Fig. 6.19 indicates the effect of the moisture content in developing these upper and lower Mohr envelopes of the same soil. The upper boundary represents the Mohr envelope of the partially saturated specimens (at natural water content), while the lower boundary represents the Mohr envelope of the fully saturated specimens of the same soil at the same dry unit weight. These boundaries affected by the soil density, moisture condition, soil type, the activeness of the cementing bond between the particles, etc. Mohr's envelopes of each soil were plotted to end up with these boundaries taking into consideration the above factors which affect the strength of the soil. Table 6.13 shows the summary of the results obtained from the triaxial tests carried out on fully saturated

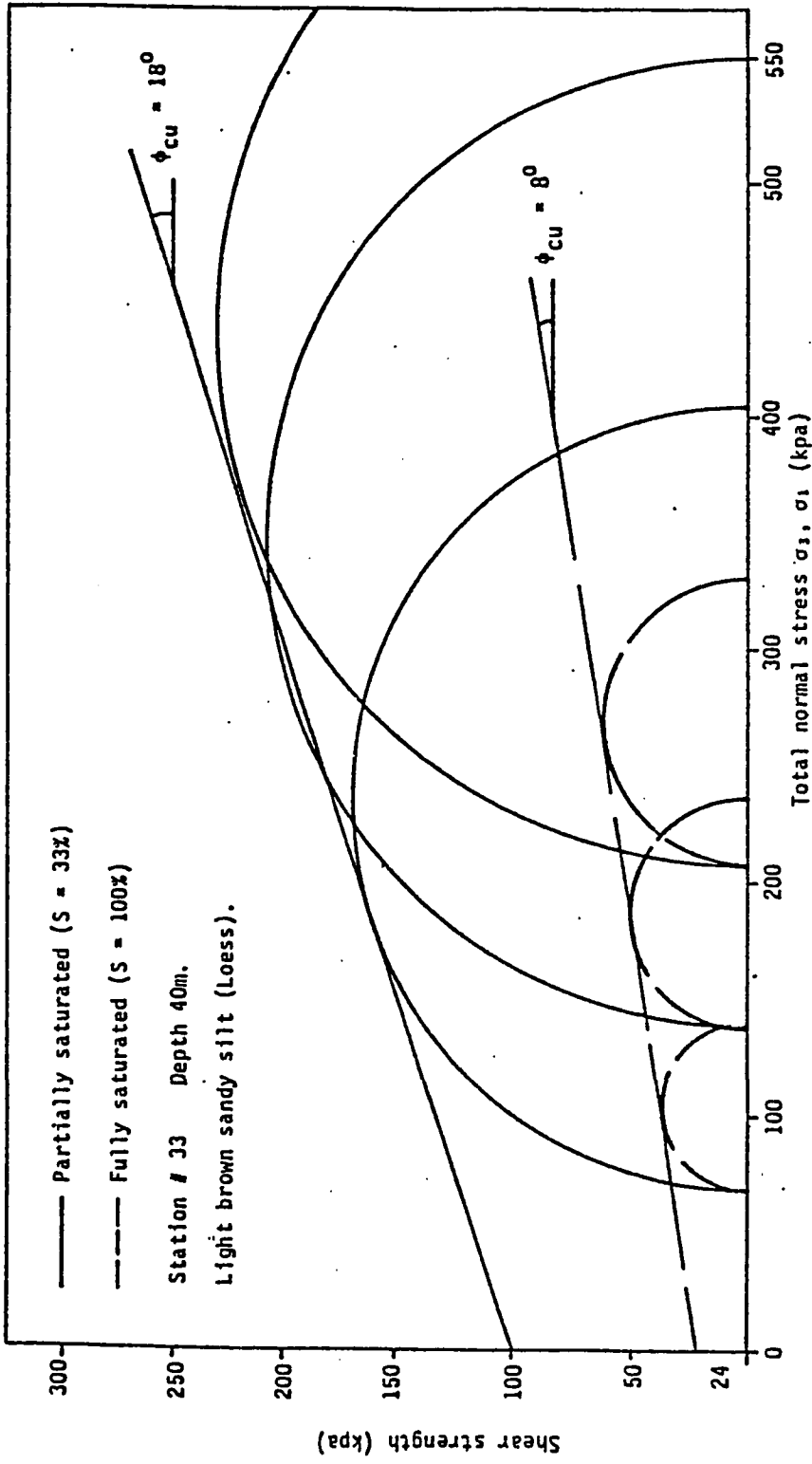


Fig. 6.19: Partially saturated and fully saturated Mohr's Envelope.

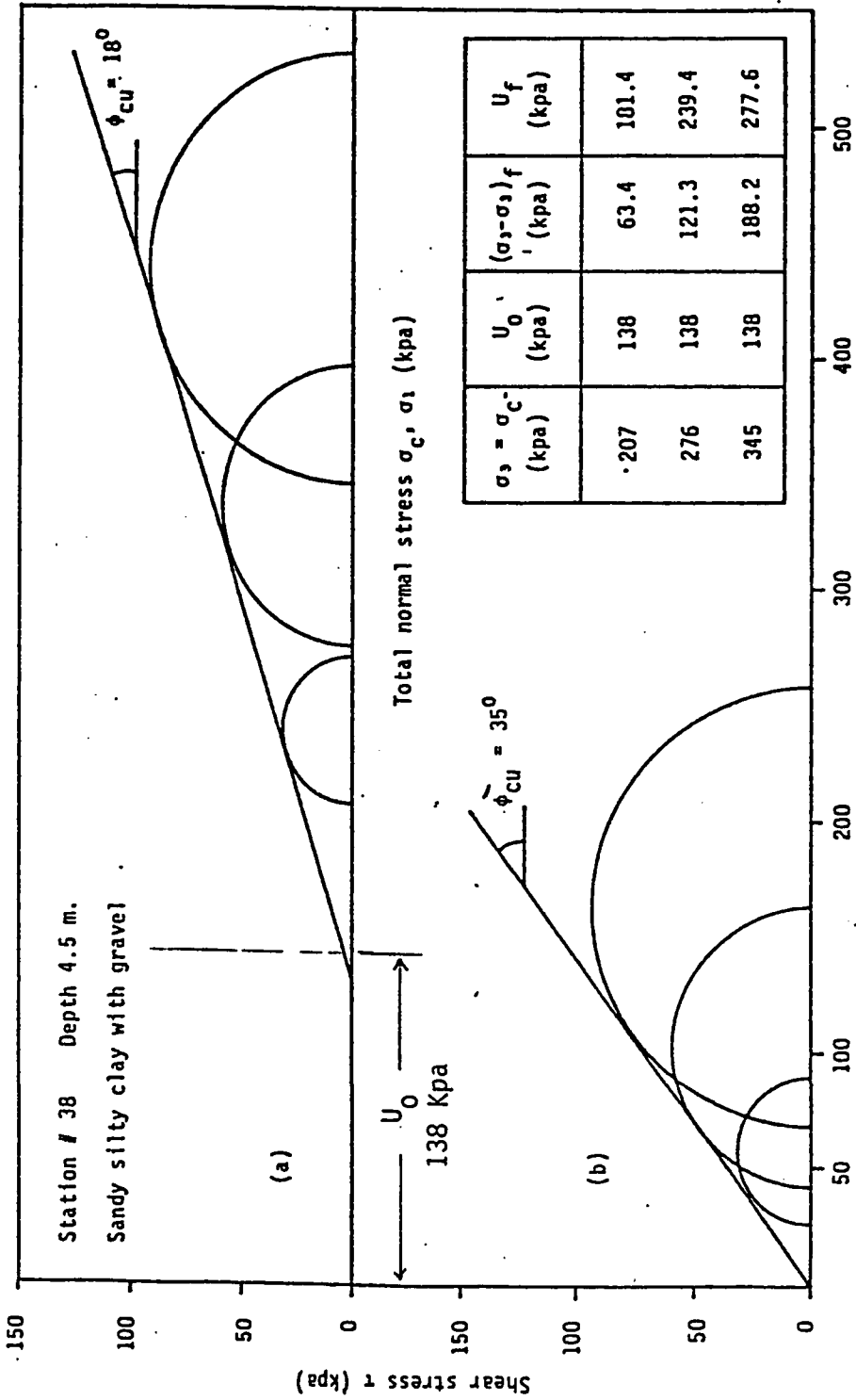


Fig. 6.18: Mohr's circles and failure envelopes in terms of:  
(a) Total Stress  $\sigma_c$   
(b) Effective Stress

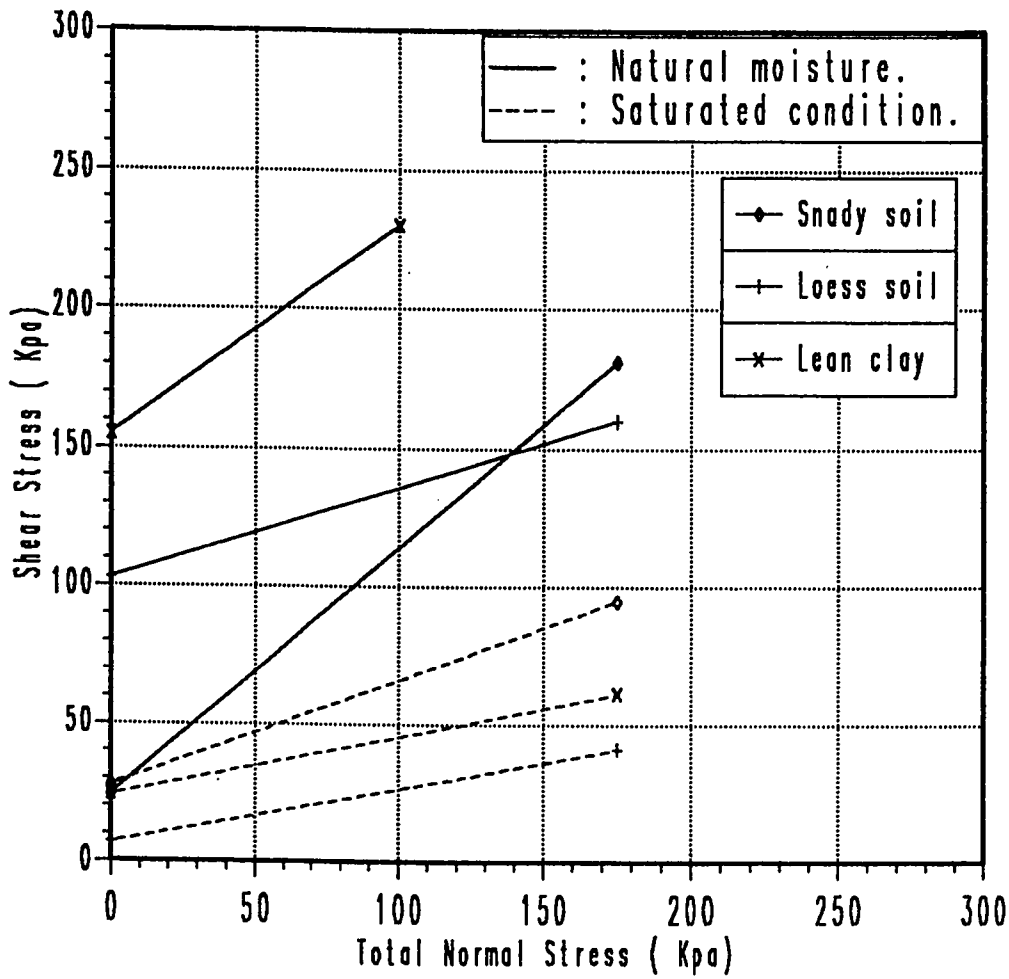


Fig. 6.20 : Mohr envelope boundraies of the different soils for both natural and saturated conditions

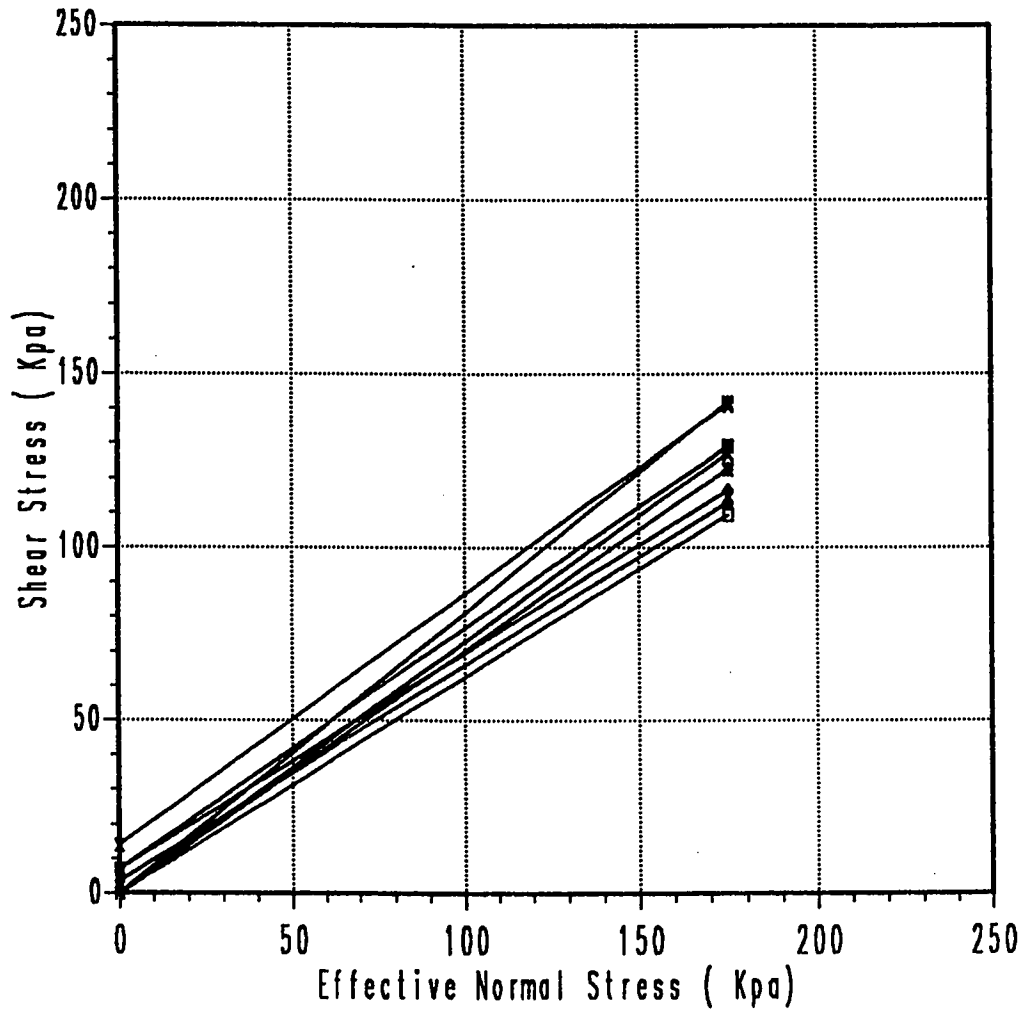


Fig. 6.21 : Mohr envelope boundraies of the different soils in term of the effective stresses

specimens, while Table 6.12 shows the same results of the same tests carried out on partially saturated specimens. The variation in shear stress and the total normal stress of the two tests conditions were plotted in Fig. 6.20 for all the different soils. Fig. 6.21 shows this variation for soil, units (3, 4, 5, 6 and 7) in terms of the effective stress. There is no great variation in the effective friction angle. This variation of loess soils in term of the effective stresses is shown in Appendix D - 11.

### 6.3.3 Analysis and Correlations

The pattern of the stress-strain and pore water pressure-strain curves were found to be similar to those of normally to slightly over consolidated soils, as found by many investigators such as Bishop and Henkale (1962), Atkinson and Bransky (1974). Soils which possess  $A_f$  in the range 0.7 to 1.4 are normally consolidated, while those which have values in the range 0.3 to 0.7 are slightly over consolidated (Fadlul allah, 1985). These observations coincide with the stress history of the different soils as detected by one-dimensional consolidation tests mentioned in Section 6.2. The effective stress path exhibited mostly positive pore water pressure even for lean clay soils.

The strain at failure  $\epsilon_f$  resulting from partially and fully saturated sample for the lean clay, sandy lean clay and silty clayey sand with gravel is approximately the same (5%), while it is different for

loessial soils, sandy silt and sandy silty clay with gravel. It is higher for the partially saturated samples (20%) than the fully saturated samples (7%). This may be due to the structure, fabric and the disturbance effects. The bond strength of the saturated undisturbed samples is weakened by wetting. Upon shearing, these samples fail through the weakened points. The remoulded loess samples which were tested in partially saturated condition lost their natural fabric. That is why they failed at low strain. In addition, those remoulded samples were more homogeneous than the undisturbed ones. In other words, the pores and particles arrangements existed in a more uniform state. Subsequently, the rearrangement of particles during shearing required large deformation before reaching failure. Most of the remoulded samples fail by bulging, while some of the natural samples fail in a brittle way which indicates the homogeneity effect (Plate 6.3).

The values of  $E_s$  of the different investigated soils obtained from both tests conditions are within the ranges reported by Bowles (1982) as can be seen in Table 6.14.

Since the measurements of both air and pore water pressures, during the undrained shearing stage, are greatly difficult to obtain in case of the partially saturated soils, total normal analysis was used (Das, B. ,1984, Peck, Hanson and Thurnborn ,1974 and Bishop and Henkle, 1962). Fig. 6.20 shows the total normal stresses of both partially and fully saturated tested soils. Referring to the figure

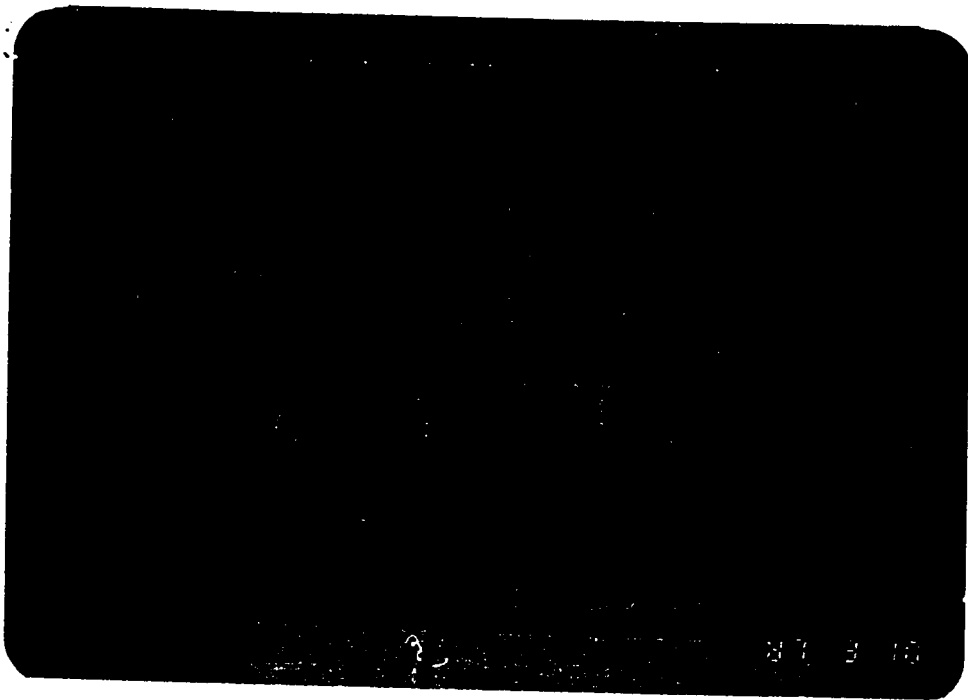


Plate 6.3 : Two failure types of triaxial compression specimens.

Table 6.14: Typical Range of Values for the Static Stress-Strain Modulus  $E_s$  for Selected Soils (Field values depend on stress history, water content, density, etc. (Bowles, 1982)).

Soil	$E_s$	
	ksf	Mpa
<b>Clay</b>		
Very soft	50-250	2-15
Soft	100-500	5-25
Medium	300-1000	15-50
Hard	1000-2000	50-100
Sandy	500-5000	25-250
<b>Glacial till</b>		
Loose	200-3200	10-153
Dense	3000-15 000	144-720
Very dense	10 000-30 000	478-1440
<b>Loess</b>	300-1200	14-57
<b>Sand</b>		
Silty	150-450	7-21
Loose	200-500	10-24
Dense	1000-1700	48-81
<b>Sand and gravel</b>		
Loose	1000-3000	48-144
Dense	2000-4000	96-192
<b>Shale</b>	3000-300 000	144-14 400
<b>Silt</b>	40-400	2-20

(6.20) the different soils exhibited a relative high shear resistance when they were tested at their natural moisture content. On contrast, the figure indicates also a lower shear resistance of the same soils when they were saturated before testing. Moreover, the figure indicates certain generalized trends which may be pointed out. The soils which were tested under saturation conditions are concentrated in the lower part of the figure having a consistent slope and are within a narrow range. On the other hand, the soils which were tested at natural moisture are concentrated on the upper part of the chart within a wider range. The silty clayey sand with gravel (sandy soil) exhibited a different trend due to its different composition. It exhibited a considerable drop due to wetting in the total internal friction angle from  $42^{\circ}$  to  $21^{\circ}$ , whereas the clayey and loessial soils exhibited a reduction in the total of both cohesion and friction angle. The reduction in shear resistance of the loessial soils affected also by its dry density, loessial soils of a higher dry density exhibited a higher reduction in the total cohesion and a lower reduction in the total internal friction, while the opposite is true with respect to the loessial soils of low dry density as shown in Fig. 6.22. The stiff lean clay soils exhibited a high drop in both total cohesion (155 kpa - 24 kpa) and total internal friction angle ( $37^{\circ}$  -  $12^{\circ}$ ).

The reduction in dry strength due to wetting can be related to some interference factors. The soil composition (including, cementing agents, percentage of the different texture, fabric, etc.) and the capillary forces between particles (the natural moisture content) are

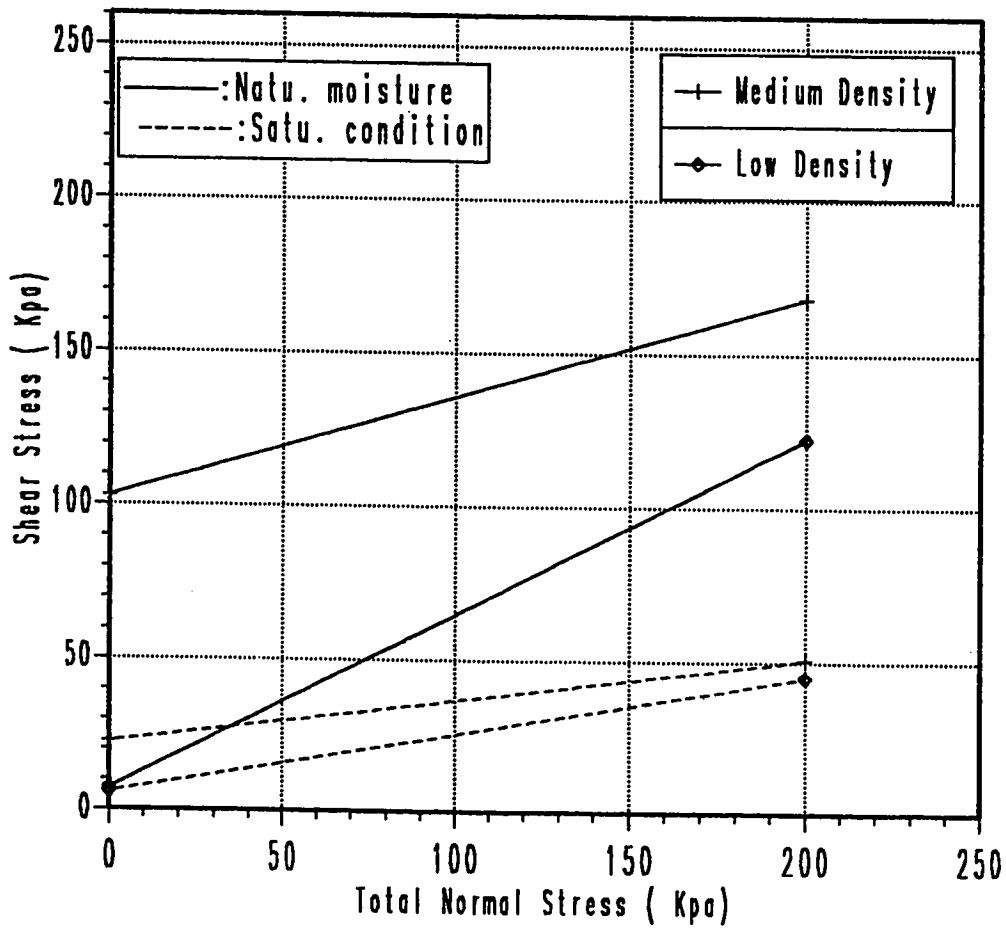


Fig. 6.22 : Upper and lower boundrais of Mohr envelopes of Loess under different moistures and densities

the most factors affecting the reduction mechanism.

The grain particles of the fine soils are kept in a bulky grains forms either by the accumulation of the clay particles in the junction of the grains giving a buttress type of support and/or by chemical precipitation which cemented the particles together. Holtz and Gibbs (1951) indicated that this bond is of high strength when dry and of low strength when wetted. Clemence (1981) explained these weaknesses in bond strength due to collapsing in the bonding mechanism as water is added. He observed that, the lower the water content, the higher the bond strength. Clemence (1981) found that the collapse in strength is more immediate in the case where the grains are held together by capillary suction (as lean clay soil), slow in the case of chemical cementing and much slower in the case of clay buttresses. Plate 6.2 shows the failure in the bonding agent due to saturation and loading as detected by SEM from the sandy silt soil (loess).

The other main factor which reduces the dry strength upon wetting is the capillary forces or the internal water tension between particles. Since the soils within the study area (semi arid region) commonly possess low water content, the particles are held strongly together by these capillary forces. Upon wetting, these forces are lost and the particles relax causing a moderate swelling within the soil. The clay particles that coat the coarser materials act as a lubricating agents. Upon wetting the coating materials are softened

and capillary forces are rapidly lost. During shearing stage for the wetted samples, a great reduction in shear strength was observed as detected in the stiff lean clay soil (Spangler and Handy, 1982). Clemence (1981) defined the strength results from capillary tension as a temporary strength. He stated that for the densest packing of uniform spherical grains, the maximum capillary forces occur at 10% moisture.

Fig. 6.21 shows the variation in the effective shear strength. The effective shear resistance of the different soils is relatively high. The soils exhibited low cohesion and relative high internal friction angle in terms of the effective stress. The consistent slope of the failure envelopes seems to be varied in a narrow range from  $32^{\circ}$  to  $39^{\circ}$ . The cohesion varies from almost 0.0 to 14 kpa. This relatively high shear strength in terms of the effective stress is more related to the soil composition. Most of the studied soil composition contain high quartz, kaolinite and calcite. Quartz and kaolinite give high shear strength, as shown in Fig. 6.23, while calcite may be destroyed or weakened by wetting and loading. In the natural moisture condition calcite, as a bonding agent itself, contributes to high bond strength. In the saturated condition, upon loading in the consolidation stage, the bond due to calcite may breakdown and particles may become closer leading to a higher shear strength in term of the effective stresses. This high friction angle and low cohesion stress reflect the effect of consolidation processes in breaking down the particle bond, fabric structure, thus allowing for more close

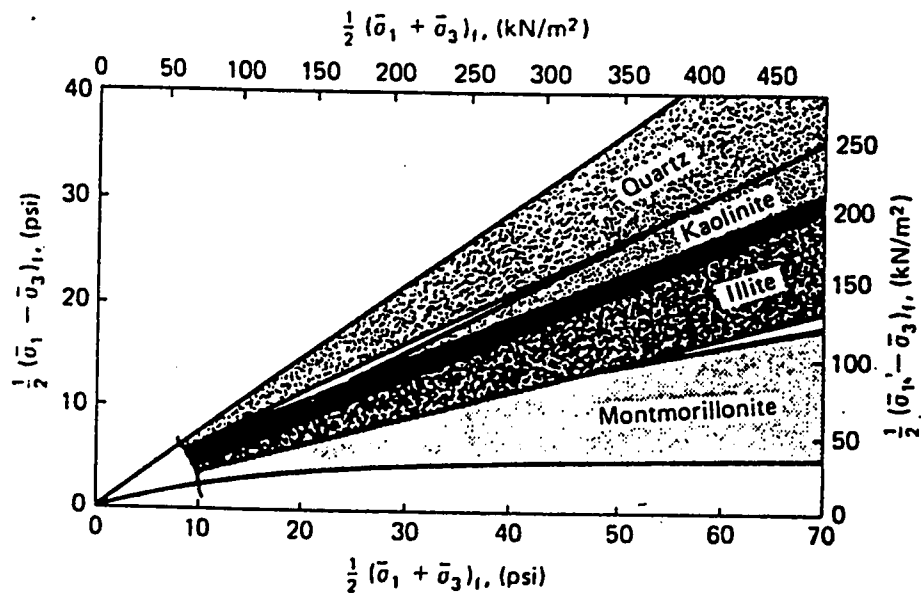


Fig. 6.23: Ranges in Effective Stress Failure Envelopes for Pure Clay Minerals and Quartz (Mitchell, 1976).

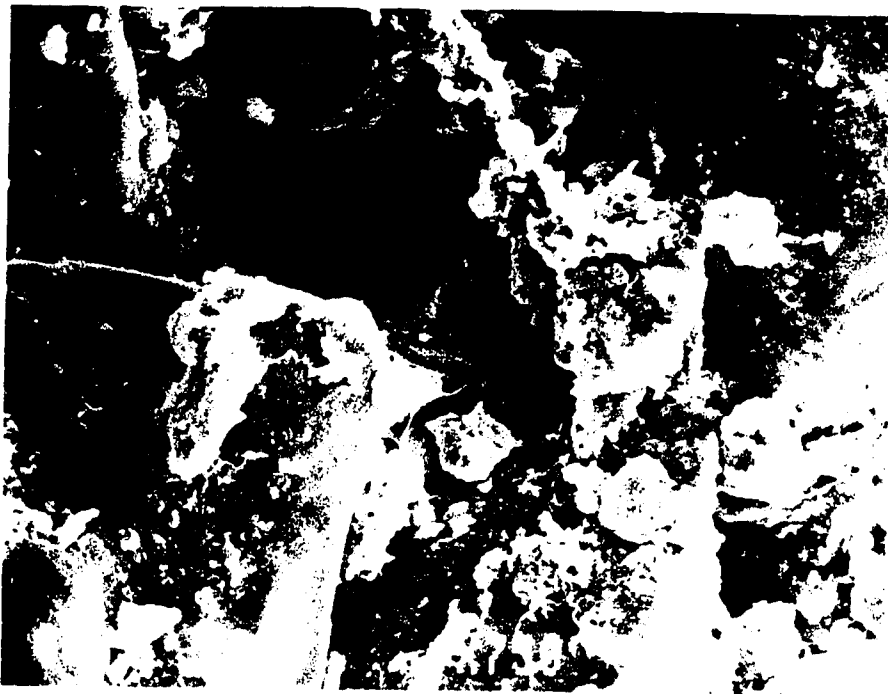


Plate 6.4 : Failures on masonry bearing wall of one floor building resting on the expanding lean clay, 'Merriah'.

particle contact. This contact becomes more pronounced in the soils containing higher coarse material contents such as the silty clayey sand with gravel and the sandy silty clay with gravel. Plate 6.4 shows this type of grain to grain contact, resulted from the break in bond strength as detected in the failure surface of the triaxial specimen (saturated sandy silty clay with gravel soil). It indicates also the dilution and leaching of cementing agent, calcite, out of the contact surface as shown by the white colour.

The obtained values of  $\phi_{cu}$  from consolidated undrained triaxial tests for natural conditions in term of the total stresses are within the ranges of the internal friction angle obtained from SPT as shown in Table 6.15. Holtz and Gibbs (1951) carried extensive research on Loess soils. Generally, all the obtained engineering properties in this study are within the limits of the results obtained by them. Table 6.16 indicates the index properties of some loess soils along with the variation in the internal friction angle as water content varies. These results coincide with the obtained values of internal friction angle from both partially and fully saturated conditions.

Table 6.15 : Empirical values for  $\phi$ ,  $D_r$  and unit weight of granular soils based on the standard penetration number with corrections for depth and for fine saturated sands. (Bowles, 1982).

Description	Very loose	Loose	Medium	Dense	Very dense	
Relative density $D_r$ *	0	0.15	0.35	0.65	0.85	1.00
Standard penetration no. $N$		5-10	8-15	10-40	20-70	> 35
Approx. angle of internal friction $\phi$ †	25-30°	27-32°	30-35°	35-40°	38-43°	
Approx. range of moist unit weight $\gamma$ , pcf (kN/m <sup>3</sup> )	70-100‡ (11-16)	90-115 (14-18)	110-130 (17-20)	110-140 (17-22)	130-150 (20-23)	

\* Depends on  $p_v$  ranging from 70 to 500 kPa. Low value of  $N$  corresponds to lesser  $p_v$ .

† After Meyerhof (1956).  $\phi = 25 + 25D$ , with more than 5 percent fines and  $\phi = 30 + 25D$ , with less than 5 percent fines. Use larger values for granular material with 5 percent or less fine sand and silt. See also Eq. (4-10) for estimate of  $\phi$ .

‡ It should be noted that excavated material or material dumped from a truck will weigh 70 to 90 pcf. Material must be quite dense and hard to weigh much over 130 pcf. Values of 105 to 115 pcf for nonsaturated soils are common.

Table 6.16 : Characteristics of China Loess  
 (After Wu Zhi-hui and Xie Ding-yi,  
 ASCE, 1987).

Index	Lanchow Loess	Xian Loess		Lowchuan
		No.1	No.2	Loess
Dry density $\text{KN/m}^3$	11.8-13.7	12.3-13.8	13.1-17.2	12.7-13.1
Initial water content %	16.3-28.7	19.1-23.0	14.2-31.0	9.7-12
Void ratio $e$	0.96-1.30	0.96-1.20	0.58-1.07	1.00-1.20
Plastic limit $w_p$	16.3-19	17-19		19.7
Liquid limit $w_l$	24.0-32	30-32		30.7
Shear strength $C$ , kps	16-26	20		30-80
$\phi$ degrees	16-18	22		32-34

## Chapter 7

### DESIGN CONSIDERATION AND SITE IMPROVEMENTS

The observed soil distribution within the study area require great care to chose the most appropriate foundation design. The existence of stiff fissured clay as a medium expansive soil in the top surface followed by sandy silt as a collapsible loess complicates the problem. In addition, the existence of fine soils interbedded with or sometimes mixed with coarse soils demands more investigations and great cautions to select the strength and consolidation properties and subsequently the suitable foundation design.

The occurrence of the stiff dark fissured lean clay in the first meter below the ground surface makes the removing of this layer beneath the foundation the best economical and practical solution even in case of one story light structure. In some cases, this soil may extend to a greater depth and in rare cases it may occur again at about 3.0m below the ground surface as found in Station # 17. If that is the case, the applied stress resulting from the dead loads of the super structure must be greater than the expected swelling pressure. The suspended ground slab should be used to avoid direct contact pressure between slab and soil which allow for expansion of soil. Failure in the basements or light structures resting on this soil, were observed as shown in Plate 6.1. Since this soil exists mostly on the top layer it causes a great trouble for highway and

roads pavements. The replacement of this soil by another suitable material is the best solution. Lime treatment and compaction on the wet site of optimum could be used to reduce the swelling potential of such surficial soil.

Some structures have been supported by foundations resting on two or more different levels. This leads to different interaction between the bearing layers and the superstructure according to these different soils. For example many structures may have part of the foundations resting on this lean clay soil and the other foundations resting on the sandy silty loess or granular soils. Such conditions have to be considered and suitable safe design has to be considered.

On the other hand, the existence of loessial collapsing soils, including the sandy silt and the sandy silty clay with gravel represents the major problem and the most difficult soil as a foundation material in the region. Problems of consolidation and stability are frequent in loessial deposits and other collapsible soils. The high degree of consolidation (or settlement) of such soils when loaded or wetted can be a considerable problem that has to be considered in designing structures on loessial foundations. Controlling settlement is the main problem in such design because shear resistance is dependent upon the consolidation that takes place. The settlement and subsequently the shear resistance are dependent upon the moisture content, the dry density and the plasticity of the loess (Braja, D., 1984). The moisture content is the first main factor which con-

trols the design considerations in case of loessial soils of the sandy area as well as other loess deposits. The design considerations of structures resting on loess (collapsing) due to moisture condition have to be analyzed in two phases. The first phase is the low moisture content and the second phase is the wetted condition or relatively high moisture state.

The dry loess, in general, has high bond strength and is often capable of supporting relatively large loads without excessive settlements. Clevenger (1956) and Clemence (1981) indicate that natural loess soils can support the normally assigned loadings with less settlement when they have moisture content below 15% regardless of density. The caution of the sudden failure in loess due to the breakdown in the bond strength has to be considered. Such sudden failure can take place if the applied load exceeds the critical load. Such sudden collapse was shown by Peck, Hansen and Thornburn, (1974) by carrying out the plate load tests on different loess soils having different moistures as shown in appendix E-1. They indicated the effect of moisture content in controlling the value of the critical supported loads. For moisture content 13% about 870 Kpa was the ultimate while it dropped to about 250 Kpa at 29% moisture content. The spread footings can be built on collapsible loess if great cautions are taken to prevent the rising in moisture under structures. This rise in moisture can take place in any of the following forms (Clemence, 1981):

- 1) Local or shallow wetting resulted from water source as pipelines or uncontrolled drainage of surface water.
- 2) Intense, deep, local wetting of soil caused by water discharge of industrial effluents or irrigation.
- 3) Rise in water table resulting from water source outside the collapsing soil area.
- 4) The change of evaporation condition due to a surficial obstruction that cause a condensation of steam and accumulation of water.

These general forms cause either a slow and uniform rise in moisture or localized and may cause rapid rising in moisture which develop the differential settlement problem. The last situation was detected within the study area. Four adjacent masonry buildings exhibited severe cracks in the internal and the external bearing walls in Moammr area, Old Sana'a city.\* These cracks resulted from the collapsing in the soil structure beneath the bearing walls as a result of seeping the water from a broken pipeline into the soil beneath the collapsing sides. Damage resulting from the differential settlement in form of hair cracks within the reinforced structures having isolated foundation were also observed. Plate 7.1 shows the cracks in the reinforced concrete wall of a new one story building that has rested on the top of the sandy silt layer in Hada area (new Hada city). The hair cracks in finishing of beams, slabs and walls

-----

\*The Prominent was the consultant for the owners.

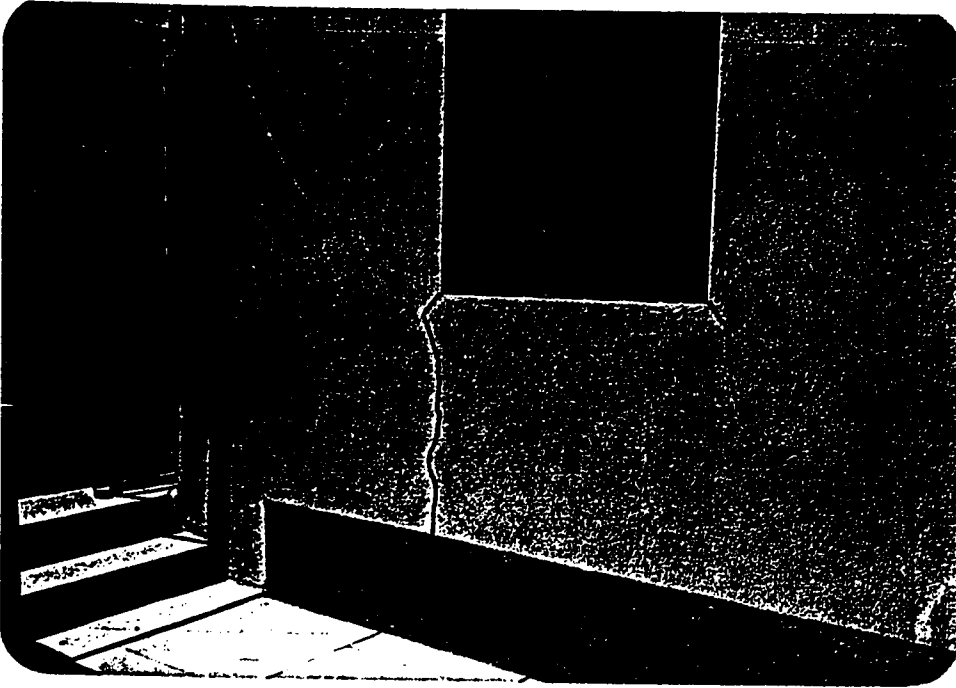
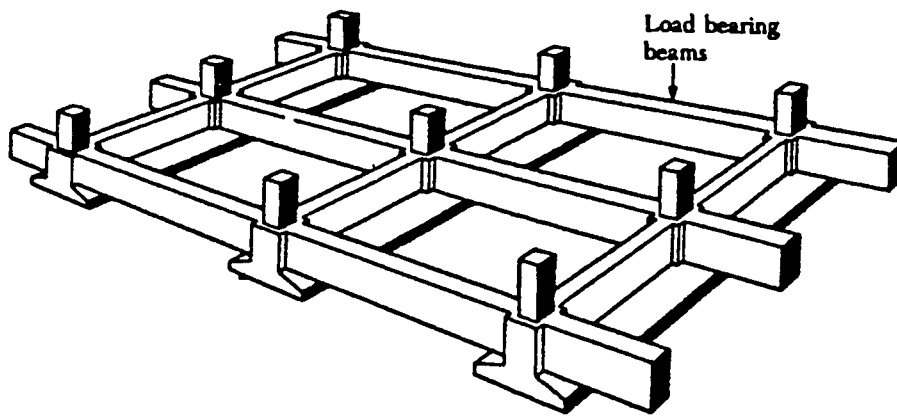


Plate 7.1 : Cracks on a reinforced concrete wall of one floor building resting on surficial collapsing soil in Hada Region.

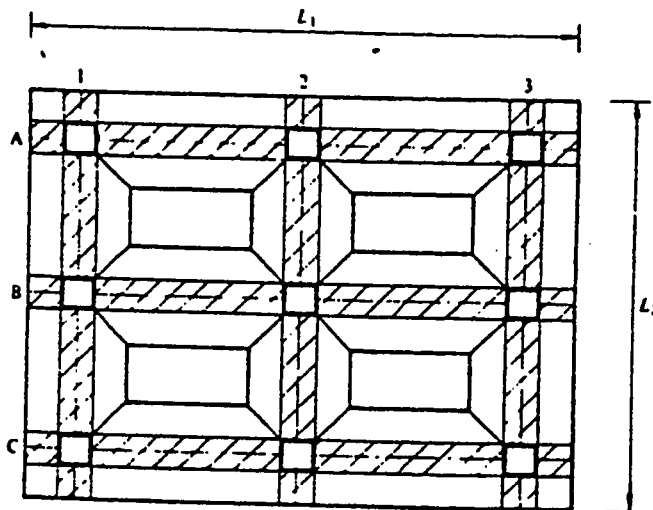
are common in most of the available structures. A main source of increase in the moisture within the study area is the existence of the septic tank of each structure (pit hole) nearby the building. Another significant factor is the increase in the planted area, of most houses, that surrounds the building or located at the side of the building. Another contributing factor for the damage of structures resting on collapsing soil is the dynamic loads effect. An area of 100 km away of the study area (Thamar area in 1983) was subjected to an earthquake which was felt in Sana'a area. Palka, J., (1985) indicated that when dynamic loads are encountered, shearing strength of loess soils decreases by about 40% as humidity increases. Generally, keeping the soil at its natural low moisture is difficult to control. During site investigation some soil samples had a water content higher than 15%. Consequently, design based on the natural dry strength of the loessial soils would be in error if the foundation ever becomes wetted (Holtz and Gibbs, 1951).

The second moisture content phase is the wet state, at which wetting of the loess causes the most pronounced settlement condition. Rise in moisture may result in two different considerations, either low bearing capacity may reach 25 kpa (Bowles, 1982) with restricting the settlement to minimum or an excessive settlement associated with increase in bearing capacity. The last situation is the most common and such excessive settlement upon wetting has caused concern to designers and has made research imperative (Holtz and Gibbs, 1951). The problem comes into the picture as a high possibility for the

differential settlement to take place. Holtz and Gibbs (1960), indicated that when the natural moisture content is expected to reach more than 20 percent, the moisture at which the bond between particles relatively highly weakened, the differential and total settlement have to be considered. For such condition using continuous footing to minimize the differential settlement is safer than using the isolated footing. Fig. 7.1 shows a typical strip footing that is used on collapsible soils (Clemence, 1981). The figure shows the using of a stiff continuous footing in one direction to transfer the columns loads into soil while longitudinal load bearing beams are used to minimize the differential settlements and increase the foundation stiffness (Fig. 7.1.a). In case of heavier structure, the strip footing with stiffness in two directions is desirable as shown in Fig. 7.1.b (Zeevaert, 1972). In the situation where the area of strip footing becomes close to 50 per cent of the projected area of the building, it is more economic to use a continuous mat foundation. Clemence (1981) and Bowles (1982) suggested, that if large settlements are expected under building heavy structures, drilled-pier and pile foundations may be considered to control settlement. The selection of the suitable bearing layer demands more experience and deeper site investigation since the bed rock is very deep. The geological studies showed this great variation in depth of the quarternary sediments (alluvial and aeolian deposits) from non-existence to almost 300m thick. Heavy structures on loessial soils collapse easily due to heavy load or wetting. The water content affects greatly the value of the critical stress. That is



a)



(b)

Fig. 7.1 : Continuous strip footing in collapsing soil:

- a) Continuous in one direction with load bearing beam, (After Clemence, 1981), and
- b) Continuous in two directions, (After Zeevaret, 1988).

why wetting is considerably more effective in breaking-down the bond than loading. However, the foundation must be proportional in such a manner that the critical stresses are not exceeded. A factor of safety of 2.5 to 3.0 should be used to calculate the allowable soil pressure (Das, B. 1984).

The collapsing problem due to wetting or breaking down the bond strength under high loading arises mainly in soils having low densities. Holtz and Gibbs (1960) and Bowles (1982) indicated that the probability of extreme settlement is not great for densities above 90 lb per cu ft ( $14.8 \text{ gm/cm}^3$ ) and voids ratio less than 0.85. The surficial loess soil which exists mostly below the first meter down from the ground surface is characterized by having low dry density (about  $13.4 \text{ gm/cm}^3$ ) while the loess soils have higher dry unit weight. When loess is compacted, relatively high density is obtained, bond strength is destroyed and grain to grain becomes more in contact. Consequently, a higher strength, less consolidation and less tendency to collapse are achieved. Most of the foundations within Sana'a area have been constructed at 1.0 to 2.0 m below the surface which are in the range of the collapsing soil. If it is suspected that the upper layers of soil may get wet and collapse at some time after construction of the foundations, several improvements may be considered. Table 7.1 summarized the general suggested improvement techniques (ASTM, 1978). Improving the soil can be done either by causing a collapsing in the bond strength before construction or by increasing

the bond strength by injection certain materials or solutions specially in case of the already available structures.

The existence of those highly collapsible soils in the first three to four meters below the surface makes the use of the conventional compaction improvement more economical and more effective after removing the top soil than the other methods. Ponding of or flooding with water before roller compaction is expected to give high improvement results (Beles, A. A., and Schaly, 1976).

The sample of the sandy silt (Station # 40 at 2.5 m) exhibited a relatively higher dry unit weight (15.0 kpa) and lower void ratio (0.92). The layer from which this sample was obtained was subjected to truck movement during the excavation of the trench. This type of movement caused, to some extent, a compaction of this layer. When a specimen of this layer was tested in the oedometer test, it did not show the tendency for collapse as shown in Fig. 7.2. A low value of the collapsing potential  $C_p$  equal to 1.0 was obtained (Table 6.10).

This identification coincides with the other identification shown in Table 6.9. The tested specimen of the sandy silt (Station # 42 at 1.2m) gave a value of  $C_p$  equal to 7.2 as shown earlier in Fig. 6.10.

This last sandy silt sample had a low dry density ( $12.8\text{gm/cm}^3$ ). Comparing the results of these two tested specimens (both of which are sand silt loess) indicates the effect of compaction in increasing the density, reducing the voids ratio and subsequently reducing the

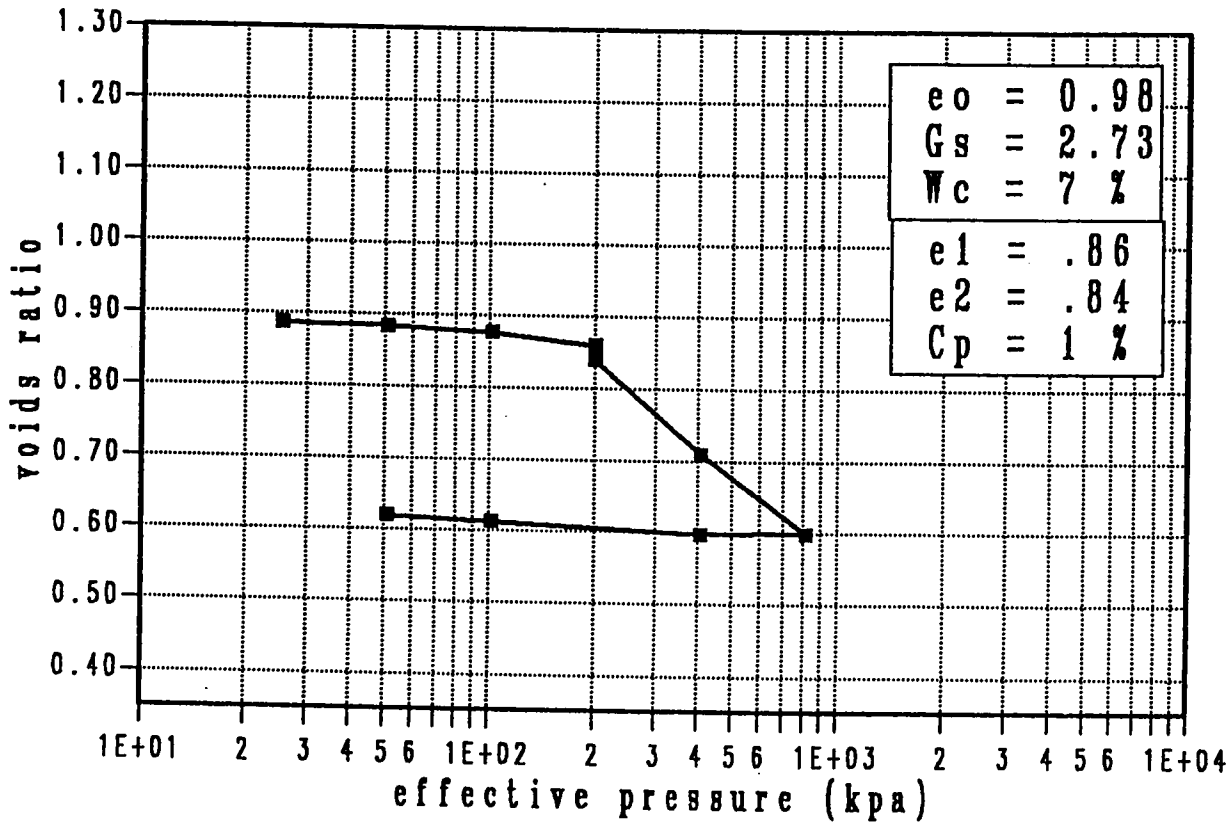


Fig. 7.2 : Effect of densification in reducing the collapsing potential tendency

tendency to collapse. The use of grout injection methods may not be more economic due to the existence of granular materials in between the loess deposits which may require large amount of grouts. Several investigators recommended the use of flooding by ponding in order to stabilize surficial loess. Beles, A. A. and Schally (1967) indicated that prewetting by ponding can be used with good technical and economical results. They also indicated that preflooding is an effective method of compacting slumping soils characterized by low cohesiveness and a predominance of structural bond, not only in the lower but also in the higher horizons. A layer of 17m thick of Terkum loess which is similar in its composition to the loess of the study area exhibited a slump of 110 cm after the first two months of flooding the surface as indicated by Balaev, L. G. (1967). He indicated also that preliminary flooding of such loess soils in combination with surface compaction is convenient stabilization method. The thermal stabilization method has been used successfully in stabilizing loessial soils. This method was used to raise the bearing capacity underneath a collapsed warehouse from  $8 \text{ kg/cm}^2$  up to  $25 \text{ kg/cm}^2$ . The warehouse is now in normal service after improving the loessial soils down to 5.0m beneath the foundations (Vorobkov, L., Kasperskii, O. and Karpjenko, V., 1967).

If the collapsible soil is improved, the behavior of the soil is modified and medium to low compressibility capacity may be obtained. The allowable bearing capacity for improved deposits ranges from

1 kg/cm<sup>2</sup> to over 4 kg/cm<sup>2</sup> (Zaevaert, 1972). The ultimate bearing capacity reached up to 25 kg/cm<sup>2</sup>, when loess deposit was improved by thermal stabilization (Vorobkov, L. et al, 1967). However, the settlement should be estimated in accordance with the new stress-strain characteristics of the soil encountered and environmental hydraulic conditions at the proposed site. When major changes in humidity under the foundations of high buildings (of heavy loads) are expected to take place, a great caution and deeper site investigation are essential to arrive at the most appropriate solutions.

## Chapter 8

### SUMMARY AND CONCLUSION

Based on the field and laboratory investigation programs that were carried out on Sana'a area, the capital of Yemen Arab Republic, the following conclusions are drawn:

- 1) The available Quaternary sediments within Sana'a Plain mainly resulted from both the alluvial depositional system in forms of alluvial fans, flood plain and wadi deposits and wind depositional system in the form of wind-laid deposits.
- 2) A relative regular soil profile is common condition, in spite of the great variation in the available soil types. The relatively regular profile is mostly a repetitive layering system of both water-laid and wind-laid deposits.
- 3) The available granular soils have different colours, textures and forms. They vary from well to poorly graded sand and gravel with or without silty clay matrix. While most of the fine soils are of the loess formation type - mainly of the prime loess type within the first three to four meters below the ground surface and of modified loess, secondary type, below the previous type.
- 4) The most common nonclay minerals are quartz, albite, calcite, aragonite, augite and hematite, while the predominant clay mineral is kaolinite.

- 5) The chemical analysis indicated that all soils are alkaline with high calcium carbonate and iron oxide contents and low organic matter and sulphate contents. So no special treatment for foundation is needed. The silty clayey matrix within the granular soil and the stiff fissured lean clay soil, top layer, are moderately erodeable.
- 6) The microstructure and the fabric of the fine soils varies from an open metastable fabric, collapsible fabric, with high chemical precipitations in loess soil to well oriented fabric of close-packed arrangement in form face to face aggregation with edge to edge and high clay precipitations in lean clay soils.
- 7) The deformation characteristics of the fine soils are of two different types. A swelling behavior of medium type is the characteristics of the over-consolidated dark stiff fissured lean clay which exists mostly as a top layer, with a maximum thickness of 1.5m. It exhibited a swelling pressure of about  $1.0 \text{ kg/cm}^2$  and a swelling potential of 2.6%. The second deformation type, loess formations exhibited a moderate to high collapsing behavior under wetting and loading.
- 8) The stress history of the fine soils are within the range of the normally to slightly over-consolidated state except the stiff fissured lean clay which exhibited a relatively high over-consolidated stress history.

- 9) Generally all soils are characterized by having high shear strength when they have low moisture content and drastic decrease in strength as moisture content increases, so the foundation design in dry state may be in error whenever the foundation becomes wet.
- 10) Critical state parameters were established for the different fine soils in the saturated condition.
- 11) Great caution has to be considered in the foundation design to overcome both the expansion in case of construction on stiff fissured lean clay soil, top layer, and collapsing in case of loessial soils.

### Future Research

For future research, the following researches are suggested:

- 1) Identification of the boundaries of coarse and fine soils formation in the horizontal direction.
- 2) Site improvement for both the top expansive soil from the transportation aspects and for the collapsing soils from geotechnical point of view.
- 3) Most appropriate foundation system for collapsing soil under the available layering system, such as a strip continuous or mat foundation, (Clemence, 1981).
- 4) The deeper site investigation in case of special structures.

## REFERENCES

- Agha Shaher, G. (1984), Geography of Natural Yemen (North Yemen), By Al Annwar Publisher, Demuscas Syria.
- Aldo, R. (1971), Standard Penetration Tests on Collapsible Soils, Fourth Pan American Conf. on Soil Mech. and Foundation Engineering, pp. 77-84.
- Altschaeffl, A.G. (1982), Discussion of Design Consideration for Collapsible Soils, Proc. Am. Soc. Civil Engrs., J. Geotech. Eng. Div., 108, Gt1:674-676.
- ASTM (1971), Sampling of Soil and Rock, Special Technical Publication No.483, Philadelphia.
- ASTM (1978), Soil Improvement, by ASCE, New York.
- ASTM (1972), Annual Standard, Part II, April.
- Atkinson, J. H. and Bransby, P. L. (1978), The Mechanics of Soils: An Introduction to Critical State Soil Mechanics, McGraw-Hill Book Co., London.
- Baleav, L. G. (1967), Prognosis of Slumping Deformation of Loess Soils, Geotechnique.
- Barden, L. A. McGown and K. Collins (1973), The Collapse Mechanism in Partly Saturated Soil, Engineering Geology, 7, pp.49-60.
- Bates, R.L. and Jackson, J.A (1980), Glossary of Geology, 2nd Ed. Am. Geol. Inst., Falls Church, Va. 751 PP.
- Bear, F. E. (1964), Chemistry of the Soil, 2nd Edition, Reinhold Publishing Corporation, New York.

- Beles, A. A., Stanculescu and Schally, V. R. (1969), Prewetting of Loess-Soil Foundations for Hydraulic Structures Fifth International Conference in Soil Mechanics and Foundation Engineering.
- Bell, F. G. (1981), Engineering Properties of Soils and Rocks, Butterworth & Co. Ltd.
- Bishop, A. W., and Henkel, D. J. (1962), The Measurement of Soil Properties in Triaxial Test, 2nd Edition, Edward Arnold Ltd., London.
- Bowles, Joseph E. (1984), Physical and Geotechnical Properties of Soil, McGraw-Hill Book Co., New York.
- Bowles, Joseph E. (1978), Engineering properties of Soils and Their Measurement, McGraw-Hill Book Co., New York.
- Bowles, Joseph E. (1982), Foundation Analysis and Design, McGraw-Hill Book Co., New York.
- Bull, W. B. (1972), Recognition of Alluvial-Fan Deposits is the Stratigraphic Record, Recognition of Ancient Sedimentary Environments, Soc. Econ. Planotologists and Mineralogists, Spec. Publ. No. 16, Tulsa, Okla, pp. 68-83.
- Clemence, S. P. and Finber, A. O. (1981), Design Consideration for Collapsible Soils, ASCE, GT3, pp. 305-317.
- Clevenger, W. A. (1956), Experience with Loess as Foundation Material, ASCE Proceedings, Paper No. 1025, July.
- Das, B. M. (1984), Principles of Foundation Engineering, Wadsworth, Inc., Belmont, California.
- Denisov, N. J. (1951), Settlement Properties of Loessial Soils, Soviet

- Science, U.S.S.R. Government Publishing Office, Moscow.
- Dhawian, A. W. (1981), Characteristics of AL Ghat Collapsing Soil, Symposium in Geotechnical Problems in Saudi Arabia.
- Dudley, John H. (1970), Review of Collapsing Soils, Journal of the Soil Mechanics and Foundation Division, ASCE, Vol. 96, No. SM3, Proc. Paper 7278, May, pp. 925-949.
- Dusseault, M. B. Scott, J. D. and Moran, S. (1985), Smectatic Clays and Posts Reclamation Differential Subsidence of Strip Mine Areas, Applied Clay Science, 1.
- El Anbaawy, M. I. (1985), Geology of Yemen Arab Republic, Sana'a University, Sana'a.
- Fadlul Allah, K. M. A. (1985), Geotechnical Properties of Subsoil in Other Area, North Jeddah, Thesis presented to the Faculty of Earth Sciences, King Abdulaziz University, Jeddah.
- Geukens, F. (1966), Geology of the Arabian Peninsula Yemen, Geological Survey Professional Paper 560-B, U.S.
- Gibbs, H. J. and Bara, J. P., (1962), Predicting Surface Subsidence from Basic Soil Tests, Special Technical Publication No. 322, ASTM.
- Gray, T. Lobdell (1981), Hydroconsolidation Potential of Palouse Loess, ASCE Proceeding Vol. 10 7, No. GT6, June.
- Gibbs, H. J., Hilf, J. W., Holtz, W. G. (1960), Shear Strength of Cohesive soil, Soil Mechanics and Foundation Division, Research Conference on Shear Strength of Cohesive Soil, Colorado University.

- Gillott, J. E. (1987), Clay in Engineering Geology, by Elsevier Science Publishers, Amsterdam.
- Glennie, K. W. (1970), Desert Sedimentary Environments, Developments in Sedimentology, V. 14 . Elsevier, New York.
- Goildstein, J. I., Newbury, D. E., Echlin, P., Joy, D. C., Flori, C. and Lifshin, E. (1981), Scanning Electron Microscopy and X-Ray Microanalysis, Plenum Press, New York.
- Grim, R. E. (1968), Clay Mineralogy, 2nd Edition, McGraw-Hill Book Company, New York.
- Grolier, M. J. and W. C. Overstreet, W. C. (1978), Geological Map of Yemen Arab Republic, U.S. Geological Survey, Reston, Virginia, U.S.A.
- Head, K. H. (1982), Manual of Soil Laboratory Testing, Pentech Press, London.
- Holtz, W. G. and Hilf, J. W. (1961), Settlement of Soil Foundations Due to Saturation, Fifth International Conference on Soil Mechanics and Foundation Engineering, Vol. 1, pp. 673-679.
- Holtz, W. G. and Gibbs, H. J. (1951), Consolidation and Related Properties of Loessial Soils, ASTM, Symposium on Consolidation Testing of Soils, STP No. 126.
- Houston, S. L., Houston, W. N. and Spadola, D. J. (1988), Prediction of Field Collapse Soils Due to Wetting, Journal of the Soil Mechanics and Foundation Division, ASCE Proceeding, Paper No. 22107, January.
- International Society for Soil Mechanics and Foundation Engineering

- (1981), The International Manual for the Sampling of Soft Cohesive Soil, Tokyo University Press, Tokyo, Japan, 1981.
- Italconsult (1973), Water Supply for Sana'a and Hoddidah, Report of 3 volumes, Rome.
- Jennings, J. E. and Knight, K. (1975), A Guide to Construction on or with Materials Exhibiting additional Settlement due to Collapse of Grain Structure, Sixth Regional Conf. for Africa on Soil Mech. Found. Eng. pp. 99-105.
- John Lowe and Thaddus, C. (1960), Use of Back Pressure to Increase Degree of Saturation, Soil Mechanic and Foundation Division, Research Conference on Shear Strength of Cohesive Soil, Colorado University.
- Jones, D., and Van Alphen, G. (1980), Collapsing Sand - A Case History, Seventh Regional Conference for Africa on Soil Mechanics and Foundation Engineering, Accra.
- King, J. and Abu Ghanem, A. E. (1983), Soil Survey of the Yemen Arab Republic, Thesis Presented to New York State College of Agriculture and Life Sciences.
- Kruck, W. (1983), Geological Map of the Yemen Arab Republic, Federal Institute for Geosciences and Natural Resources, Hanover, Federal Republic of Germany.
- Krynine, D. P. and Judd, W. R. (1957), Principles of Engineering Geology and Geotechnics, McGraw-Hill Book Company.
- Lambe, W. T. (1951), Soil Testing for Engineering, John Wiley and Sons, Inc., New York.

- Lampe, T.W. and Martin, R.T. (1953), Composition and Engineering Properties of Soils Vol 1, Highway Res. Board, Proc., 32:576-590
- Lovell, C. W., and Richard, L. Wiltshire (1987), Engineering Aspects of Soil Erosion, Dispersive Clays and Loess, Geotechnical Special Publication by ASCE, New York, April.
- M. Minkove (1985), Geotechnical Problems of the Bulgarian Loess Soil, Eleventh Int. Conf. on Soil Mech. and Found. Engg. V. 4, pp. 2435-2442.
- Mc Gowen, J. H. and Garner, L. H. (1970), Physiographic Features and Stratification Types of Coarse-Grained Point Bars Modern and Ancient Examples, Sedimentology, 14:77-112.
- Ministry of Public Works (1985), Two Reports of Two Locations Within Sana'a Region, Sana'a, 1985
- Mitchell, James K. (1976), Fundamentals of Soil Behavior, John Wiley and Sons, Inc., New York.
- Mustaffa Isa, A. (1985), Geographical Study of Sana'a Region, Thesis Presented to Sana'a University, Sana'a.
- Northey, R. D. (1969), Engineering Properties of Loess and other Collapsible Soils, Seventh International Conference on Soil Mechanics and Foundation Engineering, Mexico City, pp. 445-452.
- Palka, J., and Naboczyk, J. (1985), Settlement of Foundations on Loess Soils, International Soil Mechanics and Foundation Engineering, V. 4., 1985.

- Peck, R. B., Hanson, W. E. and Thurnborn, T. B., (1974), Foundation Engineering, Wiley, New York.
- Rallings, R. A. (1966), An Investigation of the Causes of Failure of Farm Dams in the Brigalow Belt of Central Queensland, Bulletin 10, Water Resources Foundation of Australia.
- Rhoades, J. D. (1982), Cation Exchange Capacity, Methods of Soil Analysis , Agronomy Monograph No. 9.
- Richard, A. Davis (1983), Depositional Systems, Prentice-Hall, U.S.A..
- Robert, G. Lukas (1980), Densification of Loess Deposits by Pounding, ASCE, GT4, pp.435-446.
- Sherard, L. E., Dunnigan, P. and Decker, R. S. (1976), Identification and Nature of Dispersive Soils, Journal of Geotechnical Engineering Division, ASCE, GT4, April.
- Siliva, J. A. (1971), Geology and Engineering Behavior of Expansive Clay from Cazenga Region-Land, Fifth International Conference in Soil Mechanics and Foundation, Africa.
- Skempton, A. W. (1954), The Pore Pressure Parameters A and B, Geotechnique, Vol. 4, No. 4.
- Smart, P. and Tovey, N. K. (1981), Electron Microscopy of Soils and Sediments: Example, Butler and Tanner Ltd., London.
- Smalley, I.J. and Cabrera, J.G. (1969), Particle association in Compacted kaolin. Nature, 22: 80-81
- Spangler, M. G., and Handy, R. L. (1982), Soil Engineering, 4th edition by Harper and Row Publishers, New York.

- Terzaghi, K., and Peck, R. (1976), Soil Mechanics in Engineering Practice, by John Wiley and Sons, Inc..
- Tomlinson, M. J. (1980), Foundation Design and Construction, Fourth edition, Pitman Publishing, London.
- Vickers, B. (1983), Laboratory Work in Soil Mechanics, 2nd Edition, Granada Publishing, Great Britain.
- Vorobkov, L. N., Kaspeski, O. A., and Karpienko, V. M. (1967), Thermal Stabilization of Loessial Soils, Geotechnique.
- Weaver, C., and Pollard, L. (1973), The Chemistry of Clay Minerals, Elsevier Scientific Publishing Co., Amsterdam.
- Wray, W. K. (1986), Measuring Engineering Properties of Soil, Prentice-Hall, A division of Simon and Schuster, Inc., Englewood Cliffs, U.S.A..
- Young, R. N. and Townsend, F. C. (1986), Consolidation of Soils: Testing and Evaluation, ASTM.
- Zeevaret, L. (1983), Foundation Engineering for Different Subsoil Conditions, Van Nostrand Reinhold Publishing Co., New York.

## APPENDICES

Appendix...A

Appendix...B

Appendix...C

Appendix...D

Appendix...E

**APPENDIX A****A - 1 : Triaxial Test Set-up****A - 2 : Triaxial Test Procedures****A - 3 : Oedometer Test Procedures**

## A-1

## Triaxial Test Set-up

*The test set-up consisted of the following units:*

- i) A 10 ton capacity compression machine was used for applying the deviator stress to the specimens during shearing stage.
- ii) Triaxial cell from Wykeham France Ltd. were used to test specimens.
- iii) Two self-compensating mercury systems were used for applying the water back pressure, while in case of the gas back pressure a cylinder tube under a high gas pressure was used to feed a smaller one (through a regulator) from which  $CO_2$  was obtained through another regulator.
- iv) The cell pressure was obtained from a water tank which was obtained from a cylinder tube through a regulator. This cylinder tube was supplied by the air pressure from a compressor through another regulator.
- v) An indicator was used to measure the pore water pressure inside the specimen during the shearing stage.
- vi) A null indicator filled partially with mercury was used to check the degree of saturation before consolidation and shearing stage.
- vii) Auxiliary items used in the test set-up included standard

filter paper, porous stones, rubber membranes, and a vacuum pump. Both top and bottom ends of a specimen were covered by porous stone along with a filter paper between the specimen and the porous stone to prevent clogging of the porous stone by fine particles.

## A-2

**Triaxial Test Procedure:**

This test is not yet standardized. The procedure that was followed is similar in principle to that described by Bishop and Henkel (1962).

The CIU-Test was conducted using the following steps:

- i) The specimen was prepared and its actual height, weight and diameter were recorded.
- ii) A porous stone was placed on the pedestal followed by a filter paper and the specimen.
- iii) The rubber membrane was put around the specimen with the help of the membrane stretcher so that the membrane covered the pedestal and there was sufficient length available at the upper end to cover the top cap.
- iv) Two rubber O-rings were placed successively over the membrane covering the pedestal.
- v) The sides of the specimen were gently rubbed by the palm of the hands from down upward to remove entrapped air without disturbing the specimen.
- vi) A filter paper, a porous stone and the top cap was placed on the specimen. The upper end of the membrane was pulled up to cover the top cap, and finally a pair of O-rings were placed over the membrane over the

top cap.

- vii) The cell body was placed in position and sealed to its base by turning the three fixed screws while the piston was allowed to touch the top at its central groove.
- viii) The cell was filled with distilled water while air was allowed to escape.
- ix) The cross arms of the compression frame along with the proving ring was lowered to allow the proving ring to touch the piston. The strain gage was set in position.
- x) Taking the advantages of carbon dioxide being heavier than the air and its ability to dissolve in water,  $CO_2$  was inserted into the specimen under a continuous constant pressure. This pressure was less than the cell pressure with one psi at least (7 to 9 psi), in order to remove the air from the specimen.
- xi) After one hour in case of silty sandy specimens to three hours in case of silty clay ones, gas pressure was stopped and the back water pressure was applied (9 psi). The cell pressure and the back pressure were raised simultaneously in steps of 5 psi keeping the difference about one psi at least (cell pressure higher than the back pressure). A time gap of about 5 minutes were allowed in each of these steps. The degree of saturation were checked by using the null indicator till the desirable degree of saturation was reached.

- xii) After reaching the full saturation the cell pressure was raised into the required confining pressure (Cell pressure minus back pressure). The drainage valve was opened to allow the consolidation stage till the pore water inside the specimen was equal to the back pressure ( $u = 0$ ).
- The specimen was loaded in a constant rate of about 0.002"/min., taking the reading of the deviator stress, the deformation and the pore water pressure till the failure took place, the back pressure and the cell pressure were brought to zero.
  - The specimen was removed from the cell and the final dry weight of the specimen was determined.
  - The above procedures were repeated for the other two specimens from the same soil under two different confining pressures.

## A-3

## Consolidation Test Procedures

- 1) The empty ring was weighed and its internal diameter was measured.
- 2) The specimen was cut and trimmed into ring, then the ring and specimen were weighed. The trimmed soil was used to obtain water content and specific gravity of the same soil.
- 3) A filter paper was placed over the bottom porous stone, then the sample was placed in the consolidation cell over the filter paper.
- 4) The cell was fit in load frame and loading yoke was set up.
- 5) Adjusting the beam and setting the dial gage were done before adding the first load increment to weights hunger.
- 6) The specimen was saturated by adding water, then first load was applied on specimen.
- 7) The specimen was loaded incrementally starting either from  $0.31 \text{ kg/cm}^2$  or  $0.26 \text{ kg/cm}^2$  and continued up to  $10.1 \text{ kg/cm}^2$  or  $8.32 \text{ kg/cm}^2$  followed by unloading to  $1.26 \text{ kg/cm}^2$  or  $1.04 \text{ kg/cm}^2$ , then finally reloading again to  $10.1 \text{ kg/cm}^2$  or  $8.32 \text{ kg/cm}^2$ . The period of consolidation under each loads increment was 24 hours and the load increment was unity (i.e. every load except the first one was double that was applied before).

- 8) During consolidation under each increment of loads the dial readings were taken along with time in minutes at 0.25, 0.5, 1, 2, 4, 8, 15, 30, 60, 120, 240, 480 and 1440.
- 9) After the final reloading the cell was drained and the specimen was removed and weighed.
- 10) The specimen was dried in oven under  $105 \pm 0^\circ\text{C}$  then its dry weight was obtained.
- 11) The obtained dial readings were plotted against the square root of time on arithmetic scale and the coefficient of consolidation was determined by using initial straight line portion of the plot (Taylor, 1942).
- 12) Finally, the void ratio was plotted against the logarithm of effective pressure allowing the determination of compression index ( $C_c$ ), swelling index ( $C_s$ ) and the preconsolidation pressure ( $\sigma'_p$ ) which was done using Schmertmann method (Bowles, 1982). These results are shown in the following chapters.

**APPENDIX B**

**B - 1 : Flow Diagram of the USCS.**

**B - 2 : Plasticity Chart**

**B - 3 : Table of AASHTO Classification System.**

**B - 4 : Diagram of AASHTO classification System.**

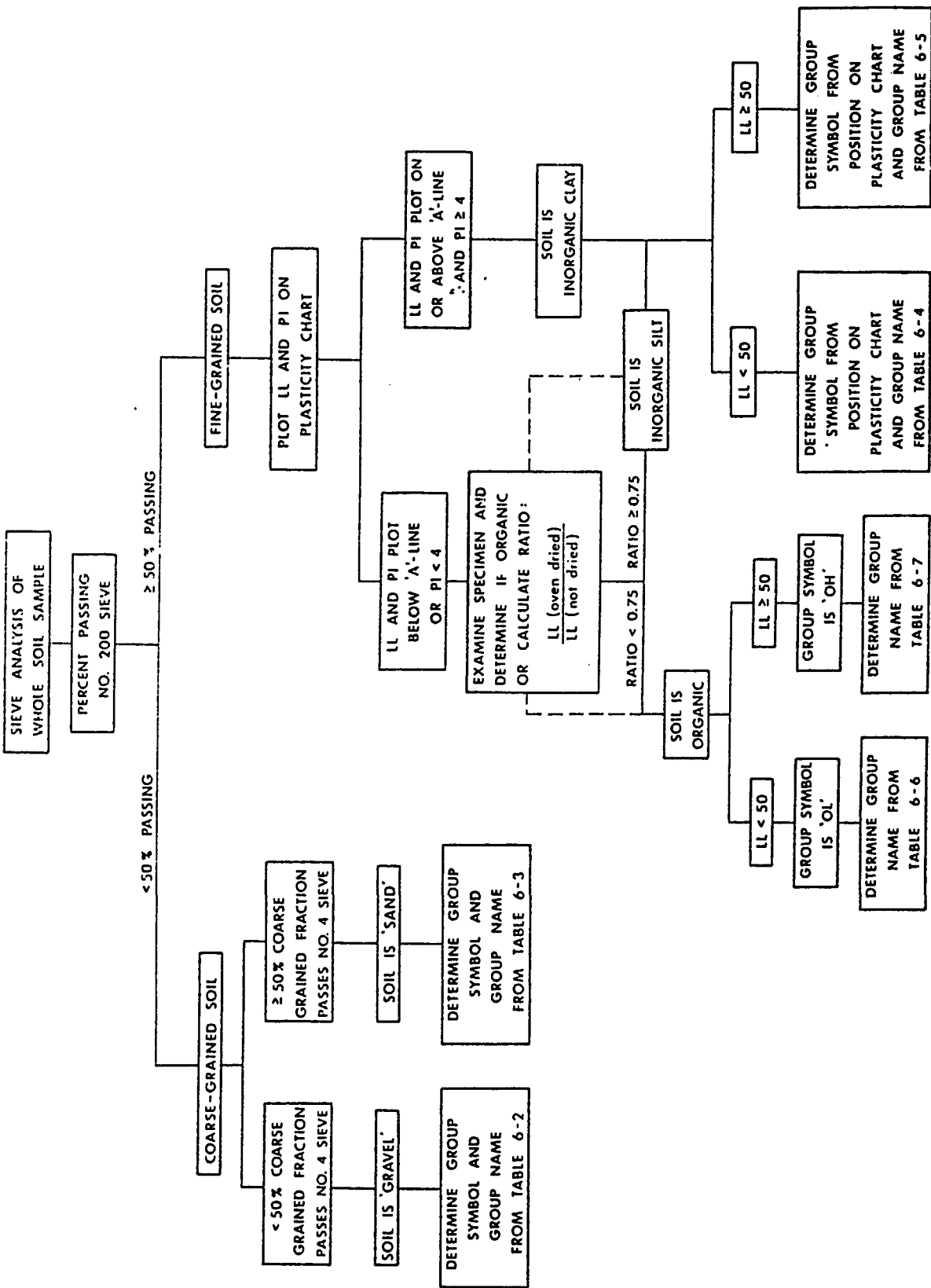
**B - 5 : Tables of Coarse Soils After USCS.**

**B - 6 : Tables of Fine Soils After USCS.**

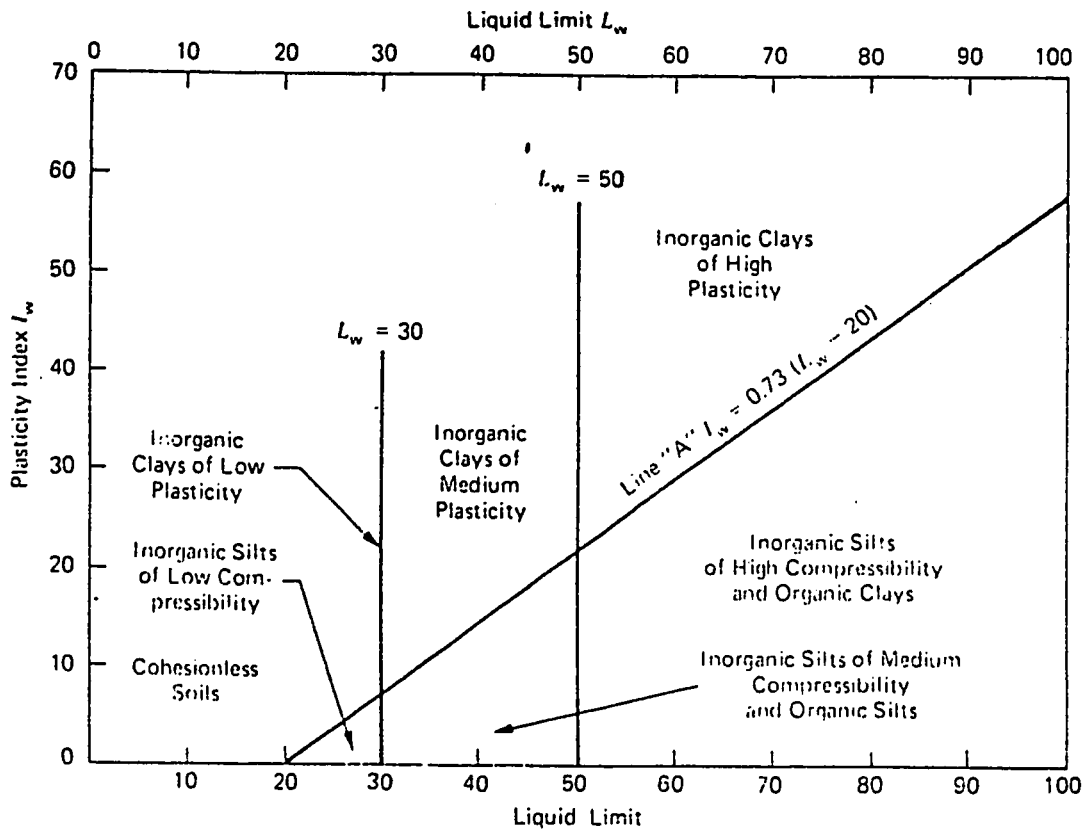
**B - 7 : Soil Correlation Using N Values.**

**B - 8 : Field Soil Identification.**

**B - 9 : Summary of Engineering Properties(USCS).**



B-1: Flowchart for determining the group symbol of the Unified Soil Classification System.

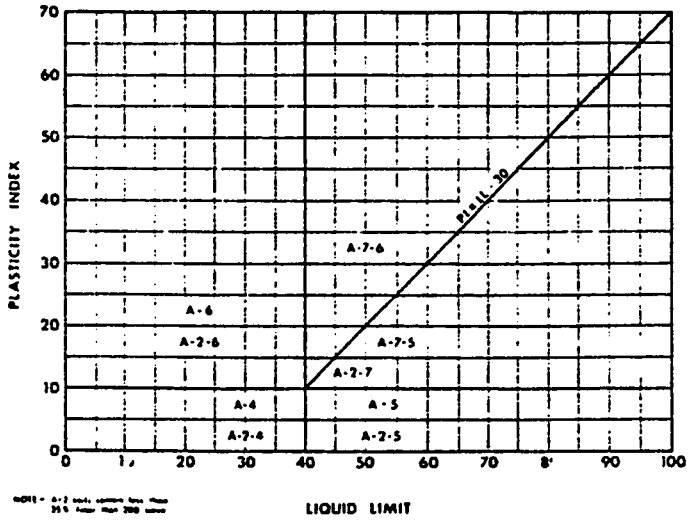


B-2: Plasticity chart.

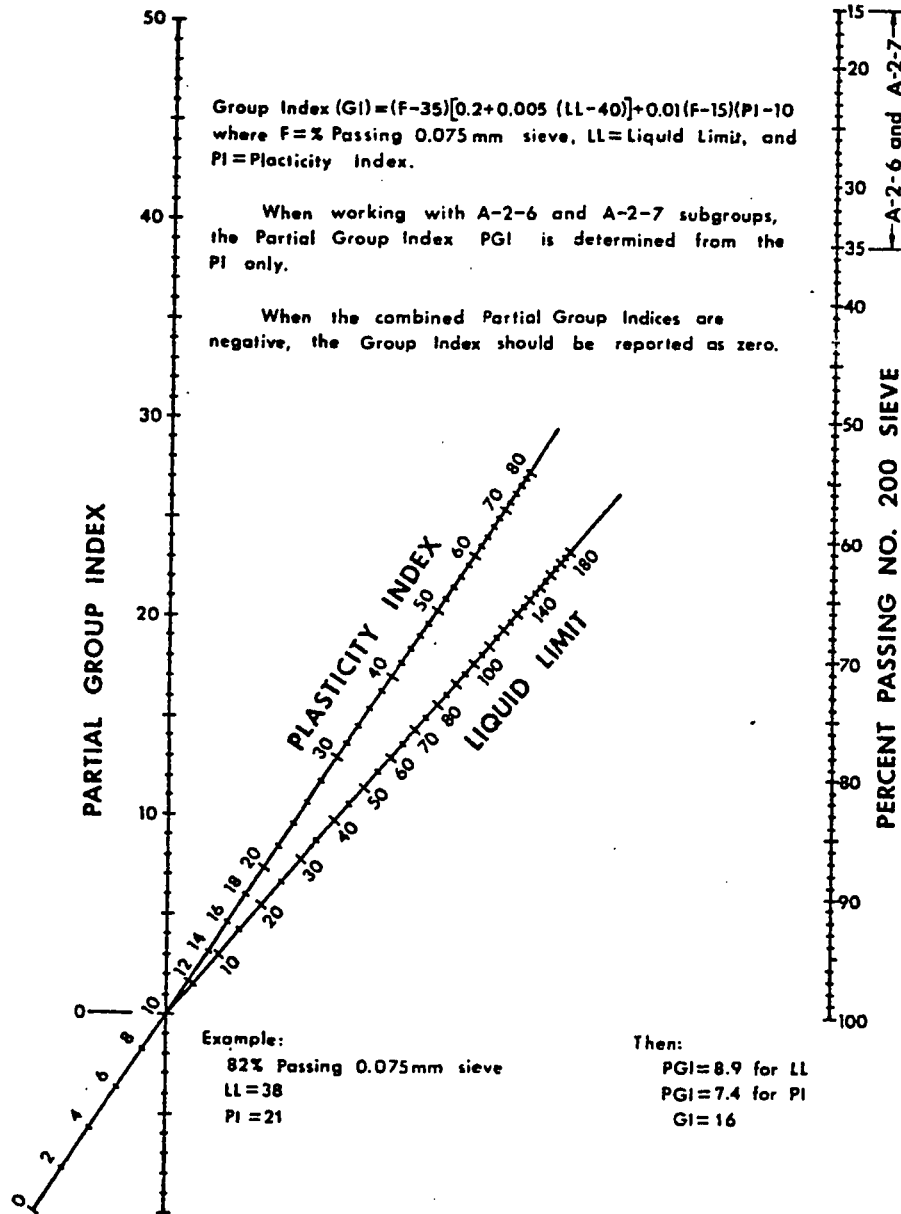
**B - 3: Classification of Soils and Soil-Aggregate Mixtures (with Suggested Subgroups)**

General Classification	Granular Materials (35% or less passing No. 200)				Silt-Clay Materials (More than 35% passing No. 200)						
	A-1		A-2	A-3	A-4		A-5		A-6		
Group Classification	A-1-a	A-1-b	A-2	A-2-4	A-2-5	A-2-6	A-2-7	A-4	A-5	A-6	A-7
Sieve analysis, percent passing:											
No. 10											
No. 40		50 max.	51 min.								
No. 200		25 max.	10 max.	35 max.	35 max.	35 max.	35 max.	36 min.	36 min.	36 min.	36 min.
Characteristics of fraction passing											
No. 40:											
Liquid limit				40 max.	41 min.	40 max.	41 min.	40 max.	41 min.	40 max.	41 min. <sup>a</sup>
Plasticity index		6 max.	NP	10 max.	10 max.	11 min.	11 min.	10 max.	10 max.	11 min.	11 min.
Usual types of significant constituent materials		Stone fragments, gravel and sand	Fine sand	Silty or clayey gravel and sand	Silty or clayey gravel and sand	Silty or clayey gravel and sand	Silty or clayey gravel and sand	Silty soils	Silty soils	Clayey soils	Clayey soils
General rating as subgrade				Excellent to good							Fair to poor

<sup>a</sup> Classification procedure: With required test data available, proceed from left to right on above chart and correct group will be found by the process of elimination. The first group from the left into which the test data will fit is the correct classification.  
<sup>b</sup> Plasticity index of A-7-5 subgroup is equal to or less than L.L. minus 30. Plasticity index of A-7-6 subgroup is greater than L.L. minus 30 (see Fig. 14.1).



B-4: Diagram of ASSHTO Classification System.



Group Names for Coarse-Grained Soils Classified as "Sands" in the Unified Soil Classification System

Percent passing No. 200 sieve	Coefficients of uniformity and curvature	Classification of fine-grained portion from plasticity chart	Group symbol	Percent sand or gravel	Group name
<5%	$C_u \geq 6$ and $1 \leq C_c \leq 3$	—	SW	<15% Gravel	Well-graded sand
			SP	$\geq 15\%$ Gravel	Well-graded sand with gravel
	$C_u < 6$ and/or $C_c < 1$ or $C_c > 3$	ML or MH	SW-SM	<15% Gravel	Poorly graded sand with silt
			SP-SM	$\geq 15\%$ Gravel	Poorly graded sand with silt and gravel
5-12%	$C_u \geq 6$ and $1 \leq C_c \leq 3$	CL, CH, or CL-ML	SW-SC	<15% Gravel	Well-graded sand with clay (or silty clay)
			SP-SC	$\geq 15\%$ Gravel	Well-graded sand with clay and gravel (or silty clay and gravel)
	$C_u < 6$ and/or $C_c < 1$ or $C_c > 3$	ML or MH	SP-SM	<15% Gravel	Poorly graded sand with silt
			SP-SC	$\geq 15\%$ Gravel	Poorly graded sand with clay (or silty clay)
>12%	—	ML or MH	SM	<15% Gravel	Silty sand
			SC	$\geq 15\%$ Gravel	Silty sand with gravel
	—	CL or CH	SC-SM	<15% Gravel	Clayey sand with gravel
			SC-SM	$\geq 15\%$ Gravel	Silty, clayey sand with gravel

Group Names for Coarse-Grained Soils Classified as "Gravels" in the Unified Soil Classification System

Percent passing No. 200 sieve	Coefficients of uniformity and curvature	Classification of fine-grained portion from plasticity chart	Group symbol	Percent sand or gravel	Group name
<5%	$C_u \geq 4$ and $1 \leq C_c \leq 3$	—	GW	<15% Sand	Well-graded gravel
			GP	$\geq 15\%$ Sand	Well-graded gravel with sand
5-12%	$C_u < 4$ and/or $C_c < 1$ or $C_c > 3$	ML or MH	GW-GM	<15% Sand	Poorly graded gravel with silt
			GW-GC	$\geq 15\%$ Sand	Well-graded gravel with silt and sand
	$C_u \geq 4$ and $1 \leq C_c \leq 3$	CL, CH, or CL-ML	GW-GC	<15% Sand	Well-graded gravel with clay (or silty clay)
			GP-GC	$\geq 15\%$ Sand	Well-graded gravel with clay and sand (or silty clay and sand)
>12%	$C_u < 4$ and/or $C_c < 1$ or $C_c > 3$	ML or MH	GP-GM	<15% Sand	Poorly graded gravel with silt
			GP-GC	$\geq 15\%$ Sand	Poorly graded gravel with silt and sand
	—	CL, CH, or CL-ML	GP-GC	<15% Sand	Poorly graded gravel with clay (or silty clay)
			GC-GM	$\geq 15\%$ Sand	Poorly graded gravel with clay and sand (or silty clay and sand)
>12%	—	ML or MH	GM	<15% Sand	Silty gravel
			GC	$\geq 15\%$ Sand	Silty gravel with sand
	—	CL or CH	GC-GM	<15% Sand	Clayey gravel with sand
			GC-GM	$\geq 15\%$ Sand	Silty, clayey gravel

# B-6: Tables of Fine Soils After USCS

Group Names for Coarse-Grained Soils Classed as "Gravels" in the Unified Soil Classification System

Percent passing No. 200 sieve	Coefficients of uniformity and curvature	Classification of fine-grained portion from plasticity chart	Group symbol	Percent sand or gravel	Group name	
<5%	$C_u \geq 4$ and $1 \leq C_c \leq 3$	—	GW	<15% Sand	Well-graded gravel	
				$\geq 15\%$ Sand	Well-graded gravel with sand	
	$C_u < 4$ and/or $C_c < 1$ or $C_c > 3$	—	GP	<15% Sand	Poorly graded gravel	
				$\geq 15\%$ Sand	Poorly graded gravel with sand	
5-12%	$C_u \geq 4$ and $1 \leq C_c \leq 3$	ML or MH	GW-GM	<15% Sand	Well-graded gravel with silt	
				$\geq 15\%$ Sand	Well-graded gravel with silt and sand	
		CL, CH, or CL-ML	GW-GC	<15% Sand	Well-graded gravel with clay (or silty clay)	
				$\geq 15\%$ Sand	Well-graded gravel with clay and sand (or silty clay and sand)	
	ML or MH	GP-GM	<15% Sand	Poorly graded gravel with silt		
			$\geq 15\%$ Sand	Poorly graded gravel with silt and sand		
	CL, CH, or CL-ML	GP-GC	<15% Sand	Poorly graded gravel with clay (or silty clay)		
			$\geq 15\%$ Sand	Poorly graded gravel with clay and sand (or silty clay and sand)		
	>12%	—	ML or MH	GM	<15% Sand	Silty gravel
					$\geq 15\%$ Sand	Silty gravel with sand
CL or CH			GC	<15% Sand	Clayey gravel	
				$\geq 15\%$ Sand	Clayey gravel with sand	
CL-ML	GC-GM	<15% Sand	Silty, clayey gravel			
		$\geq 15\%$ Sand	Silty, clayey gravel with sand			

Group Names for Coarse-Grained Soils Classed as "Sands" in the Unified Soil Classification System

Percent passing No. 200 sieve	Coefficients of uniformity and curvature	Classification of fine-grained portion from plasticity chart	Group symbol	Percent sand or gravel	Group name	
<5%	$C_u \geq 6$ and $1 \leq C_c \leq 3$	—	SW	<15% Gravel	Well-graded sand	
				$\geq 15\%$ Gravel	Well-graded sand with gravel	
	$C_u < 6$ and/or $C_c < 1$ or $C_c > 3$	—	SP	<15% Gravel	Poorly graded sand	
				$\geq 15\%$ Gravel	Poorly graded sand with gravel	
5-12%	$C_u \geq 6$ and $1 \leq C_c \leq 3$	ML or MH	SW-SM	<15% Gravel	Well-graded sand with silt	
				$\geq 15\%$ Gravel	Well-graded sand with silt and gravel	
		CL, CH, or CL-ML	SW-SC	<15% Gravel	Well-graded sand with clay (or silty clay)	
				$\geq 15\%$ Gravel	Well-graded sand with clay and gravel (or silty clay and gravel)	
	ML or MH	SP-SM	<15% Gravel	Poorly graded sand with silt		
			$\geq 15\%$ Gravel	Poorly graded sand with silt and gravel		
	CL, CH, or CL-ML	SP-SC	<15% Gravel	Poorly graded sand with clay (or silty clay)		
			$\geq 15\%$ Gravel	Poorly graded sand with clay and gravel (or silty clay and gravel)		
	>12%	—	ML or MH	SM	<15% Gravel	Silty sand
					$\geq 15\%$ Gravel	Silty sand with gravel
CL or CH			SC	<15% Gravel	Clayey sand	
				$\geq 15\%$ Gravel	Clayey sand with gravel	
CL-ML	SC-SM	<15% Gravel	Silty, clayey sand			
		$\geq 15\%$ Gravel	Silty, clayey sand with gravel			

**B-7: Penetration Resistance and Soil Properties on Basis  
of the Standard Penetration Test**

Sands (Fairly Reliable)		Clays (Rather Unreliable)	
Number of Blows per ft, $N$	Relative Density	Number of Blows per ft, $N$	Consistency
0-4	Very loose	Below 2	Very soft
4-10	Loose	2-4	Soft
10-30	Medium	4-8	Medium
30-50	Dense	8-15	Stiff
Over 50	Very dense	15-30	Very stiff
		Over 30	Hard

**B-8: Qualitative and Quantitative Expressions for Consistency  
of Clays**

Consistency	Field Identification	Unconfined Compressive Strength $q_u$ (tons/sq ft)
Very soft	Easily penetrated several inches by fist	Less than 0.25
Soft	Easily penetrated several inches by thumb	0.25-0.5
Medium	Can be penetrated several inches by thumb with moderate effort	0.5 -1.0
Stiff	Readily indented by thumb but penetrated only with great effort	1.0 -2.0
Very stiff	Readily indented by thumbnail	2.0 -4.0
Hard	Indented with difficulty by thumbnail	Over 4.0

B-9: Soil Characteristics pertinent to Construction According to Soil Classification (After Unified Soil Classification)

Symbol (1)	Name (2)	Value as substrate when not subject to frost action (3)	Value as substrate when not subject to frost action (4)	Value as base when not subject to frost action (5)	Potential frost action (6)	Compressibility and expansion (7)	Drainage characteristics (8)	Compaction equipment (9)	Max. unit dry weight at optimum moisture (lb/ft <sup>3</sup> ) (10)	Typical design values	
										CBR (11)	Subgrade modulus $k$ (lb/in <sup>2</sup> ) (12)
GW	Well graded gravels or gravel sand mixtures, little or no fines	Excellent	Excellent	Good	None to very slight	Almost none	Excellent	Crawler-type tractor, rubber-tired roller, steel-wheeled roller	2.00-2.25 (125-140)	40-80	80-135 (300-500)
GP	Poorly graded gravels or gravel-sand mixtures, little or no fines	Good to excellent	Good	Fair to good	None to very slight	Almost none	Excellent	Crawler-type tractor, rubber-tired roller, steel-wheeled roller	1.75-2.75 (110-140)	30-60	80-135 (300-500)
GM	Silty gravels, gravel-sand mixtures	Good to excellent	Good	Fair to good	Slight to medium	Very slight	Fair to poor	Rubber-tired roller, sheepfoot roller; close control of moisture	2.00-2.35 (125-145)	40-60	80-135 (300-500)
GC	Clayey gravels, gravel-sand mixtures	Good	Fair	Poor to suitable	Slight to medium	Slight	Poor to practically impervious	Rubber-tired roller, sheepfoot roller	1.85-2.15 (115-135)	20-30	55-135 (200-500)
SW	Well-graded sands or gravelly sands, little or no fines	Good	Fair	Poor to suitable	Slight to medium	Slight	Poor to practically impervious	Rubber-tired roller, sheepfoot roller	2.10-2.35 (130-145)	20-40	55-135 (200-500)
SP	Poorly graded sands or gravelly sands, little or no fines	Good	Fair	Poor	None to very slight	Almost none	Excellent	Crawler-type tractor, rubber-tired roller	1.75-2.10 (110-130)	20-40	55-110 (200-400)
SM	Silty sands, sand-silt mixtures	Fair to good	Fair	Poor to not suitable	None to very slight	Almost none	Excellent	Crawler-type tractor, rubber-tired roller	1.70-2.15 (105-135)	10-40	40-110 (150-400)
SC	Clayey sands, sand-clay mixtures	Fair to good	Fair to good	Poor	Slight to high	Very slight	Fair to poor	Rubber-tired roller, sheepfoot roller; close control of moisture	1.90-2.15 (120-135)	15-40	40-110 (150-400)
ML	Inorganic silts and very fine sands, loess, silty or clayey fine sands or clayey silts with slight plasticity	Poor to fair	Poor	Not suitable	Slight to high	Slight to medium	Poor to practically impervious	Rubber-tired roller, sheepfoot roller	1.60-2.10 (100-130)	10-20	27-80 (100-300)
CL	Inorganic clays of low to medium plasticity, gravelly clays, sandy clays, silty clays, lean clays	Poor to fair	Poor	Not suitable	Slight to high	Slight to medium	Poor to practically impervious	Rubber-tired roller, sheepfoot roller	1.60-2.15 (100-135)	5-20	27-80 (100-300)
OL	Organic silts and organic silt-clays of low plasticity	Poor	Not suitable	Not suitable	Medium to very high	Slight to medium	Fair to poor	Rubber-tired roller, sheepfoot roller; close control of moisture	1.45-2.10 (90-130)	15 or less	27-55 (100-200)
MH	Inorganic silts, micaceous or diatomaceous fine sandy or silty silts, elastic silts	Poor	Not suitable	Not suitable	Medium to high	Medium	Practically impervious	Rubber-tired roller, sheepfoot roller	1.45-2.10 (90-130)	15 or less	14-40 (50-150)
CH	Inorganic clays of high plasticity, fat clays	Poor to fair	Not suitable	Not suitable	Medium	High	Practically impervious	Sheepsfoot roller, rubber-tired roller	1.45-1.85 (90-115)	15 or less	14-40 (50-150)
OH	Organic clays of medium to high plasticity, high plasticity organic silts	Poor to very poor	Not suitable	Not suitable	Medium	High	Practically impervious	Sheepsfoot roller, rubber-tired roller	1.30-1.75 (80-110)	5 or less	7-27 (25-100)
U	Peat and other highly organic soils	Not suitable	Not suitable	Not suitable	Slight	Very high	Fair to poor	Compaction not practical			

**APPENDIX C**

**C - 1 : Computer Out Put of the X-Ray Analysis  
of Sandy Silt Soil Station 33 at 1.8m.**

**C - 2 : Natural Chemical Composition of the Earth Crust.**

## C - 1: X-ray Computer Output

PEAKS

09-NOV-87 14:45

-----

Listed DI file name : GAONE3.DI  
 Raw data file name : GAONE3.RD

Sample identification : GAONE3GASOUSHEETED  
 Date of measurement : 1-NOV-87  
 Generator settings : 45 kV, 30 mA

Step size, count time : 0.010 deg, 1.00 s  
 Angle range (2theta) : 3.005 - 79.995 deg  
 A1, A2 wavelengths : 1.54056, 1.54435 Ang

Range in d-spacing : 1.1984 - 29.3770 Ang  
 Monochromator used : Yes  
 Maximum peak counts : 784. cts, 784. cps

S.E.C. function applied :

$$0.00003 \times 2\theta^2 + -0.00412 \times 2\theta + 0.15866$$

Peak no	Angle (deg)	Tip width (deg)	Peak (cts)	Backg (cts)	D spac (Ang)	I/Imax (%)	Type			Qual
							A1	A2	Ot	
1	7.1700	0.06	62.	114.	12.3187	7.96	X	X		1.26
2	8.8150	0.80	90.	135.	10.0232	11.51	X	X		5.37
3	17.5975	0.32	53.	135.	5.0357	6.80	X	X		1.15
4	19.6850	0.32	299.	169.	4.5061	36.86	X	X		6.92
5	20.7825	0.16	188.	169.	4.2706	23.94	X	X		1.51
6	21.7650	0.48	55.	237.	4.0800	6.98	X	Y		1.66
7	23.7575	0.64	59.	276.	3.7421	7.56	X	X		1.26
8	25.2750	0.24	67.	310.	3.5208	8.58	X	X		1.48
9	26.5700	0.16	784.	313.	3.3520	100.00	X	X		11.48
10	27.7525	0.64	199.	372.	3.2118	25.36	X	X		9.55
11	33.1325	0.32	96.	266.	2.7016	12.25	X	X		4.37
12	34.6475	0.24	156.	269.	2.5862	19.93	X	X		1.12
13	35.5925	0.24	272.	342.	2.5203	34.73	X	X		2.88
14	35.9550	0.36	225.	342.	2.4957	28.70	X	X		4.57
15	37.2950	0.20	48.	335.	2.4090	6.07	X	X		1.20
16	37.8325	0.12	237.	328.	2.3760	30.25	X	X		2.57
17	39.4225	0.32	21.	289.	2.2838	2.70	X	X		1.48
18	40.1375	0.40	108.	231.	2.2453	13.80	X	X		2.63
19	41.8975	0.40	102.	259.	2.1544	13.01	X	X		2.51
20	42.4125	0.12	48.	272.	2.1295	6.07	X	X		1.07
21	43.3100	0.48	12.	269.	2.0874	1.56	X	X		1.15
22	44.0300	0.16	28.	269.	2.0549	3.58	X	X		1.02
23	45.5850	0.64	32.	240.	1.9884	4.14	X	X		1.48
24	48.1000	0.48	31.	225.	1.8901	4.00	X	X		1.58
25	50.1300	0.12	102.	225.	1.8182	13.01	X	X		1.05
26	54.0850	0.56	130.	234.	1.6942	16.58	X	X		3.55
27	54.8925	0.40	128.	234.	1.6712	16.29	X	X		1.66
28	59.8800	0.24	117.	259.	1.5434	14.88	X	X		1.78
29	61.2375	0.96	96.	299.	1.5124	12.25	X	X		2.04
30	62.4925	0.48	10.	357.	1.4850	1.31	X	X		2.24
31	64.0075	0.32	32.	320.	1.4534	4.14	X	X		1.58
32	68.1300	0.24	108.	272.	1.3752	13.80	X	X		1.91
33	71.7500	0.96	45.	279.	1.3144	5.73	X	X		2.09
34	75.5850	0.48	35.	282.	1.2570	4.44	X	X		1.74
35	77.7050	0.48	10.	253.	1.2279	1.31	X	X		1.00

35 peaks identified  
 35 crystalline

0 amorphous

All listed

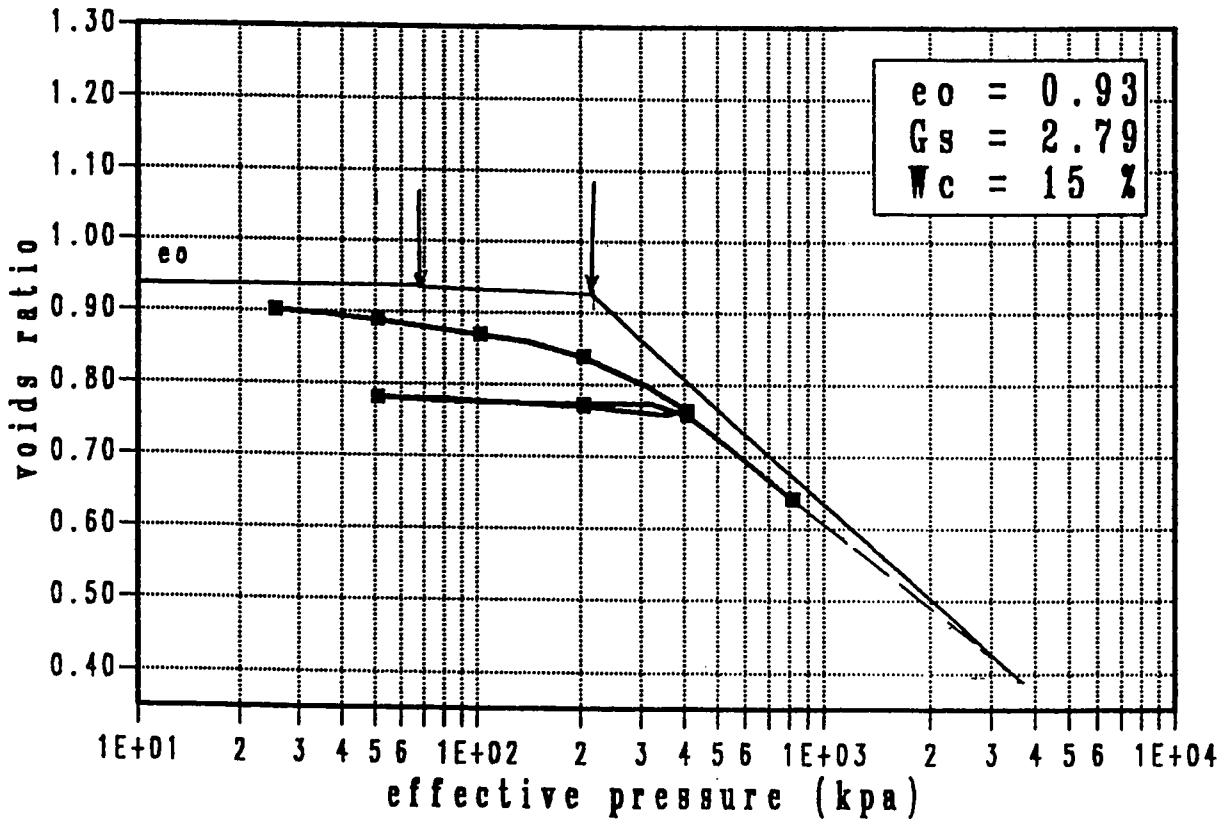
PEAKS

C-2 : Average chemical composition of the  
Earth's crust (after Bear, 1964).

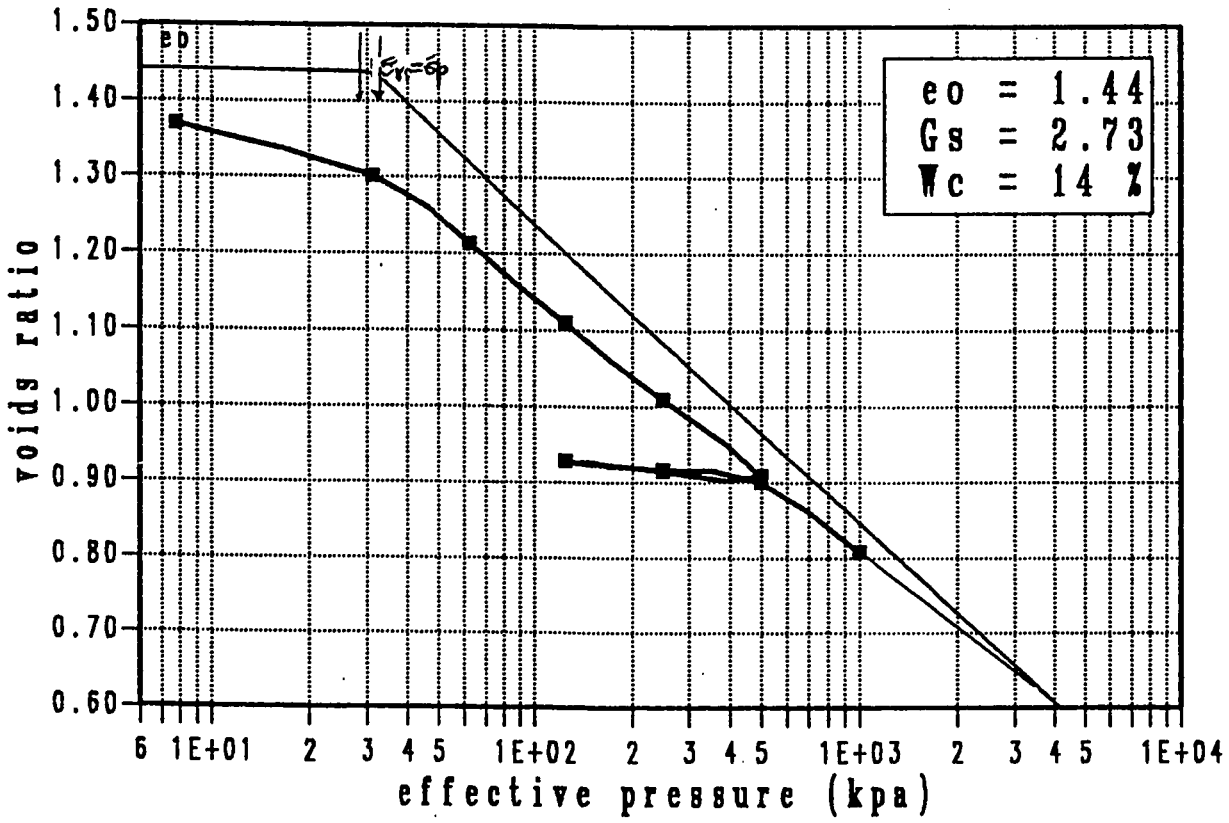
Chemical composition of crust*			
Element	%	Oxide	%
O	46.5	SiO <sub>2</sub>	59.07
Si	27.6	Al <sub>2</sub> O <sub>3</sub>	15.22
Al	8.1	Fe <sub>2</sub> O <sub>3</sub>	3.10
Fe	5.1	FeO	3.71
Ca	3.6	CuO	5.10
Mg	2.1	MgO	3.45
Na	2.8	Na <sub>2</sub> O	3.71
K	2.6	K <sub>2</sub> O	3.11
Ti	0.6	TiO <sub>2</sub>	1.03
P	0.12	P <sub>2</sub> O <sub>5</sub>	0.20
Mn	0.09	MnO	0.11
S	0.06	H <sub>2</sub> O	1.30
Cl	0.05		
C	0.04		

## APPENDIX D

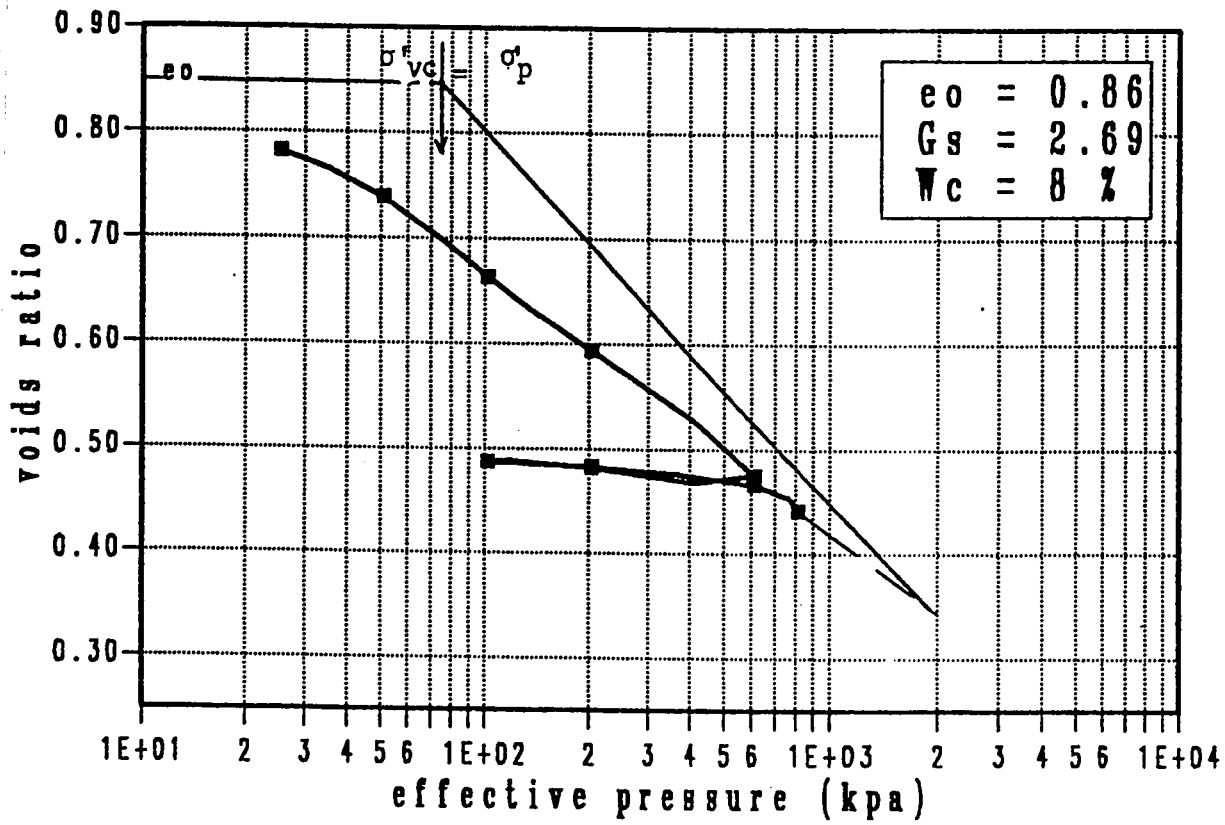
- D - 1 : e log P curve of Sandy Lean clay (Station 36 at 4.5m)
- D - 2 : e log P curve of Sandy Silt (Station 33 at 1.8m)
- D - 3 : e log P curve of Sandy Silty Clay with Gravel (Station 38 at 4.0m)
- D - 4 : Computer Program of Calculating Oedometer test results
- D - 5 : V - Ln p' of Sandy Silt (Station 40 at 2.5m)
- D - 6 : V - Ln p' of Sandy Lean Clay (Station 36 at 4.0m)
- D - 7 : Stress Strain of The Sandy Soil
- D - 8 : Pore pressure of The Sandy Silt Soil
- D - 9 : The Triaxial Computer Program
- D - 10: A representative Computer Out Put
- D - 11: Boundaries of Mohr Envelopes of Loess



D-1: e-Log  $\sigma'_{vo}$  curve of sandy lean clay soil selected from station 36 at 4.0m.



D-2: e-Log  $\sigma'_v$  curve of sandy silt selected from station 33 at 1.8m.



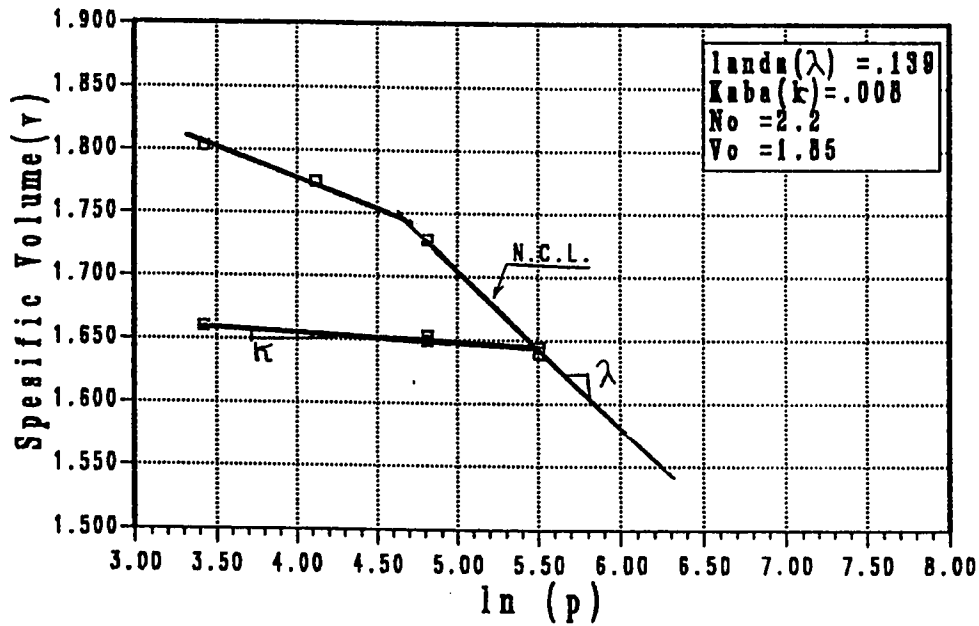
D - 3 : e-Log  $\sigma'_v$  Curve of sandy silty clay with gravel selected from station 38 at 4.5m.



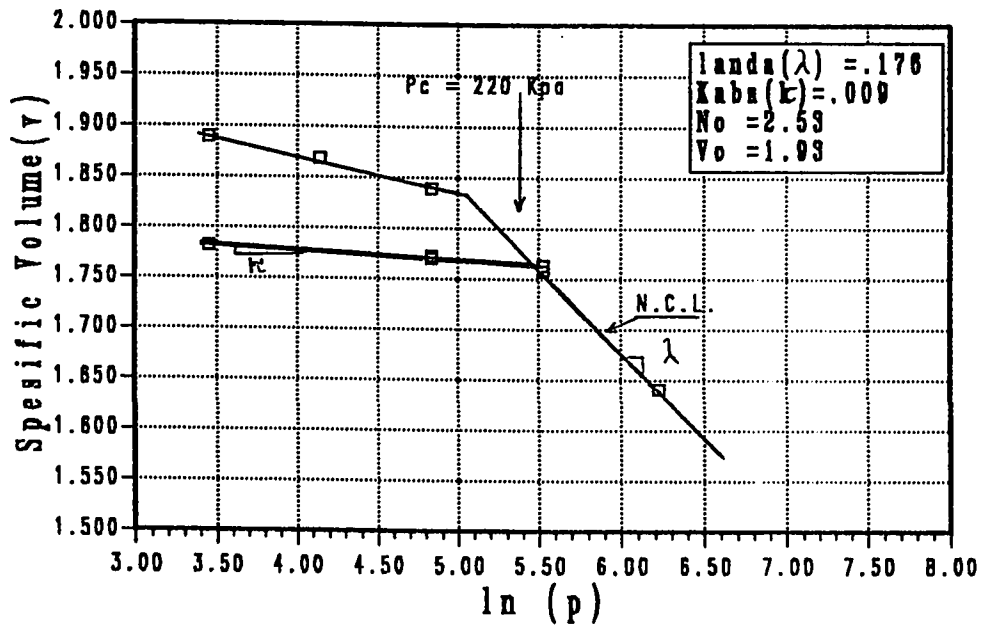
```
DO 20 I=1,N
DELH(I) =R(I) *FR
HAV = HIN -((DELH(I)+X1)/2)
HD(I)= HAV/2
X1 = DELH(I)
DELE = DELH(I)/HS
E(I) = EO - DELE
20 PRINT5,HD(I),P(I),E(I)
40 CONTINUE
5  FORMAT(3(4X,F10.3))
STOP
END
```

\$ENTRY

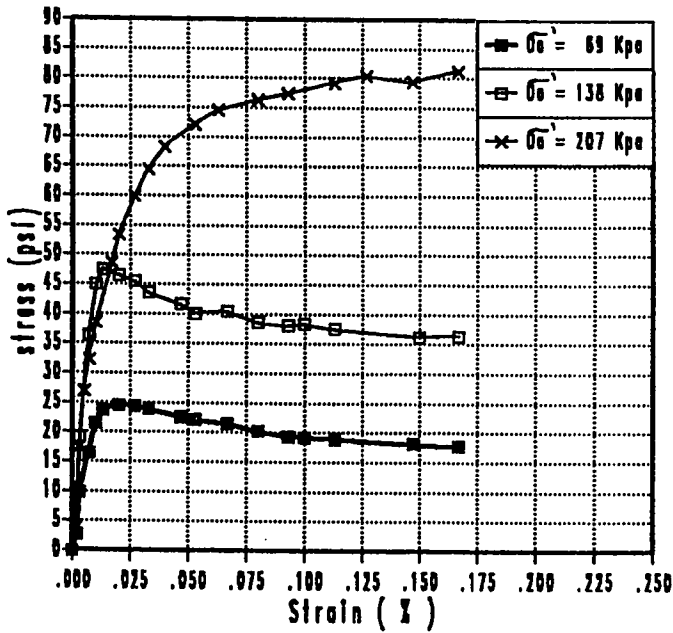
---



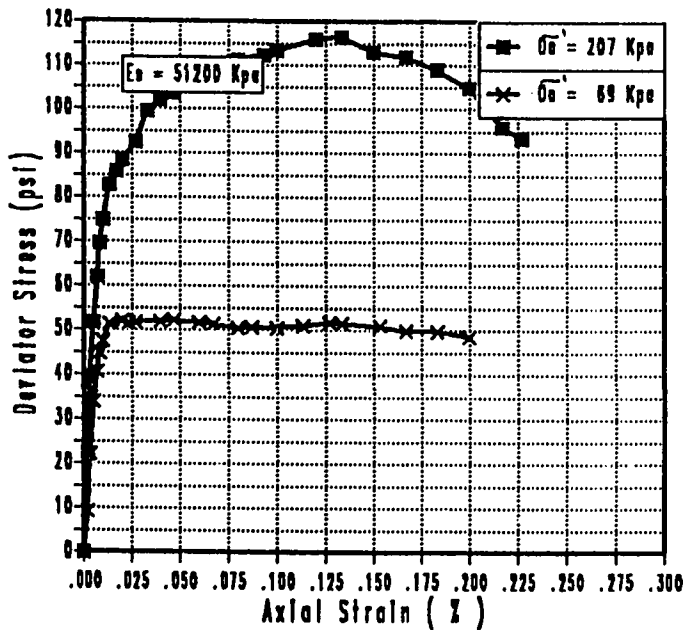
D - 5 :  $v$ - $\ln p$  space of the sandy silt (Station 40 at 2.5m)



D - 6 :  $v$ - $\ln p$  space of the sandy lean clay (Station 36 at 4.0m)

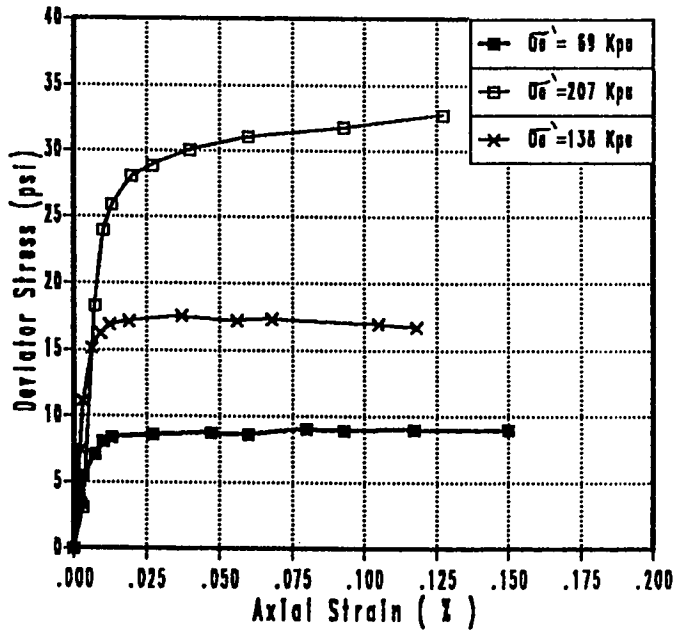


a) Saturated condition

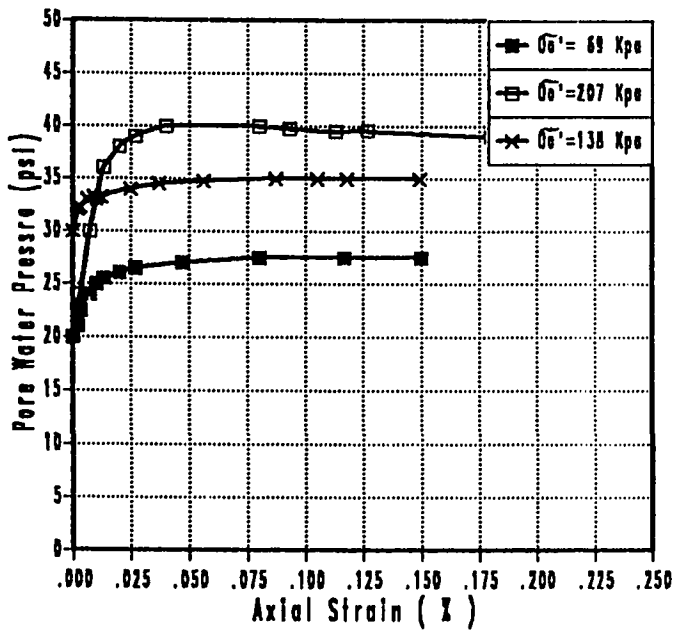


b) Partially saturated condition

D - 7 : Stress strain relation of the Silty clayey sand with gravel (Station 41 at 2.0m).



a) Stress strain



b) Pore water pressure vs. strain

D - 8 : Stress Strain relations of the sandy silt soil (Station 35 at 4.5m)

## D-9

The used computer program in calculating the  
different parameters resulted from triaxial test.

```
=====
$JOB
  DIMENSION DEFR(45),U(45),SEG1(45),Q(45),PTOT(45),PEFE(45)
+,DEVST(45),LOADR(45),STRAIN(45),ACOR(45),SEGC(1),SEG3(45)
  CHARACTER*40 TITLE(45)
  REAL LOADF,LOADR
cc-----      Number of tested samples = m -----
  READ,M
  DO 100 J = 1,M
  READ3,TITLE (J)
3  FORMAT(A40)
  PRINT4,TITLE(J)
4  FORMAT(' ',A40)
  READ ,HO,AO,DEFF,LOADF,N,SEGC(1)
c-----      Inout data -----
cc-----      HO : Intial hight of the sample -----
cc-----      AO : Intial area of the sample -----
cc-----      DEFF: Deformation factore -----
cc-----      LOADF:Load factore -----
cc-----      SEGC(1): Confined pressure -----
c-----
```

```

PRINT11,HO, AO, DEFF, LOADF, N, SEGC(1)
11  FORMAT(1X, 'HO = ', F5.3, 2X, 'AO = ', F5.3, 2X, 'DEFF
+ = ', F5.3, 'IN', 2X, 'LOADF = ', F5.3, 'LB',
+ 2X, 'NU.POINTS= ', I2, 2X, 'SEGM CON.= ', F7.4)
DO 10 I=1,N
READ , DEFR(I),LOADR(I),U(I)
10  PRINT 20 , DEFR(I),LOADR(I),U(I)
20  FORMAT (3(4X,F10.4))
C   PRINT 6,J
C 6  FORMAT (' ',8X,'-----THE INPUT OF BL8 ( ',I2,' )--')
IF ( J .EQ. 1 ) PRINT,80
80  FORMAT (///1X, 'SAMPLE OUTPUT OF TRIAXIAL TEST RESULT'
+/1X, 'STIFF FISSURED LEAN CLAY SOIL'
+/1X, 'STATION : 33 AT 0.7 METER'//)
PRINT, '-----'
+-----'
PRINT 9
PRINT7
PRINT, '-----'
+-----'
7  FORMAT(4X, 'PSI', 6X, 'PSI', 6X, 'PSI', 6X, ' % ', 5X,
+'PSI', 7X, 'PSI', 7X, 'PSI')
9  FORMAT(3X, 'SEG 1', 4X, 'SEG 3', 3X, 'WAT. PRE.', 2X,
+ 'STRAINR', 3X, 'PTOT', 5X, 'PEFE', 4X, 'SEG1-SEG3')
DO 30 I=1,N
STRAIN(I)=(DEFR(I)*DEFF)/HO

```

ACOR(I)=AO/(1-STRAIN(I))

DEVST(I)=(LOADR(I)\*LOADF)/ACOR(I)

SEG3(I)=SEGC(1)

SEG1(I)=DEVST(I)+SEG3(I)

Q(I)=DEVST(I)

PTOT(I)=(SEG1(I)+2\*SEG3(I))/3

PEFE(I)=PTOT(I)-U(I)

PRINT 40,SEG1(I),SEG3(I),U(I),STRAIN(I),PTOT(I),PEFE(I)

+,Q(I)

30 CONTINUE

PRINT, '-----'

+-----'

100 CONTINUE

40 FORMAT (7(2X,F7.3))

STOP

END

\$ENTRY

---

---

## D-10

Computer out put of the triaxial  
 results of the stiff lean clay  
 ,unit VI, (Station 33 at 0.7m).

\*\*\*\*\*

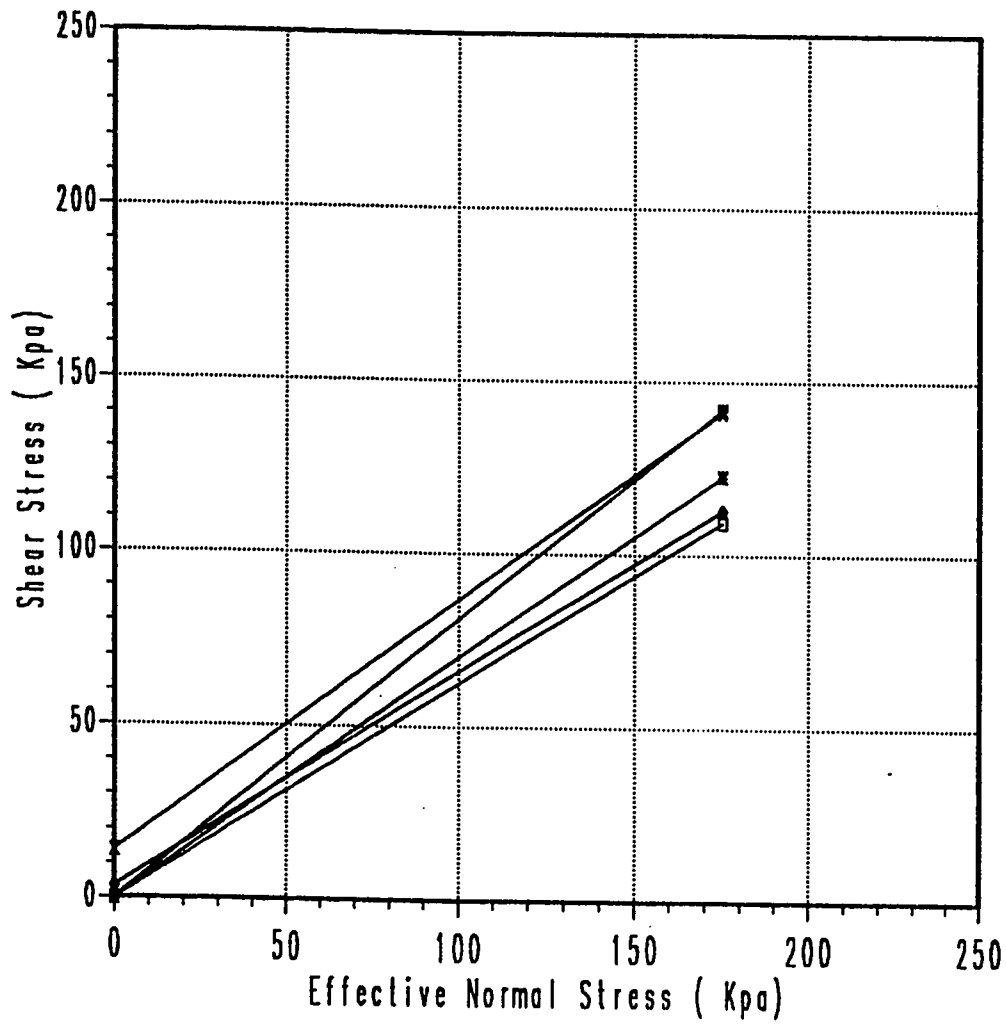
HO = 3.000 AO = 1.767 DEFF = 0.001IN LOADF = 0.598LB

SEGM CON.= 40.0000 NU. POINTS= 18

SEG 1	SEG 3	WAT.PRE.	STRAINR	PTOT	PEFE	SEG1-SEG3
PSI	PSI	PSI	%	PSI	PSI	PSI
40.000	40.000	20.000	0.000	40.000	20.000	0.000
48.447	40.000	23.500	0.002	42.816	19.316	8.447
52.817	40.000	25.500	0.003	44.272	18.772	12.817
57.145	40.000	27.750	0.007	45.715	17.965	17.145
59.097	40.000	29.250	0.010	46.366	17.116	19.097
59.967	40.000	31.000	0.017	46.656	15.656	19.967
59.899	40.000	31.500	0.020	46.633	15.133	19.899
60.094	40.000	32.500	0.027	46.698	14.198	20.094
59.956	40.000	33.000	0.033	46.652	13.652	19.956
59.818	40.000	33.500	0.040	46.606	13.106	19.818
59.543	40.000	33.750	0.053	46.514	12.764	19.543
59.723	40.000	33.750	0.060	46.574	12.824	19.723
59.615	40.000	34.000	0.080	46.538	12.538	19.615
59.945	40.000	34.000	0.093	46.648	12.648	19.945

60.105	40.000	34.000	0.113	46.702	12.702	20.105
60.098	40.000	34.000	0.127	46.699	12.699	20.098
60.424	40.000	33.750	0.150	46.808	13.058	20.424
60.588	40.000	33.500	0.167	46.863	13.363	20.588

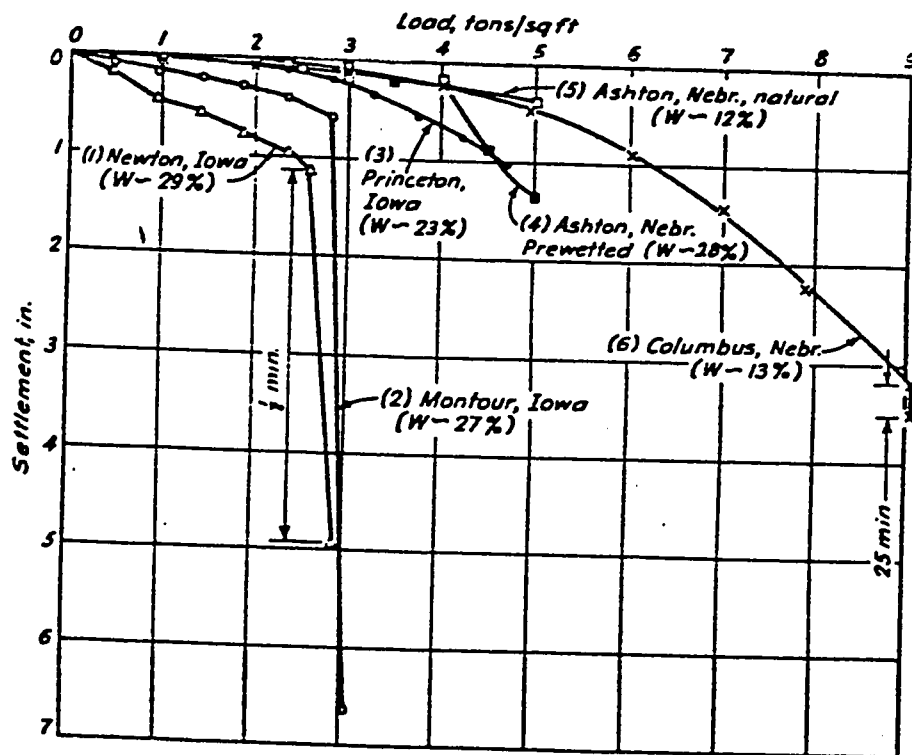
-----  
\*\*\*\*\*



D - 11: Upper and lower boundrais of Mohr envelopes of Loess in term of the effectuve stresses

**APPENDIX E**

**E - 1 : Effect of Moisture on The Critical  
Stress of Collapsing Soil**



E-1: Effect of moisture content in the critical stress of collapsing soil.

(Peckm, Hanson and Thurnborn, 1974).